EVOLUCION TECTONICA DEL MARGEN SUR-CENTRAL DEL CARIBE BASADO EN DATOS GEOQUIMICOS

MARINO OSTOS ROSALES

INTRODUCCION

Objetivos

La historia del Cretácico y Terciario en el norte de Venezuela está claramente relacionada con los tipos de márgenes litosféricos existentes entre la placa Caribe y la placa de Suramérica. Diferentes modelos de tectónica de placas han sido propuestos para explicar la evolución del norte de Suramérica. Los más antiguos se encuentran practicamente en su totalidad en el trabajo de Bonini *et al.* (1984) y los modelos más recientes han sido propuestos por Pindell *et al.* (1988) y Ross and Scotese (1988). Los modelos de tectónica de placas mencionados pueden ser agrupados en dos tendencias: (a) la primera interpreta la placa Caribe formada como el resultado de la expansión entre Norte y Sur America durante el Jurásico y el Cretácico Temprano (Maresch, 1974; Beets *et al.*, 1984) y (b) en el segundo grupo de modelos la placa Caribe fue formada en el Pacifico (placa de Farallón) y ha migrado hacia el este, entre Norte y Sur America, desde el Cretácico Tardio (Pindell *et al.*, 1988; Ross y Scotese, 1988).

De igual manera diversos modelos de tectónica de placas han sido propuestos especificamente para explicar la geología de Venezuela (Maresch, 1974; Talukdar et al., 1981; Talukdar y Loureiro, 1982; Navarro, 1983; Beck, 1985; Ostos y Navarro, 1985; Stephan, 1985). De todos estos modelos propuestos, los de Talukdar *et al.* (1981), Navarro (1983) y Ostos y Navarro (1985) muestran las mayores diferencias con el resto de los modelos propuestos, la cual consiste básicamente en la existencia de un cuenca marginal en el norte de Venezuela durante el Cretácico, la cual evolucionó en su parte sur a un borde convergente. Dicho borde desarrollo un arco de islas (La Formación Dos Hermanas del cinturón tectónico de Villa de Cura) y por consiguiente no existe una aloctonia de este cinturón tectónico, tal como es propuesta en los otros modelos, ni una correlación con las islas holandesas y venezolanas y el terreno de la Cordillera de la Costa-Margarita.

El principal objetivo de esta investigación fue el tratar de corroborar los diferentes modelos tectónicos propuestos con anterioridad y determinar cuál o cuales de estos modelos pueden explicar de una mejor manera la geología de Venezuela. Otro objetivo secundario pero de gran importancia fué el determinar la aloctonia de los diferentes cinturones tectonoestratigráficos del norte de

Venezuela, la cual es de importancia para la recontrucción de la evolución tectónica de las cuencas "foreland", al sur de los terrenos estudiados, ya que estas han demostrado ser importantes yacimientos petroliferos.

METODOLOGIA

Para alcanzar los objetivos de la presente investigación se llevaron a cabo estudios de geologia estructural, petrologia y geoquimica, en afloramientos y rocas del norte de Venezuela. Tres geotransversales fueron realizadas en el orógeno, a lo largo de las cuales análisis estructurales fueron llevados a cabo, asi como la toma de muestras para análisis microestructurales y estudios petrográficos, geocronológicos y geoquimicos. Adicionalmente, otras áreas de interes geológico fueron visitadas para la recolección de muestras. De igual manera la información disponible de la plataforma Venezolana (pozos y sismica) fue tambien integrada en esta investigación.

El análisis estructural realizado incluyó el reconocimiento de los periodos de plegamiento y fallamiento en el campo, asi como la determinación de la cinemática de la deformación en base a las microtexturas desarrolladas durante la deformación dúctil, las cuales fueron identificadas durante el estudio petrográfico de la muestras orientadas, las cuales fueron recogidas durante la fase de campo. La información mesoscópica, megascópica, y la cinemática de la deformación determinada fué utilizada para reconstruir la historia deformacional de los diferentes cinturones tectonoestratigráficos estudiados.

Las muestras también fueron estudiadas utilizando microscopia de luz polarizada con la finalidad de reconocer las asociaciones mineralógicas en las diferentes unidades tectonoestratigráficas, asi como las relaciones texturales existentes entre las diferentes fases minerales reconocidas. Basado en la identificación de las asociaciones minerales y las relaciones texturales se interpretaron las facies metamórficas, las relaciones aproximadas de P y T a las cuales fueron sometidas las rocas, asi como la interpretación de los ambientes tectónicos en los cuales las diferentes unidades pudieron haber sido metamorfizadas.

La identificación de los ambientes tectónicos de las rocas igneas máficas y félsicas fué realizado por medio del uso

de anàlisis discriminantes, para lo cual fueròn seleccionadas las muestras a analizar por medio del estudio petrogràfico, a fin de seleccionar muestras libres de alteraciones y de venas de minerales, las cuales pudieran alterar los anàlisis quìmicos. La abundancia de elementos mayoritarios y de algunos elementos trazas (incluyendo tierras raras) fue realizado por fluorescencia de rayos X (XRF) en los laboratorios de la Escuela de Geologìa, Minas y Geofìsica, Ministerio de Energìa y Minas y X-RAY ASSAY Laboratories en Canadà. Igualmente fué utilizado en los anàlisis un equipo de plasma (ICP) y de activaciòn de neutrones de X-RAY ASSAY Laboratories en Canadà.

A partir de las abundancias determinadas fueron interpretados los ambientes tectònicos para las diferentes unidades tectonoestratigràficas estudiadas, por medio de diagramas dicriminantes y la correlaciòn de los patrones de tierras raras normalizados con los publicados en la literatura.

Durante el presente trabajo se intentò determinar las edades de cinco complejos ìgneos incluidos en el orògeno, utilizando el metodo Rb/Sr en roca total, habiendo sido realizado los anàlisis en la compañìa Teledyne Isotopes INC de los Estados Unidos. En tres de los complejos analizados fue imposible determinar una buena isocrona, lo cual fue debido a la similitud en las abundancias de los isotopos de Sr y en la abundancia de Rb en las muestras analizadas. Sin embargo las relaciones isotòpicas obtenidas fueron utilizadas para interpretar ambientes tectònicos y la fuente original del magma a partir de los cuales los complejos ìgneos estudiados fueron formados.

Las isocronas obtenidas y aquellas edades isotòpicas previamente publicadas fueron integradas y analizadas criticamente, de manera de establecer de una manera aproximada la relaciòn temporal de los diversos eventos geològicos ocurridos en el orògeno estudiado.

Por ùltimo se analizò criticamente los patrones de deriva continental, asì como las reconstrucciones de placas publicadas para el Triasico-Juràsico. A partir de estos fué integrada toda la informaciòn geològica obtenida en el presente trabajo, asì como toda la previamente publicada, incluyendo un breve anàlisis de la evoluciòn de las cuencas sedimentarias Mesozoicas y Cenozoicas del norte de Suramérica y la incorporaciòn de los datos geològicos de mayor relevancia de las cordilleras Colombianas. Basado en toda la informaciòn anteriormente descrita, se procediò a verificar la posibilidad de que alguno de los modelos

previamente publicados, ya fuesen a escala regional o a escala de Venezuela, pudiesen explicar la sucesiòn de eventos geològicos reconocidos durante los analisis previos de esta investigaciòn. Al reconocer que ninguno de los modelos cumplìa con este objetivo, se elaborò un modelo de tectònica de placas que si lo cumpliese.

CONCLUSIONES

Cinturones Tectónicos

Las islas holandesas y venezolanas consisten de rocas ígneas de origen oceánico de edad Cretácico Temprano y rocas de arco de islas de edad Cretácico Tardío. Este terreno ha sido correlacionado con las unidades litológicas que constituyen el cinturón tectónico de Villa de Cura y con la parte nororiental de la plataforma venezolana.

El Sistema Montañoso del Caribe ha sido dividido en cinco cinturones tectónicos, con tres fallas regionales de rumbo este-oeste separando los cuatro cinturones que se encuentran más al sur en el sistema. El terreno de la Cordillera de la Costa-Margarita consiste de rocas que fueron afectadas por un metamorfismo de alta P y baja T, al cual se le sobreimpuso un metamorfismo con una relación intermedia de P y T. El cinturón tectónico de la Cordillera de la Costa consiste de un basamento granítico de edad Precambrica y una covertura sedimentaria de edad Mesozoica, la cual sólo fué afectada por el segundo evento metamórfico descrito para el terreno de la Cordillera de la Costa-Margarita.

El cinturón tectónico de Caucagua-El Tinaco consiste de un basamento Paleozoico, una cobertura de metasedimentos pérmicos y metavolcanicas no orogénicas y metasedimentos y metavolcánicas de edad Cretácico. El basamento de este cinturón tectónico fué afectado por un metamorfismo en la facies de la anfibolita en un régimen de baja relación P/T. La cobertura paleozoica y mesozoica muestra una asociación de minerales caracteristica de la facies de los esquistos verdes.

El cinturón tectónico de Paracotos consiste de sedimentos tipo flysch y wildflysch, megalentes de serpentinitas y ofiolitas desmembradas, interpretándose una edad de sedimentación en el rango Campaniense a Maastrichtiense. Localmente este cinturón fué afectado por un metamorfismo de muy bajo grado.

El cinturón tectónico de Villa de Cura consiste de metasedimentos (abundantes metavolcaniclásticos), las metavolcánicas del Grupo Villa de Cura, volcánicas de arco de islas y plutones máficos-ultramáficos. Las rocas de este cinturón fueron afectadas por un metamorfismo de alta P y baja T, al cual localmente le fué sobreimpuesto un metamorfismo de intermedia relación de P y T.

Edades Isotópicas

La mayoria de la edades isotópicas del norte de Suramérica están relacionadas con la orogenia que afectó el límite de placas entre el caribe y suramérica. Las edades isotópicas pueden ser correlacionadas con los siguientes eventos tectónicos: (a) un evento Jurásico de "rifting", (b) un evento metamorfico que abarca el Cretácico, (c) un episodio de levantamiento durante el Cretácico tardio y (d) un levantamiento durante el Terciario.

Edades Sedimentarias

Los fósiles en el margen de placas estudiado son escasos, lo cual es probablemente a la mala preservación causada por el intenso desmembramiento tectónico y recristalización. Sin embargo, basado en los datos disponibles las siguientes conclusiones pueden ser alcanzadas: (a) fósiles de edad Jurásico y Neocomiense han sido encontrados en mármoles en la Península de Paraguaná, en la ofiolita de Siquisique y en la Cordillera de la Costa. Estas constituyen las edades mesozoicas más viejas en el orógeno y restringen la edad de apertura del Proto-Caribe, (b) fósiles de edad Turoniense a Albiense han sido encontrados en las secuencias de piso oceánico de Aruba y Curazao, mientras que en las secuencias de arco de islas primitivo de Bonaire fósiles de edad Albiense a Coniaciense han sido identificados. Ellos probablemente permiten interpretar que el arco de islas estaba formándose mientras la expansión todavia continuaba, (c) los fósiles de edad Pérmico, Albiense y Cretácico Tardio sin diferenciar han sido identificados en el cinturón tectónico de Caucagua-El Tinaco, lo cual indica una historia geológica anterior a la apertura del Proto-Caribe, (d) los sedimentos tipo flysch en el cinturón tectónico de Paracotos contienen fósiles de edad Cretácico Tardio y Cretácico Tardio-Paleoceno. Ellos indican la edad de la sedimentación en una fosa, en una cuenca al frente de un arco volcánico o en una cuenca episutural en un terreno transpresional y (e) en el Grupo Villa de Cura han sido reportados fósiles de aguas poco profundas con una edad Aptiense-Albiense, pudiéndose asi correlacionar este grupo con las secuencias de piso oceánico de las islas holandesas. Sin embargo, el ambiente de los fósiles identificados en el Grupo Villa de Cura es sospechoso. Asi, los fósiles más bien pudieron haber sido recogidos en otra unidad tectonoestratigráfica o quizás ellos fueron incorporados tectónicamente en Villa de Cura. Esto también es apoyado por las edades isotópicas, ya que las secuencias de piso oceánico en el cinturón tectónico de Villa de Cura aparentemente son ligeramente más viejas que

las secuencias similares en las islas Holandesas, por lo que la correlación de Villa de Cura sería más bien con la ofiolita de Romeral en Colombia y con las secuencias de piso oceánico de las islas Venezolanas de Los Monjes y Los Roques.

Discordancias

Basado en las edades del basamento y de la cobertura sedimentaria determinadas isotópicamente y por el contenido fosilífero, algunas discordancias fueron reconocidas en el borde sur-central de la placa Caribe, las cuales son importantes indicadores de los eventos tectónicos que afectaron el orógeno estudiado.

La discordancia presente en las islas holandesas y venezolanas pudo haber estado relacionada con la colisión del Caribe y Suramérica. La colisión aparentemente se inicio más temprano en las islas al oeste (Cretacico Tardio) que en las islas al este (Eoceno). En la plataforma venezolana (Golfo de la Vela y Golfo Triste) las discordancias pueden ser correlacionadas con el borde colisional desarrollado en el Cretácico Tardio-Eoceno, la formación de las cuencas "pull-apart" durante el Oligoceno y la migración hacia el norte del bloque de Maracaibo-Santa Marta.

La cuenca de Carúpano en la parte noreste de Venezuela muestra una discordancia Paleoceno a Oligoceno en su parte sureste, mientras que la discordancia en los pozos perforados hacia el noroeste es Oligoceno. En La cuenca Tuy-Cariaco dos discordancias fueron reconocidas, las cuales son de edad Cretácico Tardio-Paleoceno y Oligoceno-Mioceno. La más joven quizás indica la generación de las cuencas "pull-apart", mientras que la más antigua quizás está relacionada con la colisión interpretada anteriormente.

Las cuencas de Guárico y Maturin muestran diacronismo desde el oeste hacia el este en la sedimentación de las molasas Mioceno y Plioceno. Las discordancias en el terreno de la Cordillera de la Costa-Margarita se reconocen fácilmente en la isla de Margarita, las cuales pueden ser interpretadas como consecuencia de la colisión (Cretácico Tardio-Eoceno Temprano y Eoceno Tardio-Mioceno Medio) y con la generacion de las cuencas Miocenas "pull-apart" en el borde colisional.

El Sistema Montañoso del Caribe en tierra firme muestra una discordancia al menos desde el Cretácico Tardio al Plioceno o Pleistoceno, la cual puede ser la consecuencia

del levantamiento y del desarrollo Neogeno de las cuencas "pull-apart" en el borde colisional.

Afinidad Tectónica de la Rocas Igneas

La afinidad tectónica de numerosos complejos igneos en el borde sur-central del Caribe fue determinado por medio de diagramas discriminantes de los elementos mayoritarios más inmóbiles, de los elementos de transición del grupo del hierro (Cr y Ni), de los elementos incompatibles como Zr, Y, Nb y algunas tierras raras, asi como de elementos de bajo potencial iónico como Rb. Basado en las afinidades tectónicas determinadas en el presente estudio y aquellas obtenidas en trabajos previos, se interpretó un marco geológico regional para el borde sur-central de la placa Caribe, el cual es el siguiente: (a) en los cinturones tectónicos de la Cordillera de la Costa y de Caucagua-El Tinaco fueron reconocidos granitos de interior de placas precambricos y granitos paleozoicos del tipo andino respectivamente, (b) en el cinturón tectónico de Caucagua-El Tinaco fueron reconocidos adicionalmnente tholeitas de arco de islas volcánico y de cordillera centro-oceánica, (c) tholeitas no orogénicas de edad Jurásico fueron extruidas en el graben de Espino, las cuales pueden estar relacionadas con la apertura del Caribe, (d) en los cinturones tectónicos de la Cordillera de la Costa y Paracotos y en el terreno de la Cordillera de la Costa-Margarita son reconocidas ofiolitas desmembradas, las cuales no han sido nunca datadas, pero han siempre sido interpretadas como Mesozóicas, (e) al sur de la cuenca Terciaria de Falcón ha sido reconocida una ofiolita de edad Jurásico Medio (Siquisique), (f) los basaltos de edad Jurásico Tardio-Cretácico Temprano en algunas de las islas holandesas y venezolanas (Los Monjes, Aruba, Curacao y Los Roques), en la isla de Margarita (terreno de la Cordillera de la Costa-Margarita) y en la cuenca de Carúpano representan extrusiones en cordilleras centro-oceánicas, (g) el cinturón tectónico de Villa de Cura consiste de basaltos de edad Cretácico Temprano (?) generados en una cordillera centro-oceánica ó en una cuenca oceánica marginal, (h) durante el Cretácico Tardio es reconocida la existencia de actividad magmática en un arco de islas (Aruba, Bonaire, Los Roques, La Blanquilla, Los Hermanos, Los Frailes, Margarita, en las cuencas de Carúpano y Tuy-Cariaco y en el cinturón tectónico de Villa de Cura) e (i) actividad volcánica de edad Eoceno Tardio asociada a un arco de islas volcánico es reconocida en la parte noroeste de la cuenca de Carúpano y en la isla de Los Testigos.

Metamorfismo Regional

La determinación de las condiciones del metamorfismo regional que afectaron el borde sur-central del Caribe fue realizado en base a las asociaciones de minerales reconocidas durante el estudio petrográfico, así como en las relaciones texturales existentes entre las diferentes fases minerales, las cuales fueron también determinadas durante el mismo estudio. En conclusión se puede decir: (a) el basamento del cinturón tectónico de Caucagua-El Tinaco fue afectado probablemente en el Pérmico por un metamorfismo en la facies de la granulita, (b) rocas de piso oceánico de edad Jurásico Tardio a Cretácico Temprano fueron metamorfizadas en un complejo de subducción durante la parte tardia del Cretacico Temprano a la parte temprana del Cretácico Tardio en las facies de la prehnita-pumpelita, zeolitas, eclogita y esquistos azules. Rocas de este complejo de subducción fueron reconocidas en las islas holandesas y venezolanas (Curazao), en la plataforma venezolana (Cuenca de Carúpano), en el terreno de la Cordillera de la Costa-Margarita, y en los cinturones tectónicos de Paracotos y Villa de Cura, (c) un evento de presión y temperatura intermedias ocurrió en un arco de islas durante el Cretácico Tardio; rocas afectadas por este evento metamórfico han sido reconocidas en las isla holandesas y venezolanas (Aruba, Bonaire, Los Roques, Los Hermanos, los Testigos y Los Monjes), en la plataforma venezolana (cuencas de Carúpano y Tuy-Cariaco), en el terreno de la Cordillera de la Costa-Margarita y en el cinturón tectónico de Villa de Cura. La asociación de minerales reconocidos indican un evento metamórfico en la facies de la prehnita-pumpelita, esquistos verdes y anfibolita epidótica, y (d) durante el Cretácico Tardio un evento metamórfico de intermedia a baja P/T (facies de los esquistos verdes, anfibolita epidótica y anfibolita) afectó las rocas de los cinturones tectónicos de la Cordillera de la Costa y de Caucagua-El Tinaco.

Geología Estructural

Los cinturones tectónicos del Sistema Montañoso del Caribe han sido fuertemente deformados. Cuatro fases de plegamiento fueron reconocidas. Las primera dos fases de plegamiento fueron solamente identificadas en el cinturon tectónico de Caucagua-El Tinaco y ellas probablemente fueron el resultado de una orogénesis que ocurrio durante el Permico. El cinturón tectónico de la Cordillera de la Costa tambien debio haber sido deformado durante esta orogenesis. Las dos ultimas fases de plegamiento fueron reconocidas en todos los cinturones tectónicos y ellas probablemente se generaron durante la orogénesis del

Cretàcico Tardio-Terciario. En el Sistema Montañoso del Caribe fueron reconocidas tres generaciones de fallas las cuales son: fallas transcurrentes dextrales y de corrimiento de orientaciòn este-oeste, fallas transcurrentes dextrales orientadas noroeste-sureste. Las generaciones de los sistemas de fallas reconocidos se encuentra relacionado con la generaciòn del cuarto periodo de plegamiento. También han sido reconocidas fallas normales con rumbo este-oeste, las cuales son interpretadas como posteriores a las anteriores y son en la actualidad activas.

Los indicadores cinemàticos estudiados sugieren que una cizalla hacia el sur ocurriò en los planos de foliaciòn, la cual esta relacionada con la tercera fase de plegamiento reconocida en el terreno de la Cordillera de la Costa-Margarita y en el cinturòn tectònico de la Cordillera de la Costa. Sin embargo indicadores cinemàticos en los cinturones tectònicos de Caucagua-El Tinaco, Paracotos y Villa de Cura indican en su lugar una cizalla hacia el norte, pero en todos los los terrenos se evidencia una componente dextral importante. Por consiguiente, si todos los indicadores cinemàticos se desarrollaron durante la orogénesis del Cretàcico Tardio-Terciario, el Sistema Montañoso del Caribe debiò haber sufrido cizalla dextral paralela a los cinturones tectònicos del sistema.

Cuencas Sedimentarias en el norte de Sur America

La historia de las cuencas sedimentarias del norte de Suramérica pueden tambien ayudar a interpretar la evoluciòn tectònica del borde de placas objeto del presente estudio. Las cuencas sedimentarias pueden ser divididas en cuencas del tipo Atlantico y cuencas episuturales y basado en sus historias geològicas, las siguientes interpretaciones pueden ser realizadas: (a). Las sedimentaciòn hasta el Cretàcico Tardio ocurriò en cuencas pasivas en una margen tipo Atlàntico en el norte de Sur America. Las facies sedimentarias pre-Santonienses son similares en todo el margen Atlàntico, lo cual sugiere que solamente existio hasta esta epoca una gran cuenca. A partir de esta época es cuando la gran cuenca es dividida en dos de menores dimensiones. (b). Durante el Cretàcico Tardio-Paleogeno, la sedimentaciòn en las partes màs meridionales de las cuencas tipo Atlantico fue continua, mientras que hacia el norte de la cuenca de Maracaibo esta se convierte en una cuenca "foreland" (perisutural). (c). Durante el Cretàcico Tardio, cuencas flysch se desarrollaron al norte de las cuencas Atlanticas y perisuturales. Ellas se encuentran hoy expuestas en las

islas holandesas y venezolanas (Curazao y Bonaire) y en la plataforma venezolana (Cuenca de Carúpano). Estas cuencas corresponden a una sedimentación en fosas oceánicas (deep sea trench) o "forearc basins" y probablemente estuvieron relacionadas con el borde convergente desarrollado en el norte de Sur America durante el Cretácico Tardio. (d). Sedimentos volcanogénicos de edad Eoceno han sido reconocidos al este del bloque de Maracaibo-Santa Marta, en la plataforma venezolana (Cuencas de Carúpano y de Golfo Triste) y en el terreno de la Cordillera de la Costa-Margarita en la isla de Margarita. Estos sedimentos deben haber tenido relación con el borde convergente que existió en el Terciario en el norte de Venezuela. (e) Durante el Oligoceno en la parte occidental del borde de placas entre el Caribe y Suramérica se desarrollaron cuencas "pull-apart" episuturales con un rumbo generalizado este-oeste y (f). cuencas "pull-apart" episuturales con una orientación este-oeste fueron desarrolladas en la parte central y occidental del borde de placas (plataforma venezolana y Sistema Montañoso del Caribe) durante el Mioceno y el Plioceno a Cuaternario.

Modelo de Tectónica de Placas

Basado en la información geológica disponible, es propuesto un modelo de tectónica de placas para explicar la evolución del norte de Suramérica. El modelo trata de incluir todas las variables geológicas analizadas durante el trabajo. En el modelo los cinturones tectónicos este-oeste del norte de Suramérica son alóctonos y fueron deformados como el resultado de la colisión de un microcontinente y un arco de islas contra el oeste-noroeste de Suramérica durante el Neocomiense. Los cinturones fueron inicialmente sobrecorridos en el margen oeste-noroeste de la placa suramericana, pero debido al angulo alto de oblicuidad en el borde de placas, los cinturones fueron transportados transpresionalmente hacia el noreste. El transporte tectónico hacia el noreste ocurrió desde el Santoniense-Campaniense, posteriormente a la colisión del "plateau" del Caribe y la generación de la zona de subducción con inclinación hacia el oeste, en el borde este de la placa del Caribe. El transporte tectónico hacia el noreste de los cinturones tectónicos y de la placa Caribe cambió a un transporte hacia el este, en el Eoceno Tardio, como consecuencia de la colisión de la placa del Caribe con la plataforma de las Bahamas. El cambio en la dirección de transporte tectónico es evidenciado en el norte de Suramérica por una compresión noroeste-sureste y por el desarrollo de la cuencas sedimentarias Oligocenas "pull-apart" de rumbo e ste-oeste.

En el Oligoceno Tardio se inició el transporte tectónico del bloque de Maracaibo-Santa Marta, el cual continúa en la actualidad. El transporte tectónico del bloque fue incrementado en el Mioceno por la colisión del arco de Panamá-Costa Rica. El transporte tectónico del bloque de Maracaibo-Santa Marta está causanso la generación del cinturón deformado del sur del Caribe. El borde de placas al este del cinturón deformado del Caribe se ha caracterizado por una tectónica transcurrente dextral.

ABSTRACT

TECTONIC EVOLUTION OF THE SOUTH-CENTRAL CARIBBEAN BASED ON GEOCHEMICAL DATA

MARINO OSTOS ROSALES

Northern Venezuela consists of seven east-west trending tectonostratigraphic belts which are from north to south: Dutch and Venezuelan islands (DVI), Venezuelan platform, Cordillera de la Costa-Margarita terrane (CCMT), Cordillera de la Costa belt (CCB), Caucagua-El Tinaco belt (CTB), Paracotos belt (PB), and Villa de Cura belt (VCB). Geochemical, metamorphic, and structural data were collected in several transects through these belts.

Major- and trace-element abundances in mafic and felsic rocks were determined to find the tectonic affinity of these rocks. The Precambrian basement of the CCB appears to consist of within-plate granites. The Paleozoic basement of the CTB consists of MORB's, Andean-type tholeiites, and arc granites. The mafic rocks of Mesozoic age have variable affinities: the DVI, CCMT, and VCB are underlain by MORB's, but part of the VCB has volcanic arc affinity. All felsic rocks of Mesozoic age in the DVI and CCMT are arc granites. Several periods of metamorphism have occurred in Venezuela in Precambrian and Paleozoic time. An important metamorphic event occurred in the Cretaceous. The CCMT and VCB underwent high P/low T metamorphism and subsequently low to intermediate P/T metamorphism. These events may be related to subduction and subsequent uplift, respectively. The CCB underwent an intermediate P/T metamorphism, because it probably has never been burried as deeply. The PB underwent very low-grade metamorphism possibly related to the obduction of ophiolitic thrust sheets.

Four generations of folds and three generations of faults were recognized. The first two phases of folding occurred probably in the Permian and the last two during a Late Cretaceous-Tertiary orogeny. Kinematic indicators suggest that the entire system underwent dextral shear parallel to the belts during the Late Cretaceous-Tertiary. Based on the available geologic data, a plate tectonic model is proposed. In the model the east-west trending belts of northern South America are allochthonous and deformed as a result of collision of a microcontinent (Sebastopol block) with northwestern South America. The belts were initially coupled to the overriding South American plate, but because of the large obliquity of plate convergence were transported easterly since the Late Cretaceous.

ACKNOWLEDGMENTS

The work involved in this thesis was completed with the cooperation of several persons whom I wish to acknowledge. First I wish to thank Dr. Hans G. Avé Lallemant for his patience, conscious criticism, and guidance.

I thank Enrique Navarro, Franco Urbani, Franklin Yoris, and Daniel Loureiro for discussions over the past few years.

My thanks to my wife, my children, and my parents for their moral support.

I am indebted to the Universidad Central de Venezuela, the "Consejo Venezolano de Investigaciones Cientificas de Venezuela, CONICIT", the National Science Foundation (Grant EAR-8517383 to Dr. Hans G. Avé Lallemant), and "Petroleos de Venezuela, PDVSA" for financial support.

TABLE OF CONTENTS

page

page

CHAPTER IV

STRUCTURAL GEOLOGY

CHAPTER V

GEOCHEMISTRY AND TECTONIC SETTING OF IGNEOUS ROCKS OF NORTHERN VENEZUELA

page

page

CHAPTER VIII

TECTONIC MODELS

page

CHAPTER I

INTRODUCTION

Objectives

The Caribbean Mountains system in central Venezuela is part of an east-west trending fold and thrust belt which has formed during Cretaceous and Tertiary times. However, several rock units have an older history: they may have been involved in Paleozoic (Ouachita time) and Precambrian deformational events.

The Cretaceous and Tertiary history of northern Venezuela is clearly related to the interaction of the Caribbean lithospheric plate and the South American continent. Many plate tectonic reconstructions of the Caribbean and its borderland have been proposed: most older models have been reviewed in Bonini *et al.* (1984); more recent models are by Pindell *et al.* (1988) and Ross and Scotese (1988). Plate tectonic models for the Caribbean can be grouped into two groups: one in which the present Caribbean plate is the result of Jurassic-early Cretaceous spreading between North and South America (e.g. Maresch, 1974; Beets *et al.*, 1984) and the other in which the Caribbean plate was formed in the Pacific (Farallon plate) and migrated eastward, in between North and South America, during late Cretaceous and Tertiary time (e.g. Pindell *et al.*, 1988; Ross and Scotese, 1988). As will be shown later, these two groups of models have very different consequences for the interpretation of Venezuelan geology.

The present study deals with the structural geology, petrology, and geochemistry of rocks in Venezuela. Three north-south sections were made through the Caribbean Mountains system (See Chapter III). Strip maps were made along these sections and structural analysis was performed. Samples were collected for microscopic structural analysis, for petrographic studies, and for geochemical analysis. Several additional areas of geologic interest were visited to collect samples for laboratory studies. Additionally, well and seismic data from the Venezuelan continental platform were integrated in this study.

The main objective of the present study was to test the many plate tectonic models proposed in the past and to determine which model or models can best explain the geology of Venezuela. An important secondary objective was to determine the allochthoneity of the entire Caribbean Mountains system because it may constrain the reconstructions and tectonic

evolution of the foreland basins, south of the Caribbean Mountains; basins which have been proven to be quite petroliferous.

Before discussing the field areas (Chapter III), the structural geology (Chapter IV), the geochemical results (Chapter V), the metamorphism (Chapter VI), and the age determinations (Chapter VII), it is necessary first to give an overview of the Caribbean geology and secondly, the important features of the regional geology of the southern Caribbean margin in Venezuela (Chapter II).

Overview of the Caribbean Plate

Geographically, the Caribbean Sea and the Caribbean lithospheric plate cover almost the same area. However, the boundaries of the first are well defined, whereas the boundaries of the second are somewhat problematic. The boundaries of the Caribbean lithospheric plate are in the west the west-facing volcanic arc and subduction zone of Central America (Panama-Costa Rica arc) and the North Panama deformed belt; to the north, the Motagua fault zone of Central America, Cayman trough, and Puerto Rico Trench; and in the east, the east-facing Lesser Antilles volcanic arc and subduction zone. The southern boundary is not well-defined and may in fact be a rather wide zone, locally perhaps as wide as 500 Km consisting of the South Caribbean deformed belt, the Dutch Leeward Antilles and Venezuelan Islands, the Venezuelan continental platform, and the Caribbean Mountains system of mainland Venezuela. Toward the west, in western Venezuela and Colombia, the boundary is even more problematic (Burke, 1988).

Most features of the Caribbean lithospheric plate have been reviewed in Bonini *et al. (1984)*. Here, only those features will be discussed that have direct relevance to the present study.

Caribbean Plate

Physiographically, the Caribbean plate is comprised mainly of three positive provinces (ridges, rises) and three negative provinces (basins). These provinces are from northwest to southeast: Nicaraguan rise, Colombian Basin, Beata Ridge, Venezuelan Basin, Aves Ridge, and Grenada Basin (Figure 1.1). Smaller terranes, described by Case *et al.* (1984), are not mentioned here, because they appear to be insignificant and rather poorly defined.

One characteristic of the Caribbean crust is that it is much

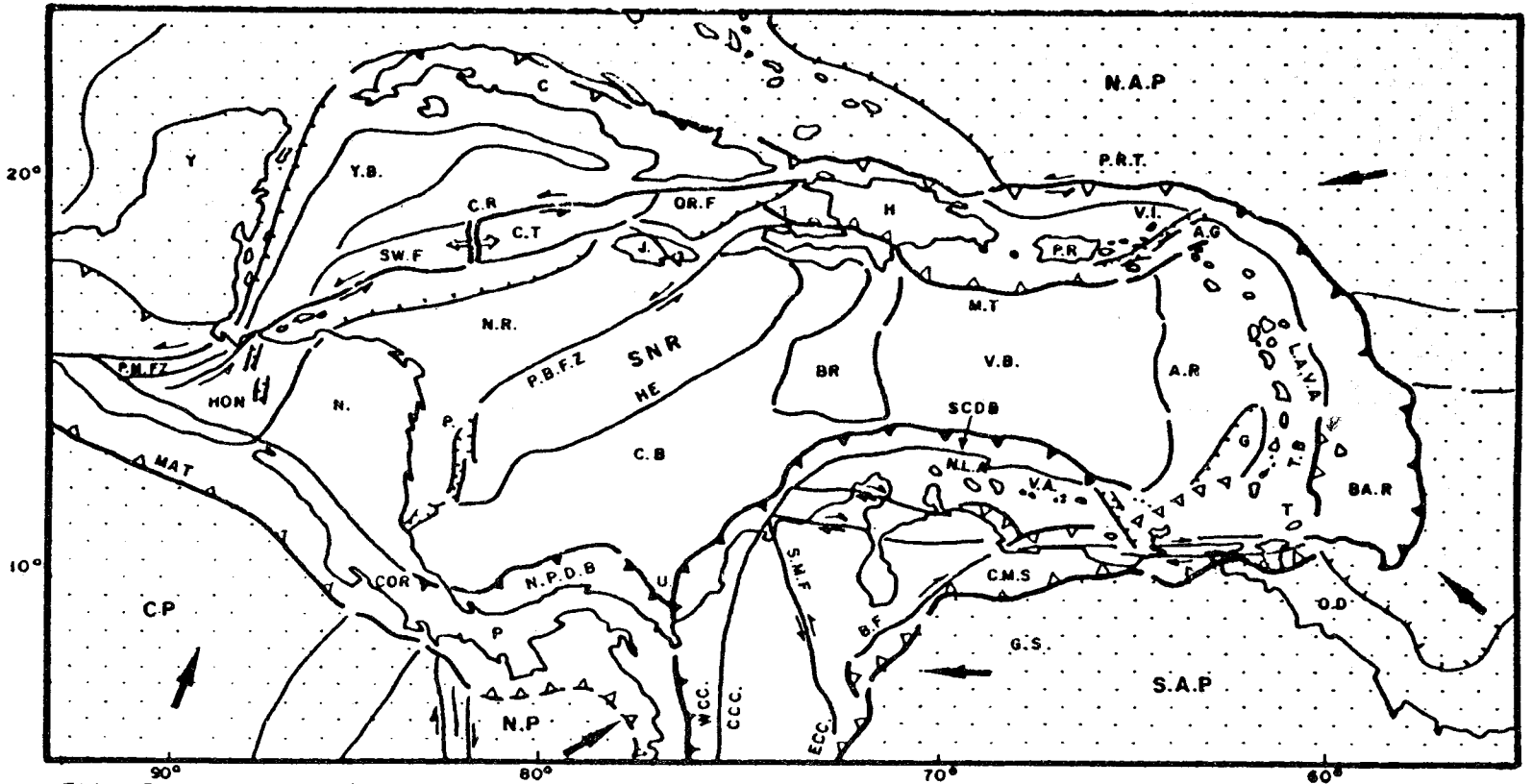

FIGURE I.1 : PHYSIOGRAPHIC MAP OF THE CARIBBEAN REGION (MODIFIED AFTER MASCLE *et al.*, 1985)

AG, Anegado GAP; AR, Aves Ridge; BR, Barbados Ridge; BF, Bocono Fault; BR, Beata Ridge; C, Cuba; CB, Colombian Basin; CCC, Central Colombian Cordillera; CMS, Caribbean Mountains System; COR, Costa Rica; CP, Cocos Plate; CR, Cayman Ridge; CT, Cayman Trought; ECC, Eastern Colombian Cordillera; G, Grenada Basin; GS, Guayana Shield; H, Hispaniola; HE, Hess Escarpment; J, Jamaica; L.A.V.A, Lesser Antilles Volcanic Arc; MAT, Middle America Trench; MT, Muertos Trench; N, Nicaragua; NAP, North American Plate; NLA, Netherlands Leeward Antilles; NP, Nazca Plate; N.P.D.B, North Panama Deformed Plate; NR, Nicaragua Rise; OD, Orinoco Delta; OR.F, Oriente Fault; PA, Panama; PBFZ, Pedro Bank Fault Zone; P.M.FZ, Polochi-Motagua Fault Zone; PR, Puerto Rico; PRT, Puerto Rico Trench; SAP, South American Plate; SCDB, South Caribbean Deformed Belt, SM.F Santa Martha Fault; SNR, Southern Nicaragua Rise; SWF, Swan Fault; T, Tobago; TB, Tobago Basin; U, Gulf of Urubo; VA, Venezuelan Antilles; VB, Venezuelan Basin; VI, Venezuelan Islands; WCC, Western Colombian Cordillera; Y, Yucatan Peninsula; YB, Yucatan Basin.

thicker than normal oceanic crust. It is 15 to 25 Km thick in the Colombian Basin, 10 to 20 Km in the Venezuelan Basin, and about 25 Km in the Grenada Basin (Case *et al.*, 1984). The crust has a thickness of 20 to more than 30 Km beneath the Nicaraguan rise, about 20 to 25 Km beneath the Beata Ridge, and 25 to 40 Km beneath the Aves Ridge (Case *et al.*, 1984). The anomalous thichness of the Caribbean crust has been related to intrusion of a thick basaltic sill in Cenomanian and earlier time; it is the so called B"-event on seismic reflection lines (Burke *et al.*, 1978). The ridges may be underlain by stretched continental or island arc crust.

The Nicaraguan rise is separated from the Colombian Basin by the northeast trending Hess escarpment (Figure 1.1). The rise has probably an oceanic to transitional crust (Edgar *et al.*, 1973). DSDP hole 152 in the Nicaraguan rise penetrated Campanian to Paleogene sediments and underlying basalt which is assumed to be the seismic horizont B" (Donnelly *et al.*, 1973; Case *et al.*, 1984). The Colombian Basin consists of an oceanic basement overlain by Campanian and younger sediments. Tholeiitic basalts intruded the oldest part of the sequences and the Campanian B" horizon can be followed across the basin to the Beata Ridge (Case *et al.*, 1984). The Colombian basin has a smooth ocean floor and it shows east trending lineations of crustal magnetism, which were tentatively interpreted (Christofferson, 1973, 1976; Watkins and Cavanaugh, 1976; Ghosh *et al.*, 1984) as having formed at a spreading center now located north or south of the present physiographic boundaries of the basin. The basin is being subducted since the Tertiary along its southwestern and southern margin beneath the North Panama and South Caribbean deformed belts, respectively (Biju-Duval *et al.*, 1978; Mascle *et al.*, 1985).

The Beata Ridge (Figure 1.1) is an uplift characterized by block-faults that trend northwest and northeast (Case *et al.*, 1984). DSDP holes have penetrated the A" horizon which consists of Eocene and older cherts and chalks (Donnelly *et al.*, 1973), the B" horizon, and Santonian, Paleogene, and Oligocene to Pleistocene deep sea marine and shallow water sediments (Edgar *et al.*, 1973; Fox and Heezen, 1975). The origin of the Beata Ridge was debated for some time; Case (1975) suggested that it was an island arc, a locus of a complex transform fault, or a block of continental crust.

However, it is now clear (Case *et al.*, 1984) that it consists of the typical Caribbean crust, deformed during the late Cretaceous-Paleogene; it is being subducted southward beneath the South Caribbean deformed belt.

The Venezuelan Basin (Figure 1.1) is by far the best known physiographic feature in the Caribbean Sea. Its stratigraphy and structure have been defined by extensive seismic surveys and several DSDP holes. The basin consists of Jurassic (?) to pre-Campanian oceanic crust (Ghosh *et al.*, 1984) of anomalous thickness, the top of which coincides with the Campanian B" reflector and overlying Campanian and younger tholeiite basalts and pelagic sediment (Saunders *et al.*, 1973; Biju-Duval *et al.*, 1978; Biju-Duval *et al.*, 1983). The basement varies from place to place; typical oceanic basement was identified by Ghosh *et al.* (1984) in the southeastern corner of the basin, where the B" reflector has an irregular appearance and the crust has a near normal thickness. Ghosh *et al.* (1984) compiled all existing magnetic data and demonstrated the presence of extensive northeast-southwest trending linear anomalies over the Venezuelan Basin, which they interpreted as having formed by seafloor spreading between 153 and 127 Ma; however, these anomalies may be related to topographic features only (Donnelly, 1989). Since the Neogene, the Venezuela Basin has been subducted under the Curacao ridge due to the component of convergence between South America and the Caribbean (Mascle *et al.*, 1979; Biju-Duval *et al.*, 1983 and Ladd *et al.*, 1984). The Aves Ridge (Fig. 1.1 and 1.2) is a north trending horstlike uplift. It consists of basalts, andesites, and late Cretaceous to Paleogene calcalkaline granodiorite intrusions (Fox and Heezen, 1975; Donnelly and Rogers, 1978), overlain by Tertiary pelagic sediments (Case *et al.*, 1984). The ridge is interpreted as a relict of an extinct island arc which was active during the late Cretaceous-Paleocene (Pinet *et al.*, 1985).

The Grenada Basin (Fig. 1.1 and 1.2) lying between the Aves Ridge and the Lesser Antilles volcanic arc, is floored by an anomalously thick oceanic crust of unknown age (Westbrook, 1975; Case *et al.*, 1984; Pinet *et al.*, 1985). The basin contains in the southern part up to 6 Km of Tertiary pelagic and volcaniclastic flysch-like sediments. The Grenada Basin is interpreted as a back arc basin with respect to the Lesser Antilles volcanic arc (Biju-Duval *et al.*, 1978; Pinet *et al.*, 1985). Speed (1985) proposed an alternative model in which the Grenada basin was a former subduction zone related to the Aves arc, and the Lesser Antilles volcanic arc was related to a subduction-zone jump.

Northern Caribbean Plate Boundary

Before the end of the Cretaceous (Pindell *et al.*, 1988) the northern boundary of the Caribbean plate consisted of the active volcanic island arc of the Greater Antilles. After the collision of this arc with the Bahama Banks (Duncan and

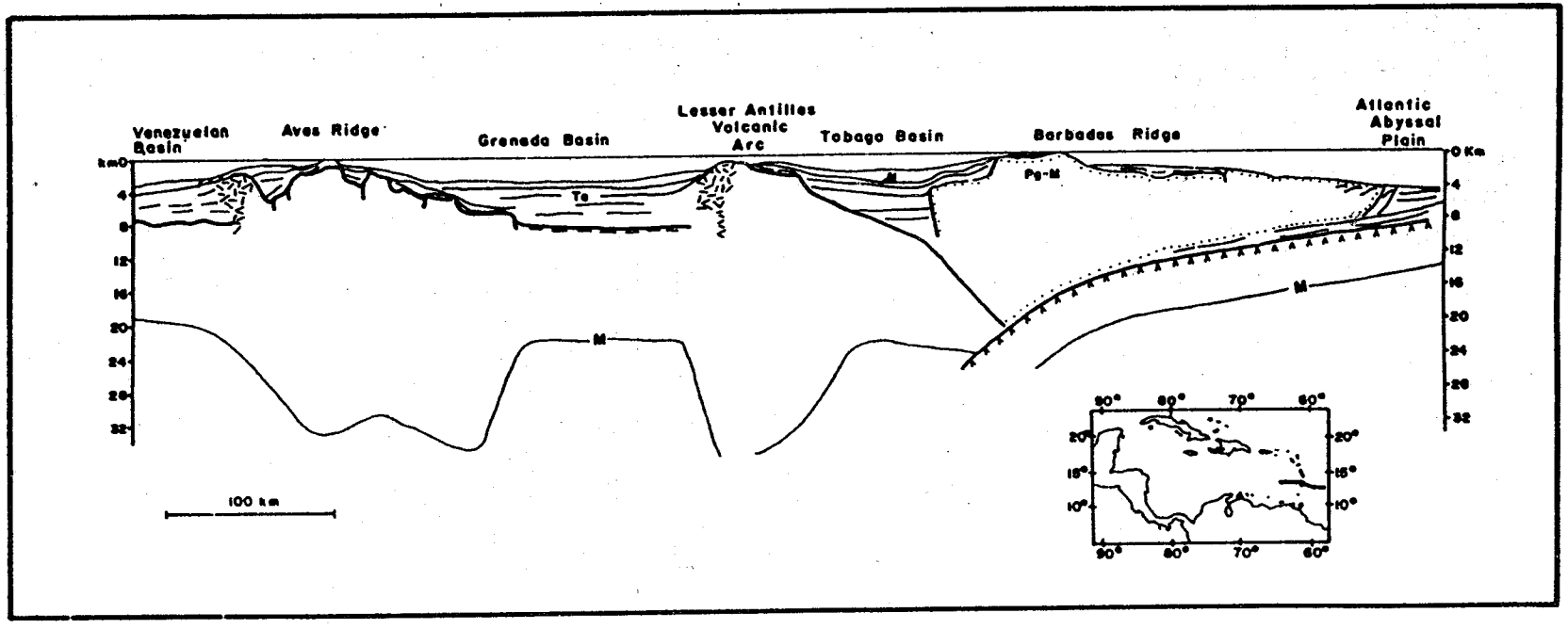

FIGURE 1.2: SCHEMATIC GEOLOGIC SECTION ACROSS THE LESSER ANTILLES VOLCANIC ARC. FROM MASCLE *et al.* (1985)

Hargraves, 1984; Burke *et al.*, 1984) a new boundary developed which is similar to the present one. The present boundary follows the Motagua fault in Central America, the Cayman trough, and the Puerto Rico Trench (Figure 1.1).

The Motagua fault zone in Guatemala has been shown to be a left-lateral strike-slip fault on the basis of focal mechanism solutions (Langer and Bollinger, 1979). The Motagua fault can be correlated with the Swan fracture zone, the southern border of the Cayman trough. Both the Swan and the Oriente fracture zones, the latter is the northern limit of the Cayman trough, are also left-lateral fault zones as indicated by earthquakes focal mechanism solutions (Molnar and Sykes, 1969; Sykes *et al.*, 1982).

There is ample evidence that seafloor spreading in the Cayman trough has occurred from the Eocene to the present. The magnetic anomaly inversions (MacDonald and Holcombe, 1978) are indicative of various rates of opening across the mid-Cayman spreading center of 2.0 $\pm$ 0.2 cm/yr for the interval 0 to 2.4 Ma and 4.0 $\pm$ 0.2 cm/yr from 2.4 to 6.0 Ma and perhaps to 8.3 Ma. The young age of the seafloor spreading history in the Cayman trough is in agreement with the high values of heat flow in the western part (2.07 HFU); the highest values tend to occur in the deepest part of the trench, while elsewhere in the trench and in the Yucatan basin to the north values range from 1 to 2 HFU (Epp *et al.*, 1970; Erickson *et al.*, 1972).

If the displacement rate of the Caribbean plate for the last 6 or 8 Ma is extrapolated to the Eocene (37 Ma), the Caribbean plate was 1400 Km west of its present position with respect to North America and the estimated displacement is just enough to close the Cayman trough and to align the margin of Yucatan with that of the Nicaraguan rise (Sykes *et al.*, 1982).

The Lesser Antilles Volcanic Arc

The eastern boundary of the Caribbean plate (Figure 1.1) is the Lesser Antilles volcanic arc. The arc is built on oceanic crust and resulted from underthrusting of the Atlantic oceanic plate beneath the Caribbean plate (Figure 1.2). The main activity of the arc started in the Miocene although the arc may have been built up on an Upper Cretaceous Paleogene arc (Pindell *et al.*, 1988). The Benioff zone is well established and reaches a depth of 200 Km (Tomblin, 1975 and Sykes *et al.*, 1982). Focal mechanism solutions indicate underthrusting of the Atlantic plate. Hinge areas, such as near Hispaniola and Trinidad are characterized by reverse faulting along gently dipping fault

planes oblique to the east-west strike-slip fault zones (Molnar and Sykes, 1969; Mann and Burke, 1984). No topographic trench has formed because of the great influx of sediments carried northward by the Orinoco River. The only deep marine trough is the Puerto Rico Trench, where little sediment influx occurs.

The Barbados accreationary prism consists of volcanogenic and silicic hemipelagic sediments and radiolarites and of melange derived from these lithologies (Torrini, *et al.*, 1985). The Barbados prism (Figure 1.1) is better developed to the south in the proximity of the South American plate (Westbrook, 1975; Mascle *et al.*, 1977). The Tobago Basin (Fig. 1.1 and 1.2), east of the Lesser Antilles volcanic arc is a forearc basin (Mascle *et al.*, 1977). The Grenada Basin is a large back-arc basin (Figure 1.2) with the sediments reaching a maximum thickness close to the Lesser Antilles volcanic arc.

Panama-Costa Rica Arc

The western boundary of the Caribbean plate is the Panama-Costa Rica arc. This boundary is somewhat more complicated than the eastern one. The arc consists mostly of Tertiary and Quaternary volcanics (Case *et al.*, 1984) but it may included older (upper Cretaceous) volcanics (Pindell *et al.*, 1988). The island arc is west facing. However, a poorly defined band of intraplate earthquakes extends along the east coast of Central America (Sykes and Ewing, 1965; Molnar and Sykes, 1969; Kafka and Weidner, 1981; Sykes *et al.*, 1982; Mann and Burke, 1984), which together with the North Panama deformed belt may indicate underthrusting of the Caribbean plate underneath the Panama-Costa Rica arc (Case *et al.*, 1984).

The Panama-Costa Rica arc was formed in the eastern Pacific in Late Cretaceous time and migrated northeastward. It collided with South America (northwest corner of Colombia) during Miocene time (Pindell *et al.*, 1988; Restrepo and Toussaint, 1988).

Southern Caribbean Plate Boundary

The boundary between the Caribbean and South American plates is not well-constrained. As mentioned before, this boundary may not be a single fault plane, but a fault zone up to 500 Km wide (Robertson and Burke, 1989). This fault zone can be divided into the following east-west trending belts from north to south: South Caribbean deformed belt, Dutch Leeward and Venezuelan islands terrane, and the Caribbean Mountains system which probably overlies the Guayana Shield with a

tectonic contact. The contact between the Dutch Leeward and Venezuelan islands terrane and the Caribbean Mountains system is complicated by the occurrence of several young sedimentary basins, probably pull-apart basins related to strike-slip faulting (Case *et al.*, 1984).

The South Caribbean deformed belt and its eastward extension, the Curacao Ridge, is a zone in which Cretaceous and Tertiary sediments are moderately deformed (Figure 1.3) as a consequence of late Miocene and younger convergence of the Caribbean and South American plates (Ladd *et al.*, 1984). The deformed belt extends from the Rancherias Basin north of Colombia to the Los Roques Trough in the east. The Caribbean oceanic crust extends southward beneath the South Caribbean deformed belt and southward-dipping reflections have been recognized within the deformed belt (Figure 1.3), indicating that probably slices of the oceanic Caribbean crust were incorporated in the belt (Mascle *et al.*, 1979; Ladd *et al.*, 1984). East of the Los Roques Trough nothing comparable to the South Caribbean deformed belt (Figure 1.4) occurs (Chevalier, 1987). Such belt did not develop; instead a major right-lateral strike-slip boundary has been recognized between the Caribbean plate and northeastern South America (Figure 1.4).

The Dutch Leeward and Venezuelan islands terrane is a disrupted chain of blocks consisting of lower to middle Cretaceous oceanic rocks and Upper Cretaceous volcanics of island arc affinity. The Venezuelan islands (Los Roques, la Blanquilla, Los Hermanos, Los Testigos, and Margarita Island) may be the easterly extension of this arc. It has been proposed that this arc was south facing and formed by convergence of the Caribbean and South American plates (Talukdar and Loureiro, 1982; Beets *et al.*, 1984; Beck, 1985). An alternative model is that it is related to the Aves/Lesser Antilles arc, but that it was disrupted by shearing along the Caribbean/South American boundary zone (Pindell and Barret, 1989). The Caribbean Mountains system on the Venezuela mainland (Figure 1.1) is a late Cretaceous-Tertiary megasuture, consisting of a Paleozoic to Precambrian basement and overlying metamorphic Mesozoic sequences. Note that Mascle *et al.* (1979) suggested that the Caribbean Mountains system was thrust southward onto the Guayana shield; in chapter VIII dealing with Plate Tectonics, an alternative model is proposed.

Whereas the Mesozoic/Paleogene boundary between the Caribbean and South American plates is rather obscure, even the Neogene/Quaternary boundary is problematic. It is clear that many east-west trending faults occur which have been proved to be dextral. In the eastern part of Venezuela

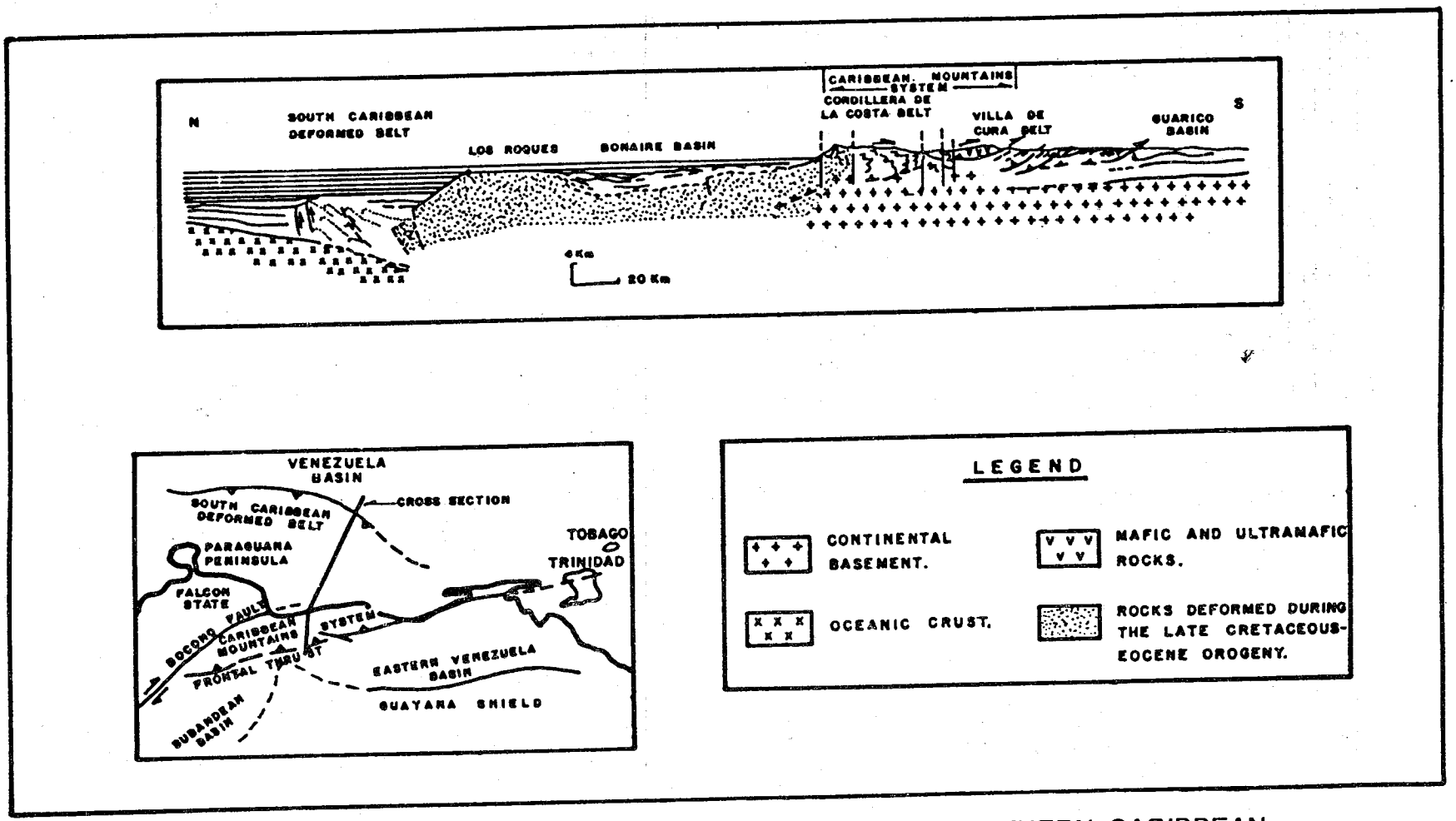

FIGURE 1.3: SCHEMATIC CROSS SECTION OF THE SOUTHERN CARIBBEAN PLATE BOUNDARY THROUGH THE SOUTH CARIBBEAN DEFORMED BELT (FROM MASCLE et al., 1979).

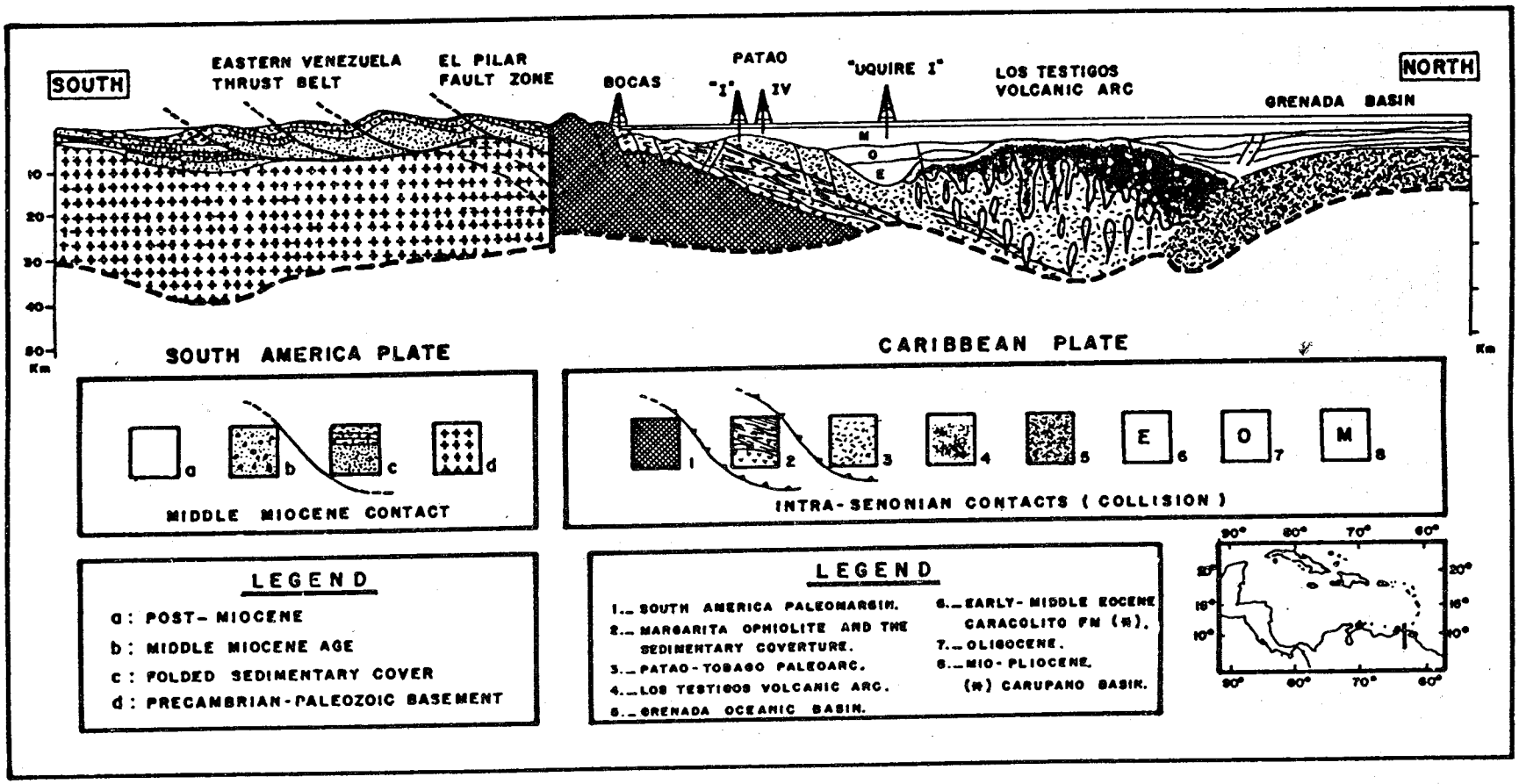

FIGURE 1.4: SCHEMATIC CROSS SECTION OF THE SOUTHERN CARIBBEAN PLATE BOUNDARY THROUGH THE ARAYA-PARIA PENINSULA (FROM CHEVALIER, 1987).

several northwest-southeast trending dextral faults (Figure 1.5) are thought to be related to the east-west faults. In western Venezuela and Colombia east-west trending dextral strike-slip faults are complicated by several sets of northwest and northeast trending strike-slip faults which may be unrelated to the interaction of the Caribbean and South America plates, but rather to the Miocene collision of the Panama-Costa Rica arc with South America (Pennington, 1981; Mann and Burke, 1984).

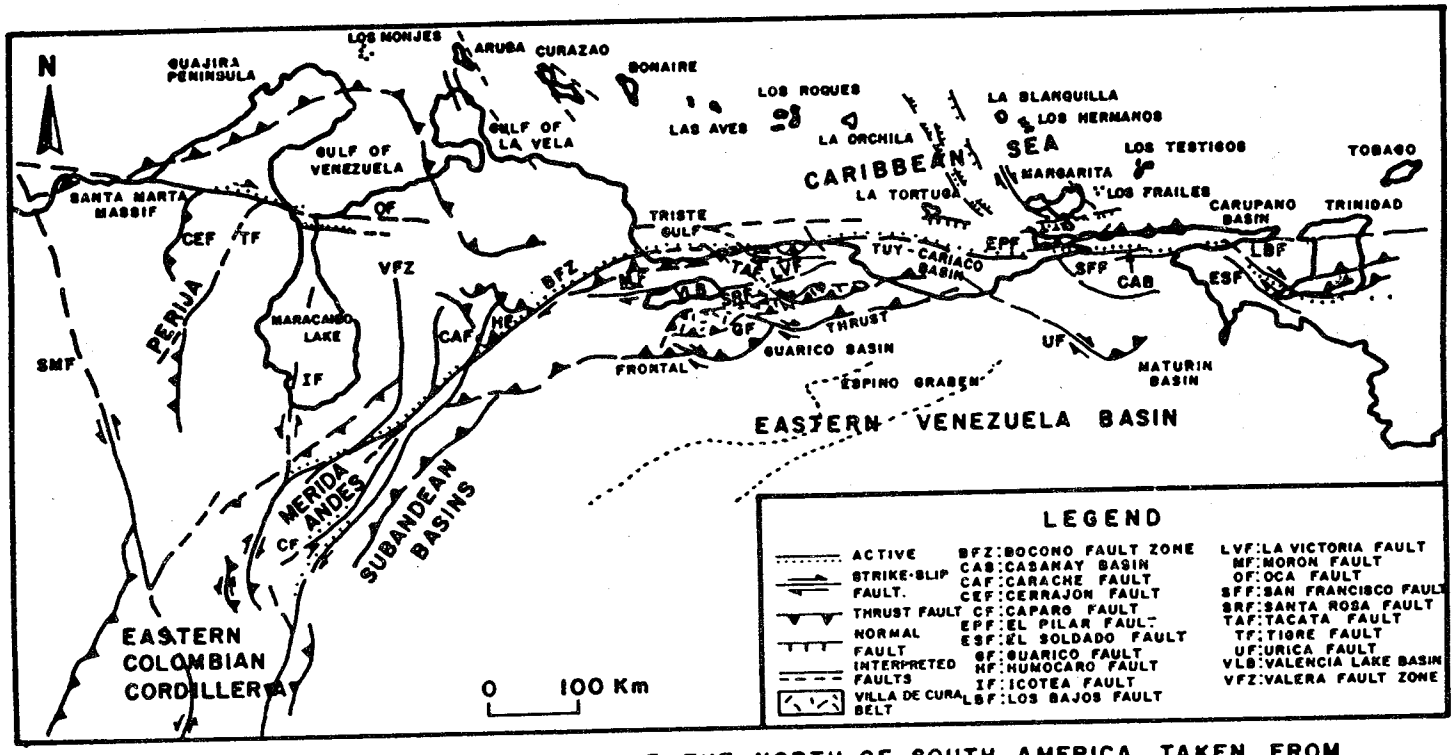

FIGURE 1.5: MAJOR TECTONIC FEATURES OF THE NORTH OF SOUTH AMERICA, TAKEN FROM BECK (1985), KELLOGG (1984), SCHUBERT (1984), AND SOULAS (1985).

CHAPTER II

GEOLOGY OF NORTHERN SOUTH AMERICA

Introduction

In this chapter, the regional geology of northern Venezuela, of some adjacent areas in Colombia, of the Dutch Leeward and Venezuela islands, and the area between the islands and the mainland, will be discussed. All the areas on the mainland are included in the Caribbean Mountains system. The Caribbean Mountains System will be divided here in three regions: a central, an eastern, and a western region. Also included here, is a short discussion of the Andean terranes and the Guayana shield.

The Dutch Leeward and Venezuelan Antilles

The Dutch Leeward and Venezuelan Antilles from west to east are Los Monjes, Aruba, Curacao, Bonaire, Los Roques, La Orchila, La Blanquilla, Los Hermanos, Los Frailes, and Los Testigos (Figure 1.5). Maresch (1974), Beets *et al.* (1984) and Bellizia (1985) correlate the lithologic units of the Dutch Leeward islands with the Villa de Cura belt in the mainland. Beets *et al.* (1984) postulated that the volcanic arc complex exposed in the Dutch Leeward islands collided with the South American plate during the Coniacian.

Los Monjes Archipelago

The Los Monjes Archipelago is the westernmost Venezuelan island group. It is located east of the Peninsula of la Goajira (Figure 1.5). It consists of nine small islands. Bellizia *et al.* (1969) and Bellizia (1972) described a complex of metagabbro and metabasalt metamorphosed in the greenschist facies, which were intruded by hornblende-quartz gabbros. Santamaria and Schubert (1974) determined a K/Ar age of 116 $\pm$ 13 Ma on amphibole from an orthoamphibolite and a K/Ar whole rock age of 114 $\pm$ 12 Ma for the same sample (See Chapter VIII).

Aruba

Aruba is underlain by a Upper Cretaceous igneous-metamorphic complex metamorphosed in the zeolite and prehnite-pumpellyite facies, overlain by Eocene and Neogene-Quaternary limestones (Helmers and Beets, 1977). The Cretaceous rocks consist of basalts and volcaniclastics (Beets *et al.*, 1984) in which ammonites of Turonian age have

been found (MacDonald, 1968). The major- and trace-element abundances of the mafic rocks are indicative of a mid-oceanic tectonic setting (Beets *et al.*, 1984). The volcanic-sedimentary unit was intruded by granitic to gabbroic batholiths (Helmers and Beets, 1977) of calc-alkaline affinity (Beets *et al.*, 1984). These rocks have K/Ar and Rb/Sr ages of 67 to 90 Ma (Priem *et al.*, 1966; Santamaria and Schubert, 1974; Beets *et al.*, 1984).

Curacao

Curacao consists of a volcanic basement underlying Upper Senonian and Danian flysch and limestones of Eocene and Neogene-Quaternary age (Beets, 1977). The volcanic basement consists of basalts of mid-oceanic ridge basalt (MORB) affinity (Beets *et al.*, 1984), chert, and limestone in which Albian ammonites have been found (Beets, 1977; Beets *et al.*, 1977). The basement is regionally metamorphosed in the zeolite and prehnite-pumpellyite facies (Beets, 1972; Beets, 1977; Beets *et al.*, 1984).

Bonaire

Bonaire is underlain by a volcanic basement overlain by Senonian-Paleocene, Eocene, and Neogene-Quaternary sediments (Beets, 1972; Beets *et al.*, 1984). The basement consists of basalts of primitive island arc affinity (PIA) and volcaniclastic sediments of Albian to Coniacian age (Beets *et al.*, 1984). It is metamorphosed in the zeolite and prehnite-pumpellyite facies (Beets, 1972; Beets *et al.*, 1984). Until the latest Maastrichtian the sediments are enterily volcaniclastic, but in the Paleocene-Eocene, continental derived detritus have been observed (Beets *et al.*, 1977; Beets *et al.*, 1984).

Los Roques Archipelago

Los Roques Archipelago is underlain by metadiabase, metagabbro, and metasediment, metamorphosed in the greenschist facies. They are intruded by silicic plutonic rocks (Schubert and Motiscka, 1972). The meta-igneous rocks have tholeiitic affinity and have Neocomian K/Ar ages, and the intrusives have calc-alkaline affinity and are of Maastrichtian age (Santamaria and Schubert, 1974).

La Orchila

La Orchila has igneous-metamorphic basement, which underlies Quaternary reefs and alluvial deposits (Gonzalez de Juana *et al.*, 1980). The basal complex consists of chlorite phyllite and schist, metadiabase, orthoamphibolite, mica gneiss,

hornblende-garnet gneiss, epidote schist, granite, granodiorite, aplite, and epidosite (Schubert and Motiscka, 1972). Two metamorphic events may have occurred, the first pre-intrusion event is an amphibolite facies event and the second is a greenschist facies event (Schubert and Moticska, 1972). No radiometric ages have been acquired.

La Blanquilla

La Blanquilla is underlain by trondhjemites, tonalites, and quartz diorites (Schubert and Moticska, 1973) of Maastrichtian to Paleocene age (Santamaria and Schubert,1974). They have calc-alkaline affinity (Santamaria and Schubert, 1974).

Los Hermanos Archipelago

Los Hermanos Archipelago consists of hornblende tonalite gneiss, pegmatite, amphibolite, epidosite, and biotite-epidote gneiss and schist, which were metamorphosed in the greenschist and epidote amphibolite facies (Schubert and Moticska, 1973). The gneiss is of Campanian to Paleocene age (K/Ar, hornblende; Santamaria and Schubert, 1974). It has calc-alkaline affinity (Santamaria and Schubert, 1974).

Los Frailes Archipelago

Los Frailes Archipelago consists of unmetamorphosed basic volcanic and intrusive rocks (Moticska, 1972; Chevalier, 1987). Santamaria and Schubert (1974) determined a whole rock K/Ar age of 66 $\pm$ 5.1 Ma for a metadiabase. Based on major- and trace-element abundances, the igneous complex has a calc-alkaline affinity (Santamaria and Schubert, 1974).

Los Testigos Archipelago

Schubert and Motiscka (1973) mapped in the Los Testigos Archipelago a basal complex consisting of mafic rocks intruded by granitic plutons. The complex was later intruded by mafic and leucocratic dikes and metamorphosed to a very low metamorphic grade. The younger intrusives yielded Eocene ages and they have calc-alkaline affinity (Santamaria and Schubert, 1974).

Venezuelan Platform

Extensive geological and geophysical research have been carried out on the Venezuelan platform by the oil industry. The best studied areas are from west to east Gulf of La Vela, Gulf Triste, Tuy-Cariaco basin, and North Paria (Carupano) basin (Figure 1.5).

Gulf of La Vela

The deepest wells in the Gulf of La Vela penetrated the basement which consists of metasediments and metaigneous rocks metamorphosed in the greenschist facies (Kiser *et al.*, 1984). Gonzàlez de Juana *et al.* (1980) and Kiser *et al.* (1984) published K/Ar ages of 83.5 Ma and 114 Ma for a quartz phyllite and a metagabbro, respectively. The basement underlies uncomformably lower Miocene sediments (Kiser *et al.*, 1984).

Gulf Triste

Several exploratory wells were drilled by the Venezuelan oil industry in the Gulf Triste. The deepest wells reached flysch sediments metamorphosed to a very low grade, which contain pelagic foraminifera of probable Early Eocene age and underly unconformably continental red beds of Eocene (?) age and/or upper Oligocene-lower Miocene shallow water deposits (Gonzàlez de Juana *et al.*, 1980; Kiser *et al.*, 1984). The Gulf Triste may be the easterly extension of the Falcon basin. It is part of the Bonaire block, which includes the Falcon and Bonaire basins that are thought to be Oligocene pull-apart basins (Muessig, 1984)

Tuy-Cariaco Basin

The Tuy-Cariaco basin is located south of the Island of La Tortuga and it includes the Cariaco Basin and the platform to the south (Figure 1.5). The Venezuelan oil industry drilled twelve exploration wells in the basin. A large amount of seismic and geochemical data are available (Talukdar and Bolivar, 1982; Bellizia, 1985). The basement consists of volcanic and subvolcanic andesites, which were metamorphosed in the prehnite-pumpellyite facies and amphibolites, mica schists, quartzites, and sheared serpentinized hornblende pyroxenite (Talukdar and Bolivar, 1982). The volcanic complex is correlated with the Villa de Cura Group and three K/Ar whole rock age determinations of 65.4 Ma, 69.5 Ma, and 78.3 $\pm$ 3.9 Ma were obtained from volcanic samples (Talukdar and Bolivar, 1982). Overlying the volcanic complex is a metasedimentary and metaigneous complex which can be correlated with the Juan Griego Group on Margarita Island (Talukdar and Bolivar, 1982; Bellizia, 1985). The basement is locally overlain unconformably by Eocene flysch-type sediments and Oligocene carbonates (Talukdar and Bolivar, 1982). Shallow water Miocene sediments are widely distributed unconformably overlying the basement, the Eocene or the Oligocene sediments (Talukdar and Bolivar, 1982).

The Carupano Basin

The Carupano basin, also known as the North Paria basin (Figure 1.5), was the focus of oil exploration by the Venezuelan oil industry and some of the geologic, seismic, and geochemical data are included in the report of Talukdar (1983) and in papers by Castro and Mederos (1985) and Pereira (1985). The oldest basement recognized in the Carupano basin consists of a sequence of basalts and quartz wackes of low metamorphic grade of the high P/low T type (Talukdar, 1983). This sequence contains Barremian to Santonian planktonic foraminifera (Castro and Mederos, 1985). The basalts have a mid-oceanic ridge affinity (Talukdar, 1983).

Locally, the basement is overlain unconformably by a Upper Cretaceous sedimentary sequence, which consists of calcareous sublitarenites, lithic arenites, and cherts. Talukdar (1983) indicates that the source of the sandstones may have been a recycled orogen on the basis of heavy minerals and the parameters of Dickinson (1970).

The wells, north of the basin, penetrated a younger basement, which consists of unmetamorphosed dark pelagic shales, sandstones, cherts, basaltic breccias, and massive basalts. The basalts were dated (whole rock K/Ar) at 87 $\pm$ 9 Ma and 102.2 $\pm$ 10 Ma (Talukdar, 1983). They have primitive island arc affinity (Talukdar 1983). The sandstones have a volcanic arc provenance (Talukdar, 1983). Near Los Testigos Island, the basement is young and consists of unmetamorphosed basaltic andesites probably related to a mature island arc (Talukdar, 1983) which is also exposed in Los Testigos island. Two K/Ar whole rock age determinations on the basalts yielded 38.6 $\pm$ 2 Ma and 33.5 $\pm$ 1.8 Ma (Talukdar, 1983). Detrital grains and heavy minerals of the locally distributed Eocene-Oligocene sandstones may have mainly a recycled orogen provenance with a minor input from a magmatic arc. The widely distributed Miocene-Quaternary sandstones have mainly a recycled orogen provenance (Talukdar, 1983).

Central Caribbean Mountains System

The "Caribbean Research Project" of Princeton University was the first systematic geologic study of the Caribbean Mountains system (Hess and Maxwell, 1949, 1953; Menendez, 1966; Bell, 1968; Maresch, 1973, 1974). Menendez (1966) divided the Caribbean Mountains system into four tectonic belts each with characteristic structural, petrologic, and geochronological features (Figure 2.1). These belts are from

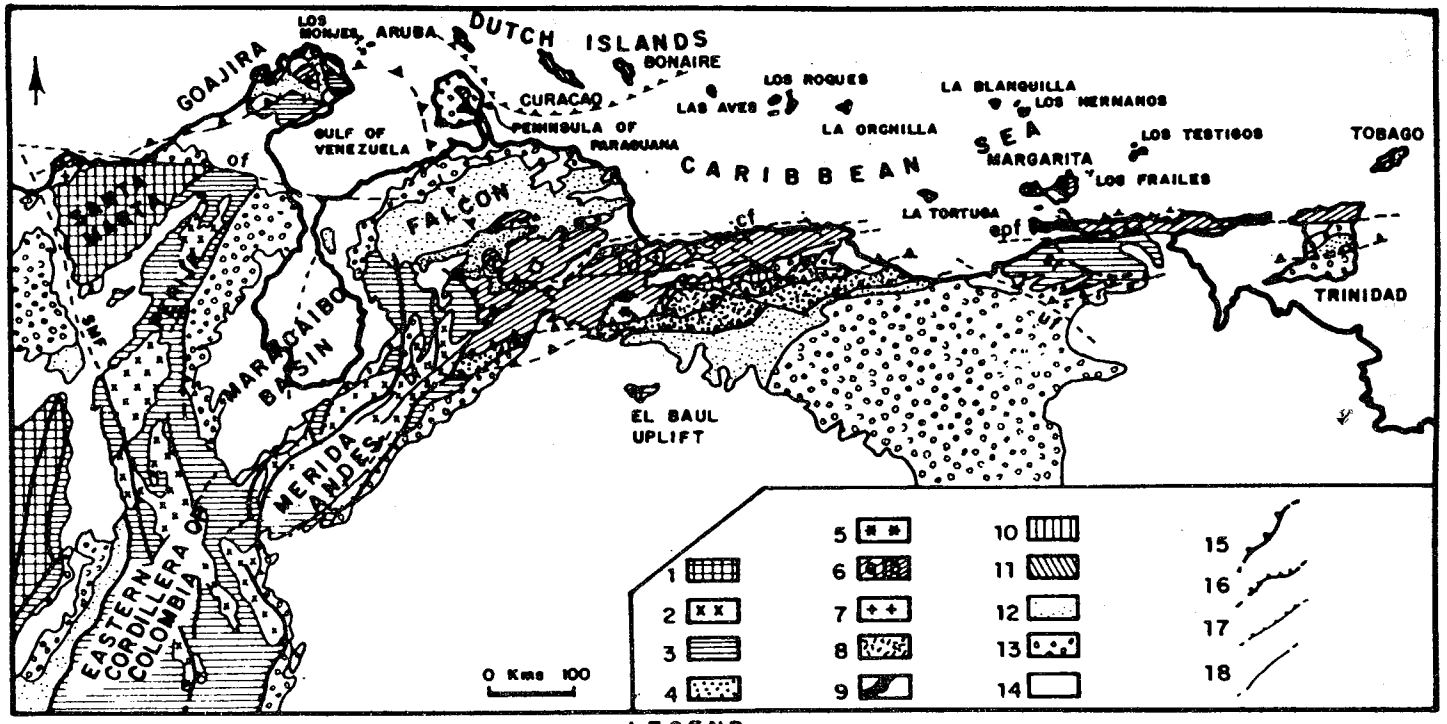

LEGEND

ANDEAN CORDILLERA AND GUAYANA PLATFORM

1. PRECAMBRIAN - PALEOZOIC BASEMENT INTRUDED BY JURASSIC, CRETACEOUS AND EOCENE GRANITES (CENTRAL COLOMBIAN CORDILLERA AND SANTA MARTA MASSIF)..
2. PRECAMBRIAN - PALEOZOIC BASEMENT IN THE EASTERN COLOMBIAN CORDILLERA, PERIJA RANGE, AND MERIDA ANDES..
3. MESOZOIC - CENOZOIC SEDIMENTARY COVER..

CARIBBEAN MOUNTAINS SYSTEM

4. PALEOCENE FLYSCH..
5. TINACO - TINAQUILLO NAPPE AND THE YUMARE COMPLEX..
6a. METAMORPHOSED JURASSIC AND CRETACEOUS (CORDILLERA DE LA COSTA BELT S.S)..
6b. ECLOGITES, BLUESCHIST, AND ULTRAMAFIC (CORDILLERA DE LA COSTA - MARGARITA BELT)
7. LATE CRETACEOUS FELSIC INTRUSIONS (CORDILLERA DE LA COSTA BELT AND THE NETHERLANDS LEEWARD AND VENEZUELAN ISLANDS..
8. METAMORPHOSED MAFIC ROCKS (VILLA DE CURA BELT AND TOBAGO ISLAND)..
9. OPHIOLITES AND ULTRAMAFIC COMPLEX..
10. LOMA DE HIERRO OPHIOLITE (SENONIAN)..

DUTCH ISLAND

11. CRETACEOUS VOLCANICS AND SEDIMENTS (VERY LOW METAMORPHIC GRADE OR UNMETAMORPHOSED..

SEQUENCES YOUNGER THAN MIDDLE EOCENE

12. OLIGO - MIOCENE..
13. MIO - PLIOCENE..
14. QUATERNARY..

MAJOR TECTONIC FEATURES

15. THRUSTING YOUNGER THAN MIDDLE EOCENE..
16. THRUSTING OLDER THAN MIDDLE EOCENE..
17. SMALL THRUST FAULT..
18. VERTICAL FAULT (MAYBE STRIKE - SLIP)
bf, BOCONO FAULT; cf, CARIBBE FAULT; epf, EL PILAR FAULT; lvf, LA VICTORIA FAULT; of, OCA FAULT; sf, SAN FRANCISCO FAULT; smf, SANTA MARTA FAULT; uf, URICA FAULT..

FIGURE 2.1 : GEOLOGIC MAP OF THE CARIBBEAN MOUNTAINS SYSTEM AND THE NORTHERN ANDEAN CORDILLERA (AFTER STEPHAN et al, 1980)

north to south; 1.- Cordillera de la Costa, 2.- Caucagua-El Tinaco, 3.- Paracotos, and 4.- Villa de Cura belts. Three majors faults trending east-west, separating the four belts are from north to south: 1.- La Victoria, 2.- Santa Rosa, and 3.- Agua Fria faults.

Cordillera de la Costa Belt

The Cordillera de la Costa belt is bound to the north by the San Sebastian right-lateral strike-slip fault and to the south by the right-lateral La Victoria fault zone (Menendez, 1966). This terrane consists of a Precambrian granitic basement and Mesozoic metasedimentary cover (Gonzalez de Juana *et al.*, 1980). During the Mesozoic this terrane resided in a passive Atlantic-type margin, upon which thick sediments of the Caracas Group were deposited (Dengo, 1951; Bellizia, 1972; Maresch, 1974; Talukdar and Loureiro, 1982; Beck, 1985). Stephan *et al.* (1980) and Stephan (1985) divided the Cordillera de la Costa belt into the Cordillera de la Costa s. s. and the Cordillera de la Costa-Margarita terrane or the Coastal Fringe-Margarita terrane (Figure 2.1). The latter consists of high P/low T metamorphosed mafic rocks exposed in the northernmost part of the belt (Tacagua, Antimano, Aroa, and Nirgua formations in the central Caribbean Mountains system), in the Peninsula of la Goajira, in the Peninsula of Araya (Copey and Laguna Chica formations), and on Margarita Island (La Rinconada and Los Robles groups).

Aguerrevere and Zuloaga (1938), Dengo (1951), Menendez (1966), and Wehrmann (1972) described in the central Cordillera de la Costa belt the following units: Sebastopol Complex, the Caracas Group (Peña de Mora Formation, Las Brisas Formation, Antimano Formation, and Las Mercedes Formation), and Tacagua Formation. Bellizia and Rodriguez (1976) recognized several other units in the Cordillera de la Costa belt, cropping out in the states of Carabobo, Cojedes, Yaracuy and Lara. These units are the Yaritagua Complex and the Aroa, Nirgua, and Mamey formations.

Sebastopol Complex

The Sebastopol Complex is the basement of the Caracas Group and it consists of granitic gneiss metamorphosed in the greenschist facies (Smith, 1952; Morgan, 1967, 1969; Wehrmann, 1972). A Precambrian-Paleozoic age has been proposed (Gonzalez de Juana *et al.*, 1980; Pimentel *et al.*, 1985). It has been correlated with the Tinaco Complex (basement of the Caucagua-El Tinaco belt; Wehemann, 1972).

Caracas Group

The Caracas Group is divided into four formations which are from bottom to top and presumably from old to young: Peña de Mora, Las Brisas, Antimano, and Las Mercedes formations (Aguerrevere and Zuloaga, 1938; Dengo, 1951; Wehrmann, 1972). The Peña de Mora Formation consists of quartz-feldspar augengneiss, biotite gneiss, quartz-muscovite schist, and minor amphibolite and marble (Wehrmann, 1972; Urbani and Quesada, 1972; Ostos, 1981). Wehrmann (1972) correlated the schists of the Peña de Mora Formation with the Las Brisas Formation. However, this is inconsistent with a Rb/Sr whole rock age of 220 $\pm$ 20 Ma (See below) determined by Kovach *et al.* (1977). The Las Brisas Formation consists of metasediments with rare amphibolite boudins, metamorphosed in the greenschist facies. The most common lithologies are: quartz-feldspar-mica schist and gneiss, quartz-sericite-graphite schist, quartz-mica-garnet schist, calcareous metaconglomerate containing microcline, quartz-muscovite-chlorite schist, and dark marble (Gonzalez de Juana *et al.*, 1980; Bellizia, 1985, Urbani and Ostos, 1987; Urbani *et al.*, 1987b; Urbani *et al.*, 1988). A Late Jurassic (Kimmeridgian) age has been proposed by Urbani (1969) and Diaz de Gamero (1969) based on *Exogyra virgula* (*DEFRANCE*) in the marbles.

The Antimano Formation consists of graphitic marble, calcareous graphitic schist, garnet amphibolite, epidote amphibolite, glaucophanite, and eclogitic amphibolite (Dengo, 1951; Wehrmann, 1972; Bellizia, 1985; Urbani and Ostos, 1987). The contacts of the Antimano Formation with the Las Brisas and Las Mercedes are concordant. A polymetamorphic history has been proposed for the mafic rocks of this unit: a first event at high P/low T (blueschist to eclogite facies) and a second intermediate P/T, in the greenschist facies (Talukdar and Loureiro, 1982) The Las Mercedes Formation consists of quartz-muscovite-calcite-graphite schist, calcareous-graphite phyllite, and graphite marble (Wehrmann, 1972; Urbani and Ostos, 1987; Urbani *et al.*, 1987b). An undifferentiated Mesozoic shallow water fauna has been recognized by MacKenzie (1966) in the State of Cojedes and by Spena *et al.* (1977) in the State of Miranda.

Tacagua Formation

The Tacagua Formation consists of sericite-epidote schist, calcareous quartz-graphite schist, amphibolite, actinolite-epidote schist, quartz-muscovite-graphite-chlorite schist, and garnet-epidote metaquartzite (Wehrmann, 1972; Ostos, 1981; Talukdar and Loureiro, 1982). The amphibolites show a

relict assemblage of an older high P/low T metamorphic event (blueschist to eclogite facies), which was overprinted by an intermediate P/T greenschist assemblage (Talukdar and Loureiro, 1982). A volcaniclastic protolith has been proposed for the Tacagua Formation (Dengo, 1951, 1953; Ostos, 1981; Talukdar and Loureiro, 1982; Urbani and Ostos, 1987). The contact with the other units of the Cordillera de la Costa belt has been interpreted by Talukdar and Loureiro (1982) as a thrust fault.

Caucagua-El Tinaco Belt

The Caucagua-El Tinaco belt (Figure 2.1) is bounded by a right-lateral strike-slip system (La Victoria fault zone) in the north and by the Santa Rosa fault in the south (Menendez, 1966; Schubert, 1984). However, Beck (1985) suggested that the belt is bounded in the north by a thrust fault located south of the La Victoria fault zone. The tectonic belt consists of a Paleozoic metamorphic basement (Tinaco Complex; Menendez, 1965) overlain by Permian metasediments (Benjamini *et al.*, 1987) interbedded with alkalic non-orogenic metavolcanics (Tucutunemo Formation; Beck, 1985b), and Cretaceous metasediments and metavolcanics (Konigsmark, 1958, 1965; Shagam, 1960; Menendez, 1965).

La Aguadita Gneiss

The Tinaco Complex consists of several units, but the only one of importance for the present study is the La Aguadita Gneiss. It consists of hornblende-quartz-plagioclase gneiss, plagioclase-quartz gneiss, and amphibolite, which were metamorphosed in the epidote amphibolite facies (Menendez, 1965; Ostos, 1984, 1985). Martin (1968) obtained a hornblende K/Ar age for the gneiss of 210 $\pm$ 10 Ma, but based on stratigraphic relations Bellizia and Rodriguez (1976) suggested a Precambrian age. The La Aguadita Gneiss was intruded in the south by trondhjemite stocks and aplite dikes (Menendez, 1965; Bellizia, 1985) and south of the city of La Victoria a quartz-hornblende diorite pluton (Smith, 1953; MacLachlan *et al.*, 1960) with blastomylonitic texture crops out (Beck, 1986), which is known as "La Guacamaya Diorite".

Tucutunemo Formation

The Permian metasediments and metavolcanics are comprised in the Tucutunemo Formation. It consists of a lower volcanic member (Los Naranjos Member), a middle detrital member, and an upper calcareous member (Beck, 1986). The metamorphic assemblage is indicative of the greenschist facies metamorphism (Bellizia, 1985). Previously (Shagam, 1960) it

was thought that this formation was of Mesozoic age, but recently Benjamini *et al.* (1987) obtained a Permian fauna in the calcareous unit.

The Los Naranjos Member is made up of two lithologic associations. The first consists of metabasalt and black phyllite, while the other is made up of metavolcaniclastics (metatuff, metabreccia) (Shagam, 1960; Beck, 1986). The metabasalts are non-orogenic tholeiites (Girard *et al.*, 1982). A Campanian (73.5 $\pm$ 1.9 Ma) K/Ar age determination was published by Beck (1986).

Cretaceous Metasediments

There are several metavolcanic and metasedimentary Mesozoic units in the Caucagua-El Tinaco belt. The Albian Chuspita Formation consists of metaconglomerate, metaquartzite, and calcareous graphite phyllite (Urbani, 1973). The Upper Cretaceos Urape Formation is made up of sericite quartz chlorite phyllite, lithic metaconglomerate, and marble lenses (Seiders, 1965). The Conoropa Formation of unknown age and it consists of metalava, aphanitic metatuff, black phyllite, metaconglomerate, and marble (Seiders, 1965). The Las Placitas Formation is of unknwon age and it consists of metaconglomerate, graphite phyllite, metagraywacke, metaradiolarite, actinolite metatuff, and metabasalt. The rocks have been affected by low grade metamorphism (Menendez, 1965). The Lower Cretaceous Pilancones Formation consists of basaltic-andesitic pillow lava, volcanic breccia, radiolarite, arkose, and limestone (Menendez, 1965; Stephan, 1982). The basaltic rocks show an non-orogenic affinity (Girard *et al.*, 1982). The Upper Cretaceous (?) Tiramuto Formation consists of pumpellyite metatuff, lithic metatuff, volcanic breccia, metabasalt, and metaradiolarite (Menendez, 1965; Bellizia and Rodriguez, 1976; González de Juana *et al.*, 1980).

Paracotos Belt

The Paracotos belt is bound to the south by the south-dipping Agua Fria thrust fault (Menendez, 1966). This belt consists entirely of the Campanian-Maastrichtian (?) Paracotos Formation (Shagam, 1960), which has a very constant foliation parallel to the Agua Fria thrust fault (Menendez, 1966). Serpentinite slices and dismembered ophiolites (Loma de Hierro Peridotite and the Tinaquillo Peridotite Complex) are common at the contacts with the Caucagua-El Tinaco belt and the Villa de Cura belt (González de Juana *et al.*, 1980). Beck (1985) combined the Paracotos Formation with the ophiolitic rocks of the Loma de Hierro and named this belt the "Loma de Hierro-Paracotos

Ophiolitic Nappe" consisting from bottom to top of: (a) an oceanic member: the Loma de Hierro Peridotite (harzburgite, serpentinite, and gabbro), (b) a Neocomian-Albian sequence of pillow lava, volcanic breccia, limestone, and radiolarite called the "Rio Guare Beds", (c) the Tiara Formation consisting of lava intruded by gabbro dikes, and (d) the uncomformably overlying Campanian-Maastrichtian Paracotos Formation.

The Paracotos Formation consists of lithic metaconglomerate with a phyllitic matrix, black siltstone, metagraywacke, green pelagic marbles, and metaconglomerate (Shagam, 1960; Beck, 1986) showing characteristic sedimentary structures of flysch and wildflysch deposits (González de Juana *et al.*, 1980). The Paracotos Formation is generally unmetamorphosed (Oxburgh, 1965; Beck, 1986); locally, it underwent very low-grade metamorphism (Konigsmark, 1958, 1965; Shagam, 1960).

The Villa de Cura Belt

The Villa de Cura belt consists of strongly deformed metasedimentary (mostly volcaniclastic) and metavolcanic rocks of the Villa de Cura Group (Shagam, 1960; Navarro, 1983), the Dos Hermanas Formation (Girard, 1981; Navarro, 1983; Beck, 1986; Urbani, 1987b), the mafic-ultramafic plutonic Chacao Complex (Murray, 1973), and the Apa Complex (Urbani, 1987b). The Villa de Cura Group is overlain unconformably by the flysch sequence of the Paleocene Guarico Formation which is part of a major flysch basin, south of the Villa de Cura belt. The flysch is overlain unconformably by a non-flysch basin of Miocene-Pliocene age (Beck, 1978). Bell (1968) subdivided the flysch and non-flysch basins into four tectonic belts. Only those units of the Villa de Cura belt relevant to the present study will be discussed here in more detail.

The Villa de Cura Group

Shagam (1960) divided the Villa de Cura Group into four units, which are from bottom to top: El Caño, El Chino, El Carmen, and Santa Isabel formations. Navarro (1983) proposed a different division with the Granofels Unit (Santa Isabel Formation) at the base of the sequence, which is overlain by the Metalava Unit (El Carmen Formation) and at the top the Metatuff Unit (El Caño and El Chino formations). The tectonic setting of the Villa de Cura Group is not certain. Beets *et al.* (1984) characterized the metalavas of the El Chino Formation geochemically as tholeiites extruded in a primitive island arc, while Navarro (1983) obtained a mid-oceanic ridge affinity for the metabasalts of the El Chino and El Carmen formations. Girard (1981) determined the

composition of clinopyroxenes from the metalavas of the El Carmen Formation and they are similar to those described from island arcs. Several whole rock, amphibole, phengite, and plagioclase K/Ar age determinations indicate an early-Late or Late Cretaceous metamorphic age (Piburn, 1968; Loubet *et al.*, 1985).

The Villa de Cura Group has undergone high P/T metamorphism (Shagam, 1960; Piburn, 1968; Navarro, 1983). The Metatuff Unit was metamorphosed in the pumpellyite-actinolite and lawsonite-albite-chlorite facies, the Metalava Unit underwent lawsonite-albite-chlorite and blueschist facies metamorphism, and the Granofels Unit was metamorphosed under the blueschist and greenschist facies conditions (Navarro, 1983).

Dos Hermanas Formation

A mainly volcanic unit outcropping south of the Villa de Cura Group, near the town of San Sebastian was named by Piburn (1977) the Tiara Formation. Girard *et al.*, (1982) renamed the unit the Dos Hermanas or Tiara Sur Formation, reserving the name Tiara Formation for the lavas and gabbro dikes in the "Loma de Hierro-Paracotos Ophiolitic Nappe", north of the Villa de Cura belt. Urbani (1987b) also recognized the Dos Hermanas Formation in Guatopo National Park (Figure 5.12).

This formation consists of volcanic breccia, ash tuff, lithic tuff, and lava (Piburn, 1968). The formation was metamorphosed under the prehnite-pumpellyite facies (Navarro, 1983). On the basis of clinopyroxene composition Girard (1981) suggested that the lavas were typical of island arcs. Loubet *et al.* (1985) suggested the same on the basis of major- and trace-elements abundances. Beck (1985) published two ages (34.7 $\pm$ 1.7 Ma and 52.2 $\pm$ 1.3 Ma), determined by the K/Ar method on metalavas from this unit. Loubet *et al.* (1985) determined two plagioclase K/Ar ages of metalavas of 119 $\pm$ 4 Ma and 112 $\pm$ 4 Ma. The Dos Hermanas Formation was overthrust to the south across the Paleocene flysch of the Guarico Formation.

Igneous rocks of the South-Central Caribbean

As the main focus of the present study is directed toward igneous rocks (their composition and their original tectonic setting), a somewhat more detailed review of these rocks will follow here.

Felsic and Intermediate Igneous Rocks

Evolved igneous rocks are present in the following tectonic belts of the central Caribbean Mountains system, from north to south:

(1) Cordillera de la Costa Belt.

Traditionally, the Sebastopol Complex in the Cordillera de la Costa belt is assumed to be the northern extension of the Guayana shield (Dengo, 1953; Smith, 1953; Bellizia, 1972; Wehrmann, 1972; , Beck, 1985; Ostos and Navarro, 1985). Granitic rocks of the Peña de Mora Formation, and similar plutons such as the Guaremal Granite, Choroni Granite, and the Colonia Tovar Granite crop out in this terrane; they were originally interpreted as syntectonic intrusions emplaced during a Late Cretaceous-Paleocene orogeny (Dengo, 1953; Urbani, 1972; Maresch, 1974; Talukdar and Loureiro, 1982; Beck, 1985), but recent data indicate that they are older and of Paleozoic-Precambrian age (Urbani, 1983; Pimentel *et al.*, 1985; Urbani, 1988). Similar Precambrian-Paleozoic igneous rocks were found in wells in the Gulf of La Vela. Such rocks are also exposed in the Paraguana Peninsula (Gonzalez de Juana *et al.*, 1980; Kiser *et al.*, 1984).

(2) Caucagua-El Tinaco Belt.

The Caucagua-El Tinaco Belt consists of felsic-intermediate basement (hornblende gneiss, and plagioclase-hornblende gneiss) intruded by metadioritic and trondhjemitic plutons (Shagam, 1960; Menendez, 1965; Mackenzie, 1966; Ostos, 1984; Beck, 1985). A Paleozoic age has been proposed for the intermediate and felsic igneous intrusions (Martin, 1968).

Mafic and Ultramafic rocks

Mafic and ultramafic rocks are widely recognized in the Caribbean Mountains system and they should be studied in the tectonic terrane framework. However, the scarcity of radiometric age data for these rocks makes it difficult if not impossible to distinguish between Paleozoic and Mesozoic belts. Bellizia (1967) suggested that the mafic and ultramafic rocks of the Caribbean Mountains System occur in two relatively ill-defined belts (Figure 2.2). The northern belt coincides in part with the Cordillera de la Costa-Margarita terrane (Stephan *et al.*, 1980; Stephan, 1985). The southern belt occurs within the Caucagua-El Tinaco belt. These ultamafic and mafic complexes occur as lenses parallel to the structure of the country rock (Bellizia, 1967) or along thrust contacts (Stephan *et al.*, 1980; Stephan,

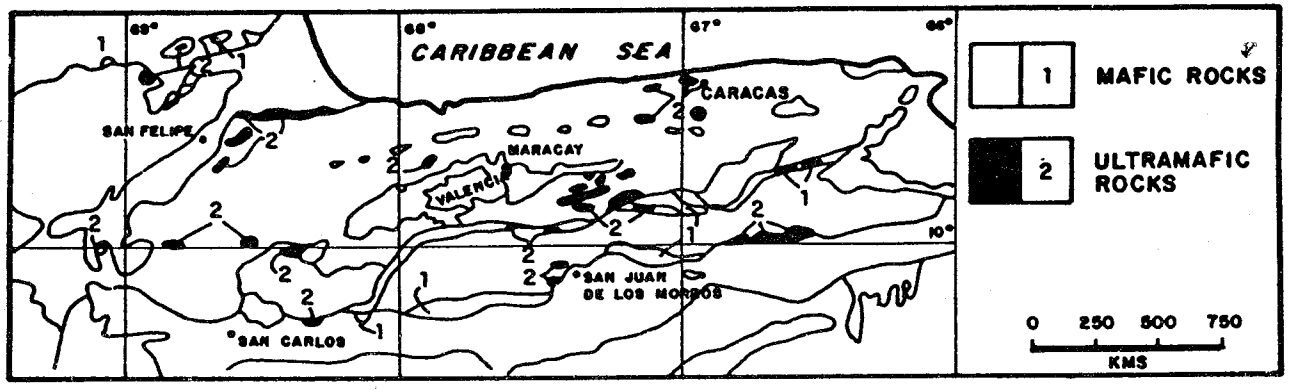

FIGURE 2.2: MAFIC AND ULTRAMAFIC IGNEOUS ROCKS IN THE CENTRAL PART OF THE CARIBBEAN MOUNTAINS SYSTEM (FROM BELLIZIA, 1967).

1985). Similar thrust contacts have been recognized between the Tinaquillo Peridotite Complex and the Loma de Hierro Nappe with their country rock (Ostos, 1984; Beck, 1985b, 1986).

The Tinaquillo Peridotite Complex is a mafic-ultramafic tectonite consisting of harzburgite, dunite, pyroxenite, serpentinite, and metagabbro (Ostos, 1984). The complex was overthrust to the north across the Las Mercedes Formation and it is conformably overlain by the Tinaco Complex (Ostos, 1984).

Urbani and Quesada (1972) defined the intermediate and mafic Todasana Complex in the Cordillera de la Costa belt, consisting of garnet amphibolite, biotite hornblende diorite, and unmetamorphosed dikes of pyroxene hornblende andesite. The complex is interpreted as a migmatitic complex, but because of the low metamorphic grade of the country rock, Urbani and Quesada (1972) suggested that the complex is allochthonous. There are also some mafic and ultramafic rocks in the southernmost Paracotos and Villa de Cura belts and in the basement of the Venezuela Llanos basin. Along the northern thrust contact of the late Cretaceous-Paleocene Paracotos belt sheared serpentinites occur (González de Juana *et al.*, 1980; Beck, 1986) and in the Villa de Cura belt several mafic-ultramafic complexes such as the Chacao and Apa complexes have been recognized (Beck, 1985, 1986; Urbani, 1988b).

Eastern Caribbean Mountains System

Rock sequences similar to the the Cordillera de la Costa belt s.s. and the Cordillera de la Costa-Margarita terrane in central Venezuela (Stephan, 1985) have been recognized in northeastern Venezuela (Margarita Island and the Araya and Paria peninsulas), in the northern area of Trinidad, and on the Tobago (Stephan, 1985; Bellizia, 1985). The Caucagua-El Tinaco belt is also correlated with the Sans Souci Formation of Trinidad and the Villa de Cura belt is correlated with the Tobago Volcanic Group of Tobago (Bellizia, 1985). In the present study, only rocks from Margarita were analyzed and thus only the geology of Margarita Island will be discussed here.

Margarita Island

The stratigraphy of Margarita Island has been studied by Hess and Maxwell (1949), Taylor (1960), Jam and Mendez (1962), González de Juana (1968), Maresch (1971, 1973), Vignali (1976, 1979), and Chevalier (1987). According to

Maresch (1973) the oldest and structurally lowest rocks of Margarita are the amphibolites of the La Rinconada Group, which were thought to be successively overlain by the Juan Griego Group and Los Robles Group (Figure 2.3). Vignali (1979) suggested that the La Rinconada Group belongs to and is interlayered with the Juan Griego Group (Figure 2.3). Chevalier (1987) believed that the La Rinconada Group is structurally overlying the Los Robles Group (Figure 2.3). The origin and relative age of several silicic igneous rocks (Matasiete Trondhjemite, Guayacan Gneiss, El Salado Granite, and the Agua de Vaca Granite) is being debated. The geometry of large bodies of serpentinite is not well known. Stephan *et al.* (1980), Beck (1985, 1986), and Bellizia (1985) correlated the Juan Griego Group with the Cordillera de la Costa belt s.s. and the other units with the Cordillera de la Costa-Margarita terrane (Figure 2.4). Chevalier (1987) suggested that the Juan Griego Group was deposited on the South America continental margin, that the La Rinconada Group and the serpentinites represent an ophiolite, that the Los Robles Group was deposited on the ophiolite, and that the granodioritic orthogneiss intruded the metaophiolites.

Juan Griego Group

The Juan Griego Group consists mainly of metasediments; the lower half is feldspar-rich and the upper is non-feldspathic (Vignali, 1979). The feldspathic unit consists of feldspathic metaquartzite, gneiss, and quartz-feldspar-mica schist, while the non-feldspathic unit consists of quartz + mica $\pm$ garnet $\pm$ graphite schist and metaquartzite interbedded with marble (Vignali, 1979; Gonzalez de Juana *et al.*, 1980). A layer of amphibole schist between the two units was recognized on the Macanao Peninsula by Vignali (1979), who correlated it with the La Rinconada Group.

The non-feldspathic unit of the Juan Griego Group contains numerous eclogite and amphibolite boudins (Navarro, 1974, 1977; Chevalier, 1987). The unit has been metamorphosed in the greenschist to epidote amphibolite facies; which overprinted an earlier eclogite assemblage (Navarro, 1974, 1977, 1981, 1987; Chevalier, 1987). Vignali (1976) suggested that the Juan Griego Group was older than Cenomanian, based on the superposition of the Los Robles Group (Figure 2.3). Chevalier (1987) correlates it with the Las Brisas Formation on the mainland, which has a Jurassic age.

Los Robles Group

The Los Robles Group consists from bottom to top of quartz-chlorite phyllite, quartz-sericite phyllite, chlorite

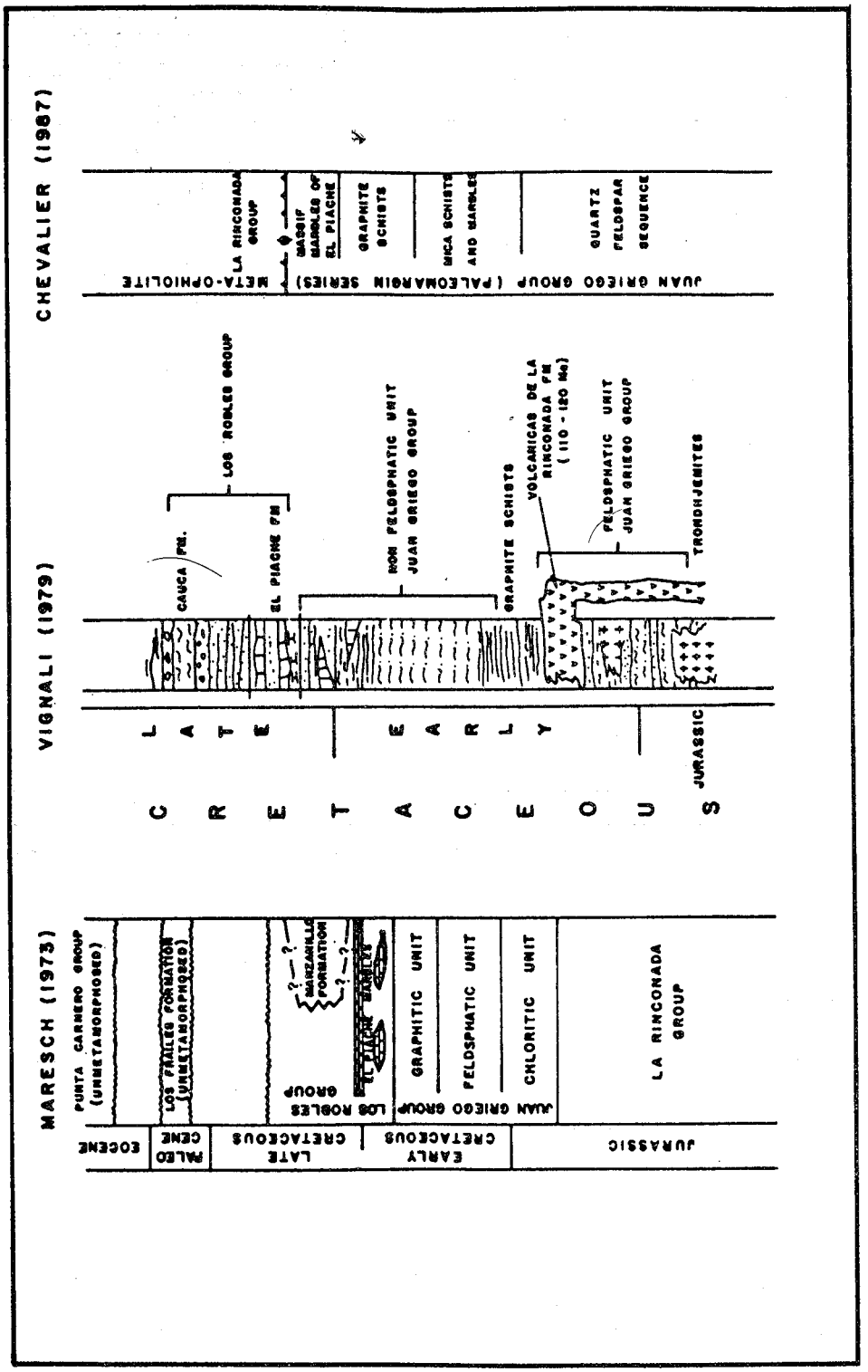

FIGURE 2.3 : JURASSIC TO PALEOCENE STRATIGRAPHY OF MARGARITA ISLAND PROPOSED BY MARESCH (1973), VIGNALI (1979), AND CHEVALIER (1987).

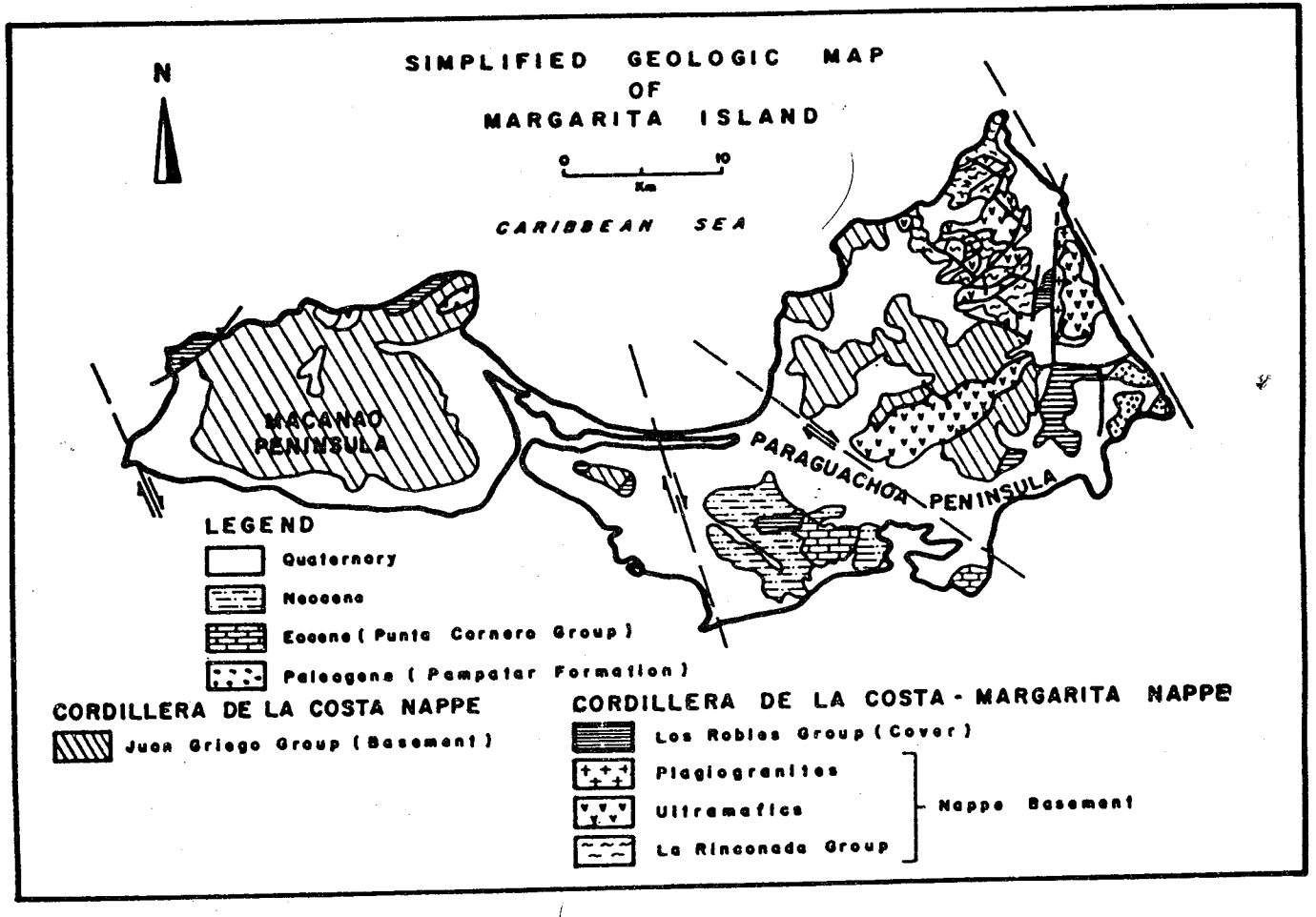

FIGURE 2.4: SIMPLIFIED MAP OF MARGARITA ISLAND (FROM BELLIZIA, 1985).

marble, dolomite marble of the El Piache Formation and calcareous quartz-sericite-chlorite phyllite, quartz-mica-chlorite schist, epidote quartzite, and metaconglomerate (Vignali, 1976, 1979). The unit has a metamorphic assemblage indicative of greenschist facies metamorphism (Carrillo and Vivas, 1986; Chevalier, 1987). The protolith of the Los Robles Group is a marine sedimentary sequence more distal and younger than the Juan Griego Group. It has a mixed continental and volcanic sourced (Chevalier, 1987). Fossils have been found in the group, which indicate a Cenomanian age (González de Juana *et al.*, 1980).

Igneous rocks

Several igneous units (ultramafic, mafic, and felsic) have been described on Margarita Island. The mafic and ultramafic units are mapped as the La Rinconada Group and serpentinites, respectively. The felsic units are formally known as the Matasiete Trondhjemite, the Guayacan Gneiss, the El Salado Granite, and Agua de Vaca Granite.

Agua de Vaca Granite

The Agua de Vaca Granite is exposed near the Village of Agua de Vaca, southeast of Cerro Matasiete (Figure 2.5). It consists of quartz, albite, chlorite, and white mica. It has a mylonitic texture (Chevalier, 1987). The granite may not be cogenetic with the Matasiete and Guayacan trondhjemites but may have developed at a plate boundary above a transitional crust (Chachati and Macsotay, 1985).

El Salado Granite

The El Salado granite is exposed near the Village of El Salado (Figure 2.5). It consists of perthite microcline, albite, quartz, epidote, white mica, and biotite (Maresch, 1973), showing a mylonitic texture (Carrillo and Vivas, 1986; Chevalier, 1987). El Salado Granite has been correlated with the Agua de Vaca Granite and Maresch (1973) proposed an intrusive relationship with the surrounding ultramafic rocks. Chevalier (1987) correlated the El Salado Granite with the intrusive felsic phase in the La Rinconada Group.

Matasiete Trondhjemite

The Matasiete Trondhjemite crops out along the western flank of the Matasiete and Guayamuri Hills (Figure 2.5). The trondhjemite is granoblastic, gneissic, mylonitic, and ultramylonitic (González de Juana *et al.*, 1980; Chevalier, 1987). It consists of oligoclase, quartz, epidote, white

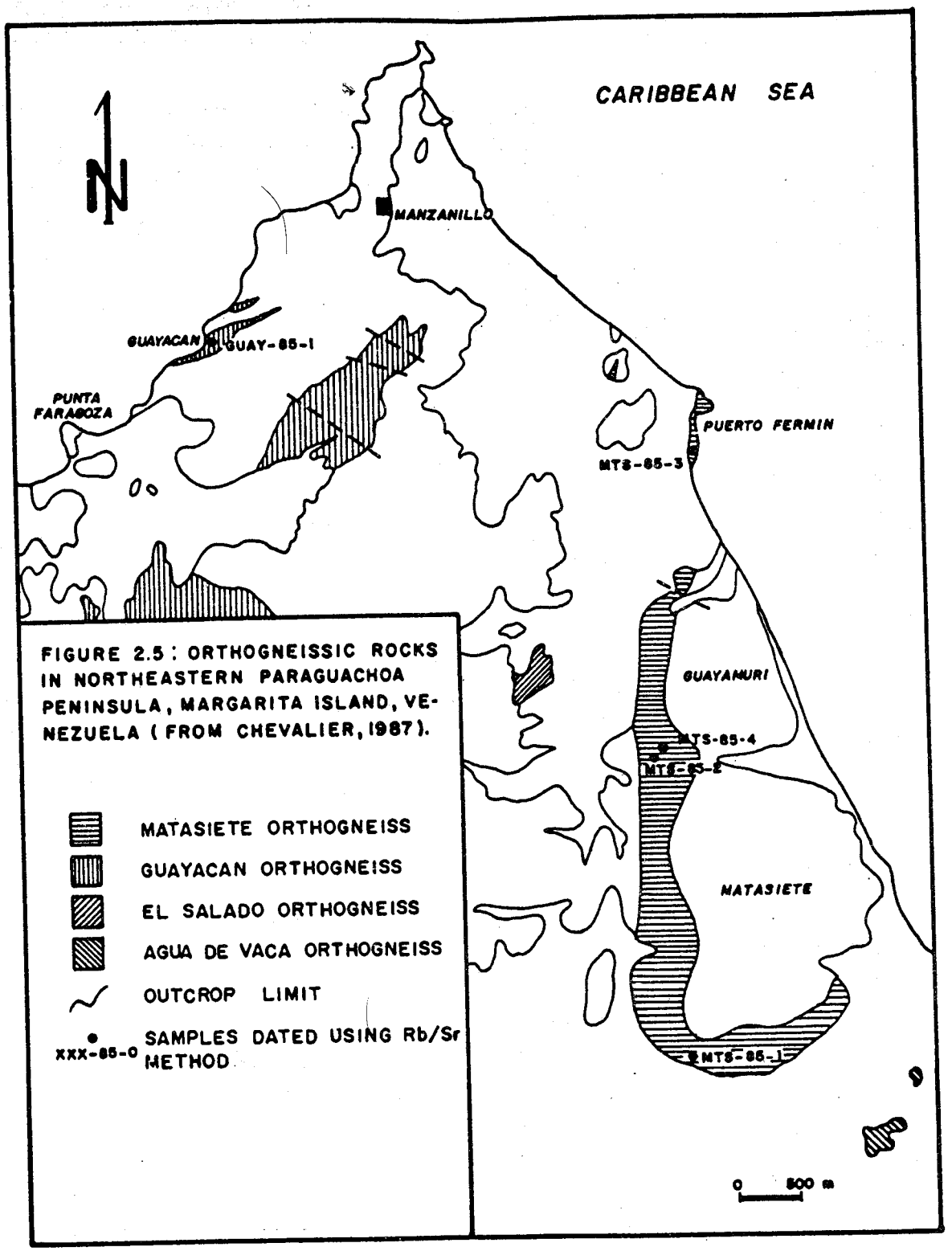

FIGURE 2.5 : ORTHOGNEISSIC ROCKS IN NORTHEASTERN PARAGUACHOA PENINSULA, MARGARITA ISLAND, VENEZUELA (FROM CHEVALIER, 1987).

mica, green amphibole, and chlorite (Carrillo and Vivas, 1986). Vignali (1979) interpreted the felsic rocks as intrusive into the Juan Griego Group, while Chevalier (1987) proposed an intrusive relationship with the La Rinconada Group.

Maresch (1973) believed that the Matasiete Trondhjemite was emplaced syntectonically and Navarro (1974) thought that it formed by melting of sediments during the orogeny. However, Schubert and Santamaria (1974) determined an island arc affinity and Chachati and Macsotay (1985) showed that it formed in an oceanic tectonic setting. Olmeta (1968) and Santamaria and Schubert (1974) determined three Campanian-Maastrichtian K/Ar ages for amphiboles from this unit and Loubet et al. (1985) obtained Maastrichtian-Paleocene and Paleocene K/Ar ages for muscovites from the trondhjemites (See Chapter VIII).

Guayacan Gneiss

The Guayacan Gneiss crops out in the northernmost Paraguachoa Peninsula (Figure 2.5). Near the contacts, it is interlayered with the La Rinconada and Juan Griego Groups (Maresch, 1973). The unit was interpreted as intrusive in the Juan Griego Group by Vignali (1979). The gneiss does not show igneous textures. It consists of quartz, albite, white mica, epidote, and chlorite (Maresch, 1973; Chachati and Macsotay, 1985). The gneiss may have intruded syntectonically and it may have been derived by partial melting from sediments (Maresch, 1973) or from the mantle in an oceanic setting (Chachati and Macsotay, 1985). Chevalier (1987) determined two K/Ar ages of micas from the gneiss, which yielded Maastrichtian-Paleocene and Paleocene ages (See Chapter VIII).

La Rinconada Group, Metagabbros, and Serpentinites

La Rinconada Group consists of amphibole gneiss and graphite-mica schist, with lenses of paragonite-amphibole eclogite and amphibolite (Maresch, 1971, 1973). Lenses and layered felsic igneous rocks are assumed to be intrusive related to the Matasiete Trondhjemite, El Salado Granite, and Agua de Vaca Gneiss (Chevalier, 1987). The stratigraphic position of the group has been a point of debate (Figure 2.3). The metamorphic history of the mafic rocks has been controversial as well. Navarro (1974), Blackburn and Navarro (1977), Stephan *et al.* (1980), and Stephan (1985) postulated a polymetamorphic history: first a high P/low T regime (blueschist to eclogite facies), which is overprinted much later by a second metamorphic event of intermediate P/T conditions. Alternatively, the metamorphic assemblages

were the result of one unique P/T path and the only difference between the Margarita and mainland rocks is that the eclogites of Margarita reached a greater depth (Maresch, 1973; Maresch and Abraham, 1981; Beets *et al.*, 1984; Chevalier, 1987).

Chevalier (1987) proposed that the La Rinconada Group and the ultramafic, and gabbroic rocks in the Paraguachoa Peninsula constitute a disrupted ophiolite. This is supported by the major and trace-element abundances of the mafic rocks analyzed by Beets *et al.* (1984) and Loubet *et al.* (1985). The K/Ar ages determined on mineral separates by Loubet *et al.* (1985) and Chevalier (1987) have a range of 37 to 98 Ma.

Western Caribbean Mountains System

Stephan *et al.* (1980) and Bellizia (1985) extended the Caribbean Mountains system to the west. It occurs in the Sierra de Santa Marta in Colombia, in the Peninsula of la Goajira, in the Peninsula of Paraguana, and in the southern part of the Falcòn State (the Siquisique ophiolites).

The Sierra de Santa Marta

The Sierra de Santa Marta (Figure 2.6) is an uplifted block with a pronounced northeasterly trending structural grain parallel to the structure of the Peninsula of la Goajira and the Sierra de Perijà (Shagam, 1975). The Sierra de Santa Marta is not isostatically compensated (Case *et al.*, 1973), and may be the result of overthrusting of continental crust over the Caribbean plate (Ramirez *et al.*, 1983).

The stratigraphy of the Sierra de Santa Marta is described in detail by Shagam (1975). The basement consists of Precambrian granulites overlain by Pennsylvanian and older low-grade metasedimentary rocks. The basement is overlain unconformably by Permian-Triassic marine sedimentary rocks and basic and siliceous volcanics, which are also overlain unconformably by spilitic or keratophyric tuff and extensive late (?) Jurassic to early Cretaceous dacitic to rhyolitic volcanism (Shagam, 1975). The Jurassic-Cretaceous vulcanics on the southeastern side of the massif were covered by a Cretaceous sequence of a basal clastics, carbonate-rich facies, and a shaley facies, and by Paleocene-Eocene molasse containing coal beds.

Shagam (1975) correlated the Cretaceous-Tertiary in the Sierra the Santa Marta with that in the Sierra de Perija and

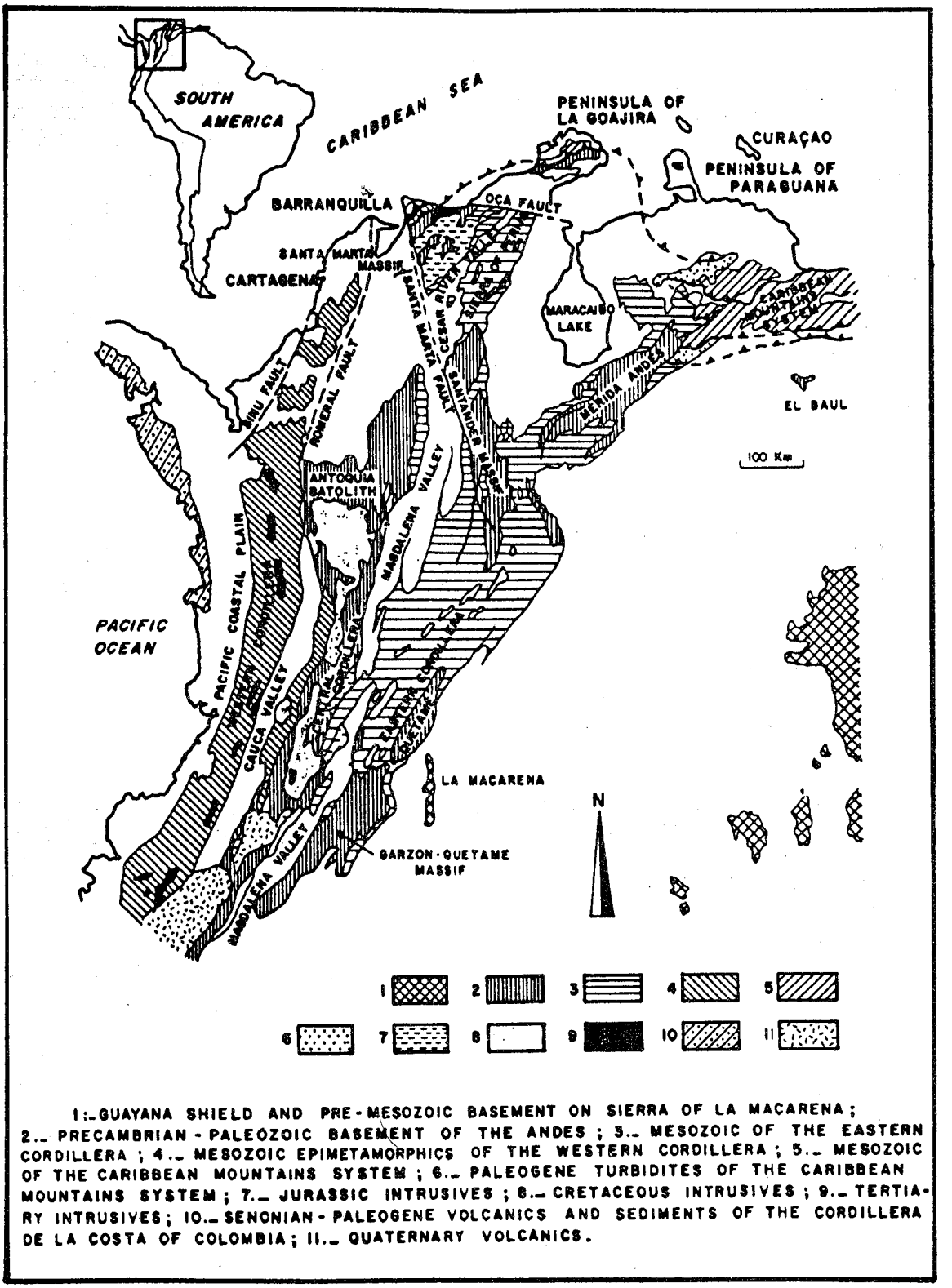

1:- GUAYANA SHIELD AND PRE-MESOZOIC BASEMENT ON SIERRA OF LA MACARENA; 2.- PRECAMBRIAN - PALEOZOIC BASEMENT OF THE ANDES; 3.- MESOZOIC OF THE EASTERN CORDILLERA; 4.- MESOZOIC EPIMETAMORPHICS OF THE WESTERN CORDILLERA; 5.- MESOZOIC OF THE CARIBBEAN MOUNTAINS SYSTEM; 6.- PALEOGENE TURBIDITES OF THE CARIBBEAN MOUNTAINS SYSTEM; 7.- JURASSIC INTRUSIVES; 8.- CRETACEOUS INTRUSIVES; 9.- TERTIARY INTRUSIVES; 10.- SENONIAN - PALEOGENE VOLCANICS AND SEDIMENTS OF THE CORDILLERA DE LA COSTA OF COLOMBIA; 11.- QUATERNARY VOLCANICS.

FIGURE 2.6: SIMPLIFIED GEOLOGIC MAP OF NORTHWESTERN SOUTH AMERICA (FROM MARECHAL, 1983 IN BELLIZIA, 1985).

in the Mérida Andes. Restrepo and Toussaint (1988) correlated the Jurassic-Lower Cretaceous volcanics of the Sierra de Santa Marta with that of La Quinta Formation in the Sierra de Perijá. An important mid-Cretaceous tectonic event may be related to the suturing of the Western Cordillera of Colombia with the Central Cordillera of Colombia. The rocks in the Western Cordillera of the Sierra de Santa Marta are the ones which Stephan *et al.* (1980) and Bellizia (1985) considered to be related to the Caribbean Mountains system.

Peninsula of La Goajira

The La Goajira Peninsula, north of the Sierra de Perijá (Figure 2.6) can be divided into four geological provinces (Gonzalez de Juana *et al.*, 1980). The La Goajira platform and La Goajira trough are south of the Cuiza fault. The Goajira arch and the Caribbe province are north of the fault (Figure 2.7).

The Goajira arch is underlain by plagioclase-hornblende-garnet gneiss, biotite-plagioclase-garnet schist, and amphibolites (Macuira Group). Bellizia (1985) correlated it with the Caucagua-El Tinaco belt and named it the "Caucagua-El Tinaco-Yumare-Siquisique Nappe". The Caribbe province is underlain by metamorphic rocks of the Bahia Honda Group. Bellizia (1985) correlated it with the Cordillera de la Costa-Margarita terrane of the Caribbean Mountains system. The Goajira platform and the Goajira trough are geologically very similar to the Mesozoic-Cenozoic sediments in the Sierra de Santa Marta, the Sierra de Perijá (Shagam, 1975), and in the Mérida Andes and Maracaibo basin (González de Juana *et al.*, 1980). The basement of these provinces consists of Precambrian and lower Paleozoic metamorphic rocks which Restrepo and Toussaint (1988) correlated with the basement of the Eastern Cordillera of Colombia.

Peninsula of Paraguana

The Peninsula of Paraguana is located south of Aruba (Fig. 2.1 and 2.6). It consists of a Paleozoic-Mesozoic igneous-metamorphic complex (González de Juana *et al.*, 1980), which has been correlated with the Cordillera de la Costa belt by Stephan *et al.* (1980) and Stephan (1985) and mafic-ultramafic complexes. The oldest rock recognized in the Peninsula is the Paraguana Granite, which consists of granite and diorite. It is intruded by felsic and mafic dikes (González de Juana *et al.*, 1980). Two U/Pb ages of 262 and 265 Ma have been determined for sphene from the granite (Martin, 1968).

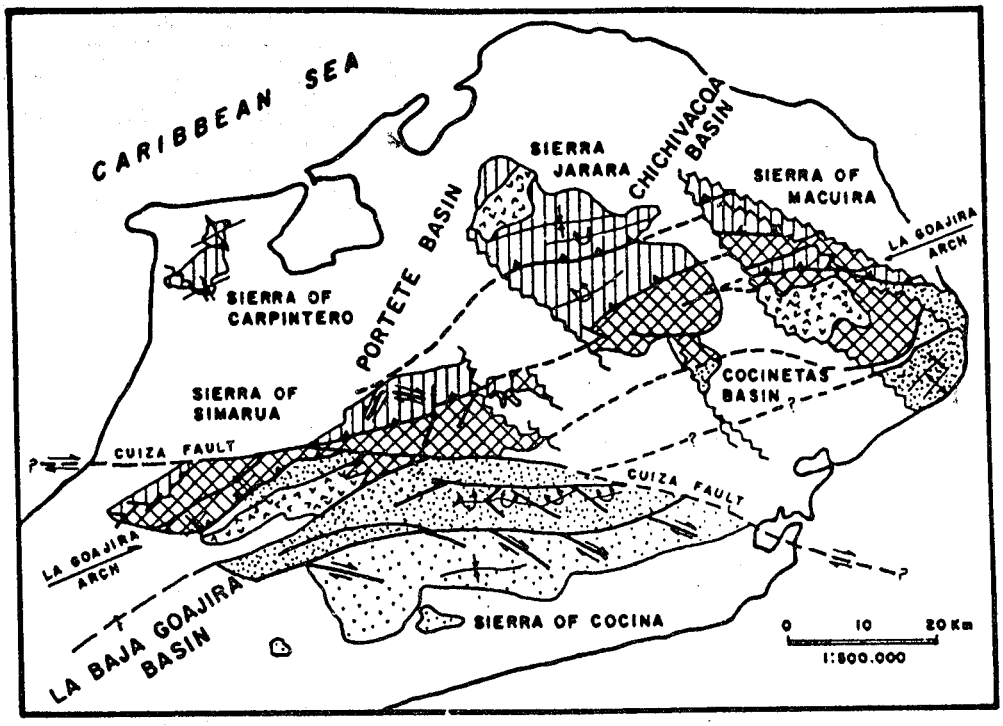

LEGEND

TERTIARY AND QUATERNARY

GRANITIC IGNEOUS ROCKS

UNMETAMORPHOSED MESOZOIC SEDIMENTS (LA GOAJIRA O COCINA BASINS)

METAMORPHOSED MESOZOIC SEDIMENTS ON THE GOAJIRA PLATFORM.

ALLOCHTHONOUS

MESOZOIC BAHIA HONDA GROUP (CORDILLERA DE LA COSTA - MARGARITA NAPPE)

PRE-MESOZOIC MACUIRA FORMATION (CAUCAGUA - EL TINACO - YUMARE - SIQUISIQUE NAPPE)

THRUST

STRIKE - SLIP FAULT

HIGH - ANGLE FAULT

TERTIARY NORMAL FAULT

FIGURE 2.7: SIMPLIFIED GEOLOGIC MAP OF THE PENINSULA DE LA GOAJIRA (FROM ALVAREZ, 1967 IN BELLIZIA, 1985).

The Pueblo Nuevo Formation consists of graphite schist and phyllite, metasandstone, conglomeratic metasandstones, metacherts, and marbles, metamorphosed in the greenschist facies (González de Juana *et al.*, 1980). A late Jurassic age for the Pueblo Nuevo Formation has been proposed, based on this unit with the Paraguana Granite may be tectonic or it is an unconformity (González de Juana *et al.*, 1980).

The mafic-ultramafic complexes of the Paraguana Peninsula are the Tausabana-El Rodeo Ultramafic Complex, the Siraba-Capuana Gabbro, and the Santa Ana Subvolcanic Complex (Martin and Arozena, 1972). The first one is a zoned ultramafic body, which consists of dunite, chromitite, harzburgite, lherzolite, olivine pyroxenite, hornblende pyroxenite, and a marginal pegmatitic gabbro intrusion (Martin and Arozena, 1972).

The Siraba-Capuana Gabbro is intrusive in the Tausabana-El Rodeo Ultramafic Complex. It consists of olivine-pyroxene gabbro, pyroxene-anorthosite gabbro, and anorthosite, which has several pyroxenite and peridotite xenolith (Martin and Arozena, 1972). The Santa Ana Subvolcanic Complex consists of aphanitic basalt, porphyritic basalt, and gabbroic basalt, which based on major-element abundances were clasified as transitional from tholeiite to Al-rich basalts (Martin and Arozena, 1972), but with additional trace element data Santamaria and Schubert (1974) suggested that the gabbros and dolerites have a tholeiitic affinity. They also determined three whole rock K/Ar ages of 120 $\pm$ 11, 129 $\pm$ 14, and 118 $\pm$ 10 Ma.

Siquisique Ophiolites

The Siquisique ophiolites, south of the Tertiary Falcòn basin (Figure 2.8) consists of gabbros and pillow lavas with shale lenses; it is intruded by basaltic dikes (Stephan *et al.*, 1980). Based on ammonites in the shaly sediments, Bartok *et al.* (1985) proposed a middle Jurassic age (Bajocian to early Bathonian) for the ophiolite. The ophiolites are overlain by a Neocomian-Albian clastic sequence and a Cenomanian-Turonian calcareous unit. The late Cretaceous sequence underlies uncomformably Paleocene calcareous clastics (Stephan *et al.*, 1980). The Siquisique ophiolites are interpreted as Caribbean oceanic crust thrust onto northern South America, earlier than the development of the northern Tertiary Falcòn pull-apart basin (Stephan *et al.*, 1980).

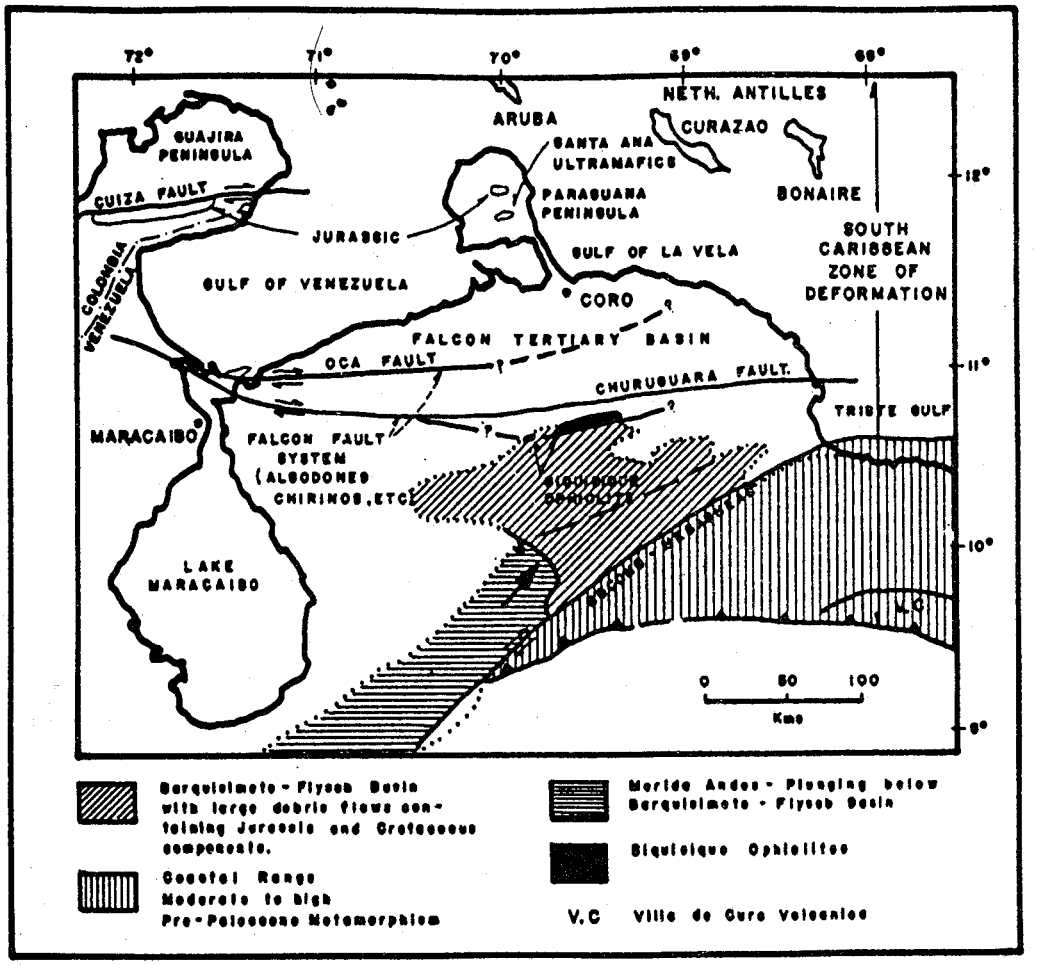

FIGURE 2.8: GENERAL LOCATION MAP OF THE SIQUISIQUE OPHIOLITES (FROM BARTOK et al., 1985).

The Andean Terranes

The Andean Terranes in the northwestern corner of South America are shown in Figures 2.6 and 2.9A. Restrepo and Toussaint (1988) divided the Andean terranes in an autochthonous and an allochthonous block. These blocks are separated by the Guaicamaro suture (Fig. 2.9B and 2.9D). Generalized stratigraphic columns of the different terranes in the autochthon and allochthon domains are given in Figure 2.9D.

Autochthonous Block

The autochthonous block includes the region east of the Eastern Cordillera of Colombia, which is shown on Figure 2.9A, as the Los Llanos physiographic province (Restrepo and Toussaint, 1988). The autochthonous block is part of the Guayana shield. The autochthonous block consists of Precambrian migmatites and granulites (Restrepo and Toussaint, 1975, 1978) which are overlain by Jurassic continental sediments, mid to Upper Cretaceous marine sediments, Paleocene to Miocene continental sediments (Figure 2.9C). All are overlain uncomformably by Miocene to Quaternary continental sediments (Restrepo and Toussaint, 1988).

Basement of the Venezuelan Llanos

The Venezuelan Llanos basin is part of the autochthonous terrane. It is subdivided into the SubAndean basins (Barinas-Apure basin) and the Eastern Venezuelan basin consisting of the Guarico and Maturin basins (Figure 1.5). The basement of the Venezuelan Llanos basin crops out in the El Baul uplift (Figure 2.6) and is found in the deepest wells in the basin (González de Juana *et al.*, 1980; Feo Codecido *et al.*, 1984). Martin (1968) published an orthoclase K/Ar age of 270 Ma for the El Baul Granite and a Rb/Sr age of 287 Ma, determined on biotite of the same granite. MacDonald and Opdyke (1974) determined two whole rock K/Ar ages of 192 and 195 Ma for rhyolites from El Baul uplift (La Guacamaya Volcanics).

Feo Codecido *et al.* (1984) published several K/Ar and Rb/Sr ages for samples of granitic basement obtained from wells in the Venezuelan Llanos basin. Two age groups may be distinguished: one in the north is between 321 and 423 Ma and the other is Precambrian (>1366 Ma) for rocks in the southern part of the basin, near the Guayana Shield.

In the Jurassic Espino Graben (Figure 1.5), a 113 m thick sequence of late Jurassic alkalic basalts (Moticska, 1985)

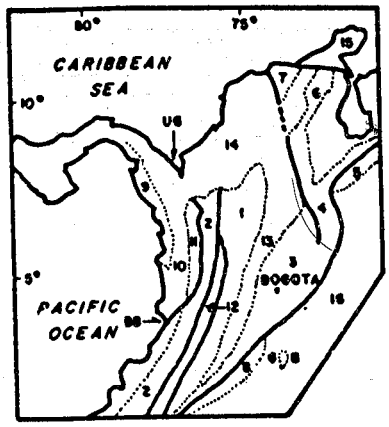

1: Central Cordillera, 2: Western Cordillera, 3: Eastern Cordillera, 4: Santander Massif, 5: Merida Andes, 6: Serrania de Perija, 7: Sierra Nevada de Santa Marta (SNSM), 8: Sierra de la Macarena and Garzón Massif, 9: Serrania de Baudó, 10: Atrato Valley, 11: Mandé Arch, 12: Cauca Valley 13: Magdalena and Cesar Valleys, 14: Caribbean coastal lowlands, 15: La Guajira Peninsula, 16: Llanos. UG-Uraba Gulf, BB-Bonaventura Bay.

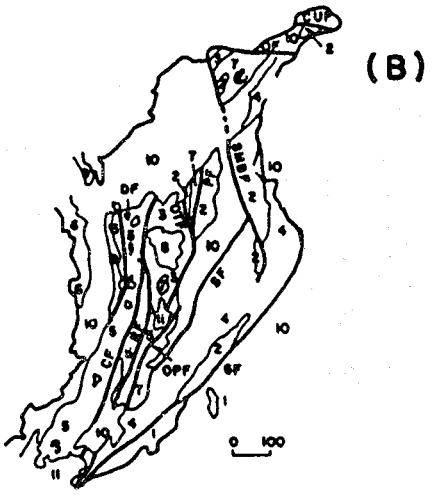

1: Precambrian metamorphic basement of the autochthonous block, 2: Precambrian and lower Paleozoic metamorphic basement of the EAT, 3: Polymetamorphic basement of the CAT, 4: Mesozoic sediments of the EAT, 5: Cretaceous basic volcanic and sedimentary rocks of the WAT, 6: Cretaceous and Cenozoic basic volcanics of the PBMT, 7: Jurassic plutonism, 8: Cretaceous plutonism, 9: Cenozoic plutonism, 10: Cenozoic sediments, 11: Pliocene to Quaternary volcanism. CF: Cauca Fault, CUF: Cuiso Fault, DF: Dabeiba Fault, GF: Guaicaramo Fault, OF: Oca Fault, DPF: Otu-Pericos Fault, PF: Palestina Fault, RF: Romeral Fault, SF: Salinas Fault, SMBF: Santa Marta-Bucaramanga Fault.

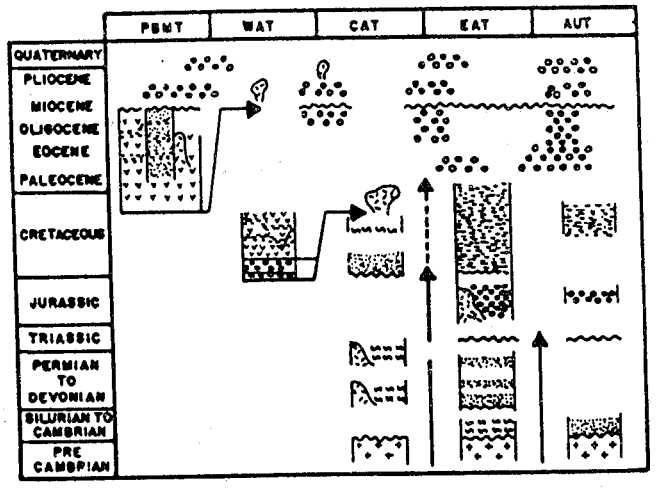

1: Precambrian basement, 2: Metamorphic event, 3: Marine sedimentation, 4: Continental sedimentation, 5: Ophiolites, 6: basic volcanism, 7: Granitoid plutonism, 8: Suture, 9: Main unconformities.

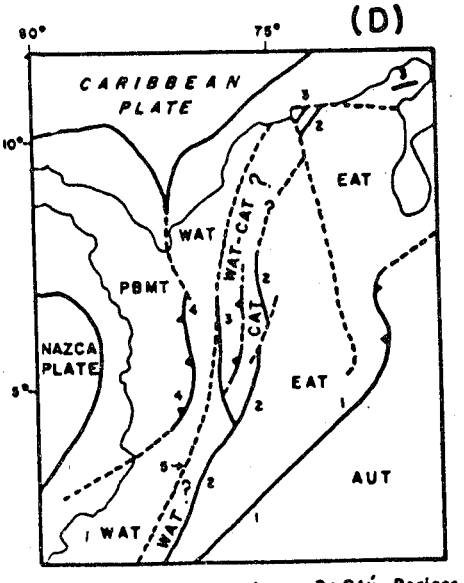

1: Guaicaramo suture, 2: Otú-Pericos suture, 3: Overthrusting front of the WAT on the CAT, 4: Dabeiba suture, 5: Cauca-Romeral Fault System. PBMT: Panamá-Baudó-Mandé Terrane, AUT: Autochthonous Block.

FIGURE 2.9: A. PHYSIOGRAPHIC MAP OF COLOMBIA AND ADJACENT REGIONS. B. SIMPLIFIED GEOLOGIC MAP OF THE COLOMBIAN ANDES. C. GENERALIZED STRATIGRAPHIC COLUMNS AND SUCCESSIVE SUTURES IN COLOMBIA. D. SCHEMATIC MAP OF THE ALLOCHTHONOUS TERRANES OF THE COLOMBIAN ANDES (FROM RESTREPO AND TOUSSAINT, 1988).

interbedded with 1540 m continental red beds have been described by Feo Codecido *et al.* (1984). The rocks of the Espino Graben (Ipire Formation) are the oldest Mesozoic rocks known in the Venezuelan LLanos basin. They have been correlated with La Quinta Formation in western South America. Overlying the Jurassic Ipire Formation or the Precambrian-Paleozoic basement is a Cretaceous-lower Tertiary transgressive and regressive sequence, similar to that in the allochthonous block (Sierra de Perijá, Sierra de Santa Marta, and Mérida Andes).

Allochthonous Terranes

The allocthonous block is located west of the Guaicaramo fault (Figure 2.9B). Restrepo and Toussaint (1988) recognized several terranes separated by sutures within the allochthonous block (Figure 2.9D). These terranes have continental or oceanic crust (Restrepo and Toussaint, 1978, 1988). The terrane with continental crust is located between the Guaicaramo and Cauca-Romeral sutures (Figure 2.9D), which includes the Eastern and Central Andean Cordillera in Colombia.

The contact between the Andean and Caribbean terranes has been located in the Sierra de Santa Marta and in the Peninsula of la Goajira (Shagam, 1975). Stephan *et al.* (1980) named this contact in the northern termination of the Mérida Andes the "transversale de Barquisimeto". The Caribbean Mountains system (Caribbean Domain) in these localities is overthrust across the allochthonous Andean terrane with continental crust (Stephan *et al.*, 1980; Beck, 1985; Bellizia, 1985).

Case *et al.* (1971), Ramirez (1983), Ramirez *et al.* (1985), and Restrepo and Toussaint (1988) recognized west of the Central Cordillera of Colombian the following two terranes with oceanic basement (Figure 2.9D): (a) The Cretaceous Western Andean Cordillera, which consists of igneous rocks of mid-ocenic ridge and island arc affinities (Bourgois *et al.*, 1985; Aspden and McCourt, 1986) and (b) The Late Cretaceous-Tertiary Panama-Baudo-Mandé terrane (Figure 2.9D), which consists of oceanic crust and an island arc accreted to the Western Andean Cordillera during the Miocene (Sillitoe *et al.*, 1982; Toussaint and Restrepo, 1982; Bourgois *et al.*, 1985; Restrepo and Toussaint, 1988). Because the geology of the autochthonous and allochthonous terranes in the Andes has no direct influence on the present study, the focus of this review will be on the Sierra de Perijá and the Mérida Andes, which are the northern extension of the Eastern Andean Cordillera in Venezuela.

Sierra de Perijá

The basement of the Sierra de Perijá consists of Cambro-Ordovician amphibolite-grade metamorphic rocks of the Perijá Series (Kellogg, 1984), which were intruded by granitic plutons of pre-Devonian, Devonian-Mississippian and Late Permian age (Bowen, 1972; Martin, 1968; Espejo, 1980). Unconformably overlying the basement is a transgressive Devonian sedimentary sequence (Bowen, 1972), which is covered unconformably by Pennsylvanian-Permian and Jurassic sediments (Figure 2.10). The Pennsylvanian-Permian sequence consists of shale, mudstone, crinoidal limestone, marl, calcareous mudstone, chert, and fossiliferous limestone (Shagam, 1975). This sequence is separated by a hiatus (Figure 2.10) from the fresh-water marl, shale, and volcanic rocks of the Jurassic La Ge Group (Shagam, 1975).

The La Quinta Formation, the major component of the La Ge Group, consists of continental sediments (red beds), tuff, hornblende andesite, dacite, and rare rhyolite (González de Juana *et al.*, 1980). Unconformably overlying the Jurassic La Ge Group is a Cretaceous-lower Tertiary section (Figure 2.10), which consists from bottom to top of a transgressive cycle (Rio Negro Formation, Cogollo Group, and La Luna Formation) and a regressive cycle (Colon, Guasare, Marcelina, Misoa, and the La Sierra formations). Kellogg (1985) identified four Cenozoic tectonic phases (Figure 2.10) and determined the ages of the uncomformities related to regional uplift during these phases, which are early Eocene (53 Ma), middle Eocene (45 Ma), late Oligocene (25 Ma), and Pliocene 3 Ma).

The Mérida Andes

The Mérida Andes are located east of Lake Maracaibo (Figure 2.6). They are the northward extension of the Eastern Andean terrane (Figure 2.9D). A review of the stratigraphy of the Merida Andes is given by González de Juana *et al.* (1980). The basement of the Mérida Andes consists of Precambrian and undifferentiated Paleozoic metamorphosed rocks (Figure 2.11A). Two phases of metamorphism have been recognized; the first of very low grade occurred in pre-Ordovician time; the later one occurred during the late Paleozoic and was of the greenschist-amphibolite facies of intermediate P/T regime (Grauch, 1975). Based on U/Pb ages determined in granites Burkley (1976) postulated three intrusive events during the Ordovican, Silurian-Devonian, and Permo-Triassic. The first two events may in reality be part of one continuous igneous event. In the southern flank of the Mérida Andes (Figure 2.11A) Ordovician and Silurian clastics and limestones have been found to overly the Precambrian-Cambrian metamorphics

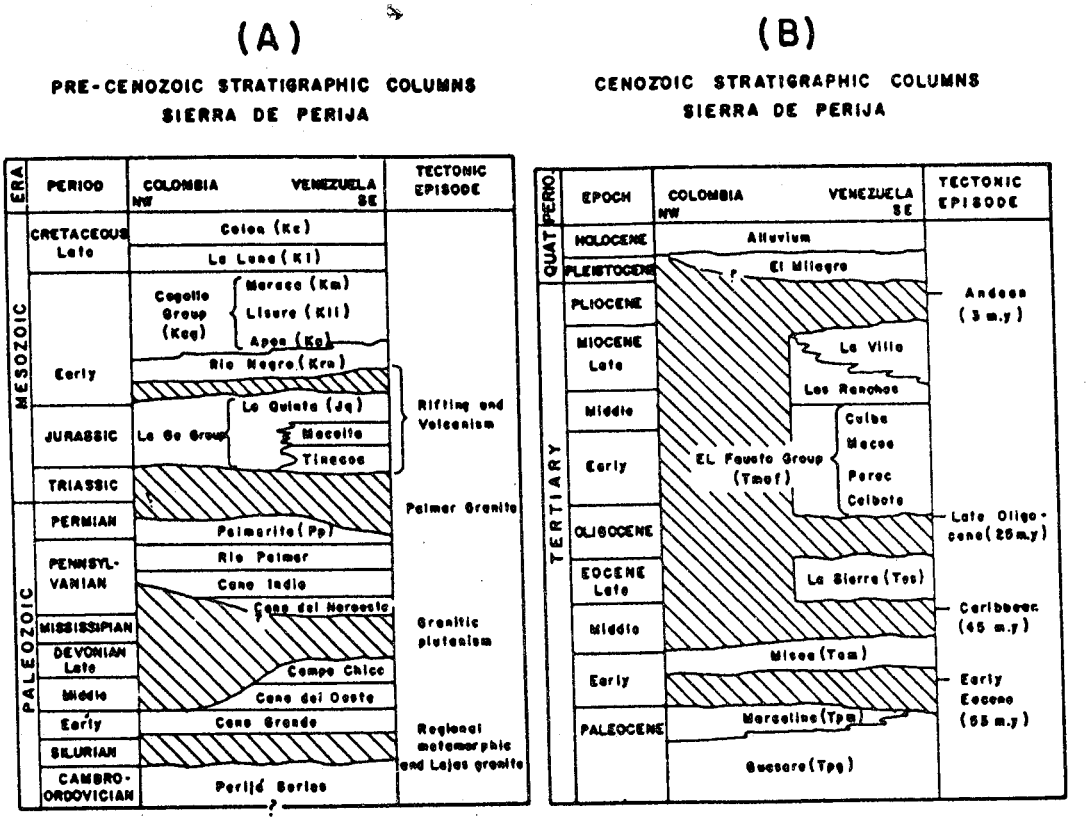

FIGURE 2.10: GENERALIZED PRE-CENOZOIC **(A)** AND CENOZOIC **(B)** STRATIGRAPHY OF THE SIERRA OF PERIJA (FROM KELLOGG, 1984).

(A)

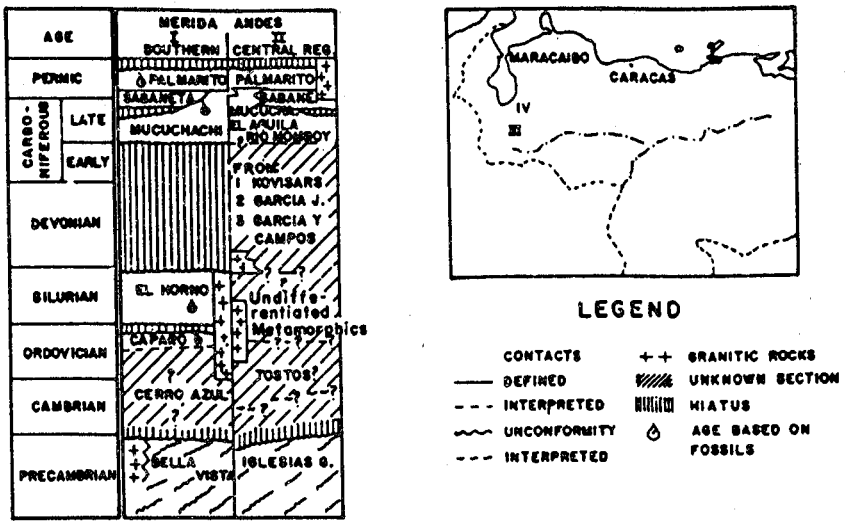

(B)

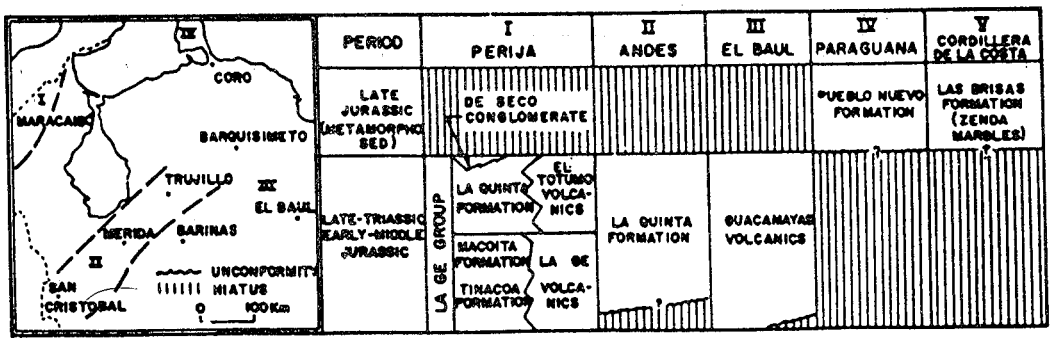

FIGURE 2.11: A. PRECAMBRIAN-PALEOZOIC STRATIGRAPHY OF THE MERIDA ANDES. **B.** TRIASSIC-JURASSIC STRATIGRAPHY OF NORTHWESTERN VENEZUELA (FROM GONZALEZ DE JUANA et al., 1980).

(González de Juana *et al.*, 1980).

The basement is overlain uncomformably by upper Paleozoic clastics, siltstone, marl, shale, and fossiliferous limestones (González de Juana *et al.*, 1980). The lower Mesozoic sedimentary sequence in the Mérida Andes (Figure 2.11B) consists of the La Quinta Formation, which consists of red clastics, tuff, shale, and calcareous siltstones (González de Juana *et al.*, 1980). Shagam (1975) and González de Juana *et al.* (1980) correlate the La Quinta Formation with La Ge Group in the Sierra de Perijá and the Guacamaya Volcanics in the Baúl Uplift (Figure 2.11B).

The Cretaceous sediments in the Mérida Andes (Figure 2.12A) consist of a lower-Upper Cretaceous transgressive cycle (Rio Negro Formation to La Luna Formation) and an Upper Cretaceous to Middle Eocene regressive cycle (Figure 2.12 B), from the Tres Esquinas Member or Colon Formation to the Mirador Formation and equivalents. González de Juana *et al.* (1980) described another middle-Upper Eocene transgressive cycle; maximum water depth was reached during the sedimentation of the flysch-type sediments of the Mene Grande Formation (Figure 2.12B). The sedimentation during the Oligocene-Pliocene in the west of Venezuela was controled by the Mio-Pliocene uplift of the Mérida Andes (González de Juana *et al.*, 1980).

Guayana Shield

Based on the petrological and tectonic observations, the Guayana shield in Venezuela is divided into four provinces: Imataca, Pastora, Cuchivero, and Roraima. The Imataca province consists of metasediments, granitic gneiss, and granitic intrusions, metamorphosed in the amphibolite and granulite facies (Dougan, 1972; Martin, 1975). Folding and partial melting occurred in the Imataca province during a 2.8 b.y. thermal event. At 2.1 b.y during the Transamazonic orogenesis (Hurley *et al.*, 1976), it was intruded by granitic magmas.

The Pastora province consists of metasediments and felsic and mafic volcanic rocks, locally intruded by gabbro and diabase dikes. The metamorphic assemblages are generally of low grade (Menendez, 1968). The terrane consists of rocks ranging in age from 2.7 b.y. to 2.0 b.y. (Martin, 1974). The Cuchivero province consists of felsic plutonic and volcanic rocks, metabasites, metasediments, and metavolcanics (Mendoza, 1977). The terrane was built up on a continental crust between 1.9 b.y. and 1.4 b.y. ago. After clastic sedimentation and felsic volcanism, regional

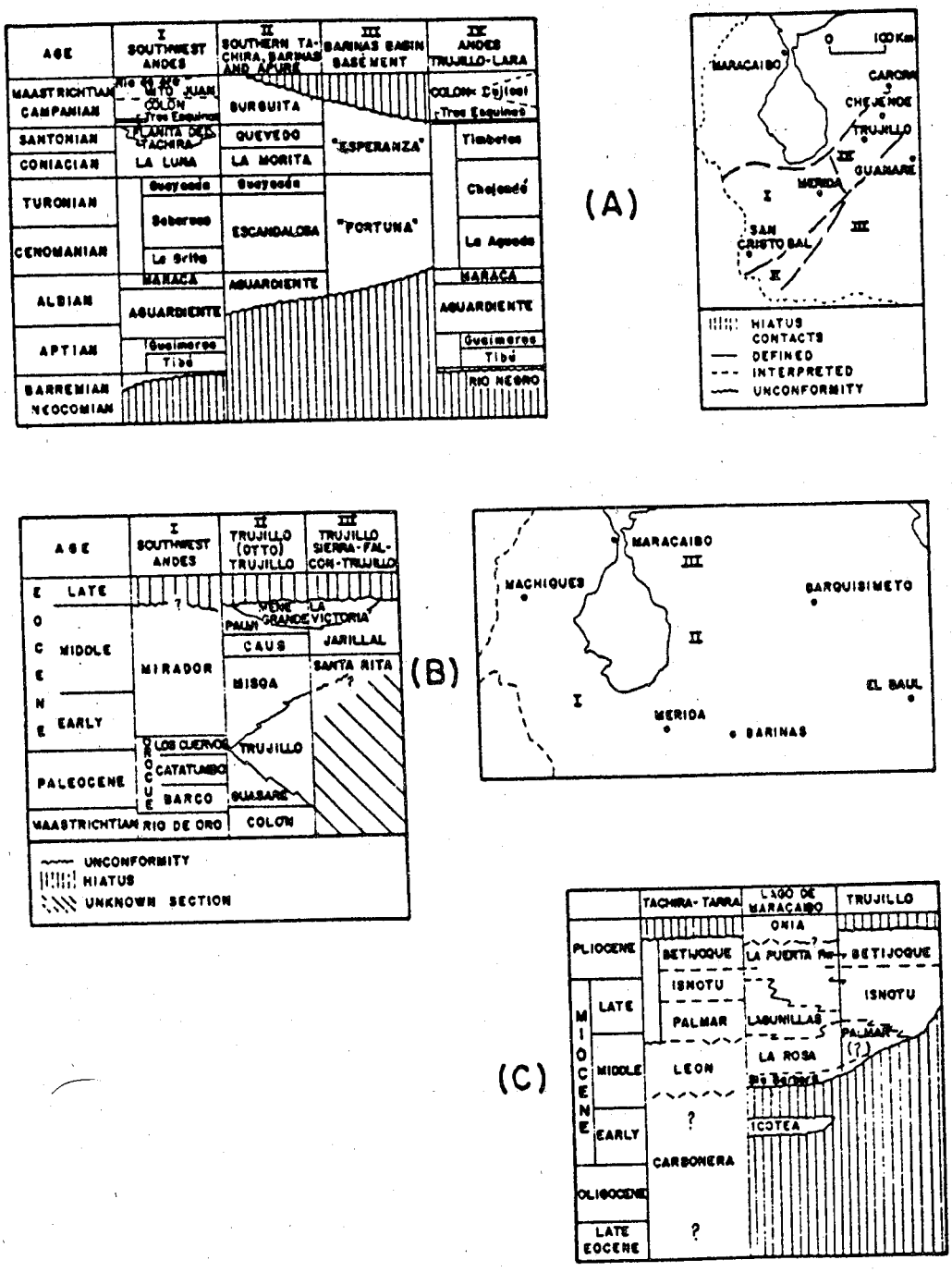

FIGURE 2.12: A. CRETACEOUS STRATIGRAPHY OF THE MERIDA ANDES AND ADJACENT REGIONS. **B.** MAESTRICHTIAN-LATE EOCENE STRATIGRAPHY OF THE MERIDA ANDES. **C.** LATE EOCENE-PLIOCENE STRATIGRAPHY OF THE MERIDA ANDES AND ADJACENT REGIONS. (FROM GONZALEZ DE JUANA et al., 1980).

metamorphism of the greenschist facies occurred, followed by a phase of granitic intrusions (Talukdar and Colvee, 1974). The Roraima Province consists of clastic sediments overlying metagabbros, granites, and diabases of the Pastora province (Ghosh, 1977). In Guyana, pyroclastic felsic beds occur in the central part of the clastic section, which have an age of 1599 Ma (Priem *et al.*, 1973).

The Guayana Shield was affected by a local thermal event, represented by the injection of tholeiitic magmas (Hawkes, 1966; Priem *et al.*, 1968; Choudhuri, 1978; Teggin *et al.*, 1985), 190 to 240 Ma ago (Priem *et al.*, 1968; MacDonald and Opdyke, 1974; Teggin *et al.*, 1985). This igneous activity in the Guayana Shield may correlate with the the volcanics of the El Baul Uplift (Gonzàlez de Juana *et al.*, 1980).

CHAPTER III

GEOLOGY OF THE STUDY AREAS

Introduction

The purpose of the present study was to get a better understanding of the tectonic setting of the terranes of northern Venezuela and to relate the deformational structures of these terranes to displacements resulting from the interaction between the Caribbean, South American, and Pacific lithospheric plates and possibly smaller microcontinental plates. The characterization of the tectonic setting is based on petrologic and geochemical studies, mainly of igneous rocks. The kinematics of deformation are based on deformational structures measured in the field but also in thin sections of orientated samples.

Three geological transects (Fig. 3.1 and 3.2) were made across the Caribbean Mountains system at a scale of 1:25.000, but reproduced in Plates 1, 2, and 3 at a scale of 1: 50.000. Additionally, several localities were visited and sampled mainly for petrologic and geochemical study. During the field work planar and linear structures (bedding planes, foliations, axial planes, crenulation cleavages, fault planes, fold axes, lineations, etc.) were measured and almost 500 samples were collected. Based on the field observations and the petrologic study carried out in the laboratory, several lithologic units were recognized and correlated with those previously described in the Venezuelan geological literature. However, in some cases, old units were redefined.

Chichiriviche-La Victoria Transect

The transect Chichiriviche-La Victoria extends from the beach along the Caribbean Sea, across the Cordillera de la Costa Range down to the town of La Victoria in the State of Aragua (Plate 1). Geologically, the transect crosses the Cordillera de la Costa-Margarita terrane and the Cordillera de la Costa belt. Along this transect several lithologic units have been distinguished; they are from north to south: (1) Nirgua Formation, (2) Peña de Mora Formation, (3) Antimano Formation, (4) Las Mercedes Formation, (5) Colonia Tovar Granite, and (7) Las Brisas Formation.

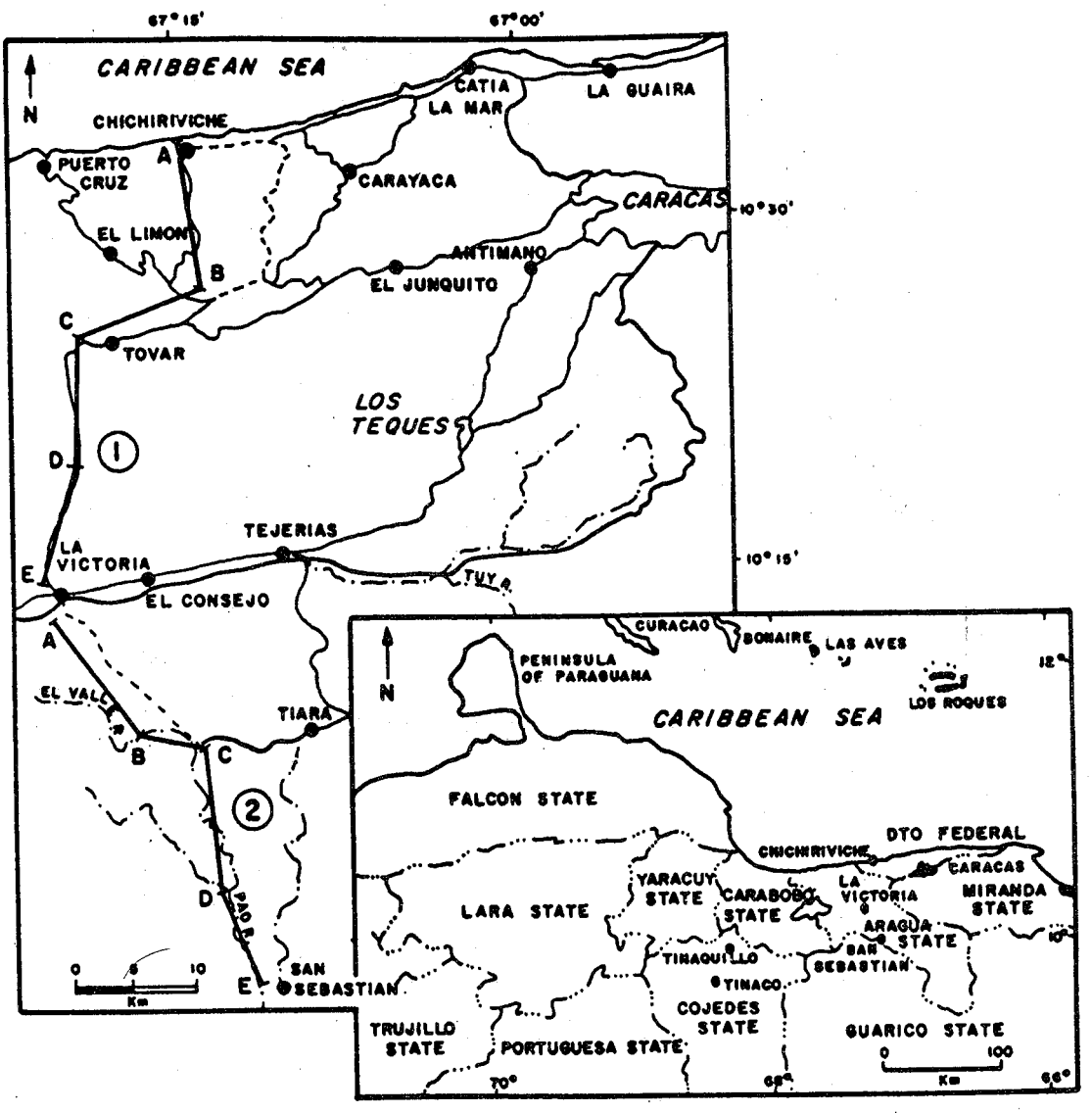

FIGURE 3.1 : LOCATION OF GEOLOGICAL TRANSECTS ACROSS THE CARIBBEAN MOUNTAINS SYSTEM. 1.- CHICHIRIVICHE - LA VICTORIA TRANSECT. 2.- LA VICTORIA - SAN SEBASTIAN TRANSECT.

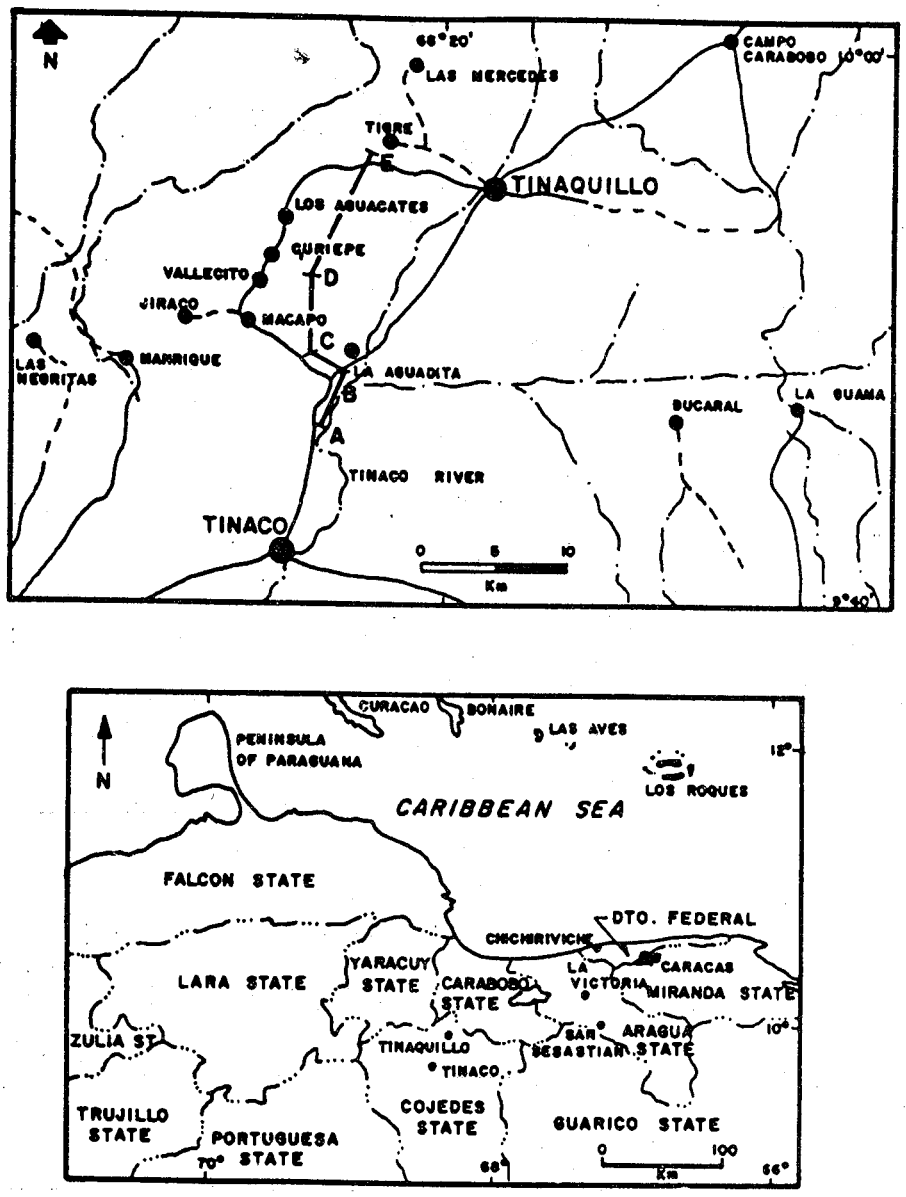

FIGURE 3.2 : LOCATION OF THE TINACO RIVER-CASUPO TRANSECT (A-E), STATE OF COJEDES.

Nirgua Formation

In the Chichiriviche-La Victoria transect, the best outcrops of the Nirgua Formation are along the shoreline and along the road through Oricao, Chichiriviche, and Puerto Cruz. Along the transect, this formation consists garnet amphibolite, quartz marble, serpentinite, and quartz-garnet-feldspar-biotite schist. Elsewhere, quartzite and glaucophanite schist occur. The amphibolites and the schists have garnet porphyroblats of up to 1.0 cm in diameter. The amphibolites and serpentinites occur as boudins and lenses 1 meter to 200 meters in lenght. Usually, the amphibolite boudins are no longer than 5 meters. The amphibolite boudins occur in the marbles and schists, while the serpentinites occur only in the schists.

The mineralogy of the amphibolites indicates that they underwent first a high P/T metamorphism (eclogite facies) and secondly a lower P/T greenschist facies metamorphism, which is also shown in the serpentinites, marbles, and schists (Chapter VI). The sheared metasedimentary matrix, the mafic-ultramafic boudins, and the flattening-shear style of deformation suggest that the unit is a tectonic melange formed in an accreationary wedge (Jacobi, 1984). The southern contact of this unit with the Peña de Mora Formation is not exposed, but a tectonic contact is interpreted (Chapter IV), along which the Nirgua Formation is thrust across the Peña de Mora Formation (Plate 1).

The age of the unit is unknown, but it is probably of Mesozoic age and the metamorphism may be Late Cretaceous (Talukdar and Loureiro, 1982). Fossils of Neocomian age have been found in the Nirgua metapelites in the State of Yaracuy (Bellizia and Rodriguez, 1968). The Nirgua Formation is correlated with the Antimano Formation on the mainland and with the La Rinconada Group on Margarita, both included in the Cordillera de la Costa-Margarita terrane (Gonzalez de Juana *et al.*, 1980; Urbani and Ostos, 1987). Based on major-element abundances Loureiro (1981) and Ostos (1981) proposed a mid-oceanic ridge affinity for this unit.

Peña de Mora Formation

The best outcrops of the Peña de Mora Formation are along the Chichiriviche River. It consists of biotite-feldspar augengneiss and schist. The "augen" are feldspars, which often have asymmetric pressure shadows. "Mica fish" and "S-C" (Berthé et al., 1979; Simpson and Schmid, 1983) surfaces also occur. Garnet is small, postectonic, and idioblastic. The schists are zones in the augengneisses and appear to have formed from the augengneiss by shearing. The

augengneiss has relict igneous textures. The mineralogy indicates that it underwent a greenschist facies metamorphism (Chapter VI). The Peña de Mora Formation is overlain by a klippe of the Antimano Formation (Chapter IV).

Traditionally, the Peña de Mora Formation has been believed to be of Mesozoic age and a member of the Caracas Group. However, recently published geologic and radiometric data indicate that the orthogneiss is not a syntectonic Mesozoic granite (Talukdar and Loureiro, 1982; Santamaria and Schubert, 1974), but that it is Precambian and Paleozoic (Urbani, 1983). The Peña de Mora Formation has been correlated with the Sebastopol Complex (basement of the Caracas Group) and with the Guaremal Granite in the State of Carabobo (Urbani and Ostos, 1987).

Antimano Formation

The Antimano Formation is well exposed along the Chichiriviche River and along the road between the villages Chichiriviche and Colonia Tovar. It consists of garnet amphibolite and albite-chlorite schist. The amphibolites have garnet porphyroblasts, which locally are 1 cm in diameter. The schists have albite porphyroclast with well developed symmetric pressure shadows. The amphibolite is a massive body, 1500 m long and 800 m wide, and is concordant with the schists. The contact with the Peña de Mora was not observed, but the Antimano Formation is interpreted to be a klippe (Chapter IV). The metamorphic assemblage recognized microscopically (Chapter VI) indicates that the formation first underwent a high P/ low T eclogite facies metamorphism and secondly an intermediate P/T greenschist facies metamorphism. The Antimano Formation has been correlated with the other mafic bearing units (Tacagua and Nirgua formations) in the central part of the Cordillera de la Costa-Margarita terrane.

The metamorphism of the unit (Chapter VI) and the major-element abundances (Loureiro, 1981; Ostos, 1981) suggest that it has formed in a mid-oceanic ridge setting and was metamorphosed in an accreationary wedge. The rocks of this unit have never been dated radiometrically. Maresch (1974), Talukdar and Loureiro (1982), and Beck (1986) believe that the unit is derived from basalts related to the Mesozoic rifting event between North and South America.

Las Mercedes Formation

The best outcrops of the Las Mercedes Formation in the northern flank of the Cordillera de la Costa Range are near the head waters of the Chichiriviche River (Mendoza, 1978)

and along the road between La Peñita and El Porton de la Colonia Tovar (Plate 1), but in these localities the weathering and the tropical jungle make it difficult to study the unit in detail. In the southern flank of the Cordillera de la Costa range, the formation is best exposed, along the Colonia Tovar-La Victoria road and the Aragua River (Plate 1). The Las Mercedes Formation consists of calcareous graphite schist and phyllite and quartz marble. The unit is crosscut by calcite, siderite, and quartz veins; such veins occur also in fold hinges. The schist has rare pyrite crystals with pressure shadows. The marble beds (from 5 cm to 5 m thick) are interlayered with the calcareous schists; their contacts are sharps, which may indicate an original bedding. The largest marble package is in the northern flank of the Cordillera de la Costa belt (Plate 1), where it is over 200 m thick. The contact of the Las Mercedes Formation with the Peña de Mora Formation and the Colonia Tovar Granite may be a low-angle normal fault or an original sedimentary contact, while the southern contact with the Las Brisas Formation is interpreted as a thrust fault (Chapter IV).

Microscopical study shows that the metamorphic assemblage is characteristic of the greenschist facies metamorphism (Chapter VI). The rocks of this unit have never been dated radiometrically, but Mesozoic fossils in the biohermic marbles have been found (Bellizia, 1972). The tectonic setting of this unit is unknown but a restricted basin between a Mesozoic Caribbean island arc and South America has been proposed (Talukdar and Loureiro, 1982).

Colonia Tovar Granite

The Colonia Tovar granite is well exposed near the head waters of the Tuy River close to La Colonia Tovar and along the road between the Porton de la Colonia and Pie del Cerro (Plate 1). However, this unit is not well preserved due to the tropical weathering which changes it to a clay and quartz rich soil. The unit consists of quartz mica gneiss crossed by abundant quartz veins of a maximum thickness of 20 cm. The Colonia Tovar granite has a gneissic texture with feldspar porphyroclasts, but it shows rarely augengneissic texture. The contact with the Las Mercedes Formation may be a low-angle normal fault or a sedimentary contact, while the northern contact with Las Mercedes Formation is a thrust contact (Chapter IV). A microscopic study shows that it contains more quartz and less mica than the Peña de Mora Formation. The mineralogic assemblage of this unit indicates that it underwent a greenschist facies metamorphism.

The protolith of this unit was thought to be Mesozoic

syntectonic granite and it was correlated with the Guaremal and Rancho Grande granites (Wehrmann, 1972). However, new radiometric data of the Guaremal Granite suggests a Precambrian to Paleozoic age (Urbani, 1983, 1988). Thus, it can be correlated with the Peña de Mora Formation. It may be the basement above which the Mesozoic Caracas Group was deposited.

Las Brisas Formation

The Las Brisas Formation is exposed close to La Victoria, along the Aragua River and along the road between Pie del Cerro to La Victoria. It consists of calcareous metagraywacke and metaconglomerate, quartz schist, and rare calcareous quartzite. The coarser lithologies are the most abundant in the study area. They contain rounded quartz and feldspar porphyroclasts. The original bedding is well preserved and it parallels the foliation. The mineralogic assemblage of the unit indicates that it underwent a greenschist facies metamorphism (Chapter VI). The southern contact of this unit is covered by Quaternary sediments, but it has been interpreted to be the La Victoria right-lateral strike-slip system (Menendez, 1966). The northern contact with the Las Mercedes Formation is interpreted as a thrust contact, along which the Las Brisas Formation is thrust across the Las Mercedes Formation (Chapter IV).

The rocks of this unit have never been radiometrically dated but near Caracas shallow water Late Jurassic fossils occur (Urbani, 1969). The Las Brisas Formation has been correlated with the feldspathic unit of the Juan Griego Group on Margarita Island (Vignali, 1976, 1979). The Las Brisas Formation may have been deposited on the South American Atlantic-type margin which developed in the Jurassic by rifting and separation of North and South America (Maresch, 1974; Talukdar and Loureiro, 1982).

La Victoria - San Sebastian Transect

The La Victoria-San Sebastian transect is the southerly extension of the Chichiriviche-La Victoria transect. Both transects are approximately north-south trending. The southern transect goes through the Caucagua-El Tinaco belt (Guacamaya Metadiorite and Tucutunemo Formation), the Paracotos belt, and the Villa de Cura belt. It terminates at the contact with the foreland fold and thrust belt (Plate 2). Along the transect several lithologic units have been distinguished; they are from north to south: (1) the Tucutunemo Formation, (2) La Guacamaya Metadiorite, (3) Paracotos Formation, and (4) Villa de Cura Group and Dos

Hermanas Formation.

Tucutunemo Formation

The Tucutunemo Formation, in particular its lower member, the Los Naranjos Volcanics, is well exposed along the Toro River and along the road from La Victoria to La Candelaria (Plate 2). The Tucutunemo Formation consists of muscovite-chlorite schist, volcanic-rich metaconglomerate, quartz marble, graphite phyllite, and amphibolite. Volcanic-rich metaconglomerate, graphite schist, and amphibolite boudins are the characteristic lithologies of the Los Naranjos Member. The schistose section is best exposed along the transect and it frequently shows well developed kink bands and crenulation cleavage.

The contact with the La Guacamaya Metadiorite north of the Taguayguay fault is interpreted as a normal fault. In the south, the contact of the Tucutunemo with the Paracotos Formation and with unnamed serpentinite bodies is probably also a low-angle normal fault (Chapter IV). The metamorphic assemblage of the Tucutunemo Formation indicates that it was metamorphosed in the greenschist facies (Chapter VI). The metamorphic age of this unit is Campanian-Maastrichtian (Chapter VIII) as determined by K/Ar dating (Beck, 1986). A Permian age of deposition has been suggested by the fossils found by Benjamini *et al.* (1987). Shagam (1985) correlated the marbles of the Tucutunemo Formation with the Palmarito Formation in the Andean terranes of northwestern South America. Beck (1985b, 1986) suggested a mid-oceanic ridge affinity for the amphibolite boudins in the Tucutunemo Formation.

La Guacamaya Metadiorite

The La Guacamaya metadiorite defined by MacLachlan *et al.* (1960) is well exposed along the road between La Victoria and La Candelaria and from the head waters of the Curujujul River to the confluence with the Toro River (Plate 2). The metadiorite looks very fresh in the field but microscopic studies show a strong alteration of the plagioclase. These rocks vary from massive to sheared; locally a well developed foliation and lineation occur. Mineralogically, the unit consists of plagioclase-hornblende and plagioclase-hornblende-augite gneisses. The foliation is nematoblastic, being defined by shape orientation of hornblende and quartz. Texturally, flaser and mylonite structures are frequent in this metaigneous body. A microscopic study shows that the quartz crystals are recrystallized to shape orientated neoblasts; rare kinked plagioclase occurs, and hornblende porphyroblasts are rimming clinopyroxenes.

The contact of the Guacamaya metadiorite with the Tucutunemo Formation south of the Taguayguay fault is interpreted as a thrust fault (Chapter IV). The metamorphic assemblage of these rocks indicate that they underwent an amphibolite facies metamorphism (Chapter VI). The rocks of this igneous body have never been dated radiometrically, but MacLachlan *et al.* (1960) suggested that they intruded into the Precambrian La Aguadita Gneiss (basement of the Caucagua-El Tinaco belt) during the Paleozoic.

Paracotos Formation

The Paracotos Formation is very well exposed along the Pao River, down streams of the confluence with the Paito River (Plate 2). An additional reference section in the studied area is along the road that parallels the Pao River between the villages La Candelaria and Guaipo (Plate 2). The Paracotos Formation is a flysch deposit consisting of lithic metagraywacke and metaconglomerate, lithic schist, calcareous phyllite, and marble. Metagraywacke boudins occur frequently in the phyllites. The more common lithologies are schist, phyllite, and metasandstone. The coarser lithologies usually show volcaniclastic and volcanic fragments larger than 0.25 cm in lenght. The marbles occur as layers of up to 2 meters and as larger exotic blocks. Mesoscopic folds and kink bands are common in the pelitic part of the unit. The original bedding in the unit is preserved and parallels the foliation.

The northern contact with the serpentinites and with the Tucutunemo Formation is interpreted to be a low-angle normal fault, while the southern contact with the Villa de Cura Group is assumed to be a thrust fault (Chapter IV). The metamorphic assemblage of the Paracotos Formation indicates that it underwent very-low grade prehnite-pumpellyite facies metamorphism (Chapter VI). Late Cretaceous fossils in marbles from the Paracotos Formation have been recognized (Oxburgh, 1965). It has been correlated with the southern unmetamorphosed Tertiary Guarico flysch (Menendez, 1966).

Villa de Cura Group and Dos Hermanas Formation

The Villa de Cura belt in the transect studied consists of the Villa de Cura Group (Shagam, 1960; Navarro, 1983) and Dos Hermanas Formation (Girard, 1981; Girard *et al.*, 1982; Beck, 1986). The Villa de Cura Group is well exposed along the Pao River between the village of Casupo and the Tres Picos Hill (Plate 2). The Dos Hermanas Formation has good outcrops from the Tres Picos Hill down to the contact with the Tertiary foreland sediments, approximately four km down streams (Plate 2). Along the transect three lithologic

units in the Villa de Cura Group were distinguished; they are from south to north: the Granofels Unit, the Metalava Unit, and the Metatuff Unit.

The Granofels and Metatuff units are heavily deformed. Many structures such as "S" and "Z" folds, extension veins, crenulation cleavages, and kink bands have been observed. The Granofels Unit consists of quartz-feldspar schist, granofels, metaradiolarite, chlorite schist, and metaspilite. The most abundant lithology in this unit is the chlorite schist, but the characteristic lithology is the granofels. A microscopic study shows that the granofels contains rounded quartz porphyroclasts, which suggest a sedimentary protolith.

The Metalava Unit consists of metatuff, medium-grained metasedimentary rocks, and pyroxene metalavas. The most abundant lithology is the metatuff, but the most characteristic lithologies are the metalavas, in which rarely pillow structures have been observed.

The Metatuff Unit consists of laminated and banded metatuff (more than 90 %) and metaspilites. The Granofels and the Metalava units have the highest content of metalavas and deep-sea sediments, while the Metatuff Unit is mainly a volcaniclastic unit. The contact of the Villa de Cura Group with the Paracotos Formation is interpreted as a south-dipping thrust fault (Agua Fria fault). The southern contact with the Dos Hermanas Formation is also interpreted as a thrust fault, but it is dipping north (Chapter IV; Plate 2). The mineralogic assemblages of the Villa de Cura Group indicate that it underwent a high P/ low T metamorphism. The metamorphic zones in the Villa de Cura Group vary from north to south: pumpellyite-actinolite, lawsonite-albite, lawsonite-glaucophane, glaucophane-epidote, barroisite, and glaucophane-barroisite, which suggests a metamorphic path from the pumpellyite-actinolite facies to the blueschist facies. However, the foliation is defined by the orientation of a greenschist and pumpellyite-actinolite paragenesis; thus, a lower P/T greenschist facies metamorphism overprints the earlier high P/ low T metamorphic assemblages (Chapter VI).

Isotopic K/Ar ages ranging from 77 to 107 Ma have been determined for the Villa de Cura Group (Chapter VIII) and Aptian-Albian fossils were described by Johnson (1965). The Villa de Cura Group has been correlated with the island arc sequences on the Dutch Leeward Islands (Maresch, 1974; Beets *et al.*, 1984; Beck, 1985b, 1986; Bellizia, 1985). The tectonic setting of these rocks is debatable. Based on major- and trace-element abundances (Beets *et al.*, 1984)

and on pyroxene composition (Loubet *et al.*, 1985) an island arc tectonic affinity has been proposed. Instead, Navarro (1983) based on major- and trace-element abundances and on the metamorphic path, interpreted that it has a mid-oceanic ridge affinity.

The Dos Hermanas Formation consists of pyroxene lava, volcanic breccia, and tuff. Original igneous structures, such as pillows, volcanic agglomeration, lava channels, and lava brecciation are preserved in this unit. The formation is mostly made up of tuff and breccia. The tuff consists of ash and lapilli size fragments of volcanic rocks and rarely mineral fragments. The southern contact of the Dos Hermanas Formation was interpreted as a thrust contact, along which it was thrust southward across the Tertiary flysch sediments (Chapter IV; Plate 2). A microscopic study shows that the Dos Hermanas Formation underwent prehnite-pumpellyite metamorphism (Chapter VI). Four K/Ar ages for the Tiara Sur Formation which has been correlated with the Dos Hermanas Formation (Beck, 1986) are from 34.7 Ma to 119 Ma (Chapter VIII). Based on major- and trace-element abundances and on pyroxene composition, Girard (1981) and Navarro (1983) believe that the lavas of the Dos Hermanas Formation are derived from basalts and andesites extruded in an island arc environment.

Tinaco River - Casupo Transect

The Tinaco River-Casupo transect (Plate 3) crosses the Caucagua-El Tinaco belt near the village La Aguadita, along the nearby Tinaco River, through the Tinaquillo Peridotite Complex, and in the north the Las Mercedes Formation of the Cordillera de la Costa belt. The tectonostratigraphic units studied in this transect are from south to north: (1) the La Aguadita Gneiss of the Tinaco Complex, (2) the Tinaquillo Peridotite Complex, and (3) the Las Mercedes Formation.

La Aguadita Gneiss

The La Aguadita Gneiss is well exposed along the Tinaco River south of the confluence with the Macapo River (Plate 2). It consists mainly of hornblende-plagioclase gneisses intruded by trondhjemites. Even though regional metamorphism and deformation have affected the complex, cross-cutting relationships can still be observed. The trondhjemite is a stock, which appears to be cogenetic with the abundant trondhjemitic sills and dikes (thickness from 20 cm to 10 meters). Toward the contact with the Tinaquillo Peridotite Complex, the Tinaco Complex changes to feldspar-quartz schists and gneiss, the textures of which suggest both

igneous and sedimentary protolith.

The gneiss contains amphibolite layers, boudins, and lenses. The feldspar-quartz schists contain rarely thin layers (thinner than 10 cm) of mica and chlorite-rich schist and phyllite, which resembles a sedimentary bedding. The amphibolite boudins and lenses occur in the feldspar-quartz schists (dimensions of 0.5 meters to 30 meters). The contact of the La Aguadita Gneiss with the Tinaquillo Peridotite Complex appears to be concordant (Chapter IV; Plate 3).

A microscopic study of the gneisses and trondhjemites along the Tinaco River shows several relict igneous textures overprinted by shear textures (Chapter VI); the amphibolite layers toward the contact with the Tinaquillo Peridotite Complex and the hornblende-rich gneisses in the Tinaco River have commonly hornblende rimming pyroxene relicts, which may indicate that the complex has undergone an amphibolite facies metamorphism, that overprints an earlier granulite facies metamorphism (Chapter VI). The later event also affected the rocks of the Tinaquillo Peridotite Complex. The rocks of the La Aguadita Gneiss have been dated by the K/Ar method, which yielded ages from 112.4 to 684 Ma (Chapter VIII). The La Aguadita Gneiss has been correlated with the Sebastopol Complex (MacKenzie, 1960), which is the Precambrian-Paleozoic basement of the Cordillera de la Costa belt.

Tinaquillo Peridotite Complex

The Tinaquillo Peridotite Complex is very well exposed in the northern hill of the Tetas de Tinaquillo (Plate 3). It consists of harzburgite, dunite, serpentinite, metagabbro, and pyroxenite. It has a mylonitic foliation and a well developed mineral lineation (Chapter IV). The harzburgite is the most abundant lithology and pyroxenite is the less frequent lithology. The latter is cross-cutting the foliation or parallels it. The harzburgites show a very well developed porphyroclastic texture, with enstatite and spinel as the most common porphyroclasts.

The dunites are interlayered with the harzburgites, the layers reaching maximum thickness of 30 cm. The serpentinites are mainly located toward the contact with the Las Mercedes Formation, although some serpentinization also occurred toward the contact with the La Aguadita Gneiss. The metagabbros are most ubiquitous toward the northern and southern contact of the complex. They occur in lenses, 50 meters to over 2000 meters long. The metagabbros have rare hornblende porphyroblasts and garnet porphyroclasts 1.5 cm

in length.

In the north, the Tinaquillo Peridotite Complex is in thrust contact with the Las Mercedes Formation (The Manrique thrust). In two outcrops along the Manrique fault (Plate 3), folds in the Las Mercèdes Formation suggest that the Tinaquillo Peridotite Complex was thrust northward across the Las Mercedes Formation. A K/Ar age determination of pyroxene presumably from the Tinaquillo Peridotite Complex yielded an age of 684 ± 55 Ma (Urbani, 1982). Beck (1985b, 1986) correlated this unit with the lower Cretaceous Loma de Hierro ophiolite.

Las Mercedes Formation

The Las Mercedes Formation crops out north of the Manrique thrust (Plate 3) which is the contact of the Las Mercedes Formation with the Tinaquillo Peridotite Complex. This formation is not well exposed. It consists of calcareous graphite phyllite and quartz marble. The Las Mercedes Formation is intensely folded. Calcite, siderite, and quartz veins cross-cut the foliation and occur also in fold hinges. The marble layers vary from beds of a minimum thickness of 3 cm to marble packages, over 50 meters thick, concordant with the foliation in the phyllites. The phyllites frequently show extension veins filled with calcite and pyrite crystals with pressure shadows filled with calcite fibers.

The mineralogic assemblage of the Las Mercedes Formation indicates that it underwent a greenschist facies metamorphism (Chapter VI). The Mesozoic fauna described by MacKenzie (1960, 1966) within the thick marbles indicates a biohermal origin. The Las Mercedes Formation has been correlated with the non-feldspathic unit of the Juan Griego Group of Margarita Island (Vignali, 1979). Talukdar and Loureiro (1982) suggested that it was deposited in a basin between the Cretaceous Caribbean island arc system and South America.

CHAPTER IV

STRUCTURAL GEOLOGY

Introduction

As described before, the Caribbean Mountains system is divided into four tectonic belts each of which has characteristic lithologies and ages (Menendez, 1966). The tectonic belts are from north to south: (a) Cordillera de la Costa belt, which is bounded to the north by the San Sebastian strike-slip fault and to the south by the La Victoria right-lateral strike-slip fault system, (b) Caucagua-El Tinaco belt bounded to the south by the Santa Rosa normal fault, (c) Paracotos belt, which is bounded to the south by the Agua Fria thrust fault, and (d) Villa de Cura belt, which toward the south is in thrust contact with Paleogene sediments (Figures 1.4 and 2.1). Stephan *et al.* (1980), Beck (1985), and Stephan (1985) divided the Cordillera de la Costa belt into de Cordillera de la Costa s.s. and the Coastal Fringe-Margarita terrane or Cordillera de la Costa-Margarita terrane. The latter is exposed along the coast and it is thrust southward across the Cordillera de la Costa belt s.s. (Figure 1.4). The Cordillera de la Costa-Margarita terrane consists mostly of high P/low T metamorphosed mafic rocks.

The structural history of each belt was determined in the field by studying the style and by measuring the orientation of the deformational structures. These structures include brittle (faults) and ductile (folds) structures. Unfortunately, however, faults are rarely exposed in the region, and their orientation and sense of slip were only inferred. Folds were studied by measuring their axial planes and their axes. Foliations and cleavages are generally subparallel to the fold axial planes and were also measured. Several generations of folds occur in the area. Relative ages of the phases of deformation responsible for the different generations of folds were determined by studying cross cutting relationships. The relationships between folds and faults is obscure, because the faults are not exposed. However, an attempt has been made here to relate faults and folds on the basis of dynamic compatibility.

The structural history of each belt was also studied in the laboratory. Thin sections of orientated samples were studied with the petrographic microscope not only to determine the composition of the rocks (Chapter III) and the metamorphic

grade (Chapter VI), but also to look for and analyze kinematic indicators to determine sense of shear of the different phases of deformation.

Meso- and Mega-scopic Structures

The Cordillera de la Costa Belt

The Cordillera de la Costa belt is characterized by east-west and northwest-southeast trending strike-slip faults, northeast-southwest to east-west trending thrust faults, and east-west trending antiforms and synforms (Dengo, 1951; Wehrmann, 1972; Urbani and Ostos, 1987; Urbani *et al.*, 1987b; Urbani *et al.*, 1988). A structural analysis of the Cordillera de la Costa belt was carried out during this research along the Chichiriviche-La Victoria transect (Plate 1) and in El Avila National Park, north of Caracas (Figure 5.2).

First Deformation: D_1

The oldest structures observed in the field are isoclinal folds with an axial-plane foliation (S_1) and a mineral lineation (L_1). This first phase of deformation is clearly recognizable in the metasedimentary sequences (Las Brisas and Las Mercedes formations). In the dismembered ophiolites (amphibolites and serpentinites) and in the granitic gneisses of the Peña de Mora Formation and Colonia Tovar Granite, a strong foliation occurs (S_1), but no isoclinal folds were found. The foliation (S_1) in the metasediments and serpentinites is lepidoblastic; a nematoblastic schistosity is developed in the amphibolites, while the basement has a mylonitic foliation.

The foliation in the granitic Peña de Mora Formation along the Chichiriviche-La Victoria transect dips generally very gently to the north, although there are a few southerly dips (Figure 4.1A). The lineations are subhorizontal and trend east-northeast-west-southwest (Figure 4.1A). Poles to the foliation of the Peña de Mora Formation in El Avila National Park form a north-south trending girdle; most foliations dip gently to the north (Figure 4.1B). Only few lineations were measured; they are subhorizontal and trend northwest-southeast to east-west (Figure 4.1B).

Poles to the foliation in the Caracas Group and the Colonia Tovar Granite along the Chichiriviche-La Victoria transect are contained in a north-south striking girdle and most of the foliations dip shallowly to the south (Figure 4.2A). The mineral lineations are variable but tend to plunge

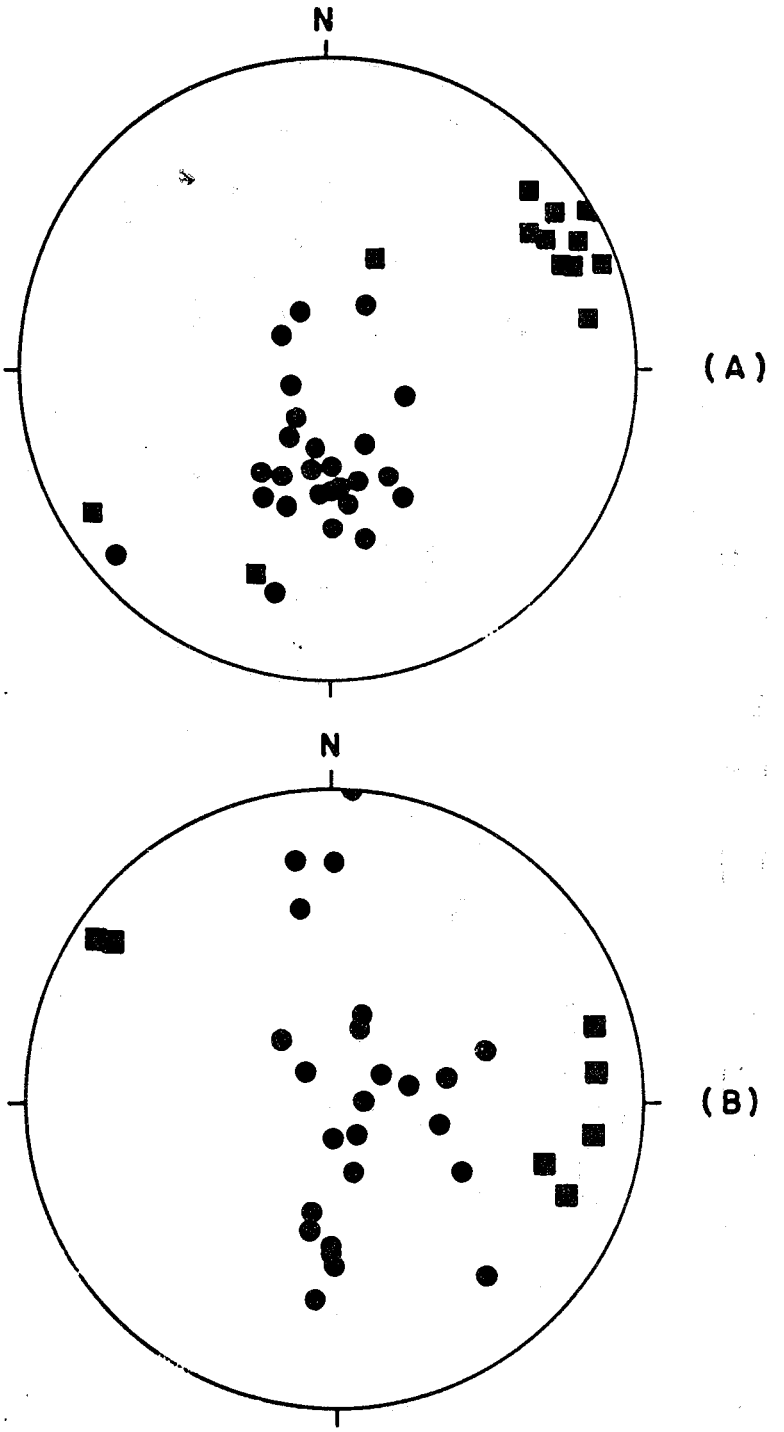

FIGURE 4.1 : EQUAL-AREA, LOWER-HEMISPHERE PROJECTION OF POLES TO FOLIATION (S_1 , dots) AND MINERAL LINEATIONS (L_1, Squares) IN THE PEÑA DE MORA FORMATION ; A. CHICHIRIVICHE - LA VICTORIA TRANSECT, B. EL AVILA NATIONAL PARK..

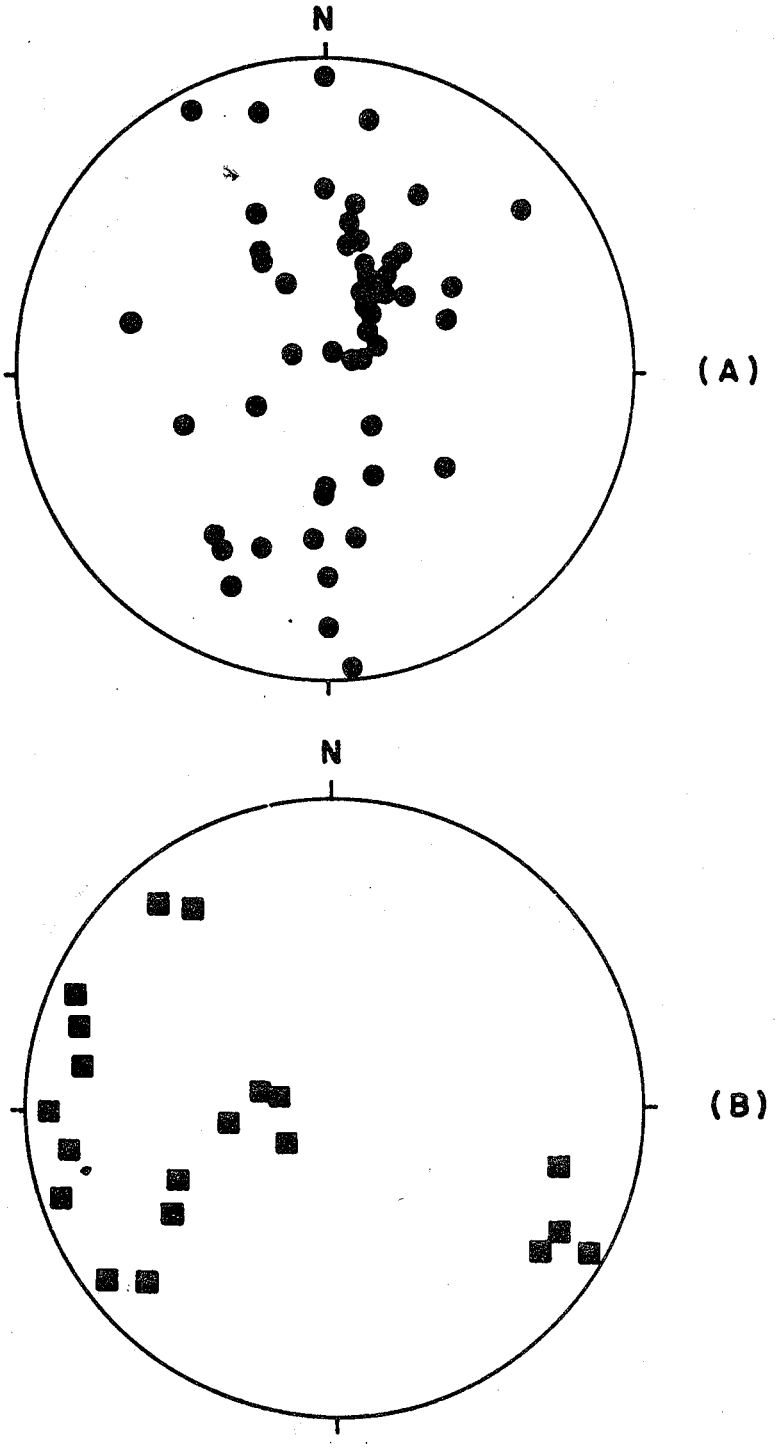

FIGURE 4.2 : EQUAL-AREA, LOWER-HEMISPHERE PROJECTION OF A. POLES TO THE S_1 FOLIATION (dots) AND B. L_1 MINERAL LINEATIONS (Squares), IN THE CARACAS GROUP AND THE COLONIA TOVAR GRANITE.

gently to moderately to the west (Figure 4.2B).

A dismembered ophiolite in El Avila National Park north of Caracas was mapped by Ostos (1981). This area was revisited several times to obtain samples for geochronology and to redetermine better the contacts between the units. For comparison, the foliations in the dismembered ophiolite are shown in Figure 4.3A. The poles to the foliation form a broad north-south trending girdle, with a maximum of foliations dipping to the north.

Second Deformation: D_2

As can be seen on the maps of the geologic transect and cross section (Plate 1), the penetrative S_1-foliations in the granitic basement are folded into large wavelength, gentle to open folds and in the metasediments into shorter wavelenght open folds. The north-south trending girdle of S_1 poles (Figure 4.2A and 4.3A) supports this folding event. The folds trend approximately east-west.

Additionally, mesoscopic folds ("S and Z") are associated with this second deformation; they are better developed in the metasediments. The fold axes generally plunge gently to the west-southwest (Figure 4.3B). The poles to D_2 axial planes form a broad northwest-southeast trending girdle; most axial planes dip gently to the southeast (Figure 4.3B).

A crenulation cleavage was frequently observed in thin sections of the metasediments and in few cases an incipient micaceous orientation was observed in these cleavages planes. Several measurements were made in the field and frequently a genetic relationship between the mesoscopic folds and the crenulation cleavage was observed. The crenulation cleavage has variable orientation; it shows a strong maximum striking northeast-southwest and dipping moderately to the southeast (Figure 4.4).

Faults

The Cordillera de la Costa belt is crosscut by many faults. As they are not exposed, their orientation and kinematics were mostly derived from the study of airphotos and radar imagery. For the present study, airphoto and radar imagery interpretation was carried out on the areas that were studied geologically. The results are completely in accord with more regional studies by Bellizia and Pimentel (1976) and Schubert (1984). Schubert (1984) proposed that the east-west strike-slip faults are right-lateral, based on the development of pull-apart basins. The offset of the northwest-southeast strike-slip faults is not well

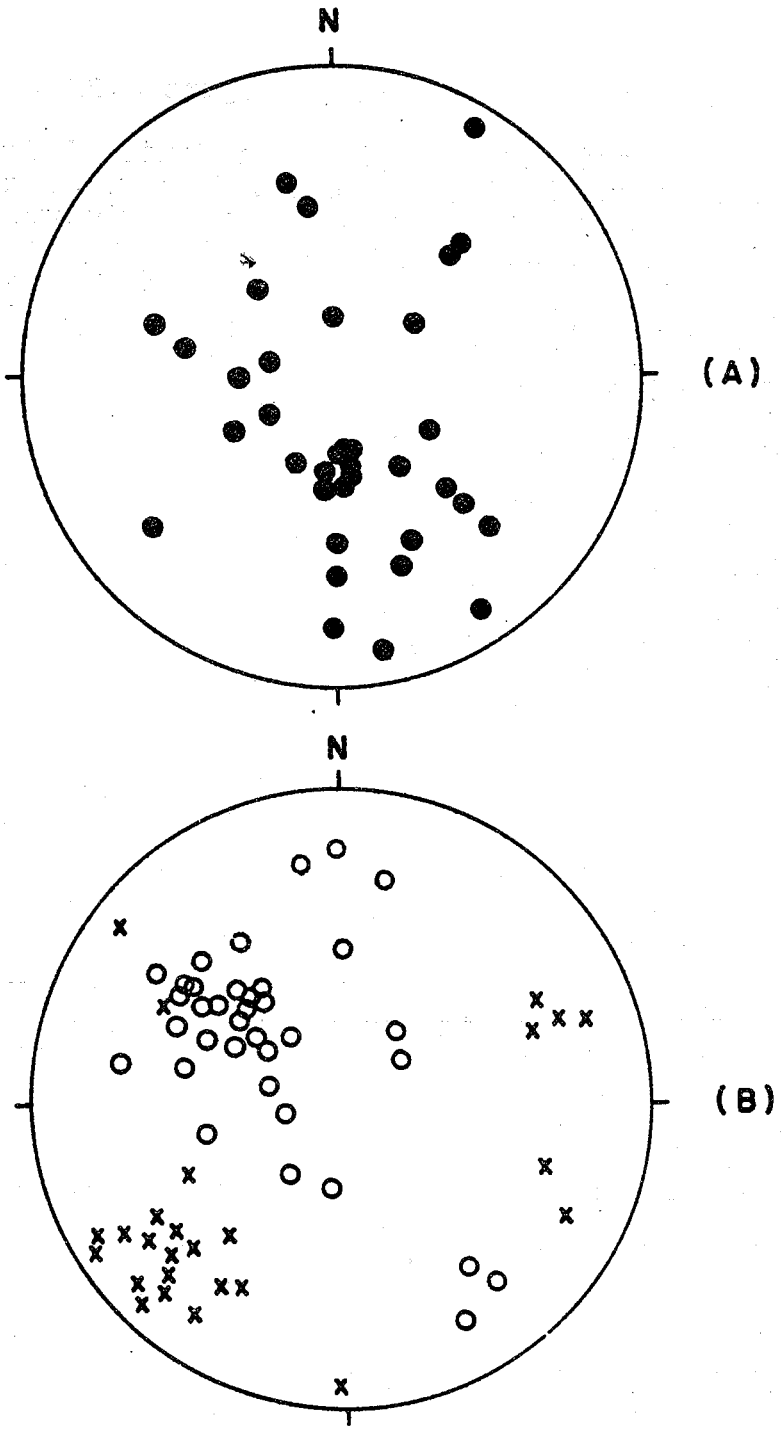

FIGURE 4.3 : EQUAL-AREA, LOWER-HEMISPHERE PROJECTION OF A. POLES TO S_1 FOLIATION (dots) IN ANTIMANO FORMATION AND THE SERPENTINITE UNIT IN EL AVILA NATIONAL PARK AND B. POLES TO S_2 AXIAL PLANES (empty dots) AND β_2 FOLD AXES (crosses) IN THE CORDILLERA DE LA COSTA BELT, ALONG THE CHICHIRIVICHE-LA VICTORIA TRANSECT..

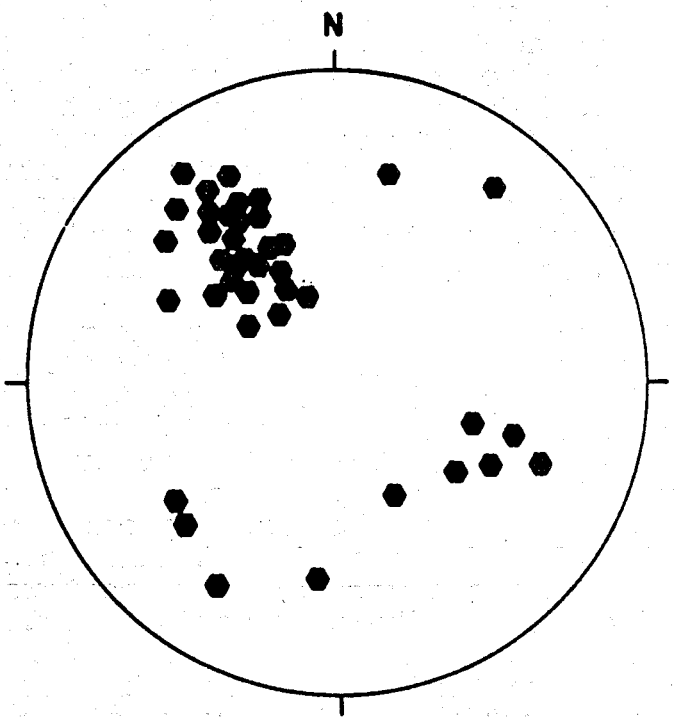

FIGURE 4.4 : EQUAL-AREA, LOWER-HEMISPHERE PROJECTION OF POLES TO THE CRENULATION CLEAVAGE (hexagons) IN THE CORDILLERA DE LA COSTA BELT, ALONG THE CHICHIRIVICHE-LA VICTORIA TRANSECT..

constrained. However, Beck (1985b, 1986), Soulas (1985) proposed a right-lateral offset along a major northwest-southeast strike-slip fault (Tacata fault; Figure 1.4), in the south-central Caribbean Mountains system, also based on pull-apart basins (Santa Lucia basin). The east-west trending thrust faults have been interpreted as south vergent faults by Stephan *et al.* (1980) and Beck (1985b; 1986).

In the study area (Plate 1), the contacts between the granitic Peña de Mora Formation and the Antimano and Nirgua formations are tectonic as indicated by the melange belt overlying the Peña de Mora Formation. Futhermore, the high P/low T metamorphic relict assemblage of the Antimano and Nirgua formations, indicates that they must have been thrust on top of the granitic basement. The contact between the granitic basement and the Las Mercedes Formation does not show metamorphic discontinuity; thus, this contact may be a depositional contact, although no erosional features were identified. Or it may be a low-angle normal fault.

The Mesozoic Caracas Group shows a complex relationship with the Paleozoic Colonia Tovar Granite (Plate 1). In the north, the Colonia Tovar Granite overlies the Las Mercedes Formation, suggesting a thrust contact, while in the south the granite underlies the Lower Cretaceous Las Mercedes Formation suggesting a low-angle normal fault relationship. To the south, the Jurassic Las Brisas Formation is overlying, clearly along a thrust contact, the Lower Cretaceous Las Mercedes Formation. The northwest-southeast trending right-lateral strike-slip faults (Plate 1) crosscut the second phase folds and regionally, they offset the thrust faults (Figure 2.2). Thus, they may be tear faults related to the thrusting. The trace of the east-west trending La Victoria right-lateral strike-slip fault is located in the southermost part of the Chichiriviche-La Victoria transect (Plate 1), where Schubert (1984) proposed the development of the Valencia Lake pull-apart basin. There are not kinematic indicator on this fault. The trace of the San Sebastian right-lateral strike-slip fault was not found during the study of the transect, because it is assumed that it lies futher north, along the platform (Figure 1.4).

The east-west trending thrust and right-lateral strike-slip faults and the northwest-southeast trending right-lateral strike-slip faults can be interpreted as having formed during the development of a compressive bridge (Gamond, 1987). The east-west right-lateral strike-slip faults are the primary structures. The left-stepping "en-echelon" northwest-southeast trending right-lateral strike-slip faults are secondary structures. The large compressive

bridge between two secondary faults causes upward displacement by folding and thrusting. The fold axes may have a sigmoidal shape and may rotate toward an east-west trend. The Gamond-model may explain the east-west trending thrusts and D_2 folds recognized in the area. If the contact between the Peña de Mora Formation and the Caracas Group is a low-angle normal fault, it could also have been the consequence of the extension along the main east-west dextral strike-slip system. Thus, it can be also included in the second phase of deformation.

Caucagua-El Tinaco Belt, State of Aragua

The structural geology of the Caucagua-El Tinaco belt is as poorly known as the other belts in the Caribbean Mountains system. The structural information available is very spotty. Menendez (1966) interpreted the east-west Santa Rosa fault, which is bounding the belt to the south as a thrust fault. Beck (1985) proposed that the Loma de Hierro ophiolite and the Rio Guare Beds were overthrust to the north during an Early Cretaceous orogeny. Beck (1985b, 1986) and Soulas (1985) recognized a right-lateral offset along the northwest-southeast trending Tacata fault. This fault may have been active during the Neogene.

In the present study, the Caucagua-El Tinaco belt was examined along the La Victoria-San Sebastian transect, in the State of Aragua (Plate 2). The deformation of the belt south of La Victoria seems least complex, but this may be due to the weathering and to the bad exposures. Still, different structures were observed and two phases of deformation were recognized.

First Deformation: D_1

The oldest structures observed along the La Victoria-San Sebastian transect are developed in the metasediments and metavolcaniclastics of the Tucutunemo Formation. They consist of isoclinal folds and an intense foliation parallel to fold axial planes. The foliation (S_1) is also a penetrative structure in the La Guacamaya Metadiorite, but no isoclinal folds were observed. The poles to the foliations occur in a north-south girdle; the majority of foliations dip southerly (Figure 4.5A). Lineations are not easily recognized but a few mineral lineations were measured (Figure 4.5B). They tend to plunge toward the southwest.

Second Deformation: D_2

As can be seen on the geologic map and the cross section

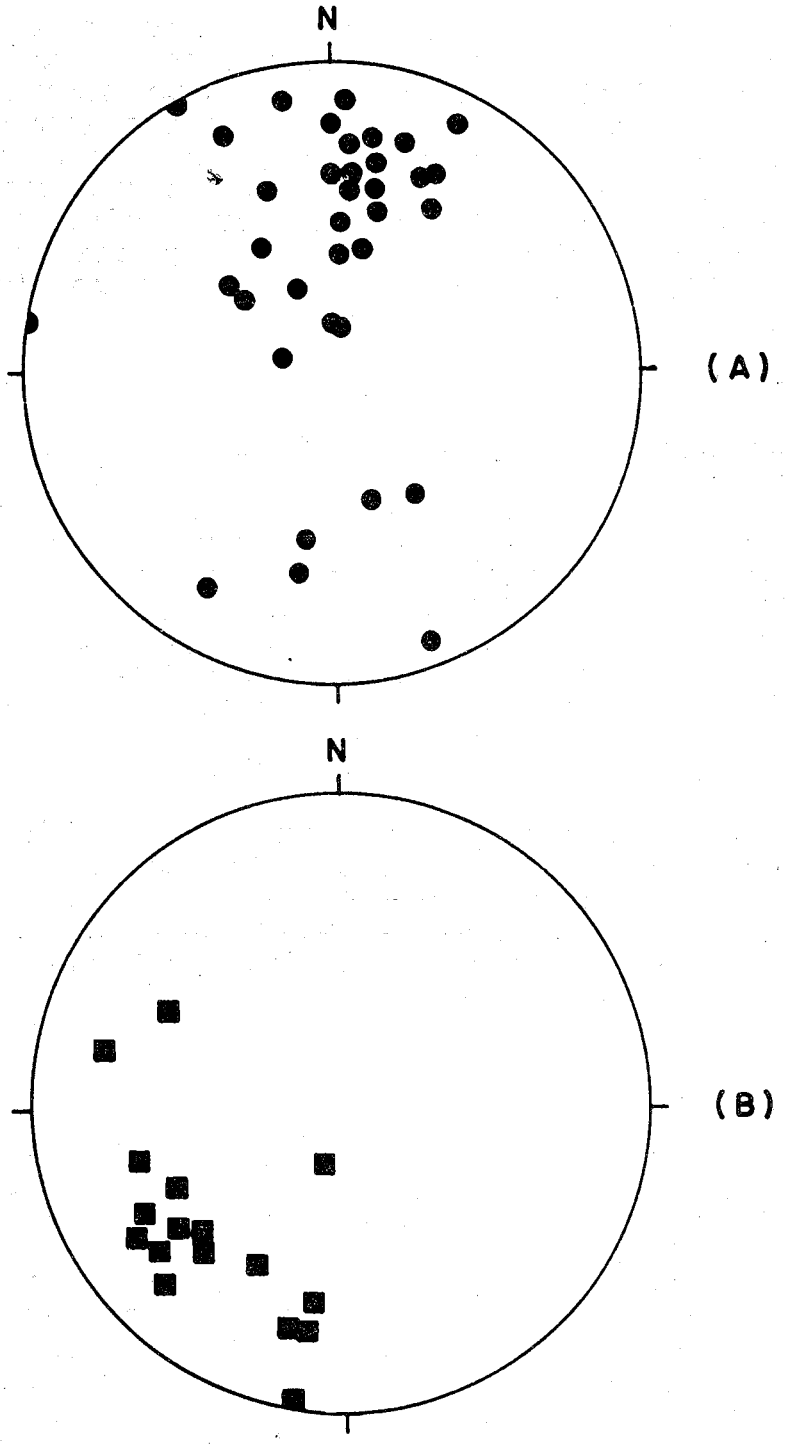

FIGURE 4.5 : EQUAL-AREA, LOWER-HEMISPHERE PROJECTION OF A. POLES TO S_1 FOLIATION (dots) AND B. L_1 MINERAL LINEATIONS (squares) IN THE CAUCAGUA-EL TINACO BELT, ALONG THE LA VICTORIA-SAN SEBASTIAN TRANSECT.

(Plate 2), the foliations (S_1) are folded into large wavelength, open folds, which are best developed in the Permian Tucutunemo Formation. The north-south girdle development of S_1 foliations is also the result of this event (Figure 4.5A). The constructed megascopic S_2 axial planes strike east-west to northwest-southeast and dip steeply to the south and southwest. No mesoscopic folds associated with the map-scale folds were observed; only in two outcrops of the Tucutunemo Formation a crenulation cleveage was formed in the hinge of a large fold.

Faults

The Caucagua-El Tinaco belt is separated from the Cordillera de la Costa belt by the La Victoria fault zone, which has been interpreted as a right-lateral strike slip fault, based on the occurrence of Tertiary basins along the fault, which appear to be pull-apart basins (Schubert, 1984). Two faults of the Neogene La Victoria fault system, the Suata and the Taguayguay faults, cut through the El Caucagua-El Tinaco belt in the studied area (Plate 2) and they are assumed to be right-lateral as well (MacLachlan *et al.*, 1960).

In the south, the contact of the Caucagua-El Tinaco belt with the Paracotos belt is marked by foliated sepentinites. This contact, the Santa Rosa fault was interpreted by Menendez (1966) as a normal fault. However, these serpentinites are in the same structural position as the Loma de Hierro ophiolite to the east, which Beck (1985b) interpretated as a thrust sheet. The foliation in the Caucagua-El Tinaco belt is subparallel to the thrust fault, which dips 50^{o} to the south; no kinematic indicators were determined for the fault.

The Tucutunemo Formation is in tectonic contact with the Precambrian-Paleozoic basement (La Guacamaya Metadiorite) south of the town La Victoria. This contact may be a sheared unconformity, or it is a low-angle normal fault. No evidence for one or the other could be found. Near the Taguayguay fault (Plate 2), the Permian Tucutunemo Formation underlies the Lower Paleozoic la Guacamaya Metadiorite. The contact must be a thrust fault which dips 40^{o} to 50^{o} to the north. The foliation in the metadiorite is parallel to the interpreted thrust fault.

The age of the faulting is unknown. However, the thrust faults could have formed at the same time as the D_2 folding event. Two northwest trending faults may be tear faults related to D_2. The two east-west trending dextral strike-slip faults could also be related to D_2 according to the

scheme of Gamond (1987).

Caucagua-El Tinaco Belt, State of Cojedes

The Caucagua-El Tinaco belt was also studied along the Tinaco River-Casupo transect (Plate 3). The Caucagua-El Tinaco belt in this area consists of the El Tinaco (La Aguadita Gneiss) and Tinaquillo Peridotite complexes. In the complexes, Ostos (1984) recognized north-south trending antiforms and synforms, which were refolded about east-west axes near the thrust contact with the Mesozoic Las Mercedes Formation. Based on kinematic indicators and petrofabric analysis of quartz and olivine, Ostos (1984) suggested that the complexes were emplaced by thrusting toward the northwest probably during the Late Cretaceous. However, the internal structures of the complexes may very well have formed during Paleozoic time (Ostos, 1984).

First Deformation: D_1

The rocks of the Tinaco complex are penetratively deformed with a well-developed foliation (S_1), which in few outcrops is seen to be parallel to the axial planes of mesoscopic isoclinal folds. These folds are very rare and difficult to find; they are most clearly distuinguishable in the hornblende gneiss, where it contains thin felsic intercalations. The poles to the foliations form a steep northeast-southwest striking girdle (Figure 4.6A). Lineations are well developed in the hornblende gneiss, where the nematoblastic texture is defined by the parallel alignment of amphiboles. The lineations are not well developed in the plagioclase-rich gneiss with its granoblastic texture. The lineations in the Tinaco Complex plunge moderately to the southeast (Figure 4.6B).

Toward the contact with the Tinaquillo Peridotite Complex, the Tinaco Complex contains increasing amounts of metasedimentary rocks and amphibolite layers; the latter are frequently boudinaged. The oldest structure in the Tinaquillo Peridotite Complex is an intense foliation parallel to fold axial planes; this foliation is a mylonite foliation and it generally dips shallowly to the south (Figure 4.7A). The foliation (S_1) is characterized by strongly flattened orthopyroxene crystals. Generaly, a very well developed mineral lineation is present, which primarily is the result of the parallelism of elongate orthopyroxenes. The lineations plunge gently to the southeast (Figure 4.7B).

Second Deformation: D_2

The foliation (S_1) has been refolded into megascopic open

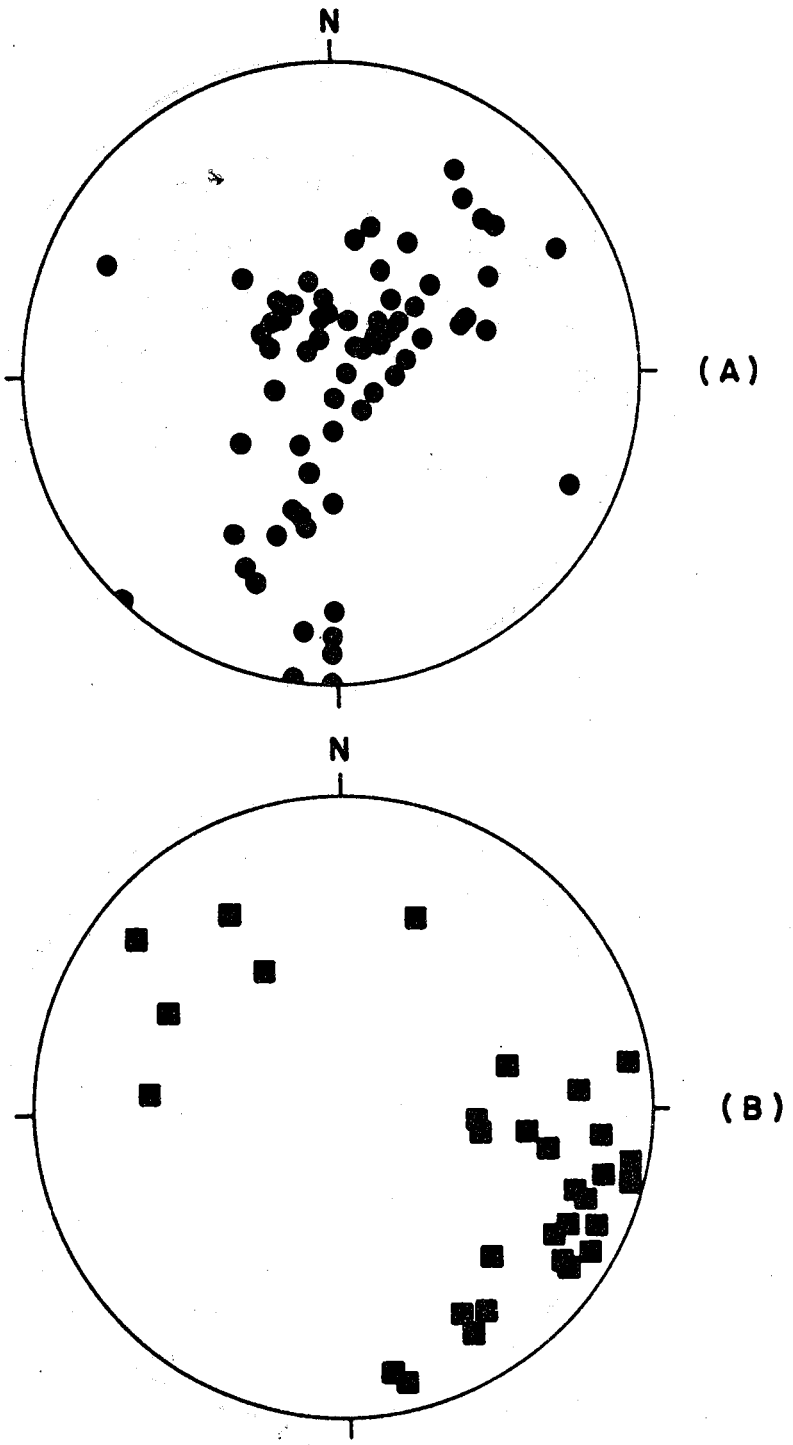

FIGURE 4.6: EQUAL-AREA, LOWER-HEMISPHERE PROJECTION OF A. POLES TO S_1 FOLIATION (dots) AND B. L_1 MINERAL LINEATIONS (squares) IN THE TINACO COMPLEX (la Aguadita Gneiss), ALONG THE TINACO RIVER-CASUPO TRANSECT.

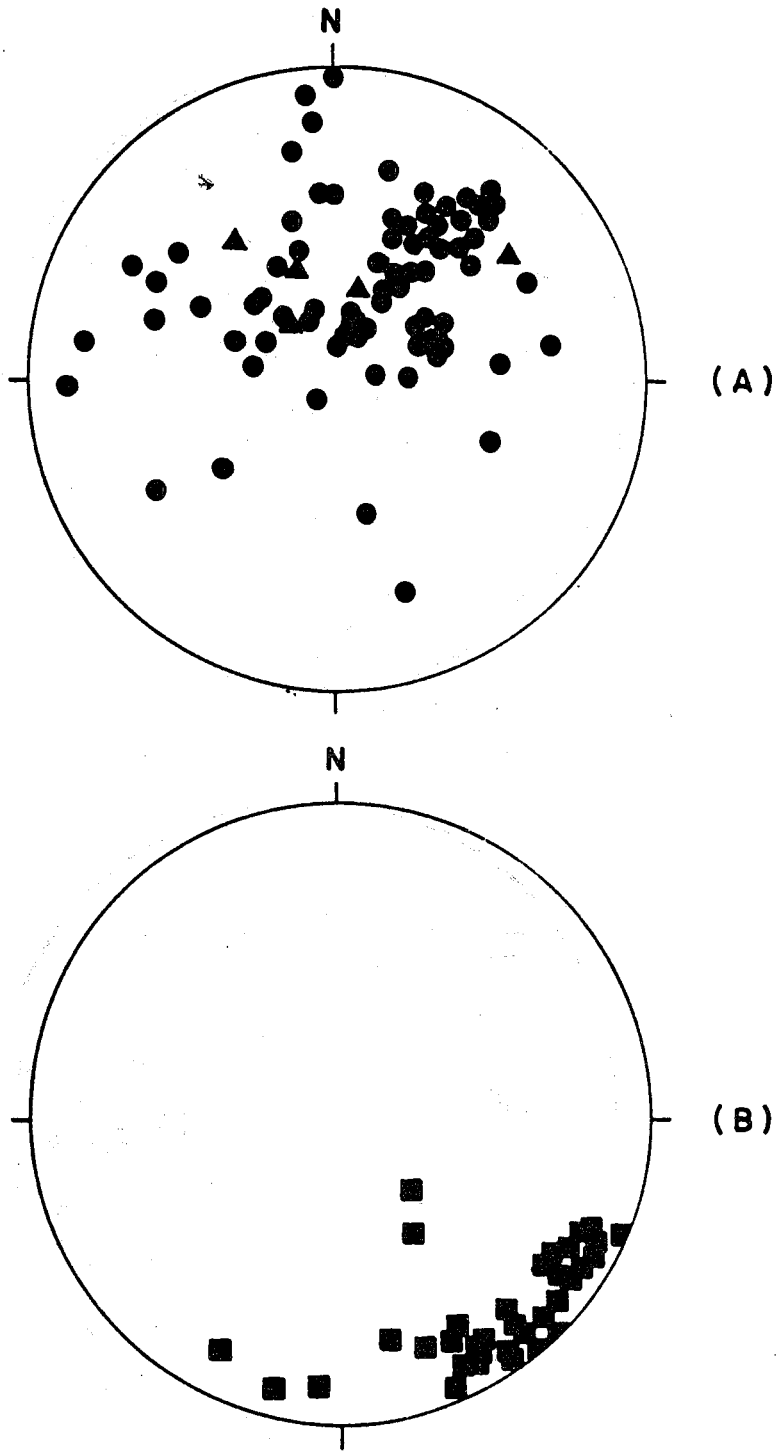

FIGURE 4.7: EQUAL-AREA, LOWER-HEMISPHERE PROJECTION OF A. POLES TO S_1 MYLONITE FOLIATION (dots) AND S_3 SERPENTINITE FOLIATION (TRIANGLES) AND B. L_1 MINERAL LINEATIONS (squares) IN THE TINAQUILLO PERIDOTITE COMPLEX, ALONG THE TINACO RIVER-CASUPO TRANSECT..

to gentle folds. The S_1 mesurements just south of the Tinaquillo Complex and in the Las Mesas-Macapo River area (Plate 3), indicate that the fold axes plunge gently to the south-southeast and the mapped axial planes of the folds are steep and strike approximately north-south. These second phase megascopic folds in the Tinaco Complex are continuous with the second phase folds in the Tinaquillo Peridotite Complex, which are well developed near the Minas de Amianto (Plate 3) where the S_1 mesurements indicate that the fold axis plunges gently to moderately to the south-southwest. There are no mesoscopic structures observed related to this phase of deformation.

Third Deformation: D_3

Further south, near and along the Tinaco River a third phase of folding is present. The structural cross section on Plate 3 indicates the presence of the deformation phase in the deepest part of the Caucagua-El Tinaco belt. The northeast-southwest girdle development of S_1 foliations is the result of this event (Figure 4.6A). The mesoscopic folds related to this deformation phase have mostly northwest-southeast axial planes, with variable dips (Figure 4.8). A few kink bands were measured and their orientation is similar as the axial planes of the mesoscopic "S" and "Z" folds (Figure 4.8). The third phase of deformation refolded the Tinaquillo and Tinaco complexes as can be seen in the Tinaquillo Peridotite Complex near La Montañita (Plate 3). Throughout the Tinaquillo Peridotite Complex a fracture cleavage has been found. This cleavage strikes generally northwest-southeast and dips steeply to the southwest (Figure 4.8B). The orientation of this cleavage is very constant and it parallels the kink bands measured near the Tinaco River; Thus, the cleavages may be related to the third phase of folding.

The Tinaquillo Peridotite Complex is thrust northward along the Manrique fault across the low-grade metamorphic rocks of the Las Mercedes Formation (Plate 3). The fault dips between 30° and 40° to the south parallel to the foliation in the complex and parallel to the structure in the Las Mercedes Formation (Plate 3). The thrust fault is exposed in two localities (Plate 3) and south-dipping folds related to the thrust in the Las Mercedes Formation may indicate a northerly thrusting of Tinaquillo across the Las Mercedes Formation. Several north-south striking faults were mapped by MacKenzie (1960) and reexamined during the present study. These faults offset the Manrique thrust fault (Plate 3). Based on field observations and aerial photograph interpretation, these faults are interpreted to be steep or vertical. They may be tear faults related to the north

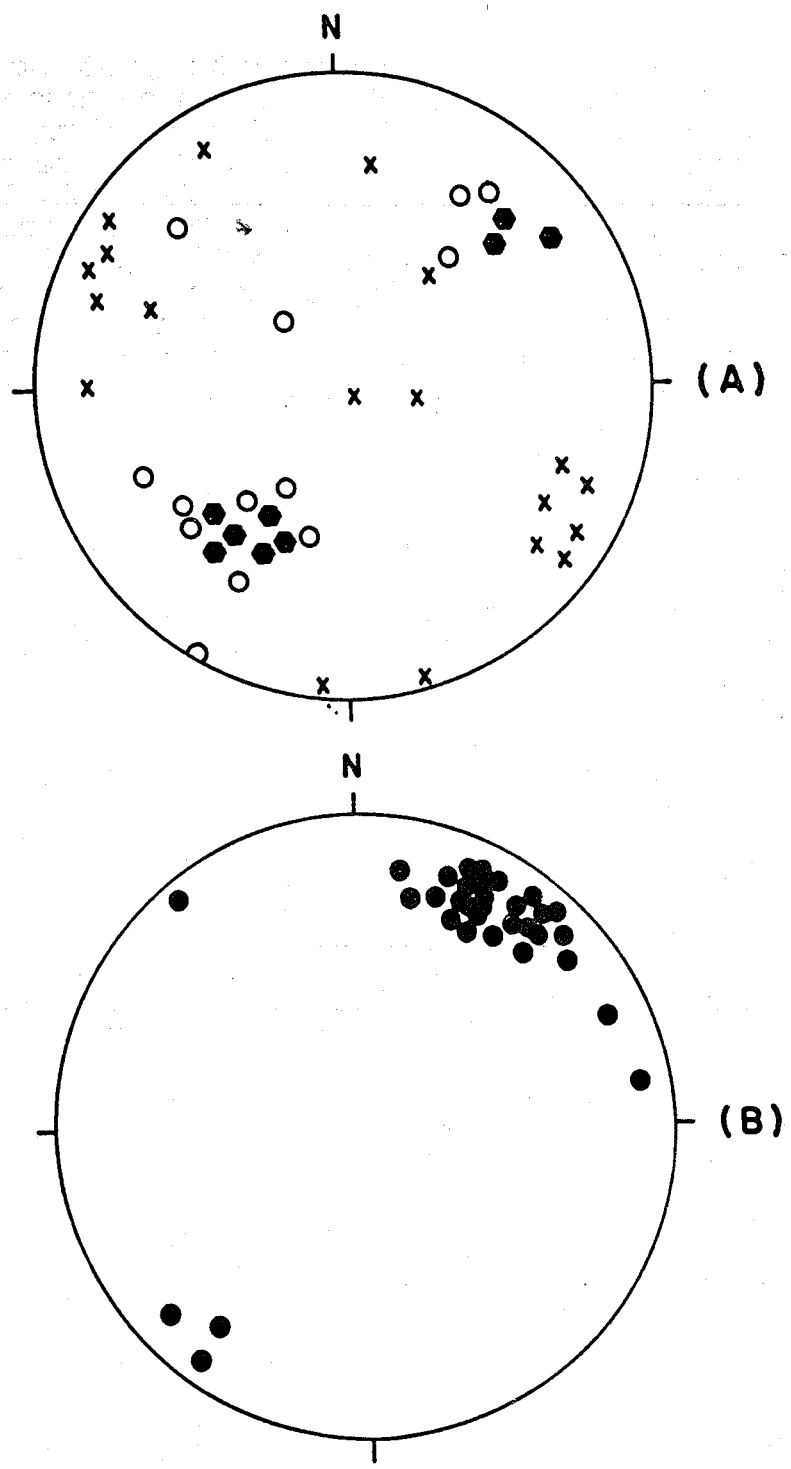

FIGURE 4.8: EQUAL-AREA, LOWER HEMISPHERE PROJECTION OF **A.** POLES TO S(3) AXIAL PLANES (circles), BETA (3) FOLD AXES (crosses), AND POLES TO D(3) KINK-BAND BOUNDARIES (hexagons) IN THE TINACO COMPLEX AND **B.** POLES TO FRACTURE CLEAVAGE IN THE TINAQUILLO PERIDOTITE COMPLEX.

directed thrusting along the Manrique fault.

The age of the D_1 deformation in the Tinaco and Tinaquillo complexes is unknown. It may be Cretaceous and contemporaneous with the D_1 deformation in the Cordillera de la Costa belt, but it is more likely that it is Late Paleozoic or even older. $^{40}Ar/^{39}Ar$ dating is underway to settle this problem. The thrust faults and tear faults are probably related to the D_3 folding. As the thrusting is probably synchronous with D_2 in the las Mercedes Formation, the D_3 folding is probably Cretaceous.

Paracotos Belt

The Paracotos belt was studied along the La Victoria-San Sebastian transect (Plate 2). Based on cross-cutting relationships two phases of folding were recognized.

First Deformation: D_1

The rocks of the Paracotos Formation are penetratively deformed. The most obvious structure is a moderately to well developed foliation (S_1), which often is parallel to the original stratification (S_0). The foliation dips steeply to the southeast (Figure 4.9A). Two types of lineations are developed (a) a lineation formed by parallelism of detrital micas and (b) a stretching lineation expressed by paralellism of elongate fragments of tuffaceous laminations and thin beds. The lineations plunge moderately to the southeast (Figure 4.9A).

Second Deformation: D_2

The foliation (S_1) has been refolded into megascopic tight to close folds (Plate 2). The S_1 measurements indicate that the fold axis plunges to the southeast and the axial plane is steep and strikes approximately east-west. Mesoscopic "S" and "Z" folds and kink-bands related to the megascopic folds were recognized (Figure 4.9B). The poles to the axial planes occur in a northeast-southwest girdle. They have shallow dips to southwest and steaper dips to the northeast. The fold axes have variable orientations (Figure 4.9B). The kink bands are vertical and strike approximately southeast-northwest (Figure 4.9B).

The northern and southern contacts of the Paracotos belt are the east-west trending Santa Rosa fault zone and the Agua Fria fault, respectively (Plate 2). The Santa Rosa fault zone was interpreted as a normal fault by Menendez (1966) and as a thrust fault by Beck (1985b; 1986). Based on the metamorphic discontinuity between the Paracotos and

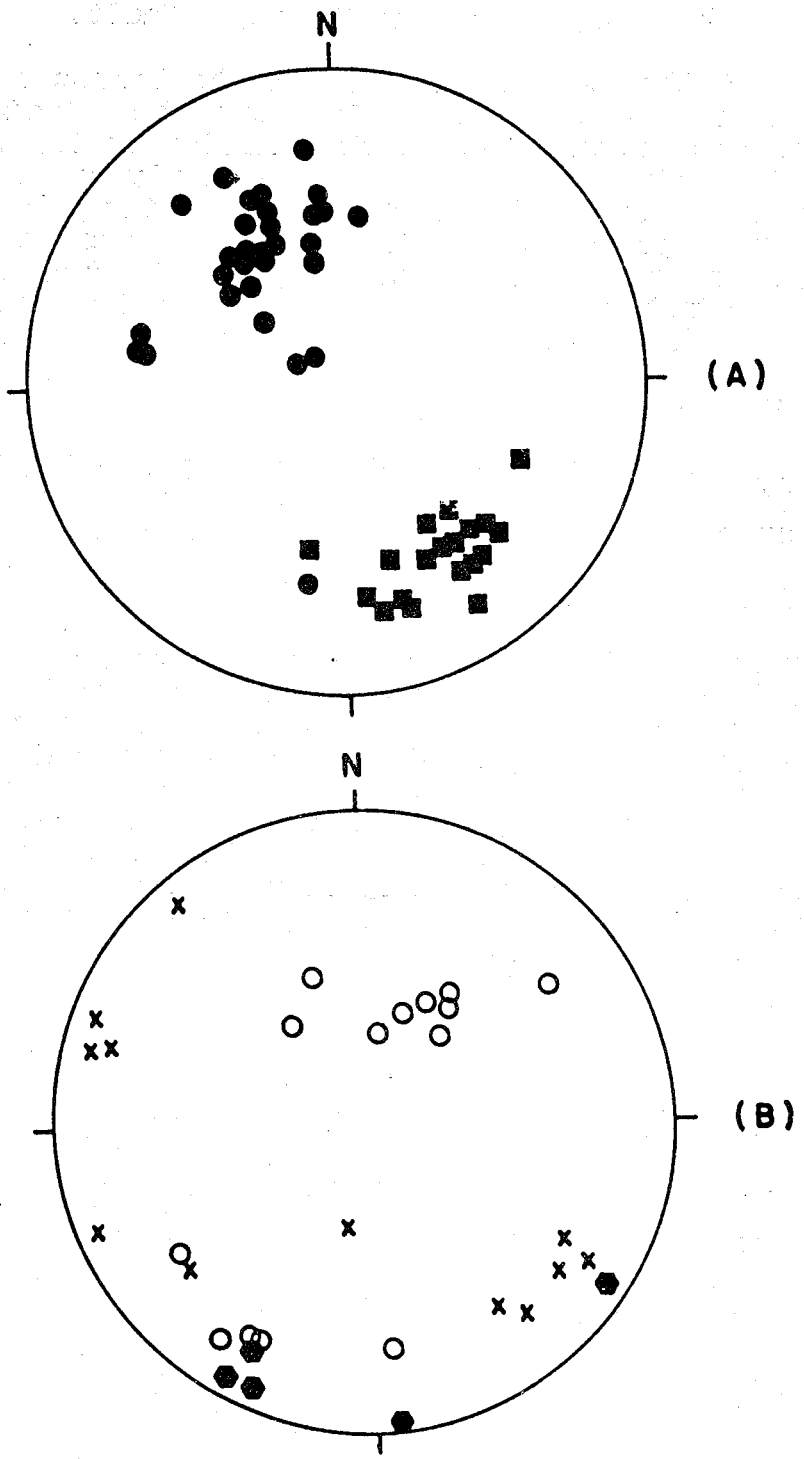

FIGURE 4.9: EQUAL-AREA, LOWER HEMISPHERE PROJECTION OF **A.** POLES TO S(1) FOLIATION (dots) AND MINERAL LINEATIONS (squares) AND **B.** POLES TO S (2) AXIAL PLANES (circles), BETA (2) FOLD AXES (crosses), AND POLES TO S(2) KINK-BANDS (hexagons) IN THE PARACOTOS BELT.

Caucagua-El Tinaco belts, it is here assumed that the Santa Rosa fault is a normal fault.

The Agua Fria fault bounds the Paracotos belt to the south (Plate 2). It juxtaposes the Lower Cretaceous Villa de Cura belt across the Upper Cretaceous Paracotos belt. Although there does not seem to be a discontinuity in the metamorphic grade between the Villa de Cura and Paracotos belts, the Agua Fria fault is interpreted as a thrust fault. The east-west folding and thrusting must have occurred during the second phase of deformation of the Paracotos belt.

Villa de Cura Belt

Deformation of the Villa de Cura belt was studied along the La Victoria-San Sebastian transect (Plate 2). It is clear that within the Villa de Cura belt, there are a strongly deformed sequence (Villa de Cura Group) and a massive, relatively undeformed volcanic and volcaniclastic unit (Dos Hermanas Formation). The deformation described below is only based on observations made in the Villa de Cura Group, in which two phases of deformation where recognized.

First Deformation: D_1

The oldest structure recognized in the field is the original stratification S_0 , which is roughly parallel to the foliation S_1. The original bedding is recognized only in the sequences with major lithologic contrast, such as chert, metapelite, and metatuff. Locally, isoclinal folds with a penetrative foliation parallel to their axial planes are preserved. The foliation strikes west-northwest and dips gently to moderately to the southwest (Figure 4.10A). The foliation is nematoblastic in the metabasalts and lepidoblastic in the metasediments. The granofels and cherts are mainly granoblastic.

On the foliation plane one can observed in general a very well developed mineral lineation which primarily is the result of parallelism of micaceous minerals, amphibole, pyroxene, and plagioclase. This lineation plunges gently to moderately to the southwest (Figure 4.10A).

Second Deformation: D_2

As can be seen on the geologic map of the Villa de Cura Group in the study area (Plate 2), the penetrative S_1 foliation is folded into short wavelenght close folds, which approximately trend southeasterly. The second phase megafolds are associated with smaller wavelenght folds. The axial planes of these "S and Z" folds (Figure 4.10B) strike

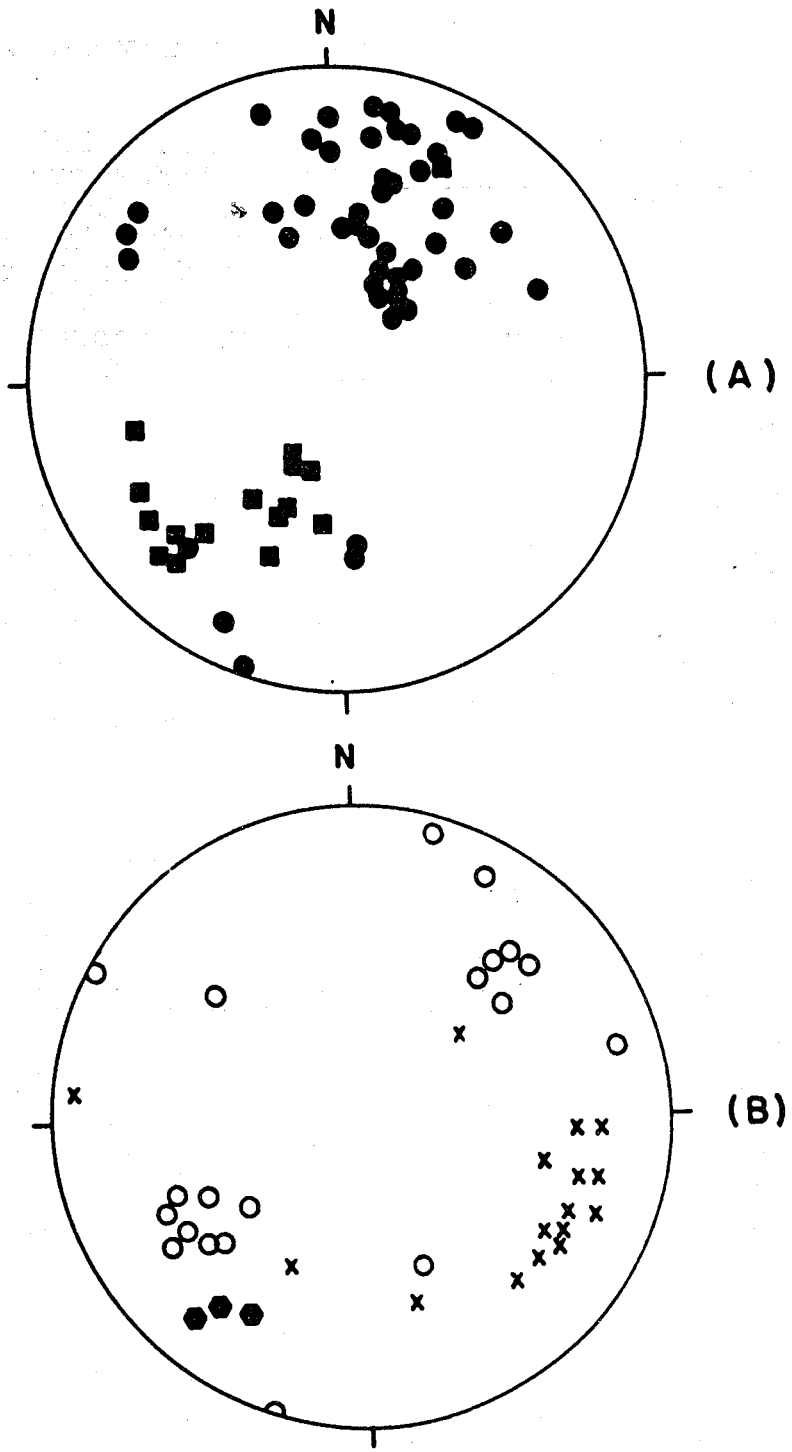

FIGURE 4.10: EQUAL-AREA, LOWER HEMISPHERE PROJECTION OF **A.** POLES TO S(1) FOLIATION (dots) AND L(1) MINERAL LINEATION (squares) AND **B.** POLES TO S(2) AXIAL PLANES (circles), POLES TO KINK-BANDS (hexagons), AND BETA (2) FOLD AXES (crosses) IN THE VILLA DE CURA BELT, ALONG THE LA VICTORIA-SAN SEBASTIAN TRANSECT.

generally northwest-southeast and dip steeply to the southwest and northeast. The fold axes plunge moderately to the southeast (Figure 4.10B). Kink bands have the same orientation and may have formed during the same phase of deformation (Figure 4.10B).

The contact of the Villa de Cura Group with the Paracotos belt in the north is the approximately east-west trending Agua Fria fault (Plate 2). This fault has been shown to dip moderately to the south (Menedez, 1966). The Lower Cretaceous Villa de Cura Group consisting at the contact of pumpellyite-actinolite facies overlies the Upper Cretaceous low-grade (prehnite-pumpellyite facies) metamorphic Paracotos Formation. Therefore, it is logical to assume that the Agua Fria fault is a thrust fault, although the sense of displacement along it could not be established. The contact between the Villa de Cura Group and the Dos Hermanas Formation is also assumed to be tectonic (Beck, 1985b). The Dos Hermanas Formation has a much lower metamorphic grade (prehnite-pumpellyite facies; Navarro, 1983) than the Villa de Cura Group. It is assumed that this tectonic contact dips steeply to the north, and thus it may be a thrust fault. The contact between the Dos Hermanas Formation and the Tertiary sedimentary rocks is also tectonic (Beck, 1985b). This tectonic contact has been interpreted to dip to the north being the frontal thrust of the Caribbean Mountains system (Menendez, 1966; Beck, 1985b).

In the southern part of the study area northwest-southeast to north-south striking faults occur, which offset the two southernmost tectonic contacts (Plate 2). On the basis of their rectilinear map pattern observed on radar imagery and airphotos, these faults are interpreted to be steep or vertical. They may be tear faults related to the east-west thrust faults.

Microtextures

Several new techniques have been developed recently to determine sense of shear in deformed rocks which allow to determine the tectonic transport direction. The most commonly used shear criteria are based on ductile deformational structures such as pressure shadows (Etchecopar and Malavieille, 1987), C-S structures (Berthé *et al.*, 1979; Simpson and Schmid, 1983), rotated porphyroclasts and rolling structures (Passchier and Simpson, 1986; Mawer, 1987; Van Den Driessche and Brun, 1987), asymmetric recrystallized tails around feldspars (Simpson and Schmid, 1983; Mawer, 1987), sigmoidal shape of deformed minerals as "mica fish" and retort-shaped

plagioclase porphyroclast (Lister and Snoke, 1984; Mainprice and Boudier, 1988), and preferred grain-boundary orientation and grain shapes (Drury and Humphreys, 1988).

Along the transects, ninety orientated samples were collected. They were cut perpendicular to the foliation and approximately parallel to the mineral lineation. Photomicrographs (Fig. 4.11 to 4.13) of some of the textures, show how the sense of shear was determined. Figure 4.11A shows a garnet with a "S-shaped" pattern of inclusions in a garnet amphibolite from south of Chichiriviche. It is indicative of a left-lateral shear during the garnet growth. These garnet crystals must have grown during the second metamorphic event discussed (Chapter VI), during which in other samples the rims of zoned garnets grew.

Figure 4.11B shows a Precambrian feldspar augengneiss from the Peña de Mora Formation, in El Avila National Park, north of Caracas. The sample shows a very well developed "C-S" structure suggesting a right-lateral shear during the recrystallization. The feldspars are porphyroclasts in a quartz bearing matrix and the "S" surfaces are defined by the orientation of quartz neoblasts, epidote, and micaceous minerals. The sample shown in Figure 4.11B is a typical example of the basement of the Cordillera de la Costa belt. It can be classified as a mylonitic gneiss according to the classification of Higgins (1971) or as a F-mylonite after the classification of mylonitic rocks of Takagi (1982, 1986).

Figure 4.12A also shows a "C-S" texture in a mylonitic trondhjemite from Cerro Matasiete on Margarita Island, indicating right-lateral sense of shear. The sample is a mylonitic gneiss according to the classification of Higgins (1971) or a F-mylonite using the classification of Takagi (1982, 1986). The plagioclase is sometimes bent and microfaulted, showing extension cracks and deformation bands. These textures are characteristic of cataclasites and mylonites-blastomylonites; thus, the texture of the rock must have been developed at transitional conditions, which according to Takagi (1986) are generated at approximately 10 km depth and at temperatures between 250^{o} and 300^{o} centigrade.

Figure 4.12B displays a locally developed "C-S" texture in a plagioclase-quartz band of a Precambrian-Paleozoic hornblende plagioclase gneiss from the Tinaco Complex in the Caucagua-El Tinaco belt, which indicates a right-lateral sense of shear. This type of kinematic indicator and the texture of the rock are very characteristic of this unit. However, they are texturally slightly different from the

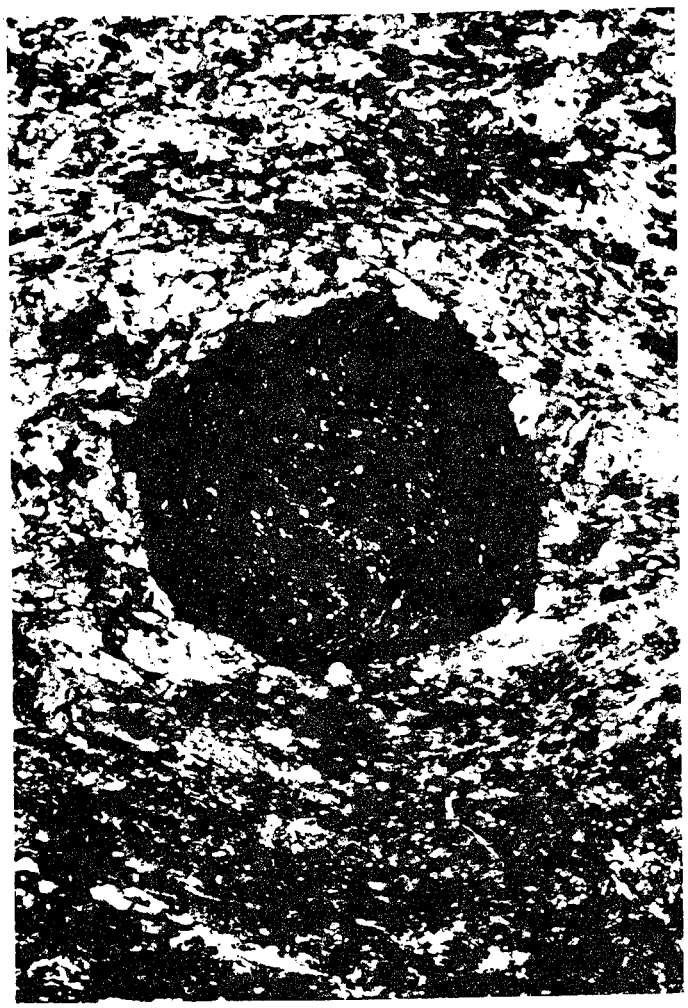

Figure 4.11A: Garnet porphyroblast with a "S-shaped" pattern of inclusions indicative of a left-lateral shear. Garnet amphibolite (Sample VO-83-9) from the Cordillera de la Costa-Margarita terrane. Long dimension= 4.2 mm.

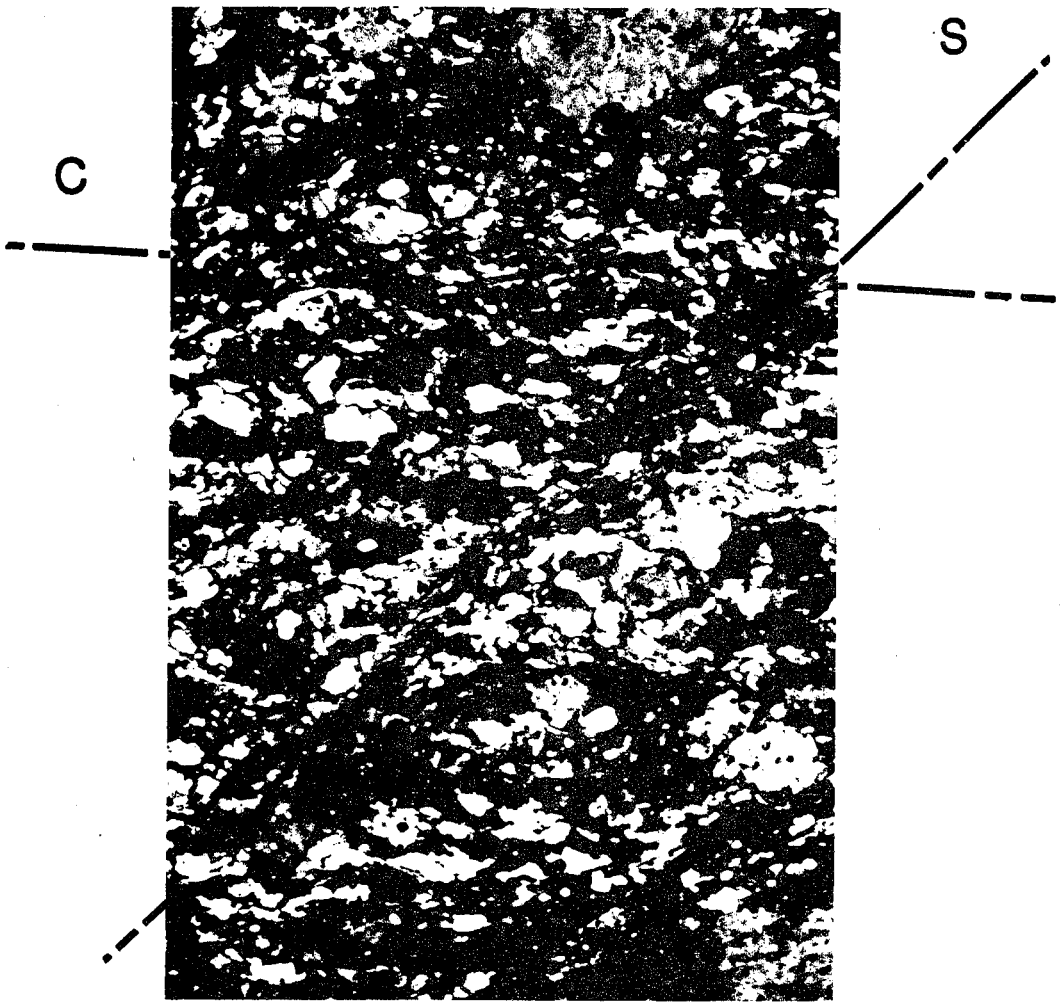

Figure 4.11B: "C-S" structure suggesting right-lateral shear in feldspar augengneiss from the Peña de Mora Formation, Cordillera de la Costa belt (Sample DF-10059). Long dimension= 4.2 mm).

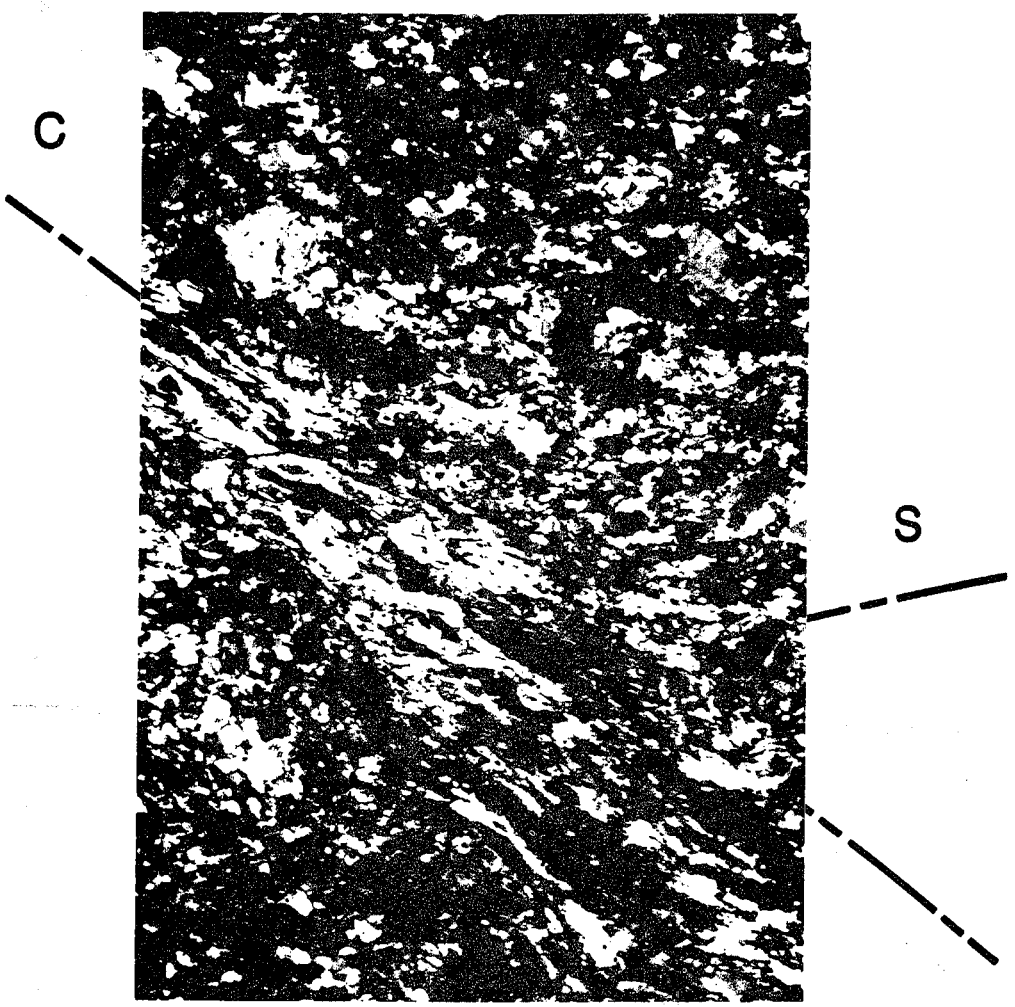

Figure 4.12A: "C-S" structure indicatives of right-lateral sense of shear in trondhjemite from Cerro Matasiete on Margarita Island (Sample VO-303). Long dimension= 4.2 mm.

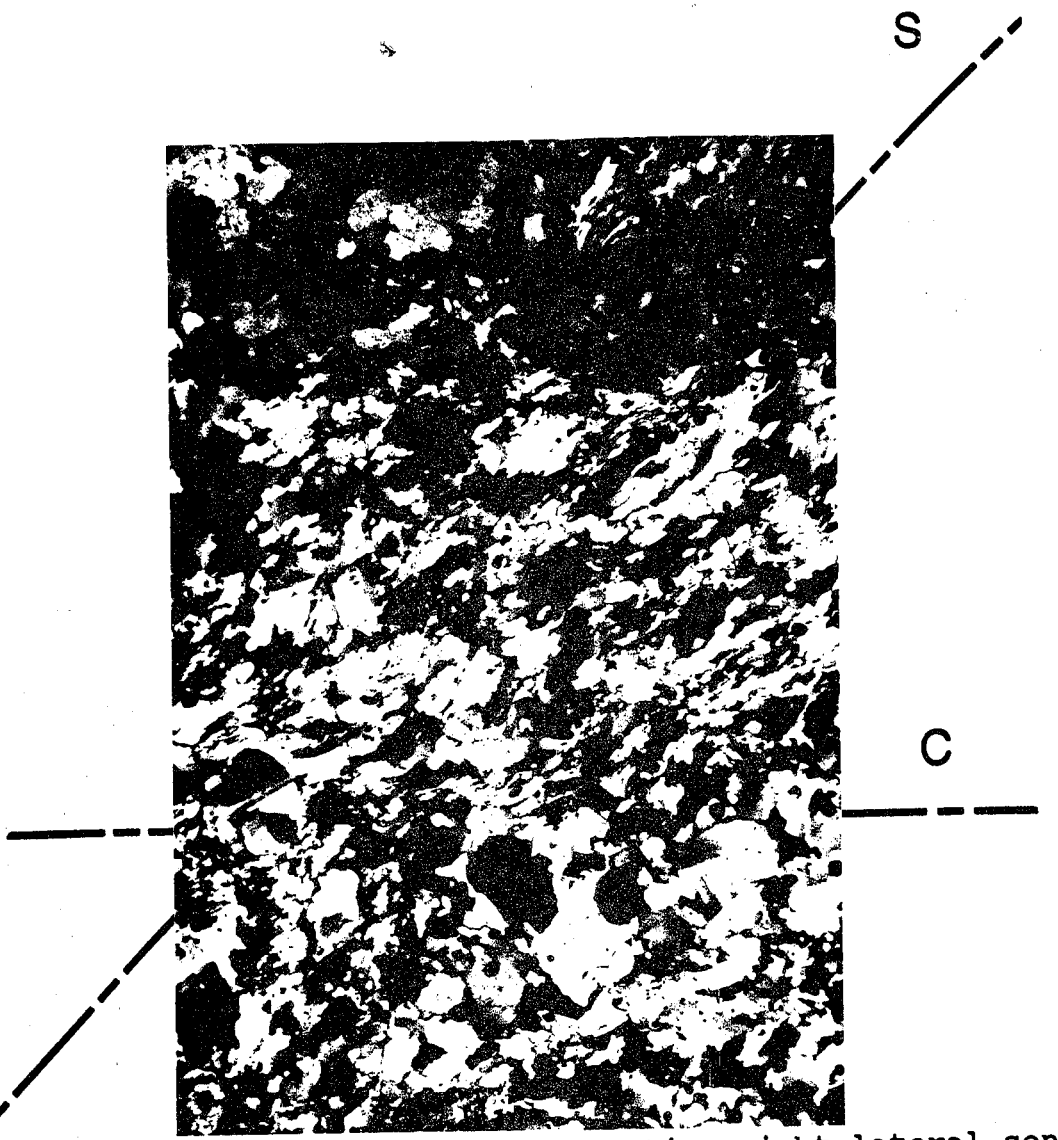

Figure 4.12B: "C-S" structure suggesting right-lateral sense of shear in a plagioclase-quartz band of a hornblende-plagioclase gneiss from the Tinaco Complex (Sample VO-83-208. Long dimension= 4.2 mm.

textures in the Peña de Mora Formation and Matasiete Trondhjemite. They have a much larger amount of porphyroclasts and cataclasis is dominant over neomineralization and recrystallization. Therefore, the gneiss from this complex is a protomylonite (Higgins, 1971) or P-mylonite (Takagi, 1982, 1986). The depth of generation of the texture may have been between 4 and 10 Km, according to Takagi (1986).

Figure 4.13A shows a pyrite-type pressure shadow (Ramsay and Huber, 1983) in an aphanitic marble from the Paracotos Formation. It indicates a right-lateral sense of shear. This type of kinematic indicator is also frequently developed in the Tucutunemo Formation (Caucagua-El Tinaco belt) and in the Las Mercedes Formation (Cordillera de la Costa belt). This pyrite-type texture is common in the belt in which the fibers always grow at the interface between the object and the matrix. The fibers are usually of quartz and frequently the growth is face-controlled, with the fiber axis growing normal to the face of the resistant crystal.

Figure 4.13B depicts a pyroxene glaucophane metalava from the Villa de Cura Group. The studied sample shows asymetric rolling structures suggesting left-lateral sense of shear.

Conclusions

Figure 4.14 summarizes the deduced senses of shear found in samples along the transects. The tectonic transport direction obtained by this analysis is not conclusive. On a regional scale, the Caribbean Mountains system does not show an uniform history of shear, which may be due to complexity of the deformation in the different tectonic belts and to the lack of a larger amount of shear data for a better discrimination of the real sense of shear. However, the following tentative conclusions can be made:

(a) The kinematic indicators in the Chichiriviche-La Victoria transect suggest that the Cordillera de la Costa belt s.s. and Cordillera de la Costa-Margarita terrane (Figure 4.14A) have a predominant dextral strike-slip tectonic transport direction parallel to the belt with an important southward component of thrusting.

(b) The kinematic indicators along the La Victoria-San Sebastian transect (Figure 4.14 B) suggest that the Caucagua-El Tinaco, Paracotos, and Villa de Cura belts have a predominant northward sense of thrusting with a small component of dextral strike-slip transport direction.

(c) The Tinaco and Tinaquillo complexes of the Caucagua-El

Figure 4.13A: Pyrite-type pressure shadow indicatives of right-lateral shear in aphanitic marble from the Paracotos belt (Sample PAR-87-3)> Long dimension= 2.6 mm.

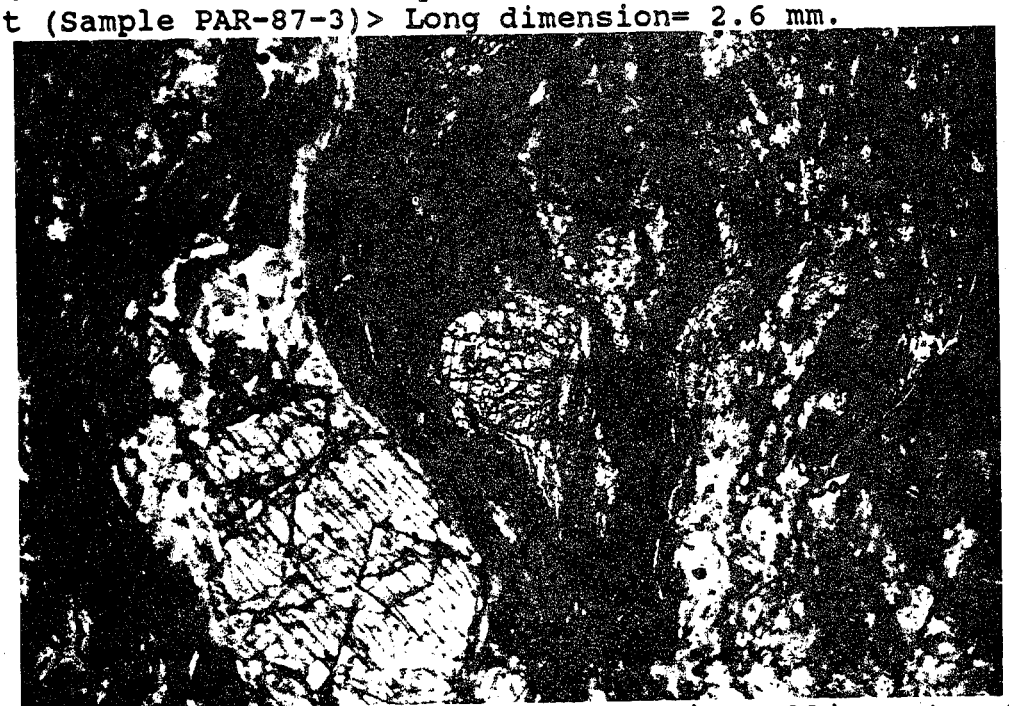

Figure 4.13B: Pyroxenes with asymmetric rolling structures indicative of left-lateral shear (north-south) in metabasalt from the Villa de Cura Group (Sample QO-839). Long dimension= 4.2 mm.

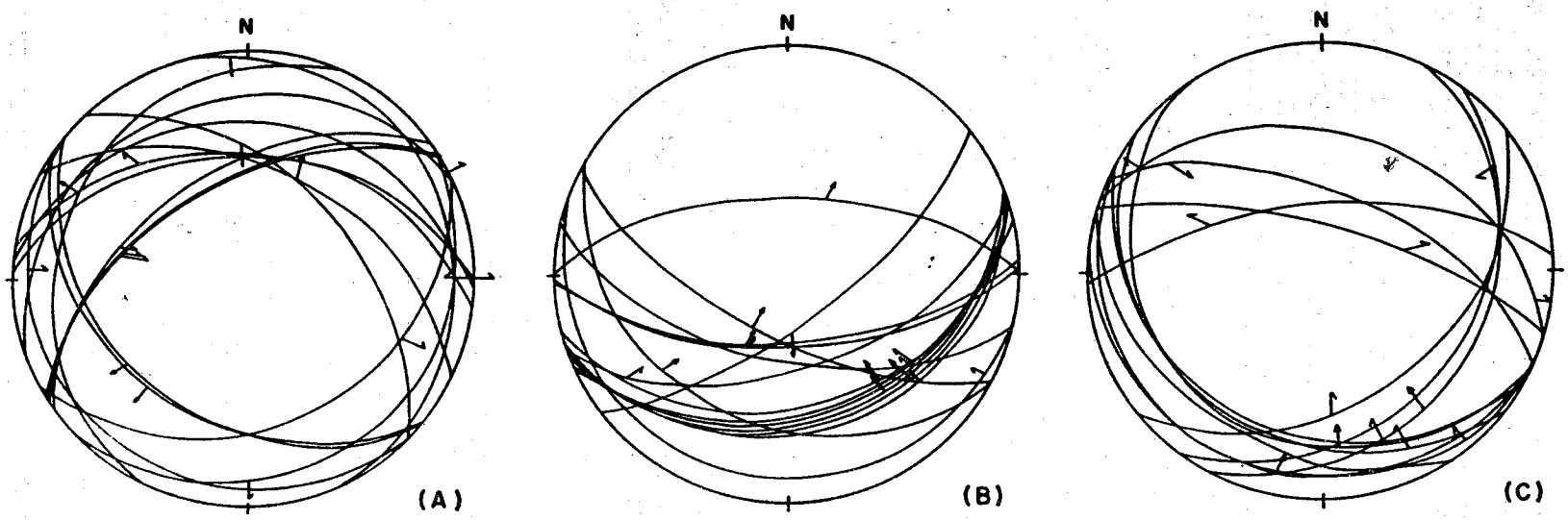

FIGURE 4.14 : EQUAL-AREA, LOWER-HEMISPHERE PROJECTION OF FOLIATION PLANES (GIRDLE) AND THE SENSE OF SHEAR (ARROW) DEDUCED FROM THE KINEMATIC INDICATORS FOR A.- CHICHIRIVICHE - LA VICTORIA TRANSECT, B.- LA VICTORIA - SAN SEBASTIAN TRANSECT, AND C.- TINACO RIVER - CASUPO TRANSECT. AN ARROW INDICATES MAINLY DIP-SLIP MOTION; IF THE ARROW POINTS TOWARD THE CENTER, IT IS THRUST MOTION, AND IF THE ARROW POINTS TOWARD THE PERISPHERY, THE MOTION IS RELATED TO NORMAL FAULTING. THE ASYMMETRIC SHEAR ARROWS INDICATE MOSTLY DEXTRAL SHEAR IN EAST-WEST DIRECTION; IF THEY POINT TOWARD THE CENTER OF THE DIAGRAM, IT IS THAT THERE IS AN IMPORTANT THRUST FAULT COMPONENT AND IF OUTWARD, A NORMAL FAULT COMPONENT..

Tinaco belt along the Tinaco River-Casupo transect have a northward sense of thrusting with a small component of dextral transport. Four kinematic indicators in the Tinaco Complex suggest dextral strike-slip (Figure 4.14C).

(d) If the kinematic indicators were developed during the Late Cretaceous-Tertiary orogenic event, the Caribbean Mountains system underwent south-directed thrusting in the north, north-directed back-thrusting in the south, and the entire system underwent dextral shear parallel to the belts.

Structural Interpretation

The study area can be divided into five tectonic belts which are very different lithologically and structurally, and which were metamorphosed at different conditions and probably at different times. From north to south the belts are: (a) The Cordillera de la Costa-Margarita terrane, (b) the Cordillera de la Costa belt, (c) the Caucagua-El Tinaco belt, (d) the Paracotos belt, and (e) the Villa de Cura belt.

The high P/T rocks of the Cordillera de la Costa-Margarita terrane are in thrust contact with the older basement of the Cordillera de la Costa belt or with the Caracas Group (Stephan et al., 1980). The Cordillera de la Costa belt is separated from the Caucagua-El Tinaco belt along the La Victoria right-lateral strike-slip system (Schubert, 1984). The Paracotos belt is separated from the Caucagua-El Tinaco belt by the Santa Rosa normal fault. The Paracotos belt is bounded to the south by the Agua Fria thrust fault (Menendez, 1966).

The tectonic belts have different metamorphic assemblages. The Cordillera de la Costa-Margarita terrane shows a high P/T metamorphic assemblage overprinted by epidote amphibolite and greenschist facies metamorphism. The Cordillera de la Costa belt shows mostly intermediate P/T and low P/T greenschist facies metamorphism. The Caucagua-El Tinaco basement shows low P/T amphibolite facies metamorphism and the Permian cover a low P/T greenschist facies metamorphism. The Paracotos belt has mostly prehnite-pumpellyite assemblages. The Villa de Cura belt shows high P/T assemblages (prehnite-pumpellyite to blueschist), which were in part overprinted by intermerdiate P/T assemblages (greenschist facies). In previous sections, the structures in each belt were discussed separately. In Table 4.1 structures from one belt are correlated with those of the other. This correlation is based on style and orientation of the structures, but also on supposed age of formation of the

TABLE 4.1 : INTERPRETATIVE STRUCTURAL HISTORY

	PHASE OF DEFORMATION				
	I	II	III	IV	V
CORDILLERA DE LA COSTA BELT			D_1 (S_1) (L_1)	D_2 (E-W FOLDS) (S-Z FOLDS) (CRENULATION CLEAVAGE) F_1 (E-W ; NW-SE DEXTRAL S-S FAULT) F_2 (E-W THRUST)	F_3 (E-W NORMAL FAULTS)
CAUCAGUA-EL TINACO BELT (SOUTH OF LA VICTORIA AND STATE OF COJEDES)	D_1 (S_1 FOLIATION) (L_1 LINEATION)			D_2 E-W TO NW-SE SUBVERTICAL AXIAL PLANE OPEN FOLDS (NW-SE KINK BANDS) F_1 (E-W; NW-SE DEXTRAL S-S FAULT) F_2 (E-W THRUST)	
CAUCAGUA-EL TINACO BELT (TINAQUILLO COMPLEX).	D_1 (S_1 FOLIATION) (L_1 LINEATION)	D_2 N-S FOLDS; SUBVERTICAL AXIAL PLANES		D_3 (OPEN FOLDS; NW-SE FOLIATION GIRDLE) (NW-SE AXIAL PLANES S-Z FOLDS) (NW-SE KINK BANDS) (NW-SE FRACTURE CLEAVAGE) F_1 - F_2 (E-W; NW-SE DEXTRAL STRIKE SLIP FAULT) (E-W; THRUST)	
PARACOTOS BELT			D_1 (S_1) (L_1)	D_2 (TIGHT TO CLOSE E-W FOLDS) (NE-SW GIRDLE ON AXIAL PLANES S-Z FOLDS) (E-W KINK BANDS) F_1 (E-W THRUST)	F_3 (E-W NORMAL FAULTS)
VILLA DE CURA			D_1 (S_1) (L_1)	D_2 (SE CLOSE FOLDS) (NW-SE KINK BANDS AND S-Z FOLDS) F_2 (E-W THRUST)	

SS = STRIKE-SLIP

structures. To avoid misunderstanding, folding phases on a regional scale will be asigned roman numerals (D_I, D_{II}, etc.).

The oldest structures (D_I) are only found in the Tinaco and Tinaquillo complexes. These structures presumably formed in Permian times but could have formed during the Late Cretaceous-Tertiary orogenic event. The kinematic indicators suggest a northwest directed thrusting with a minor component of dextral strike-slip parallel to the east-west trending belts. The Cordillera de la Costa basement must also have been deformed earlier, but the structures are obscured by the later deformation. Second phase folds (D_{II}) were formed only in the Tinaquillo and Tinaco complexes. Folds plunge to the south-southeast and have subvertical axial planes. This phase of folding may have occurred also in Permian times or during the Late Cretaceous-Tertiary orogenic event.

The D_{III} folding phase is recognized in all belts. The S_{III} foliation is rougly east-west and dips north and south, while the L_{III} lineations are roughly east-west in the Cordillera de la Costa-Margarita terrane and Cordillera de la Costa belt and southerly plunge in the Paracotos and Villa de Cura belts. The D_{IV} folding phase occurs in all belts. It is characterized by east-west trending subvertical or north and south-vergent open folds. The D_{III} and D_{IV} phases of folding probably occurred during the Late Cretaceous-Tertiary orogenic event. At least three generation of faults were have been proposed; F_1: east-west and northwest-southeast to north-south trending dextral strike-slip faults; F_2: east-west trending thrust faults, and F_3: east-west trending normal faults. The F_1 and F_2 faults are thought to have formed during the fourth phase of folding during the Late Cretaceous-Tertiary, while F_3 is interpreted to have formed later and is still active, which is supported by the continuous uplift of the Caribbean Mountains system.

The third and fourth phases of folding and the F_1, F_2, and F_3 generations of faulting are the result of one tectonic event, related to the eastward transport of the Lesser Antilles volcanic arc as has been proposed for eastern Venezuela (Ave Lallemant, 1989), while the timing of first and second phases of folding is not well constrained.

CHAPTER V

GEOCHEMISTRY AND TECTONIC SETTING OF IGNEOUS ROCKS OF NORTHERN VENEZUELA

Introduction

The distribution of basaltic volcanic rocks in relation to plate tectonic regimes is reasonably well established (Miyashiro, 1975; Miyashiro, 1978; Pearce and Cann, 1973; Pearce, 1976; Winchester and Floyd, 1977). Thus, basalt discrimination diagrams generally permit a mafic rock of unknown origin to be assigned to its most probable tectonic setting of eruption (Beccaluva *et al.*, 1979; Cann, 1970; Floyd and Winchester, 1975; Miyashiro, 1974; Miyashiro, 1975; Miyashiro, 1978; Pearce and Cann, 1973; Pearce *et al.*, 1975; Pearce, 1976; Pearce and Norry, 1979; Pearce, 1982; Pearce *et al.*, 1984; Prestvik, 1982; Shervais, 1982; Smith and Smith, 1976).

Three major eruptive types can be discriminated: (a) Mid-oceanic ridge basalts (MORB), normal-type mid-oceanic ridge basalts (N-MORB), or ocean floor basalts (OFB), extruded at divergent plate boundaries in a deep submarine environment, (b) Volcanic arc basalts (VAB), island arc tholeiites (IAT), or calcalkaline basalts (CAB) erupted at convergent plate boundaries of Andean or Japanese types, and (c) Within-plate basalts (WPB), within-plate tholeiites (WPT), and within-plate alkali basalts (WPA), extruded within a lithospheric plate. Although the majority of basalts, erupted today, can be included in the three main groups, some transitional magmas occur which have extruded in specific tectonic environments (Schilling, 1975; Sun *et al.*, 1979; Le Roex *et al.*, 1983; Pearce *et al.*, 1984), such as seamounts near ridges, incipient oceans, or abortive ridges (MORB-WPB or T-type MORB); marginal basins and fore-arc regions (MORB-VAB); supra-subduction zones (E-type MORB), and plume-influenced oceanic volcanic islands (P-type MORB).

Granitic rocks have been the object lately of similar analysis. The original classification of "S" and "I" type granites of Chappell and White (1974) and White and Chappell (1977) for granites derived by partal melting of sedimentary and igneous material, respectively, was used as a tectonic indicator. S-type granites were assumed to be product of continental collision, while I-type granite were interpreted as the product of partial melting of the mantle in Andean-type margins during post-orogenic uplift (Beckinsale, 1979; Pitcher, 1983). Later, M-type granites

were defined by White (1979) to have formed in oceanic arc settings. Oceanic plagiogranites, as defined by Coleman and Peterman (1975), also formed in such setting. Collins *et al.* (1982) described A-type granites as characteristic of anorogenic settings.

However, Pearce *et al.* (1984) demonstrated that the classification mentioned above, is difficult to apply because the boundaries between the granite types, as related to the proposed tectonic settings, are not well defined. They discovered however, that the trace elements Rb, Y, Yb, Nb, and Ta can be used for this purpose and they divided the granites into four main groups based on their geotectonic setting: 1) ocean ridge granites (ORG), 2) volcanic arc granites (VAG), which include intrusions in immature mainly tholeiitic island arcs, oceanic calc-alkaline arcs, and active continental margins, 3) within plate granites (WPG), and 4) collisional granites (COLG), comprising granites from continent-continent and arc-continent collisional settings.

Sampling

The samples analyzed in this study were collected while the geologic transects were made, and during short visits specially made with the purpose of recollecting samples in certain key areas. Some samples analyzed herein, belong to the Geological Museum, Geology Department, Universidad Central de Venezuela, or they were given to me by Drs. Enrique Navarro and Daniel Loureiro.

The samples were studied petrographically to determine whether they were suitable for chemical analysis. Several criteria were used to select or reject rock samples for chemical analysis. If pyroxenes and amphiboles were altered, the rocks were discarded. Only rarely were samples analyzed in which feldspars were altered. Samples with tiny veins of secondary minerals which by their frequency could not be avoided during sample preparation were discarded. Samples cut across by fractures with weathering products and oxides were rejected.

Discarded were also those samples which had a thick heterogeneous layering, that may have been the result of metamorphic differentiation. Samples with relict sedimentary textures were also discarded. From almost four hundred samples only approximately two hundred were chosen for analysis.

Analytical Methods

The abundances of the following elements were determined: major elements: SiO_2, Al_2O_3, TiO_2, Fe_2O_3, MnO, MgO, CaO, Na_2O, K_2O, and P_2O_5; trace elements: Cr, Ni, Zr, Y, Nb, Rb, Sr, and Rare Earth Elements (REE).

Chemical analyses of pellets of 167 samples were made by X-ray fluorescence using the Philips 1410/70 spectrometer of the Geology Department of the Universidad Central de Venezuela, which is equipped with Cr and W targets. The major-element analyses were done following a procedure described by Leake *et al.* (1969). Additionally, 40 samples were analyzed by X-ray fluorescence using a fully automated PW-1400 Philips spectrometer in the laboratories of the Ministerio de Energia y Minas de Venezuela and by inductively coupled plasma mass spectrometry and X-ray fluorescence at the X-Ray Assay Laboratories in Ontario, Canada (Table A.5.0). REE abundances were also determined in the X-Ray Assay Laboratories by radiochemical neutron activation. The international geochemical standards (Table A.5.1 in the Appendix) used for calibration were taken from Abbey (1977) and Govindaraju *et al.* (1986).

The precision of the analyses made at the Universidad Central de Venezuela was determined by measuring the concentration of each element in ten different pellets of ten samples each. The statistical data are shown in Table A.5.2 in the Appendix. The variation coefficients for sodium (5.83) and phosphorus (7.41) are too high; they are probably due to the difficulty of determining light elements (Na) and low concentrations of elements (P) by X-ray fluorescense. Additionally, the precision of the data was determined by the correlation coefficient of the calibration curves, which usually reached values between 0.98 and 0.99 for r^2. The lowest values for the correlation coefficient were determined in silicon and aluminum with values of 0.968 and 0.949, respectively.

Major-Element Geochemistry

Major element concentrations have not been used during the last years as criteria to discriminate the tectonic affinity of mafic rocks, because of their significant mobility during sea-floor metamorphism and weathering (Garcia, 1978; Pearce *et al.*, 1975; Smith and Smith, 1976; Winchester and Floyd, 1977; Winchester and Max, 1982; Wood *et al.*, 1976; Humphris and Thompsom, 1978). However, some discrimination diagrams of major-elements are sometimes useful. An example is the variation diagram K_2O-TiO_2-P_2O_5, which was proposed by

Pearce *et al.* (1975) to distinguish ocean-floor basalts from other basalt, although these elements are mobile during post-crystallization processes. The analyses of fresh, weathered, and greenschist facies rocks by Pearce *et al.* (1985) show that metamorphism has a similar effect as weathering; that is, with increased degrees of weathering and metamorphism, the compositions move steadily away from the ocean-floor field. Thus, the samples falling in the oceanic field of the diagram are very likely to be of oceanic origin.

Additionally, the bulk chemistry of the rocks must be determined before using the discrimination diagrams of minor and trace elements. On the basis of major-element compositions the samples were classified as ultrabasic, basic, intermediate, and silisic. The basic and silisic rocks will be discussed here. As no discrimination diagrams have been developed for ultrabasic rocks, the samples that were found to be ultrabasic, are not discussed here. In the present study, the terms "basic" and "mafic" will be used interchangeably. The major-element averages of the mafic samples used for discrimination of the tectonic affinity are shown in Tables A.5.3 to A.5.7 in the Appendix, while the entire data sets are shown in Tables 5.1 to 5.10 in this chapter.

Trace-Element Geochemistry

The alkalic trend in basalts can easily be distinguished from the tholeiitic trend by the enrichment in Ba, Th, Ta, and Nb, a moderate enrichment in Sr, K, Rb, Ce, and P, and a slight enrichment in Ti, Y, Yb, Sc, or Cr. Based on these trends Pearce (1982) proposed the Ti/Y-Nb/Y discrimination diagram for these igneous series. The discrimination diagrams based on the incompatible and geochemically immobile trace-element and sometimes the minor-element abundances much better discriminate between tectonic environments. Thus, the VAB basalts are characterized by an enrichment of Sr, Rb, K, Ba, Th, and sometimes Ce, P, and Sm; moreover they are characterized by a depletion of Ti, Y, Yb, and sometimes Zr, Hf, Nb, Ta, Ce, P, and Sm, relative to the N-type MORB's (Pearce, 1982).

Mid-ocean ridge basalts were subdivided by Schilling (1975) and Sun *et al.* (1979) into three different types, each one with different elemental abundances. N-type MORB's are depleted in incompatible elements (e.g. Cs, Rb, Ba, Nb, Th, U, K, light REE, P, and Ta), P-type MORB's are enriched in these incompatible elements, and T-type MORB's have abundances between N-type and P-type MORB's. Zr, Nb, and Y

are immobile during seafloor alteration and metamorphism and they show characteristic abundances in the different types of MORB's, which are not the result of partial melting (Langmuir *et al.*, 1978; Pearce and Norry, 1979). Moreover, these elements are generally more abundant in MORB's than in VIA. Thus, they are useful in discriminating tectonic settings.

Island arc tholeiites have lower contents of immobile incompatible elements than MORB's, for a given degree of fractionation (Pearce, 1982). Thus, discrimination diagrams based on immobile incompatible elements such as Ti or Y and Cr or Ni seem to discriminate between IAT and MORB; the island arc tholeiites plot separately from mid-ocean ridge basalts, having lower values of Y or Ti for a given Cr or Ni concentration (Pearce, 1982).

The trace element averages for the analyzed mafic samples are shown in Tables A.5.3 to A.5.7 in the Appendix, while the entire data sets are included in Tables 5.1 through 5.10.

Mafic Rocks

The original tectonic setting of the basaltic rocks was determined by discrimination diagrams of the most immobile major elements, the transition elements of the iron group (Cr and Ni), and the high-charge incompatible elements (Zr, Y, Nb and some of the rare REE). The elemental abundances were originally plotted on thirty three different discrimination diagrams (Table A.5.8 in the Appendix), but only a few are shown here because of similar geochemical properties of several elements which duplicate the results and because of too great mobility of some other elements. The final tectonic discrimination is most clearly represented by a few well-chosen diagrams. The REE abundances were normalized by dividing them by their respective abundance in chondrites (Haskins *et al.*, 1968).

Cordillera de la Costa Belt

Mafic rocks from the Cordillera de la Costa belt were sampled in the following areas: (a) the Chichiriviche-La Victoria transect (Plate 1), (b) an area between the Tacagua and Limon Rivers (Figure 5.1), and (c) El Avila National Park, north of Caracas (Figure 5.2). All these rocks are part of a tectonic-type melange belt with polymetamorphic assemblages (Cordillera de la Costa-Margarita terrane).

FIGURE 5.1 : LEGEND

CORDILLERA DE LA COSTA - MARGARITA TERRANE

MESOZOIC

TACAGUA FORMATION (ACTINOLITE EPIDOTE SCHIST)

ANTIMANO FORMATION (AMPHIBOLITE AND MARBLE)

ANTIMANO FORMATION (AMPHIBOLITE, CALCAREOUS MUSCOVITE SCHIST, AND MARBLE)

NIRGUA FORMATION (AMPHIBOLITE, ECLOGITE, QUARTZ-FELDSPAR EPIDOTE-ACTINOLITE SCHIST)

SERPENTINITE

AVILA GROUP

PALEOZOIC - PRECAMBRIAN

SAN JULIAN FORMATION (QUARTZ-FELDSPAR-MICA ± GARNET SCHIST AND GNEISS)

PEÑA DE MORA FORMATION (FELDSPAR-QUARTZ-MICA AUGENGNEISS)

CARACAS GROUP

MESOZOICO

CARACAS GROUP (GRAPHITIC CALCAREOUS SCHIST)

Tectonic contacts

High angle faults

•DF-2299 Samples analyzed chemically

* PM-3 Sample dated by Rb/Sr method

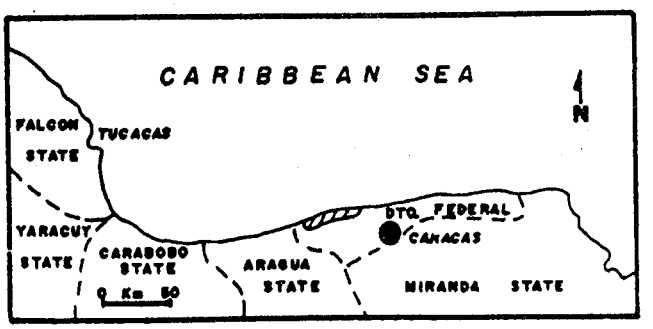

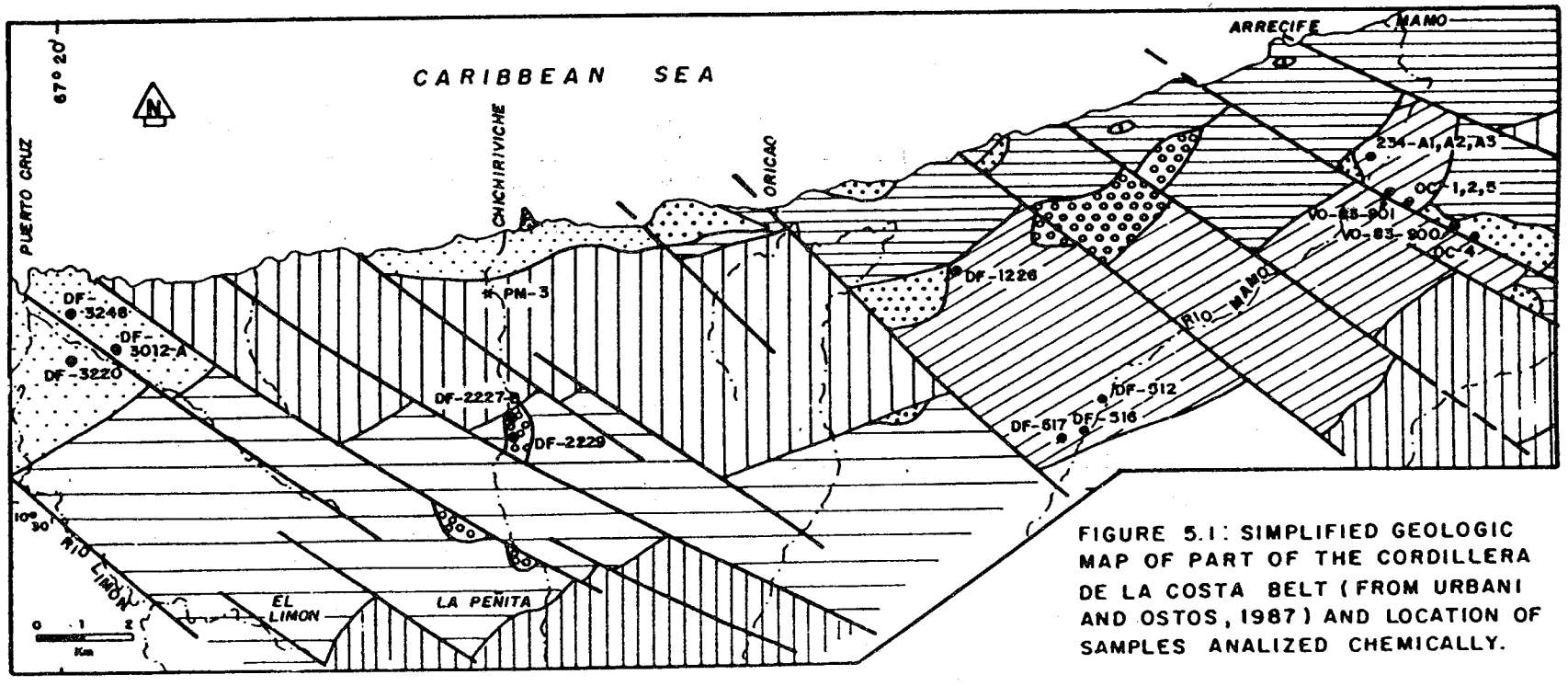

FIGURE 5.1: SIMPLIFIED GEOLOGIC MAP OF PART OF THE CORDILLERA DE LA COSTA BELT (FROM URBANI AND OSTOS, 1987) AND LOCATION OF SAMPLES ANALIZED CHEMICALLY.

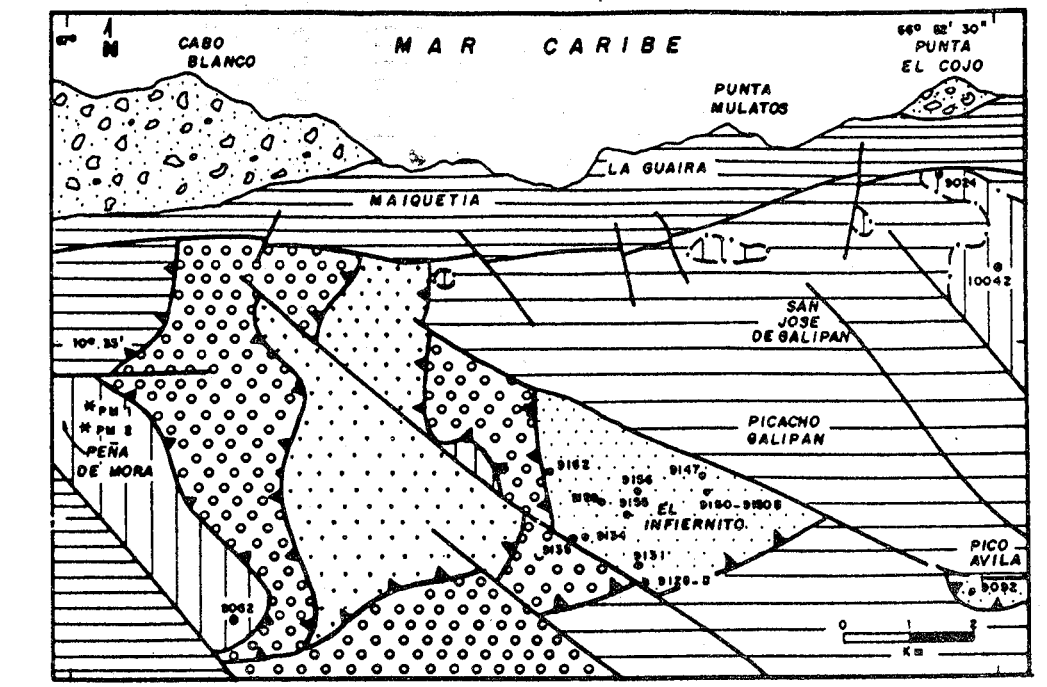

METAMORPHIC ROCKS — SEDIMENTARY ROCKS

MESOZOIC

TACAGUA FORMATION (ACTINOLITE-EPIDOTE SCHIST)

ANTIMANO FORMATION (AMPHIBOLITE, CALCAREOUS-MUSCOVITE SCHIST, AND MARBLE)

NIRGUA FORMATION (AMPHIBOLITE, ECLOGITE, QUARTZ-FELDSPAR-EPIDOTE-ACTINOLITE-SCHIST).

SERPENTINITE.

PALEOZOIC - PRECAMBRIAN

AVILA GROUP

SAN JULIAN Fm. (QUARTZ-FELDSPAR-MICA ± GARNET SCHIST AND GNEISS)

PEÑA DE MORA Fm. (FELDSPAR-QUARTZ-MICA AUGENGNEISS)

CENOZOIC

CABO BLANCO GROUP

CONGLOMERATES.

—·— Concordant contacts

—~— Discordant contacts

—▲▲— Thrust contacts

——— High angel faults

* PM-1 Samples dated by Rb/Sr method

• 9162 Samples analyzed chemically

FIGURE 5.2: SIMPLIFIED GEOLOGIC MAP OF PART OF CORDILLERA DE LA COSTA BELT (FROM URBANI AND OSTOS, 1987) AND LOCATION OF SAMPLES ANALYZED CHEMICALLY AND DATED BY Rb/Sr METHOD.

Chichiriviche-La Victoria Transect

Six amphibolite samples from the Chichiriviche-La Victoria transect were analyzed; sample locations are shown on the geologic map of the transect (Plate 1). The average elemental abundances of the six rocks are shown in Table A.5.3 in the Appendix and the entire data set is included in Table 5.1. The SiO_2 content varies from 47.64 to 55.84 %. The K_2O content varies from 0.05 to 1.06 %, but commonly is less than 0.50 %. Thus, these rocks can be classified as low-K tholeiites (Peccerillo and Taylor, 1976), typical of volcanic arcs (Jakes and White, 1972; Baker, 1982) and marginal basins (Saunders *et al.*, 1979).

The TiO_2 content varies from 0.60 to 1.55 %, but the majority of the samples have 1.00 to 1.55 %, which is characteristic of oceanic ridge and marginal basin basalts (Smewing *et al.*, 1975, Condie, 1976; Saunders and Tarney, 1979; Tarney *et al.*, 1981; Hawkins and Melchior, 1985). The Ti/Y-Nb/Y variation diagram (Figure 5.3A) indicates that the rocks from this segment of the Cordillera de la Costa belt have a tholeiitic affinity. Figure 5.3B shows the K_2O-TiO_2-P_2O_5 variation diagram, on which three of the six amphibolites have ocean floor affinity and three other samples yield non-conclusive results.

A more complete discrimination can be made on the basis of trace-element compositions. First, the data were tested for a possible within-plate affinity, but this was rejected because of the lack of the typical enrichment in Nb, P, Zr, and Ti. For example, the Zr/4-Y-2*Nb (Figure 5.4A; Meschede, 1986) and the Zr/Y-Zr (Figure 5.4B; Pearce, 1988) diagrams do not suggest a within-plate affinity but Figure 5.4A suggests a mid-oceanic ridge origin, but the data in Figure 5.4B do not discriminate between a MORB and an VIA origin.

Four of the six amphibolites have Cr/Y ratios characteristic of both IAT's and MORB's and two samples plot in the IAT field (Figure 5.5A). The binary variation diagram Ti/Cr-Ni (Pearce, 1982) suggests that four of the six samples are MORB's and two IAT's, but the compositions are close to the boundary between the two basalt types (Figure 5.5B).

Tacagua-El Limon Rivers Area

Twenty amphibolite samples from the Tacagua-El Limon Rivers area were analyzed. Major- and trace element compositions are shown in Table 5.2 and the averages are given in Table A.5.3 in the Appendix. The location of the samples is shown in Figure 5.1.

TABLE 5.1: Major- and trace-element data of amphibolites from Chichiriviche-La Victoria Transect, Cordillera de la Costa belt (Major element values in percent; trace elements in ppm).

SAMPLE	SiO2	Al2O3	TiO2	Fe2O3	MnO	MgO	CaO	Na2O	K2O	P2O5	LOI	SUM
VO-83-5	49.62	13.68	1.26	13.70	0.17	7.52	11.60	2.04	0.35	0.10	n.d	100.04
vo-83-5C	55.84	13.31	1.15	11.55	0.15	6.89	9.00	1.06	0.12	0.11	1.89	101.07
VO-83-5DA	47.64	15.09	0.60	11.07	0.14	7.74	11.00	2.87	0.05	0.20	1.98	98.38
VO-83-9	48.43	15.37	1.55	10.71	0.28	10.80	7.34	2.99	0.38	0.20	n.d	98.05
VO-83-9B	50.56	15.40	1.41	10.11	0.25	10.93	5.58	4.36	1.06	0.19	n.d	99.85
VO-83-10	50.34	15.19	1.23	10.34	0.31	11.02	5.89	3.98	0.96	0.23	n.d	99.49

	Cr	Ni	Zr	Y	Nb	Rb	Sr
VO-83-5	136	65	55	21	7.71	38	413
VO-83-5C	88	67	48	19	6.66	52	372
VO-83-5DA	116	56	67	24	7.86	43	407
VO-83-9	252	67	33	22	5.27	11	81
VO-83-9B	199	42	48	20	5.45	14	119
VO-83-10	200	75	4	18	1.00	16	174

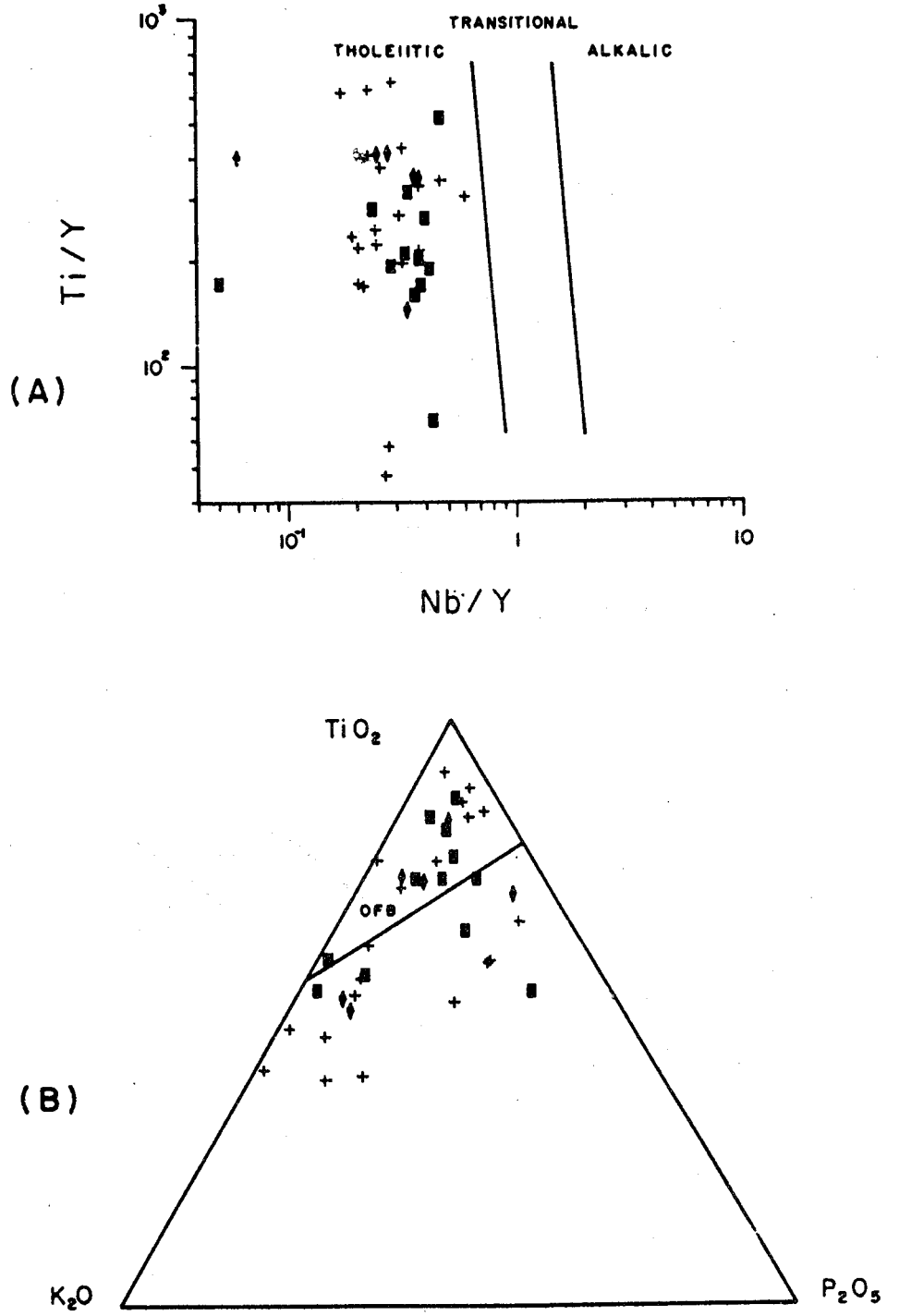

FIGURE 5.3 A-B : TECTONIC DISCRIMINANT DIAGRAMS FOR MAFIC ROCKS FROM THE CORDILLERA DE LA COSTA BELT. ♦ CHICHIRIVICHE - LA VICTORIA TRANSECT, ■ EL AVILA NATIONAL PARK, + TACAGUA - EL LIMON RIVERS AREA. A Ti / Y - Nb / Y DISCRIMINANT DIAGRAM OF PEARCE (1982). B TiO_2 - K_2O - P_2O_5 DISCRIMINANT DIAGRAM OF PEARCE et al. (1975).

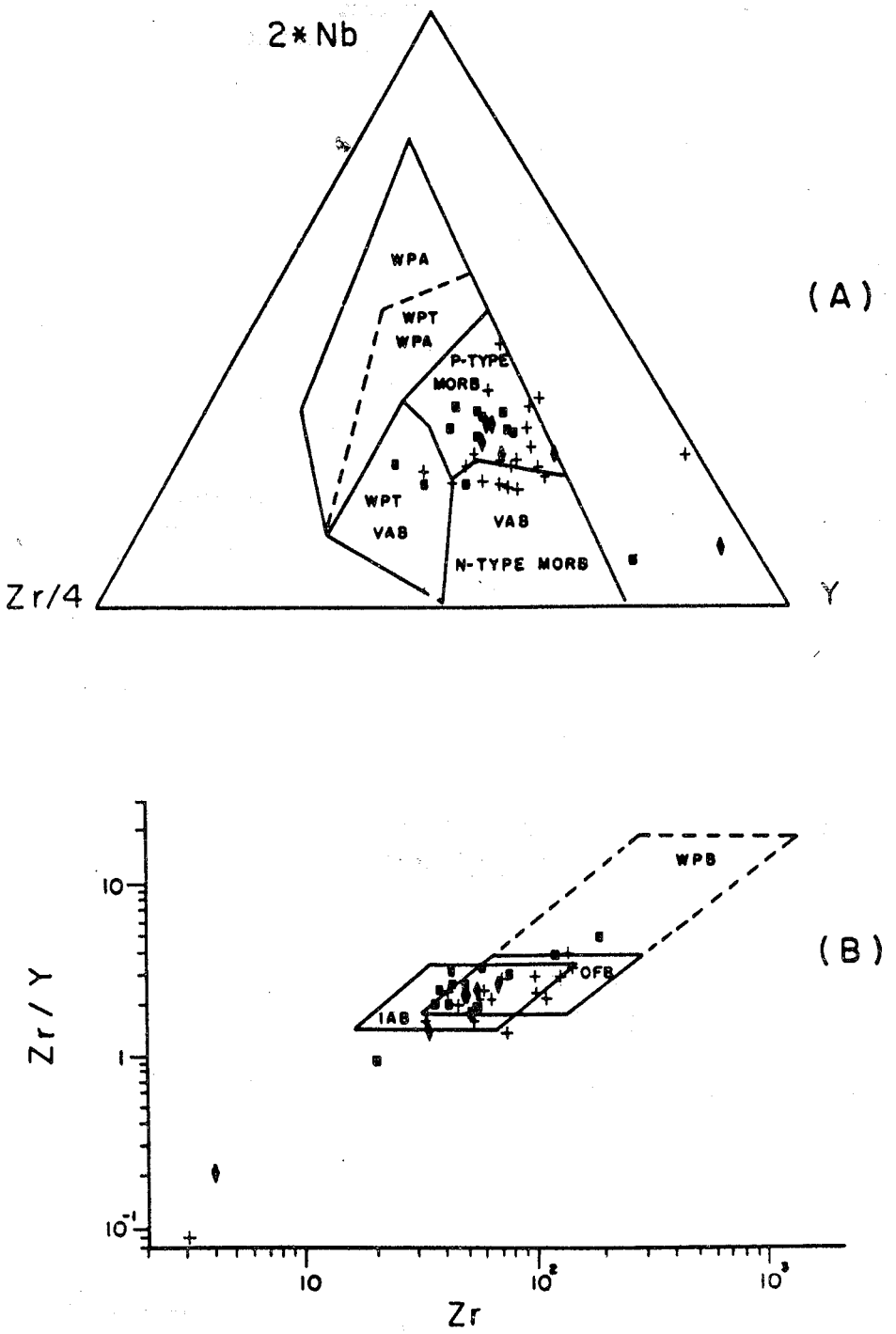

FIGURE 5.4 A-B : TECTONIC DISCRIMINANT DIAGRAMS FOR MAFIC ROCKS FROM THE CORDILLERA DE LA COSTA BELT. ♦ CHICHIRIVICHE - LA VICTORIA TRANSECT, ■ EL AVILA NATIONAL PARK, + TACAGUA - EL LIMON RIVERS AREA. A 2*Nb-Zr/4-Y DISCRIMINANT DIAGRAM OF MESCHEDE (1986) B Zr/Y-Zr DISCRIMINANT DIAGRAM OF PEARCE AND NORRY (1979).

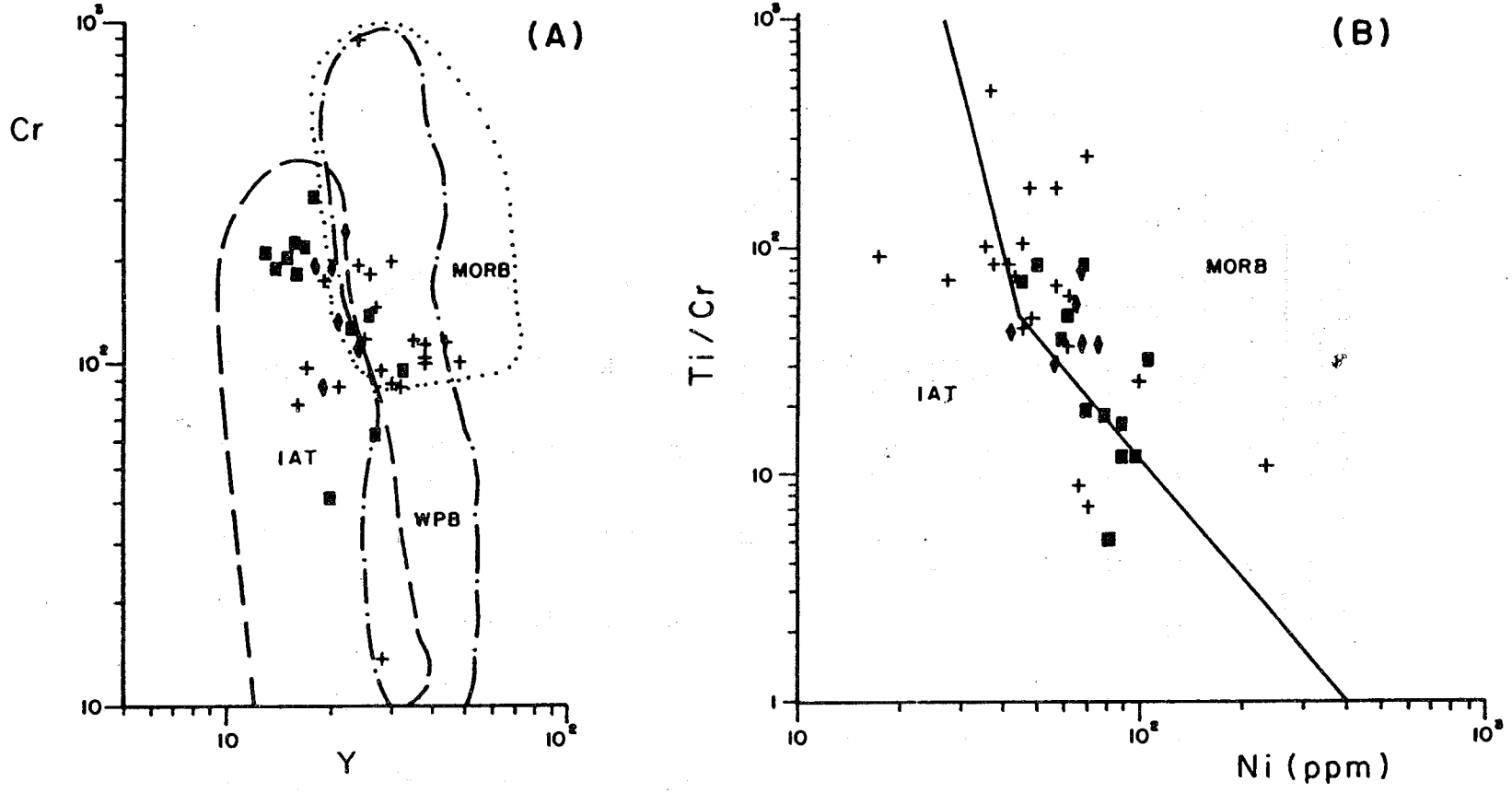

FIGURE 5.5 A-B: TECTONIC DISCRIMINANT DIAGRAMS FOR MAFIC ROCKS FROM THE CORDILLERA DE LA COSTA BELT ♦ CHICHIRIVICHE - LA VICTORIA TRANSECT, ■ EL AVILA NATIONAL PARK, + TACAGUA - EL LIMON RIVERS AREA. A Cr-Y DISCRIMINANT DIAGRAM OF MIYASHIRO (1975) AND PEARCE (1982). B Ti/Cr-Ni DISCRIMINANT DIAGRAM OF BECCALUVA et al. (1979)

TABLE 5.2: Major- and trace-element data of amphibolites from El Limon and Tacagua rivers Cordillera de la Costa belt (Major element values in percent; trace elements in

SAMPLE	SiO2	Al2O3	TiO2	Fe2O3	MnO	MgO	CaO	Na2O	K2O	P2O5
DF-234A1	41.80	17.06	0.20	16.53	0.13	12.68	8.60	2.33	0.27	0.01
DF-234A2	42.54	17.94	0.24	13.79	0.26	15.56	9.73	0.85	0.25	0.01
DF-323B	43.26	14.30	3.02	17.72	0.26	4.96	11.90	3.12	0.78	1.30
DF-412B	44.33	17.83	0.98	10.49	0.25	14.68	8.23	2.39	0.69	0.16
DF-512	48.70	12.73	0.95	15.82	0.17	7.85	7.84	3.10	0.03	0.14
DF-512B	48.41	12.82	1.36	11.77	0.22	9.77	9.37	3.15	0.25	0.17
DF-517	47.64	13.12	1.25	16.76	0.17	6.67	10.38	1.28	0.08	0.16
DF-689B	45.64	12.66	0.89	14.96	0.17	12.30	7.25	2.33	0.87	0.15
DF-1123B	48.43	15.24	1.79	16.36	0.35	8.94	5.88	3.44	0.90	0.19
DF-1226	47.02	14.41	1.11	14.09	0.19	10.53	6.91	2.21	0.68	0.16
DF-2227B	47.64	13.12	1.68	16.05	0.26	7.53	9.00	2.51	0.05	0.16
DF-2229	47.64	13.12	1.62	16.64	0.22	7.10	10.31	2.15	0.09	0.16
DF-2252	48.41	16.24	1.02	9.43	0.25	14.01	8.49	2.18	0.30	0.01
DF-3012	48.37	12.73	4.30	12.97	0.18	8.39	7.30	4.49	0.23	0.16
DF-3220	50.28	13.92	1.50	11.15	0.28	9.19	6.50	4.10	0.40	0.65
DF-3233	42.26	14.30	3.70	18.19	0.26	4.90	12.11	3.10	0.41	1.50
DF-3248	47.59	17.67	1.39	10.37	0.30	7.40	8.84	2.75	1.76	0.41
DF-3303	47.64	13.52	1.68	18.40	0.34	8.28	6.20	2.87	0.50	0.15
DF-3309B	50.77	15.65	1.14	10.26	0.25	9.88	3.10	2.19	0.52	0.52
DF-3406	51.73	15.79	1.10	9.25	0.28	8.16	6.04	3.50	1.22	0.46

	Cr	Ni	Zr	Y	Nb	Rb	Sr
DF-234A1	150	66	50	27	7.14	17	91
DF-234A2	201	71	58	24	6.41	23	135
DF-323B	99	47	51	28	6.09	21	103
DF-412B	120	48	56	25	5.99	24	116
DF-512	79	27	39	16	7.38	12	135
DF-512B	89	17	45	21	5.20	16	187
DF-517	100	43	32	17	5.27	22	102
DF-689B	207	99	52	30	6.08	30	142
DF-1123B	104	45	72	48	17.73	38	475
DF-1226	108	61	96	38	8.16	36	31
DF-2227B	118	37	106	44	9.00	54	229
DF-2229	117	41	136	38	9.19	71	259
DF-2252	90	56	132	30	9.39	56	674
DF-3012	103	69	122	38	10.61	8	99
DF-3220	88	35	96	32	9.59	9	94
DF-3233	120	56	3	35	6.00	27	103
DF-3248	189	45	52	26	15.25	18	133
DF-3303	923	234	69	24	5.39	28	210
DF-3309B	14	36	62	28	5.43	31	424
DF-3406	180	61	32	19	6.77	24	516

The SiO_2 content of the amphibolites varies from 41.80 to 51.73 % with a mean of 47.01 %. These amphibolites are the most mafic ones in the Cordillera de la Costa belt. The K_2O content varies from 0.03 to 1.76 %, but generally, it is less than 0.50%, while the TiO_2 varies from 0.20 to 3.70 %, with a mean of 1.55%. These values can be interpreted in the same way as those from the Chichiriviche-La Victoria transect. The major-element compositions are characteristic of low-K tholeiites from mid-oceanic ridges and marginal basins (Jakes and White, 1972; Peccerillo and Taylor, 1976; Saunders *et al.*, 1979; Baker,1982). Moreover, the samples with high Fe_2O_3, TiO_2, and CaO contents and low SiO_2 and MgO contents indicate an extensively alteration before metamorphism.

The amphibolites show a tholeiite affinity (Figure 5.3A). Eight samples plotted on a K_2O-P_2O_5-TiO_2 diagram (Figure 5.3B) have ocean floor affinity. The samples plotting outside of the ocean floor field may have been affected by the mobility of these elements.

The concetrations of Zr, Y, and Nb are not characteristic of within-plate basalts (Fig. 5.4A and B). Most samples (Figure 5.4A) show a P-type MORB and some a VAB or N-type MORB affinity, while Figure 5.4B does not discriminate between IAB and OFB. The discrimination diagram based on Cr-Y (Figure 5.5A) clearly shows that most of the samples are within the range of mid-oceanic ridge basalts. A similar situation can be seen in the Ti/Cr-Ni diagram (Figure 5.5B). Therefore, the amphibolites from this area probably represent tholeiitic basalts erupted at a mid-oceanic ridge plate boundary.

El Avila National Park

The twelve samples collected in El Avila National Park, north of Caracas (Figure 5.2) are mostly amphibolites with relicts of high P/T metamorphic minerals. The major- and trace-element abundances are included in Table 5.3. The average major-and trace-element abundances are given in Table A.5.3 in the Appendix. The SiO_2 content varies from 47.18 to 53.71 % with a mean of 50.27 %; TiO_2 shows a range from 0.18 to 1.18 % with a mean of 0.77 % but, generally, the values are between 0.53 and 1.18 %. The K_2O values range from 0.06 to 0.64 % with a mean of 0.19 %. Thus, the potassium content is as low as in abyssal tholeiites. The titanium content is also in the range of these tholeiites.

The amphibolite samples from El Avila National Park have Ti and Nb contents typical of tholeiites (Figure 5.3A). On the major-element diagram K_2O-P_2O_5-TiO_2 (Figure 5.3B), the

TABLE 5.3: Major- and trace-element data of amphibolites from El Avila National Park (Majo values in percent; trace elements in ppm).

SAMPLE	SiO2	Al2O3	TiO2	Fe2O3	MnO	MgO	CaO	Na2O	K2O	P2O5
DF-9092	49.10	16.67	0.18	5.14	0.09	9.51	14.00	2.26	0.14	0.01
DF-91288	53.38	14.90	1.12	9.09	0.11	7.89	12.15	2.32	0.16	0.17
DF-9131	49.83	13.91	0.47	13.45	0.15	7.53	10.50	2.00	0.28	0.07
DF-9134	52.02	13.52	0.95	12.00	0.09	6.35	11.00	1.46	0.06	0.08
DF-9135	51.15	12.50	0.91	11.93	0.13	9.23	10.83	2.34	0.12	0.21
DF-9147	53.71	12.05	1.18	11.27	0.23	8.12	10.70	2.83	0.29	0.36
DF-9150	49.21	12.12	0.65	10.29	0.14	10.90	12.07	2.01	0.14	0.41
DF-9150B	49.10	14.30	0.47	12.97	0.14	9.67	9.50	2.80	0.12	0.05
DF-9153	47.18	14.01	0.59	12.02	0.14	7.58	13.20	1.32	0.07	0.06
DF-9156	49.10	14.70	0.53	12.25	0.15	8.87	9.80	3.40	0.07	0.03
DF-9159	49.43	15.95	0.99	9.95	0.27	8.02	9.59	1.62	0.64	0.03
DF-9162	50.06	12.52	1.18	11.95	0.23	10.47	9.60	2.87	0.24	0.19

	Cr	Ni	Zr	Y	Nb	Rb	Sr
DF-9092	214	81	42	15	6.29	30	194
DF-91288	132	61	75	23	5.33	9	71
DF-9131	234	89	48	17	5.87	16	144
DF-9134	144	59	54	26	8.25	35	255
DF-9135	65	50	118	27	7.44	23	250
DF-9147	99	45	180	33	12.30	34	499
DF-9150	200	70	37	14	5.45	14	132
DF-9150B	235	97	36	16	5.99	17	180
DF-9153	42	68	2	20	1.00	14	102
DF-9156	191	89	57	16	6.54	12	124
DF-9159	321	79	40	18	5.95	18	185
DF-9162	221	106	43	13	6.01	24	314

compositions of seven amphibolites plot in the ocean floor field. A within-plate affinity iseems to be in Figures 5.4A and B. Most amphibolites have P-type MORB affinity (Figure 5.4A). On a Zr/Y-Zr plot the samples plot in the OFB/IAB field (Figure 5.4B). On the Cr-Y variation diagram most data plot in the IAT field (Figure 5.5A). However, Y values lower than 30 ppm are also common in marginal basins (Tarney *et al.*, 1981; Hawkins and Melchior, 1985) but they have not been distinguished in this diagram.

Additionally, the data plotted on a Ti/Cr-Ni binary variation diagram (Figure 5.5B) suggest a MORB affinity, but as was mentioned before, similar values of Ti, Cr, and Ni have been found in basalts in marginal basins. Unfortunately, the available data are not sufficient to differentiate these tectonic settings.

Rare earth elements (REE)

REE abundances were determined in five samples from the La Cordillera de la Costa belt (Table 5.4 and Figure 5.6); two samples from the Chichiriviche-La Victoria transect (Samples VO-83-9 and VO-83-11), one sample from the Tacagua-El Limon Rivers area (DF-2229), and two more samples from El Avila National Park (DF-9131 and DF-9156). The REE patterns for the samples from the Chichiriviche-La Victoria transect are almost flat with a slight LREE enrichment and they have a small negative Eu anomaly. The $(La/Sm)_n$ values are close to 1.00 which are common in mid-ocean ridge basalts (Jahn *et al.*, 1974). The patterns lie within the basalt envelopes of the ocean ridge basalts (Basaltic Volcanism Study Project, 1981) and do not coincide with the Japanese island arc range determined by Philpotts *et al.* (1971). They are also similar to the REE patterns of T-type MORB's for the Mid-Atlantic ridge close to the volcanic island of Tristan da Cunha, South Atlantic Ocean (Humphris *et al.*, 1985). Futhermore, the (La/Ce)n values are 0.94 and 1.06, similar to those found by Langmuir *et al.* (1977) for basalts in the Famous area, Mid-Atlantic ridge.

The pattern of the sample from the Tacagua-El Limon Rivers (DF-2229) area is also flat. The (La/Sm)n and (La/Ce)n values are 0.97 and 0.68, respectively, which are typical of ocean ridge basalts (Kay *et al.*, 1970; Jahn *et al.*, 1974) and of T-type MORB's (Sun *et al.*, 1979). The sample also plots within the ocean ridge basalt field (Basaltic Volcanism Study Project, 1981), and does not coincide with the Japanese island arc tholeiite field of Philpotts *et al.* (1971). The pattern is very similar to those of T-type MORB's of the South Atlantic (Humphris *et al.*, 1985).

TABLE 5.4: REE abundances (in ppm) of mafic and felsic rocks from the Caribbean Mountains system.

	M A F I C					F E L S I C	
	CORDILLERA DE LA COSTA	TINACO COMPLEX	TINAQUILLO	VILLA DE CURA	MARGARITA		
	DF-2229	VO-83-200	VTO-82-44	QO-843	VO-83-305	MTS-85-1	
La	20.3	51.1	5.7	17.5	23.8	39.0	La
Ce	29.5	40.6	7.4	14.8	23.4	28.3	Ce
Nd	25.1	35.2	5.0	11.7	21.8	23.5	Nd
Sm	20.9	19.6	5.6	9.3	19.5	13.5	Sm
Eu	17.9	15.1	10.2	6.4	20.4	9.1	Eu
Tb	24.5	10.2	4.1	6.1	18.4	10.2	Tb
Yb	21.2	8.7	5.6	6.7	15.5	4.4	Yb
Lu	21.7	8.7	5.6	5.9	14.6	4.3	Lu
	DF-9131	VTO-82-13	VTO-82-1168	QP-472	VO-83-3088	PM-1	
La	19.7	39.4	7.3	38.7	20.0	723.8	La
Ce	20.9	39.4	11.1	38.1	18.5	477.7	Ce
Nd	18.4	35.2	8.4	26.8	21.8	219.4	Nd
Sm	14.4	27.8	11.8	19.6	15.7	120.8	Sm
Eu	12.5	24.9	13.6	13.0	13.3	21.7	Eu
Tb	14.3	20.4	12.2	18.4	14.3	73.5	Tb
Yb	16.1	20.0	12.5	15.3	14.0	66.5	Yb
Lu	15.8	19.2	12.1	14.2	13.6	61.3	Lu
	DF-9156	VTO-82-10	VTO-82-118	VO-86-35	VO-83-315	VO-83-207	
La	7.0	49.2	1.3	15.9	13.3	51.1	La
Ce	9.8	46.7	2.5	19.7	14.8	41.8	Ce
Nd	11.7	36.9	2.5	18.4	15.1	28.5	Nd
Sm	11.3	29.3	2.1	17.0	9.9	17.0	Sm
Eu	9.4	28.8	3.3	14.8	9.1	6.6	Eu
Tb	14.3	20.4	2.0	22.4	8.2	8.2	Tb
Yb	15.8	21.2	2.4	14.6	7.8	3.4	Yb
Lu	15.5	22.3	2.2	15.5	7.1	4.0	Lu
	VO-83-9			VO-86-38	VO-83-318		
La	22.2			12.1	14.9		La
Ce	20.9			13.5	16.0		Ce
Nd	23.5			5.0	13.4		Nd
Sm	19.1			8.3	13.8		Sm
Eu	16.9			7.1	13.7		Eu
Tb	22.4			8.2	12.2		Tb
Yb	17.9			7.1	10.5		Yb
Lu	17.3			6.5	10.2		Lu
	VO-83-11						
La	19.7						La
Ce	20.9						Ce
Nd	23.5						Nd
Sm	20.5						Sm
Eu	14.4						Eu
Tb	24.5						Tb
Yb	19.9						Yb
Lu	19.5						Lu

MTS-85-1: Matasiete trondhjemite. PM-1: Pena de Mora Formation. VO-83-207: Tinaco Complex.

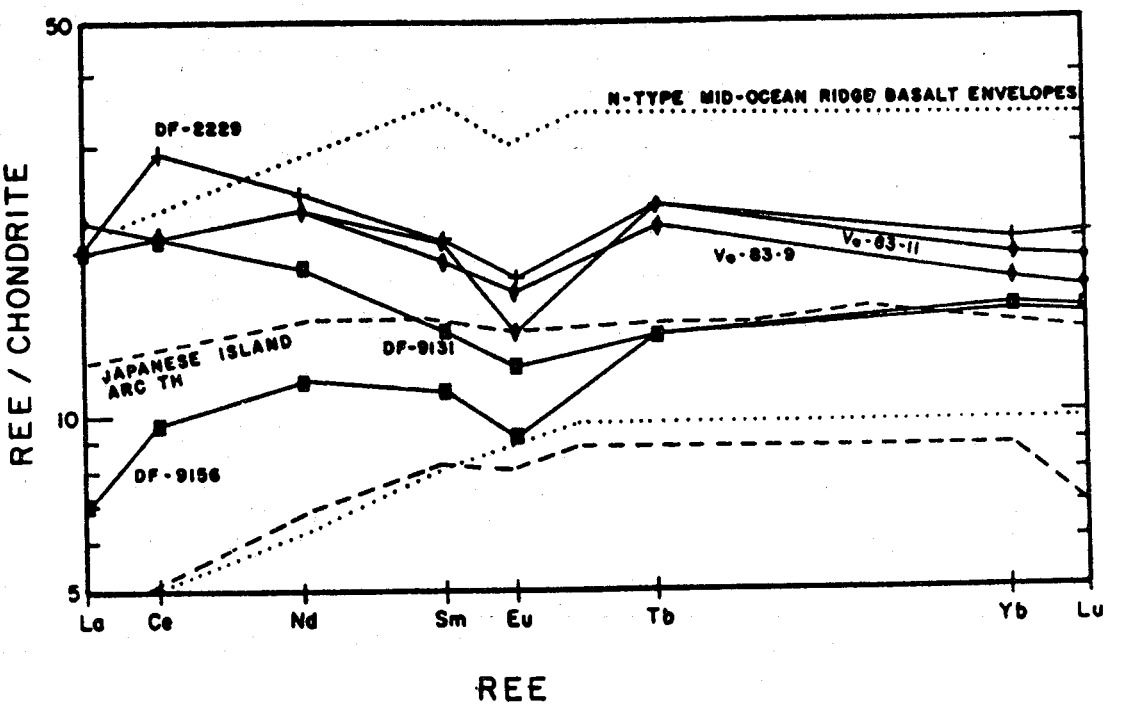

FIGURE 5.6: REE PATTERNS OF MAFIC ROCKS FROM THE CORDILLERA DE LA COSTA BELT. ♦ CHICHIRIVICHE - LA VICTORIA TRANSECT, ■ EL AVILA NATIONAL PARK, + TACAGUA - EL LIMON RIVERS AREA. THE N-TYPE MID-OCEAN RIDGE BASALT ENVELOPES IS FROM THE BASALTIC VOLCANISM STUDY PROJECT (1981) AND JAPANESE ISLAND ARC THOLEIITE ENVELOPES ARE FROM PHILPOTTS *et al.* (1971).

The REE patterns of the two samples from El Avila National Park are very dissimilar. One has a light REE enrichment (Sample DF-9131) and the other a light REE element depletion (DF-9156). The first sample has a $(La/Sm)_n$ ratio of 1.36 and a $(La/Ce)_n$ ratio of 0.94. The first ratio is not typical of oceanic ridge basalts (Jahn *et al.*, 1974). However, the $(La/Ce)_n$ is similar to those in mid-oceanic ridge basalts (Sun and Hanson, 1976), and the light REE enrichment is similar to that described in basalts from the South Atlantic spreading center (Tarney *et al.*, 1981) and the Mariana trough (Hawkins and Melchior, 1985). Sample DF-9156 shows a light REE depletion similar to that described for mid-oceanic ridges (Sun *et al.*, 1979; Schilling *et al.*, 1982) and it plots in the field of the ocean ridge basalts (Basaltic Volcanism Study Project, 1981; Humphris *et al.*, 1985). Additionally, Langmuir *et al.* (1977) recognized a light REE enrichment and depletion with concave pattern upward and downward in the Famous area (Mid-Atlantic ridge), which resembles the patterns from El Avila National Park.

Conclusions

It is certain, that the mafic rocks in the three different areas of the Cordillera de la Costa belt are tholeiites and do not have a within-plate affinity. The major-element abundances are suggestive of a mid-oceanic ridge or a marginal basin environment. Trace-element discrimination diagrams and the REE patterns are also indicative of a mid-oceanic ridge environment, but a marginal basin environment can not be excluded.

Caucagua-El Tinaco Belt

The original tectonic setting of mafic rocks from the Caucagua-El Tinaco belt was evaluated on the basis of the composition of the Guacamaya metadiorite along the La Victoria-San Sebastian transect (Plate 1), La Aguadita Gneiss of the Tinaco Complex, and the Tinaquillo peridotite complex, the latter two located in the Tinaco River-Casupo transect (Plate 3).

La Guacamaya Metadiorite

The average whole-rock major-element and trace-element abundances of samples from the La Guacamaya metadiorite are shown in Table A.5.4 in Appendix and the entire data set is given in Table 5.5. The most mafic samples found are not basic enough, to be used in the discrimination diagrams for basalts. The composition of intermediate and felsic samples from this igneous complex were plotted on discrimination diagrams for felsic rocks and will be

TABLE 5.5: Major- and trace-element data of La Guacamaya Metadiorite along La Victoria-San Sebastian Transect (Major element values in percent; trace elements in ppm).

SAMPLES	SiO2	Al2O3	TiO2	Fe2O3	MnO	MgO	CaO	Na2O	K2O	P2O5	LOI	SUM
VO-83-61	49.26	11.71	1.04	10.36	0.12	12.57	9.32	1.72	0.57	0.04	2.52	99.23
VO-83-62	56.93	16.79	0.90	10.00	0.15	4.31	5.82	2.30	1.33	0.25	1.80	100.58
VO-83-63	54.94	15.71	0.64	8.94	0.10	5.17	8.50	1.79	2.31	0.09	2.39	100.58
VO-83-65	55.51	16.06	0.79	9.24	0.14	8.28	5.81	2.18	2.11	0.18	n.d.	100.30
VO-86-17	53.80	16.61	0.31	9.65	0.11	4.64	9.30	2.33	1.02	0.08	2.44	100.29
VO-86-19	54.31	16.61	0.58	9.89	0.12	4.80	8.30	2.40	1.36	0.10	2.48	100.95

	Cr	Ni	Zr	Y	Nb	Rb	Sr
VO-83-61	40	36	68	20	8.07	41	246
VO-83-62	26	27	80	26	9.91	31	239
VO-83-63	21	24	72	23	9.53	64	222
VO-83-65	37	29	77	24	10.14	52	260
VO-86-17	30	24	44	18	10.37	58	215
VO-86-19	34	32	88	30	10.28	60	210

discussed later.

The mean SiO_2 content of the mafic samples is 54.13 %; it ranges from 49.26 to 56.93 %. The K_2O content varies from 0.57 to 2.31 %, with a mean of 1.45 %, while the TiO_2 content ranges from 0.31 to 1.04 with a mean of 0.71 %. On the basis of the abundances of SiO_2, TiO_2, and K_2O, the metadiorite appears to be related to low-SiO_2 andesites or andesitic basalts of the calc-alkaline suite (Jakes and White, 1972; Condie, 1976; Baker, 1982; Innocenti *et al.*, 1982).

The Cr content ranges from 21 to 40 ppm and the Ni varies from 24 to 36 ppm, which are within the range of calc-alkaline andesites (Jakes and White, 1972; Baker, 1982). The Zr and Y abundances are also in the range typical of calc-alkaline rocks (Jhonson, 1982; Tarney and Weaver, 1982); it seems likely that the Guacamaya metadiorite has a calc-alkaline affinity. It probably intruded into an Andean-type convergent plate boundary.

Tinaco Complex

The whole-rock compositions of ten mafic samples of the La Aguadita Gneiss from the Tinaco Complex are shown in Table 5.6 (Sample VT-83-200 through RT-87-2). The average major- and trace-element contents of the samples are displayed in Table A.5.4 in the Appendix. The SiO_2 content varies from 48.34 to 53.14 %, but generally the values are between 48.00 and 49.50 %. The TiO_2 range is from 0.25 to 1.34 % with a mean of 0.76%, while the $K2_O$ content is between 0.32 and 2.81 % with and a mean of 1.45%.

These major-element abundances are not typical of mid-oceanic ridge or marginal basin basalts (Jakes and White, 1972; Swewing *et al.*, 1975; Condie, 1976; Saunders and Tarney, 1979; Tarney *et al.*, 1981, Humphris *et al.*, 1985). The titanium content is within the range of volcanic arc basalts. The Ti/Y-Nb/Y discrimination diagram (Figure 5.7A) clearly points to the tholeiitic character of the La Aguadita Gneiss.

The K_2O-TiO_2-P_2O_5 major-element discrimination diagram (Figure 5.7B) shows a non-ocean floor affinity, but that may be due to K_2O mobility. On the $MnO*10$-P_2O_5*10-TiO_2 discrimination diagram (Figure 5.8A), the data plot in the IAT and the CAB fields. Figures 5.8B (Zr/4-Y-2Nb) and 5.9A (Zr/Y-Ti/Y) reveal clearly a non-within plate affinity of the mafic rocks from the Caucagua-El Tinaco Belt. Figure 5.8B reveals a P-type MORB affinity for the samples, but it may be due to abnormal low Zr abundances (See discussion of

TABLE 5.6: Major- and trace-element data of mafic rocks from the Tinaco and Tinaquillo complexes (major element values in percent; trace elements in ppm).

SAMPLES	SiO2	Al2O3	TiO2	Fe2O3	MnO	MgO	CaO	Na2O	K2O	P2O5	LOI	SUM
VO-83-200	49.10	11.71	0.35	11.55	0.23	10.47	11.58	1.57	1.77	0.20	1.77	100.30
VO-83-203	49.64	14.97	0.33	10.92	0.31	11.14	6.83	2.81	1.45	0.15	n.d.	98.55
VO-83-205	53.14	14.08	0.90	8.25	0.28	10.93	6.24	1.85	2.81	0.43	n.d.	98.91
VT-82-135	49.42	14.69	0.37	11.12	0.29	11.28	6.52	2.57	1.23	0.18	n.d.	97.67
VT-82-104	49.07	18.16	1.34	8.48	0.36	11.19	8.03	1.45	0.33	0.07	n.d.	98.48
VT-82-105	48.46	9.59	0.71	7.88	0.16	18.32	8.45	1.84	0.34	0.07	n.d.	95.82
VT-82-130	48.34	14.95	1.26	13.20	0.17	4.96	9.80	3.77	0.92	0.37	0.78	98.52
VT-82-1328	48.57	15.07	1.19	11.78	0.18	5.12	10.72	3.10	0.32	0.06	n.d.	47.54
VT-82-139	48.61	16.81	0.25	8.18	0.22	7.33	10.97	4.10	1.68	0.27	n.d.	98.42
RT-87-2	48.90	17.20	0.89	11.30	0.19	5.04	9.04	3.19	2.03	0.28	2.08	100.14
VT-82-44	48.34	17.03	0.20	7.99	0.11	10.36	12.43	2.04	0.15	0.01	0.34	99.00
VT-82-51	46.08	15.78	0.53	10.48	0.13	10.50	12.63	2.09	0.12	0.05	n.d.	98.39
VTO-82-52	45.10	17.98	1.18	9.64	0.18	13.20	8.30	2.85	0.44	0.08	n.d.	98.95
VTO-82-61	48.34	9.55	1.19	9.65	0.12	18.45	10.00	1.42	0.20	0.01	0.48	99.41
VT-82-100	45.97	18.97	1.64	8.92	0.30	12.69	8.03	1.45	0.33	0.07	n.d.	98.37
VT-82-101	47.68	17.83	1.36	9.19	0.29	12.08	8.55	1.61	0.21	0.04	n.d.	98.84
VT-82-114	48.80	18.69	1.17	8.33	0.20	9.60	11.64	2.72	0.27	0.04	n.d.	101.46
VT-82-116	47.18	17.03	0.42	7.62	0.24	11.08	13.08	1.81	0.57	0.01	n.d.	99.04
VT-82-1168	47.06	14.52	0.86	12.97	0.16	8.79	12.83	2.14	0.08	0.07	1.32	100.80
VT-82-118	49.88	17.45	0.26	7.88	0.25	9.35	12.23	1.32	0.02	0.01	n.d.	98.65
VTOG-31	45.35	11.21	0.58	13.21	0.15	15.86	9.70	1.68	0.25	0.06	n.d.	98.05
VTOG-82	49.26	16.00	0.20	7.75	0.11	10.41	14.68	2.00	0.12	0.01	0.64	101.18

	Cr	Ni	Zr	Y	Nb	Rb	Sr
VO-83-200	180	82	9	15	4.00	33	412
VO-83-203	232	60	52	16	6.54	17	149
VO-83-205	132	41	39	15	11.43	63	223
VT-82-135	220	68	48	18	5.73	18	731
VT-82-104	190	72	40	19	5.21	43	512
VT-82-105	1356	227	60	16	6.09	14	536
VT-82-130	130	67	44	16	2.00	6	499
VT-82-1328	150	56	46	18	5.49	32	498
VT-82-139	168	53	39	13	5.21	22	90
RT-87-2	47	24	37	14	11.00	32	605
VT-82-44	500	170	14	9	1.00	20	93
VT-82-51	601	151	14	18	5.45	17	123
VTO-82-52	583	128	31	20	5.81	11	109
VTO-82-61	920	210	19	17	1.00	12	131
VT-82-100	780	142	36	14	5.28	10	173
VT-82-101	197	57	34	22	6.72	7	52
VT-82-114	647	159	38	15	5.29	9	834
VT-82-116	736	68	31	15	6.47	11	269
VT-82-1168	330	120	21	19	2.00	12	124
VT-82-118	67	133	20	16	10.91	21	1034
VTOG-31	650	124	34	14	5.25	24	927
VTOG-82	225	97	18	18	5.31	36	394

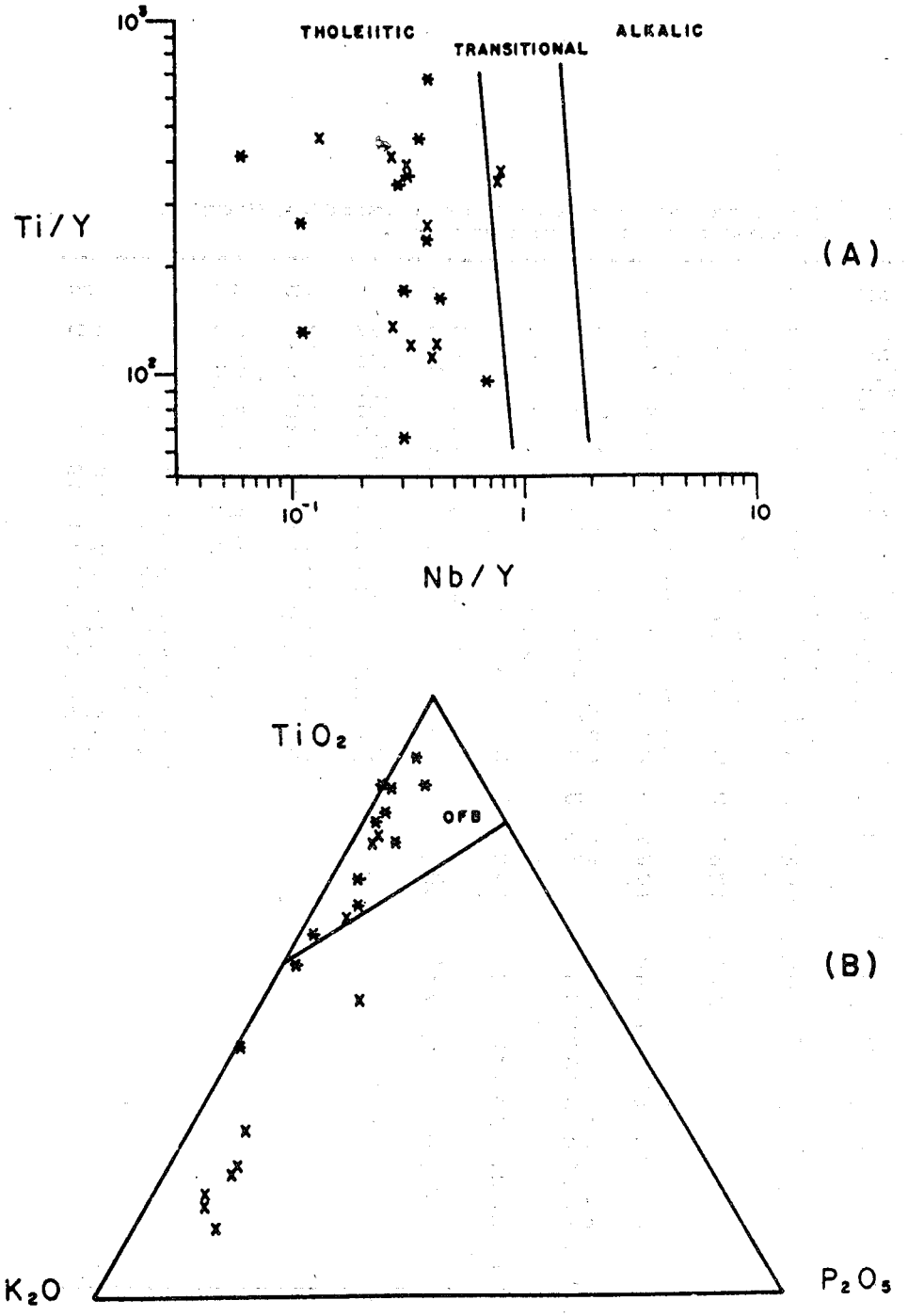

FIGURE 5.7 A-B : TECTONIC DISCRIMINANT DIAGRAMS FOR MAFIC ROCKS FROM THE TINACO COMPLEX AND THE TINAQUILLO PERIDOTITE COMPLEX. X TINACO COMPLEX, * TINAQUILLO PERIDOTITE COMPLEX. A Ti/Y - Nb/Y DISCRIMINANT DIAGRAMS OF PEARCE (1982). B TiO_2 - K_2O - P_2O_5 DISCRIMINANT DIAGRAM OF PEARCE *et al.* (1975)

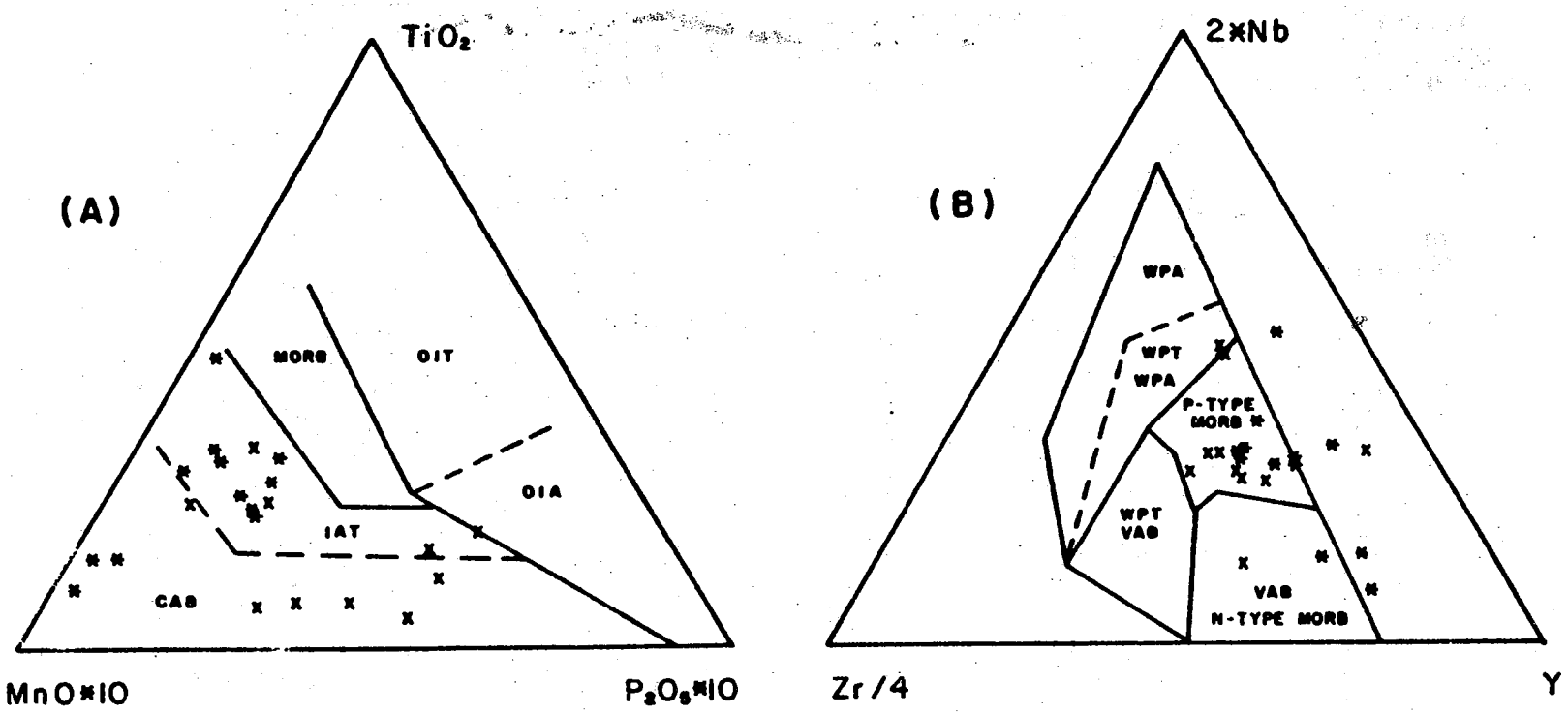

FIGURE 5.8 A-B: TECTONIC DISCRIMINANT DIAGRAMS FOR MAFICS ROCKS FROM THE CAUCAGUA - EL TINACO BELT. X TINACO COMPLEX, * TINAQUILLO PERIDOTITE COMPLEX. A TiO_2 -MnO*10- P_2O_5*10 DISCRIMINANT DIAGRAM OF MULLEN (1983). B 2*Nb - Zr/4 - Y DISCRIMINANT DIAGRAM OF MESCHEDE (1986)

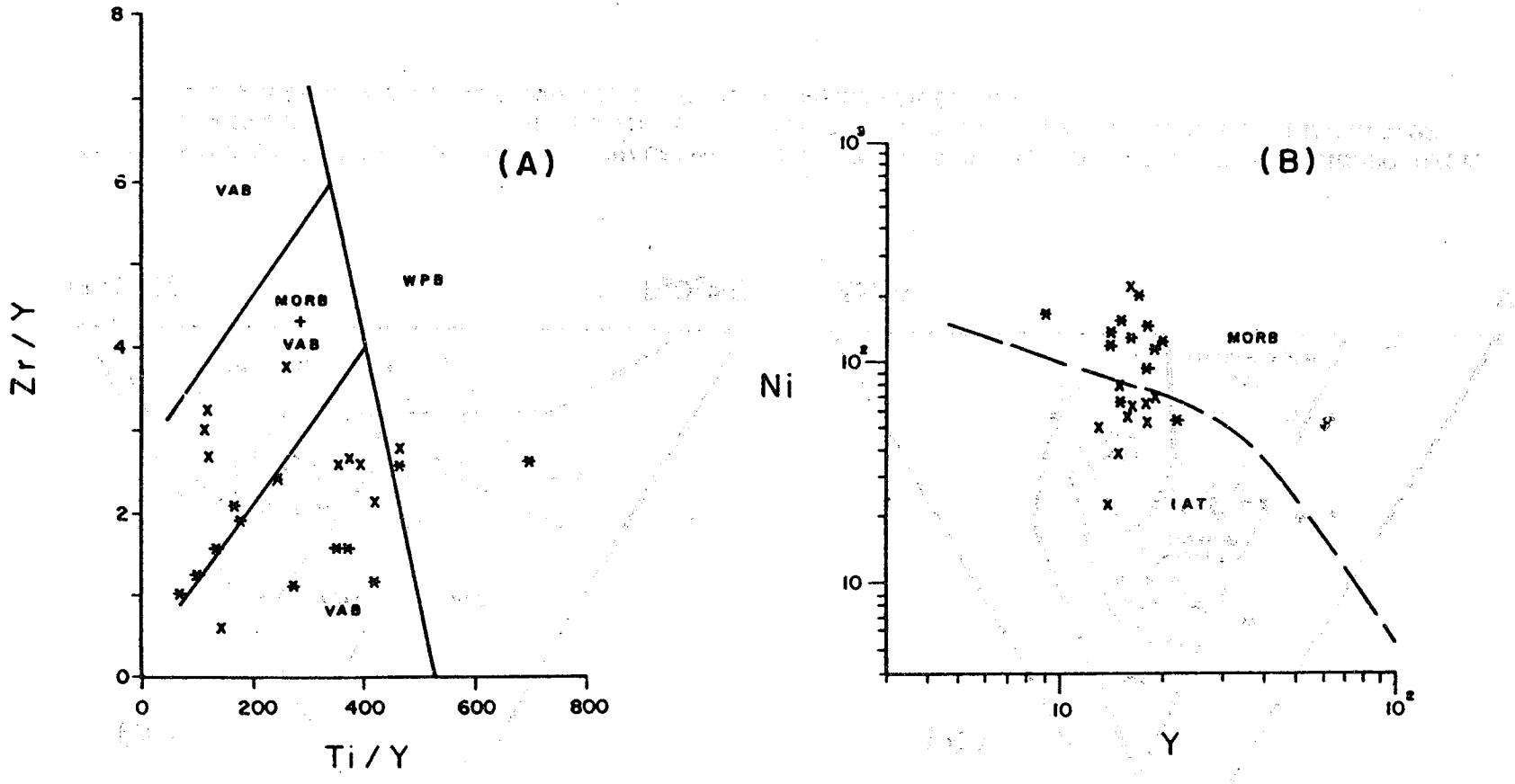

FIGURE 5.9 A-B : TECTONIC DISCRIMINANT DIAGRAMS FOR MAFIC ROCKS FROM THE CAUCAGUA - EL TINACO BELT. X TINACO COMPLEX, * TINAQUILLO PERIDOTITE COMPLEX. A Zr / Y - Ti / Y DISCRIMINANT DIAGRAM OF PEARCE AND GALE (1979). B Ni-Y DISCRIMINANT DIAGRAM OF CRAWFORD AND KEAYS (1978) AND CAPEDRI et al. (1980)

the Guacamaya Metadiorite). Figure 5.9A suggests that the rocks may have been IAB's.

The Ni-Y discrimination diagram (Figure 5.9B) also suggests that these rocks did not form at a mid-oceanic ridge. Instead, they may have been island arc tholeiites. However, a CAB affinity is not incompatible with the Ni-Y diagram (Jakes and White, 1972; Ewart and Bryan, 1973; Condie, 1976).

Tinaquillo Peridotite Complex

The major- and trace-element abundances of twelve metagabbro samples from the Tinaquillo Peridotite Complex are given in Table 5.6 (Samples VT-82-44 through the VTGO-82). The major- and trace-element averages are shown in Table A.5.4 in the Appendix. The major-element abundances are characteristic of mafic rocks: the SiO_2 content varies from 45.10 to 49.88 % with a mean of 47.42 %, which is lower than the abundances obtained for the mafic rocks of the nearby Tinaco Complex. Additionally, the range of TiO_2 contents is from 0.20 to 1.64 % with a mean of 0.80 and the K_2O abundances vary from 0.02 to 0.57 with a mean of 0.23 %. The low values of potassium are characteristic of low-K tholeiites, but due to the mobility of this element, this correlation may not be valid (Jakes and White, 1972; Condie, 1976; Peccerillo and Taylor, 1976). The TiO_2 abundances are characteristic of abyssal tholeiites and tholeiitic basalts from island arcs. Gabbros with a similar low TiO_2 content, equivalent to the island arc tholeiites, have been recognized in the Sarmientos ophiolite, which presumably formed in a marginal basin (Saunders *et al.*, 1979).

On the basis of the Ti, Y, and Nb contents, the gabbros from the Tinaquillo Peridotite Complex have a tholeiitic affinity (Figure 5.7A). The K_2O-P_2O_5-TiO_2 major-element diagram reveals a clear ocean floor tectonomagmatic affinity (Figure 5.7B) but the ternary diagram $MnO*10$-P_2O_5*10-TiO_2 shows a predominant IAT affinity (Figure 5.8A). These rocks do not have a within-plate tectonic affinity as shown by the discrimination diagram Zr/4-Y-2*Nb (Figure 5.8B) and Zr/Y-Ti/Y (Figure 5.9A). Instead, Figure 5.8B suggests that the rocks may have P-type MORB or N-type MORB affinities. Figure 5.9A suggests that the rocks have a VAB affinity. However, a better VAB-MORB discrimination was obtained by the variation diagram Ni-Y (Figure 5.9B), which clearly suggests a MORB affinity for the mafic rocks of this complex.

Rare Earth Elements (REE)

REE abundances of three mafic samples from the Tinaco Complex and three mafic samples from the Tinaquillo Peridotite Complex were determined (Table 5.4). One sample (VO-83-200) from the El Tinaco Complex was collected along the Tinaco River (La Aguadita Gneiss), another half way between the Tinaco River and the Tinaquillo peridotite complex (Sample VTO-82-130), and the third (Sample VTO-82-104) from the so-called "contact aureole" south of the Tinaquillo Peridotite Complex (MacKenzie, 1960).

The REE patterns of the samples are shown in Figures 5.10A and B. The three samples from the Tinaco Complex show a clear light REE enrichment relative to the HREE, with 20 to 50 times the chondritic abundances and almost flat patterns of the heavy REE. These patterns are very different from those of mid-oceanic ridge basalts (Basaltic Volcanism Study Project, 1981) and Japanese arc tholeiites (Philpotts *et al.*, 1971). The asymmetric pattern is also clearly different from the the Mid-Atlantic ridge basalts from Tristan da Cunha and Iceland (Schilling *et al.*, 1982; Humphris *et al.*, 1985) and the lavas of the Okmok Volcano, Central Aleutians (Nye and Reid, 1986). They are also different from marginal-basin basalts (Saunders and Tarney, 1979; Tarney *et al.*, 1981; Hawkins and Melchior, 1985).

The negative sloped REE patterns of the Tinaco Complex are similar to those of calc-alkaline rocks described by Jakes and Gill (1970), Pallister and Knight (1981), and Pearce (1982), of the basalts and basaltic andesites from Mt. Seda de Oro volcano in Sardinia, Italy (Dostal *et al.*, 1976; Dostal *et al.*, 1982), and the high Al basalts of the Chilean Andes (Lopez-Escobar *et al.*, 1977). Figure 5.10B shows the chondrite-normalized patterns of three mafic samples from the Tinaquillo peridotite complex. The samples are characterized by relatively flat REE patterns, typical of mid-oceanic ridge basalts (Kay *et al.*, 1970; Basaltic Volcanism Study Project, 1981; Humphris *et al.*, 1985), showing positive Eu anomalies that probably resulted from the acccumulation of plagioclase phenocrysts. The patterns are also quite similar to those described by Pallister and Knight (1981) for the gabbros and transitional gabbros in the Samail Ophiolite.

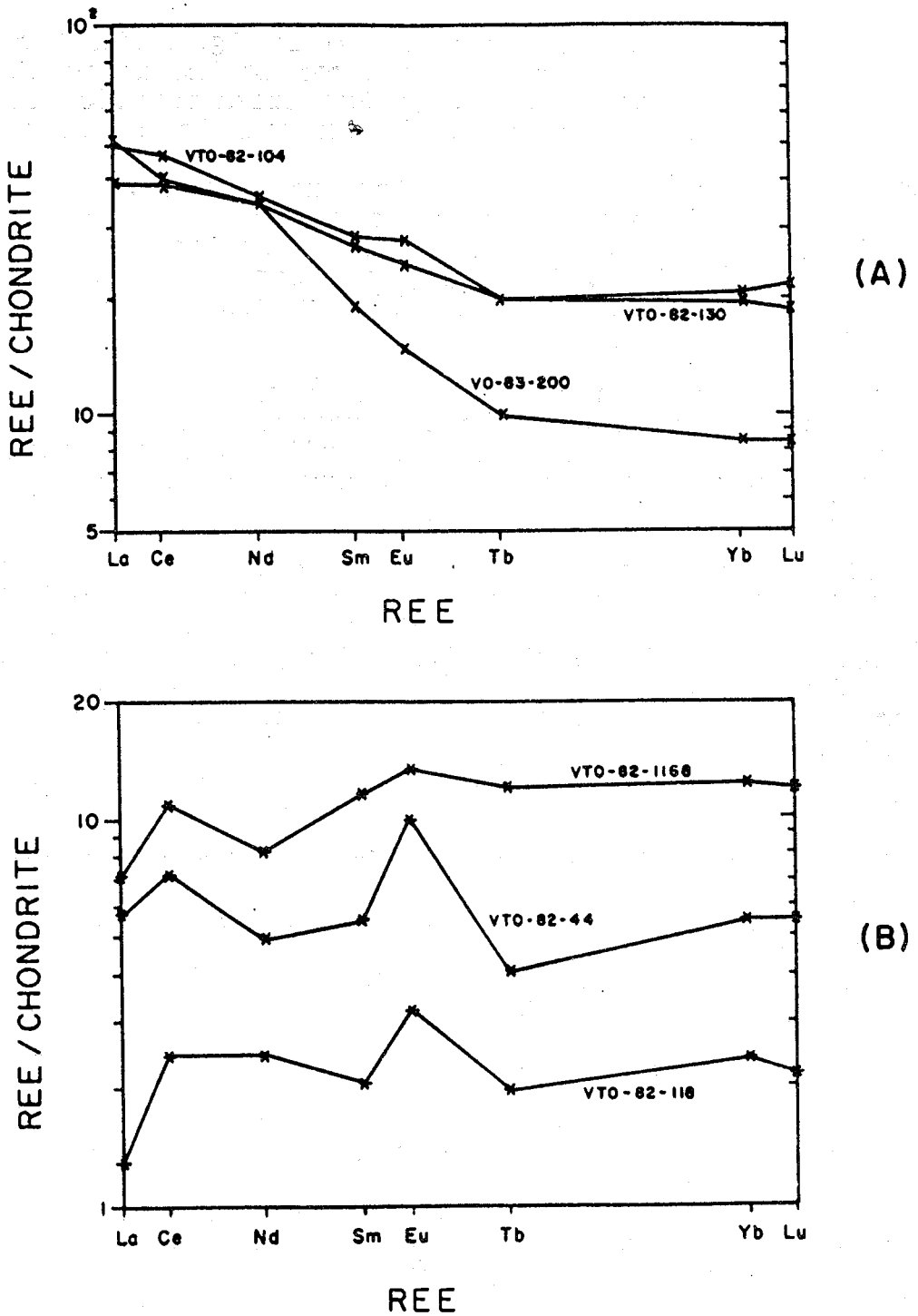

FIGURE 5.10 A-B : REE PATTERNS OF MAFIC ROCKS FROM THE CAUCAGUA-EL TINACO BELT. A TINACO COMPLEX (LA AGUADITA GNEISS). B THE TINAQUILLO PERIDOTITE COMPLEX.

Conclusions

The La Guacamaya metadiorite and the La Aguadita Gneiss (Tinaco Complex) are commonly considered as the basement of the Caucagua-El Tinaco belt. The La Guacamaya metadiorite is mostly intermediate in composition and is chemically identical with the low-SiO_2 andesites and basaltic andesites of the calc-alkaline suite of a volcanic arc. The mafic rocks of the La Aguadita Gneiss are tholeiitic, with clear volcanic arc affinities. The REE abundances and patterns are similar to those of the calc-alkaline magmatic rocks of an Andean-type margin.

The Tinaquillo Peridotite Complex has major- and trace-element abundances similar to mid-oceanic ridge basalts, marginal basins, and island arc tholeiites. A mid-oceanic ridge tectonic setting is strongly suggested by variation diagrams involving the element Ni and by the REE patterns.

An important conclusion is that the tectonic affinity of the mafic rocks in the so-called "contact aureole" of the Tinaquillo peridotite complex (MacKenzie, 1960) is different from that of the mafic rocks within the complex. Thus, the mafic rocks within the peridotite should not be interpreted as xenoliths of the country rock assimilated during a mush-like hot intrusion.

Villa de Cura Belt

The Villa de Cura belt consists mainly of two major units: the Villa de Cura Group and the Dos Hermanas Formation. Both units were sampled in the transect La Victoria-San Sebastian de los Reyes (Plate 2 and Figure 5.11). The Dos Hermanas Formation was also sampled in Guatopo National Park (Figure 5.12).

San Sebastian de los Reyes Area

Twenty five samples of the Villa de Cura belt were analyzed; eighteen samples from the Villa de Cura belt north of San Sebastian (Figure 5.11) and seven samples from Guatopo National Park (Figure 5.12). The major-element composition and the trace-element abundances of the samples from the Villa de Cura belt are shown in Table 5.7. The average major- and trace-element contents of the samples are displayed in Table A.5.5 in the Appendix.

The SiO_2 abundances range from 44.00 to 55.50 % with a mean of 47.90 %. The samples VO-86-38 and QP-403 have the highest SiO_2 values, 55.50 and 53.75 % respectively. The first is a

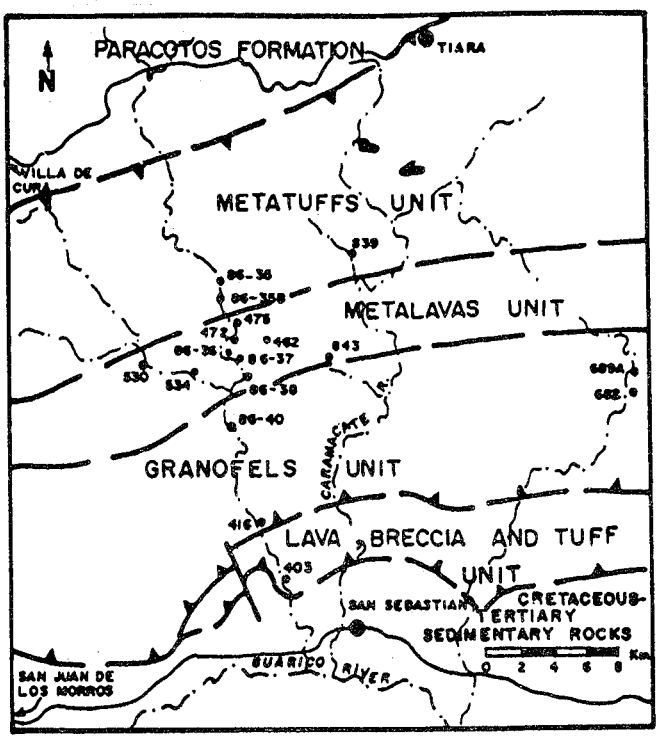

SERPENTINITES

THRUST FAULT

SAMPLES ANALYZED CHEMICALLY

FIGURE 5.11 : SIMPLIFIED GEOLOGIC MAP OF THE VILLA DE CURA BELT (FROM NAVARRO, 1983) AND LOCATION OF SAMPLES ANALYZED CHEMICALLY. THE GRANOFELS, METALAVAS, AND METATUFF UNITS CONSTITUTE THE VILLA DE CURA GROUP AND THE LAVAS, BRECCIAS, AND TUFF UNIT IS EQUIVALENT TO THE VOLCANIC TIARA SUR OR DOS HERMANAS FORMATION.

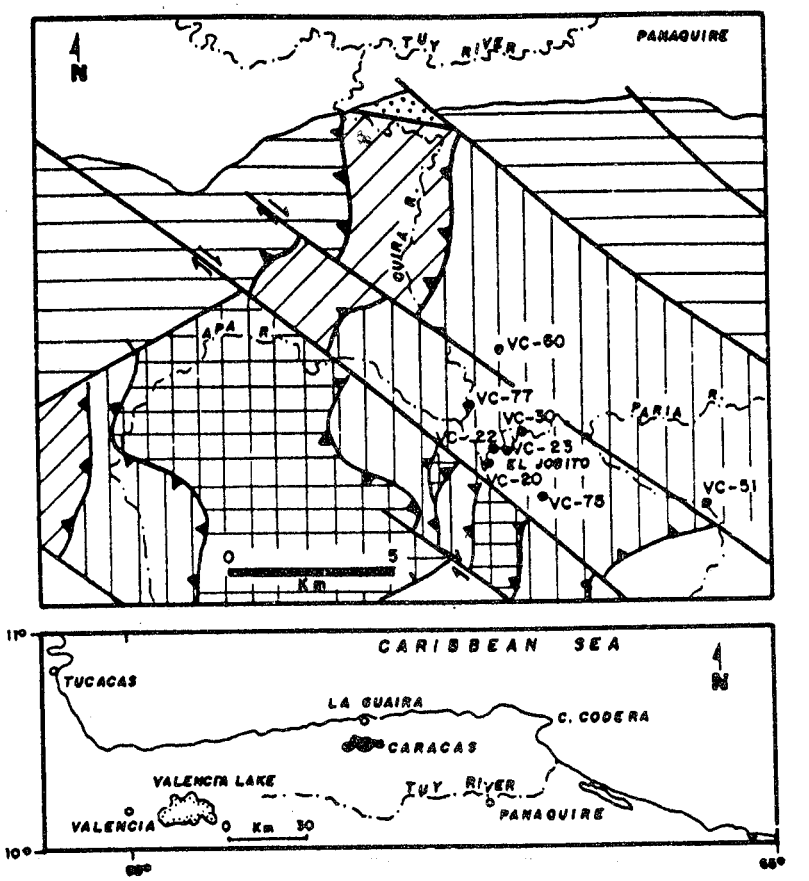

Cretaceous-Tertiary sedimentary rocks.

DOS HERMANAS Fm. (PYROXENIC METATUFF).

DOS HERMANAS Fm. (METALAVA , METATUFF , AND METABRECCIA).

APA COMPLEX (DUNITE , WHERLITE , CLINOPYROXENITE , AND GABBRO).

VILLA DE CURA GROUP.

SERPENTINITE.

FIGURE 5.12: SIMPLIFIED GEOLOGIC MAP OF THE VILLA DE CURA BELT IN GUATOPO NATIONAL PARK (FROM URBANI et al., 1987 b) AND LOCATION OF THE SAMPLES ANALIZED CHEMICALLY.

TABLE 5.7: Major- and trace-element data of metalavas from the Villa de Cura belt north of San Sebastian (major element values in percent; trace elements in ppm).

SAMPLES	SiO2	Al2O3	TiO2	Fe2O3	MnO	MgO	CaO	Na2O	K2O	P2O5	LOI	SUM
VO-86-35	45.89	15.68	1.19	10.62	0.11	8.04	8.27	1.22	0.52	0.10	n.d.	91.64
VO-86-35B	45.35	15.37	1.33	9.65	0.13	8.47	8.70	1.43	0.55	0.12	7.08	98.18
VO-86-36	44.23	15.72	0.84	10.08	0.22	14.06	6.17	1.92	0.15	0.19	n.d.	93.58
VO-86-37	44.00	16.00	0.79	10.60	0.20	14.18	6.36	2.04	0.03	0.17	6.56	100.93
VO-86-37B	44.12	15.86	0.82	10.34	0.20	14.46	6.01	1.98	0.09	0.20	n.d.	94.08
VO-86-38	55.50	16.00	0.69	8.55	0.16	4.15	8.10	2.25	1.52	0.09	2.00	99.01
VO-86-40	47.62	12.61	0.32	8.91	0.19	9.55	10.91	1.06	0.21	0.11	n.d.	91.49
QP-403	53.75	14.81	0.69	9.01	0.09	5.93	6.72	3.77	0.32	0.30	n.d.	95.39
QP-416	48.57	16.47	0.58	11.07	0.12	6.74	5.10	1.46	5.04	0.13	4.11	99.39
QP-462	48.57	14.52	0.99	9.65	0.14	8.26	10.17	2.72	0.03	0.11	4.76	99.92
QP-472	50.86	15.78	1.33	8.70	0.10	7.00	9.20	3.95	0.79	0.14	3.78	101.63
QR-475	44.72	15.78	1.74	11.55	0.16	7.47	11.70	3.01	0.20	0.20	4.03	100.56
QQ-530	54.35	16.29	0.83	10.09	0.18	6.28	4.42	1.57	3.41	0.20	n.d.	97.62
QRR-534	46.25	8.21	0.25	8.46	0.12	13.03	16.00	1.14	1.01	0.05	5.39	99.91
QH-682	51.60	14.10	1.33	10.60	0.12	5.85	8.00	3.91	3.32	0.17	1.85	100.85
QH-689A	45.53	12.42	0.52	11.07	0.16	11.30	11.60	1.43	1.06	0.17	3.45	98.71
QQ-839	45.03	12.84	0.52	11.31	0.16	11.77	12.20	1.35	0.59	0.13	3.57	99.47
QQ-843	46.25	13.68	0.52	11.65	0.16	10.41	11.70	1.60	0.66	0.15	3.92	98.47

	Cr	Ni	Zr	Y	Nb	Rb	Sr
VO-86-35	746	48	68	21	5.21	14	231
VO-86-35B	651	57	76	24	5.29	16	265
VO-86-36	803	87	64	22	5.24	10	156
VO-86-37	456	280	96	26	5.49	16	388
VO-86-37B	490	82	84	24	5.39	13	143
VO-86-38	33	119	82	24	13.00	62	231
VO-86-40	679	114	124	35	13.45	13	124
QP-403	25	43	131	36	13.03	69	371
QP-416	6	31	95	34	13.57	74	381
QP-462	191	104	82	30	15.23	9	27
QP-472	136	52	80	28	12.70	18	242
QR-475	165	65	92	31	5.99	20	255
QQ-530	37	96	102	23	12.45	52	233
QRR-534	785	124	76	19	5.30	10	111
QH-682	123	46	110	29	11.87	16	236
QH-689A	431	158	52	23	5.55	15	381
QQ-839	420	200	36	23	5.33	14	375
QQ-843	271	140	48	20	6.24	15	289

glaucophane metabasalt and is from the Metalava Unit of the Villa de Cura Group (Figure 5.11). The second is a prehnite-pumpellyite metalava from the Dos Hermanas Formation (Lava, Breccia, and Tuff Unit; Figure 5.11). The TiO_2 contents vary from 0.25 to 1.74 % with a mean of 0.85 %. The K_2O contents are between 0.03 to 3.41 % with a mean of 1.08 %. The potassium content suggests that most samples are island arc (Jakes and White, 1972; Condie, 1976; Peccerillo and Taylor, 1976) or marginal basin tholeiites (Saunders *et al.*, 1979), although the mobility of potassium makes any conclusion suspect. The higher titanium abundances (more than 1.0 %) are typical of abyssal tholeiites and the lower ones (between 0.52 and 0.84 %), are characteristic of basalts from island arcs (Jakes and White, 1972; Baker, 1982) and of some marginal basin ophiolites (Kay and Senechal, 1976; Saunders *et al.*, 1979).

The data plotted on a Ti/Y-Nb/Y diagram (Figure 5.13A) indicate a tholeiitic affinity. The K_2O-P_2O_5-TiO_2 diagram (Figure 5.13B) indicates a non-ocean floor affinity, but this diagram has also limited value. The trace- and minor-elements discrimination diagrams: Zr-3*Y-Ti/100 (Figure 5.14A), Zr/4-Y-2Nb (Figure 5.14B), and Zr/Y-Ti/Y (Figure 5.15A) indicate P-type MORB or VAB affinities for the Villa de Cura Group and a VAB affinity for the sample of the Dos Hermanas Formation (Fig. 5.14A and 5.15A). The binary Ni-Y diagram discriminating between VAB and MORB, indicates that most of the samples of the Villa de Cura Group have a mid-oceanic ridge affinity and the sample of Dos Hermanas Formation has an IAT affinity.

Guatopo National Park

The average major- and trace-element abundances for the metabasalts of the Dos Hermanas Formation from Guatopo National Park (Figure 5.12) are shown in Table A.5.5 in the Appendix and the entire data set is shown in Table 5.8. The SiO_2 content of the samples varies from 48.57 to 50.86 with a mean of 50.06 %, while the TiO_2 abundance range is between 0.55 and 1.19 % with a mean of 0.85 %, and the K_2O average is 1.08 % varying from 0.41 to 1.97 %.

The potassium content is not characteristic of low-K tholeiites; but K is mobile and thus, it is not a reliable indicator. The titanium content of most samples is typical of basalts belonging to the island arc tholeiitic series or seafloor basalts in marginal basins (Jakes and White, 1972; Saunders and Tarney, 1979; Saunders *et al.*, 1979; Baker, 1982; Hawkins and Melchior, 1985). An important difference between the Dos Hermanas Formation in Guatopo National Park and the Villa de Cura Group north of San Sebastian de los

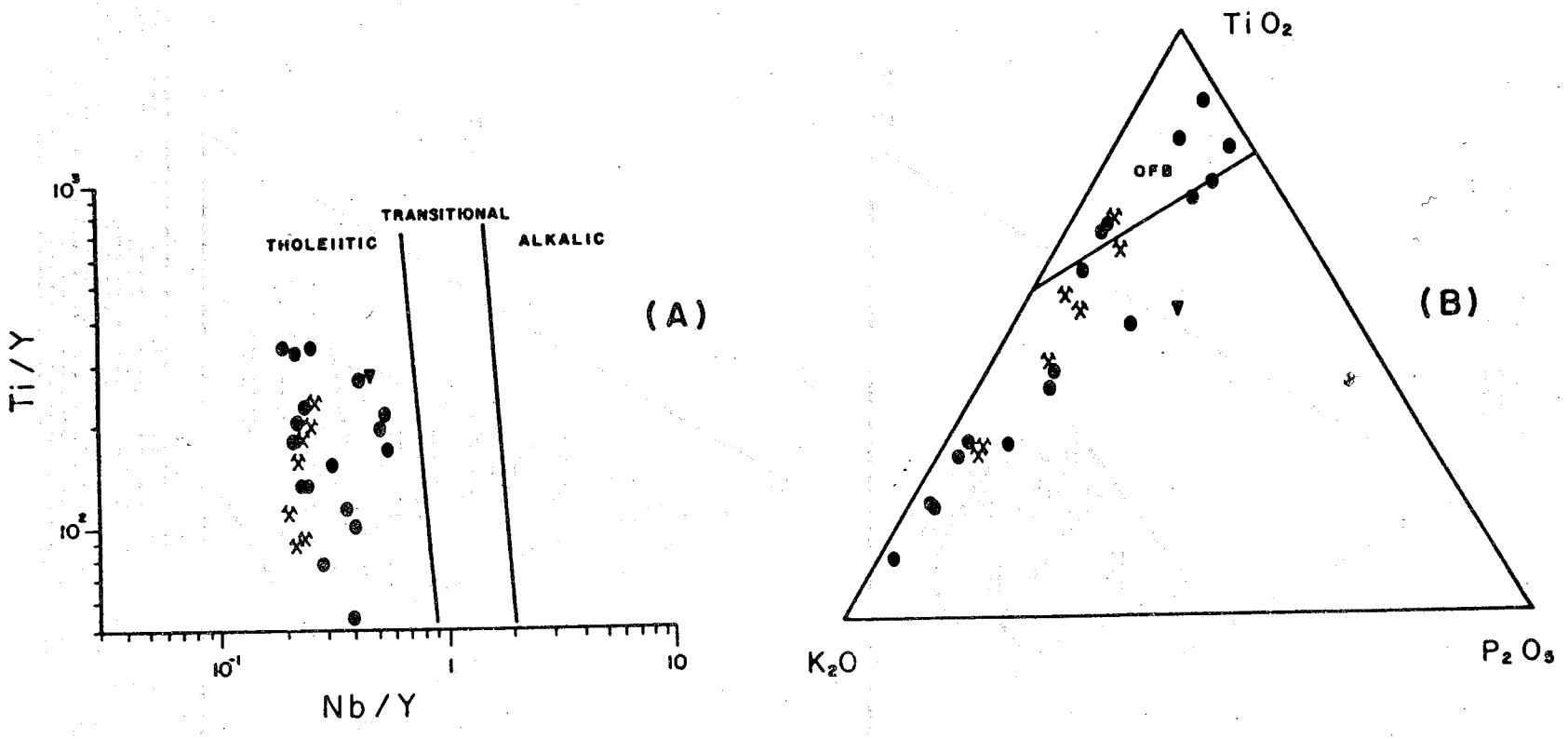

FIGURE 5.13 A-B. TECTONIC DISCRIMINANT DIAGRAMS FOR MAFIC ROCKS FROM THE VILLA DE CURA BELT. ● VILLA DE CURA GROUP NORTH OF THE TOWN OF SAN SEBASTIAN DE LOS REYES, ✕ DOS HERMANAS FORMATION IN GUATOPO NATIONAL PARK. ▼ DOS HERMANAS FORMATION NORTH OF THE TOWN OF SAN SEBASTIAN DE LOS REYES. A Ti/Y-Nb/Y DISCRIMINANT DIAGRAM OF PEARCE (1982). B TiO_2-K_2O-P_2O_5 DISCRIMINANT DIAGRAM OF PEARCE et al. (1975)

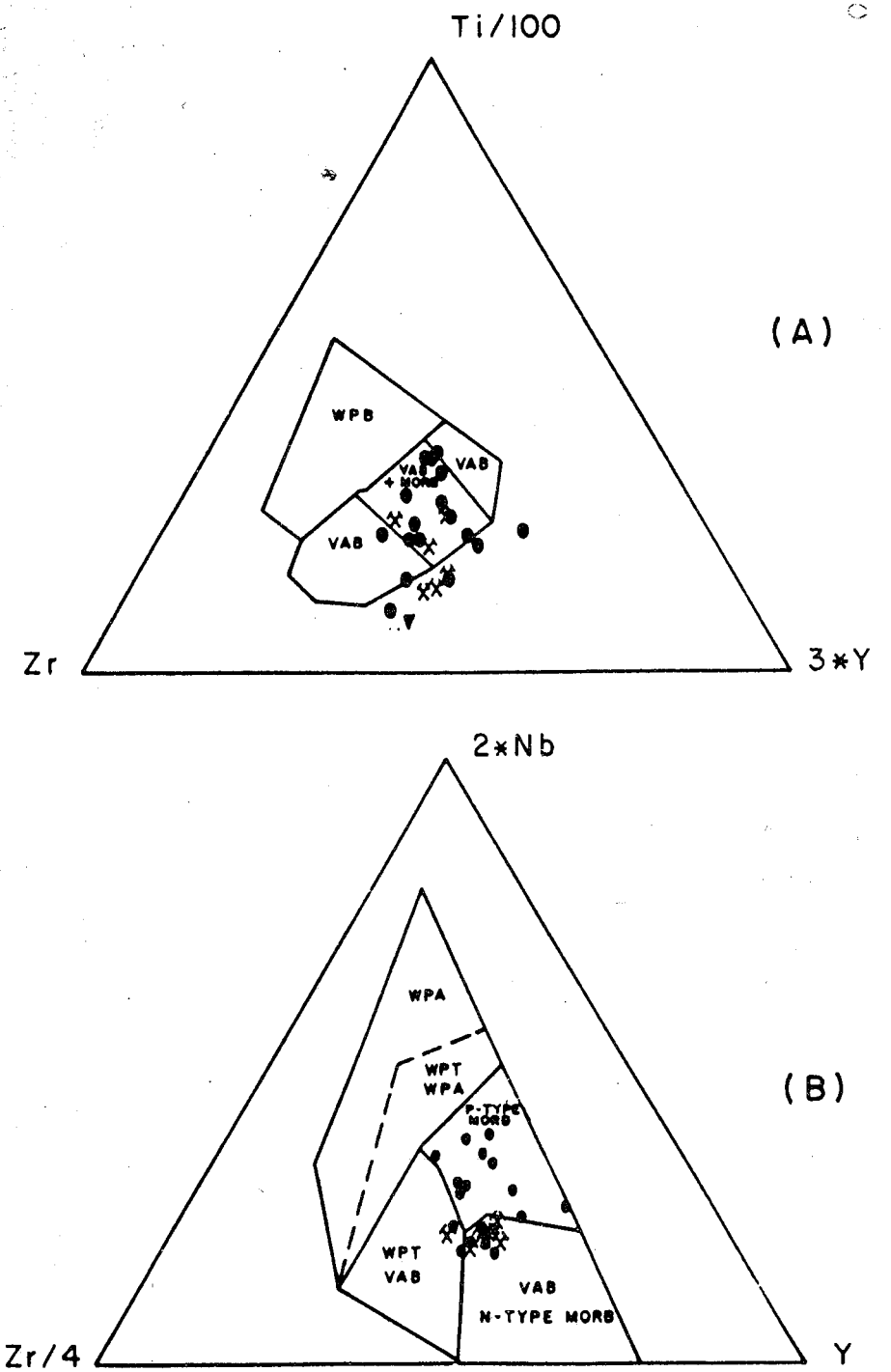

FIGURE 5.14 A-B: TECTONIC DISCRIMINANT DIAGRAMS FOR MAFIC ROCKS FROM THE VILLA DE CURA BELT. ● VILLA DE CURA GROUP NORTH OF THE TOWN OF SAN SEBASTIAN DE LOS REYES, ▼ DOS HERMANAS FORMATION NORTH OF THE TOWN OF SAN SEBASTIAN DE LOS REYES, ⚒ DOS HERMANAS FORMATION IN GUATOPO NATIONAL PARK. Ti/100-Zr-3*Y DISCRIMINANT DIAGRAM OF PEARCE AND CANN (1973). 2*Nb-Zr/4-Y DISCRIMINANT DIAGRAM OF MESCHEDE (1986)

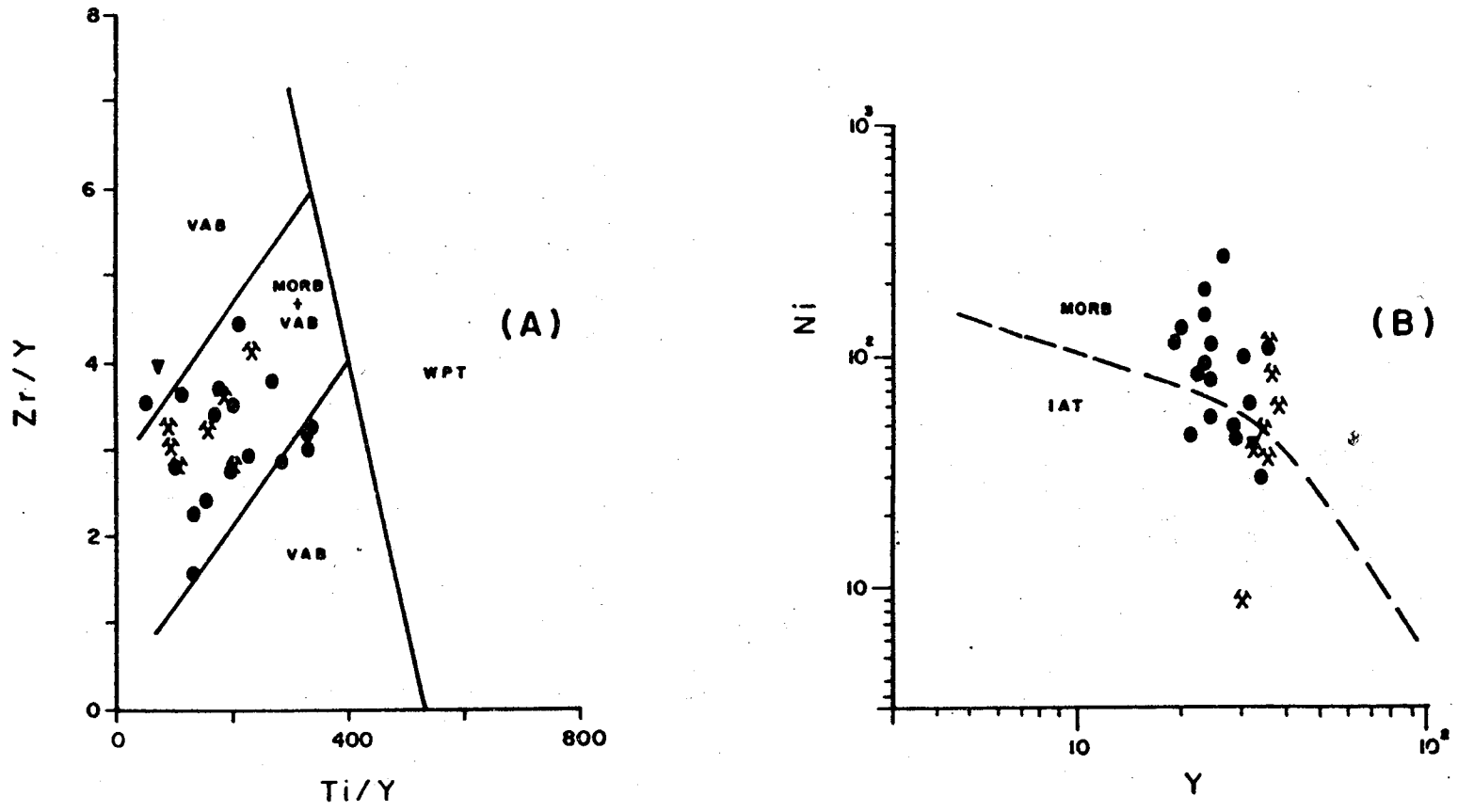

FIGURE 5.15 A-B : TECTONIC DISCRIMINANT DIAGRAMS FOR MAFIC ROCKS FROM THE VILLA DE CURA BELT. ● VILLA DE CURA GROUP NORTH OF THE TOWN OF SAN SEBASTIAN DE LOS REYES, ▼ DOS HERMANAS FORMATION NORTH OF THE TOWN OF SAN SEBASTIAN DE LOS REYES, ⚒ DOS HERMANAS FORMATION IN GUATOPO NATIONAL PARK. Zr/Y-Ti/Y DISCRIMINANT DIAGRAM OF PEARCE AND GALE (1979). Ni-Y DISCRIMINANT DIAGRAM OF CRAWFORD AND KEAYS (1978) AND CAPEDRI et al. (1980)

TABLE 5.8: Major- and trace-element data of metalavas from the Villa de Cura belt in the Guatopo National Park (major element values in percent; trace elements in ppm).

SAMPLES	SiO2	Al2O3	TiO2	Fe2O3	MnO	MgO	CaO	Na2O	K2O	P2O5	LOI	SUM
VC-20	50.67	14.19	0.55	8.76	0.27	14.03	7.74	1.78	0.60	0.11	n.d.	98.70
VC-20B	50.67	14.19	0.55	8.76	0.27	14.03	7.74	1.78	0.60	0.11	n.d.	98.70
VC-22C	48.57	15.35	0.71	8.65	0.28	11.90	7.00	4.74	1.66	0.16	n.d.	99.02
VC-23A	49.01	15.97	0.90	8.07	0.32	12.02	7.14	3.97	1.97	0.19	n.d.	99.56
VC-30A	49.16	16.29	1.08	9.66	0.38	11.31	7.40	1.61	0.48	0.17	n.d.	97.54
VC-51	50.86	14.76	1.19	10.45	0.39	8.11	6.34	4.13	0.86	0.13	n.d.	97.22
VC-60	51.50	15.97	1.09	9.52	0.28	8.61	10.50	3.39	0.41	0.10	n.d.	101.37

	Cr	Ni	Zr	Y	Nb	Rb	Sr
VC-20	360	87	117	36	8.09	7	76
VC-20B	433	122	106	35	8.22	9	83
VC-22C	86	64	107	38	7.77	16	71
VC-23A	73	52	109	34	7.41	34	77
VC-30A	14	41	90	32	7.88	23	529
VC-51	19	9	124	30	7.89	16	214
VC-60	23	38	126	35	7.91	12	845

Reyes, discussed above, is the lower content of the transition metals and the higher abundance of Zr and Y in the first.

The Ti/Y-Nb/Y discrimination diagram clearly indicates a tholeiitic character of the basaltic rocks of the Dos Hermanas Formation in Guatopo National Park. The K_2O-P_2O_5-TiO_2 ternary diagram shows a predominant non-ocean floor affinity (Figure 5.13B), although the mobility of K may invalidate this conclusion. A within-plate affinity is not indicated by the Zr-3*Y-Ti/100 diagram (Figure 5.14A), the Zr/4-Y-2*Nb diagram (Figure 5.14B), and neither by the variation diagram Zr/Y-Ti/Y shown in Figure 5.15A. Instead, a MORB-VAB affinity is suggested by Figures 5.14A and 5.15A and a VAB or N-type MORB tectonomagmatic settings by Figure 5.14B.

The discrimination between VAB and MORB can not be established in the Ni-Y diagram (Figure 5.15B). Thus, the basaltic rocks from this area could have extruded in an island arc setting, a mid-oceanic ridge, or in a transitional setting, such as a back-arc basin.

Rare Earth Elements (REE)

The REE abundances of four samples from the Villa de Cura Group near San Sebastian de los Reyes are shown in Table 5.4 and the chondrite-normalized patterns are shown in Figure 5.16. Sample VO-86-35 is characterized by a flat pattern typical of mid-oceanic ridge basalts (Basaltic Volcanism Study Project, 1981). The $(La/Sm)_n$ ratio of the sample is 0.93, which is also within the range of the mid-oceanic ridge basalts (Jahn *et al.*, 1974).

The pattern of samples QP-472 and QO-843 show a light REE enrichment and an almost flat pattern for the heavy REE. The patterns are not enclosed by the envelopes of the mid-oceanic ridges and island arc tholeiites (Kay *et al.*, 1970; Philpotts *et al.*, 1971; Schilling, 1975; Basaltic Volcanism Study Project, 1981; Humphris *et al.*, 1985). The $(La/Sm)_n$ ratios for these samples are even higher than 1.57, which is a typical value for island arc tholeiites (Jahn *et al.*, 1974). However, such values have been reported in a few samples from the Mid-Atlantic ridge (Frey *et al.*, 1968: Frey *et al.*, 1974; Langmuir *et al.*, 1977), in Pleistocene-Miocene basaltic samples from the Reykjanes Peninsula (Schilling, 1973; Wood *et al.*, 1979; Schilling *et al.*, 1982), and in the Balagne metabasalts from the Corsica Ophiolite in the western Mediterranean (Venturelli, *et al.*, 1979). The light REE enrichment has been proposed to indicate a distinct deep-mantle plume magma source (Schilling, 1973) or a more

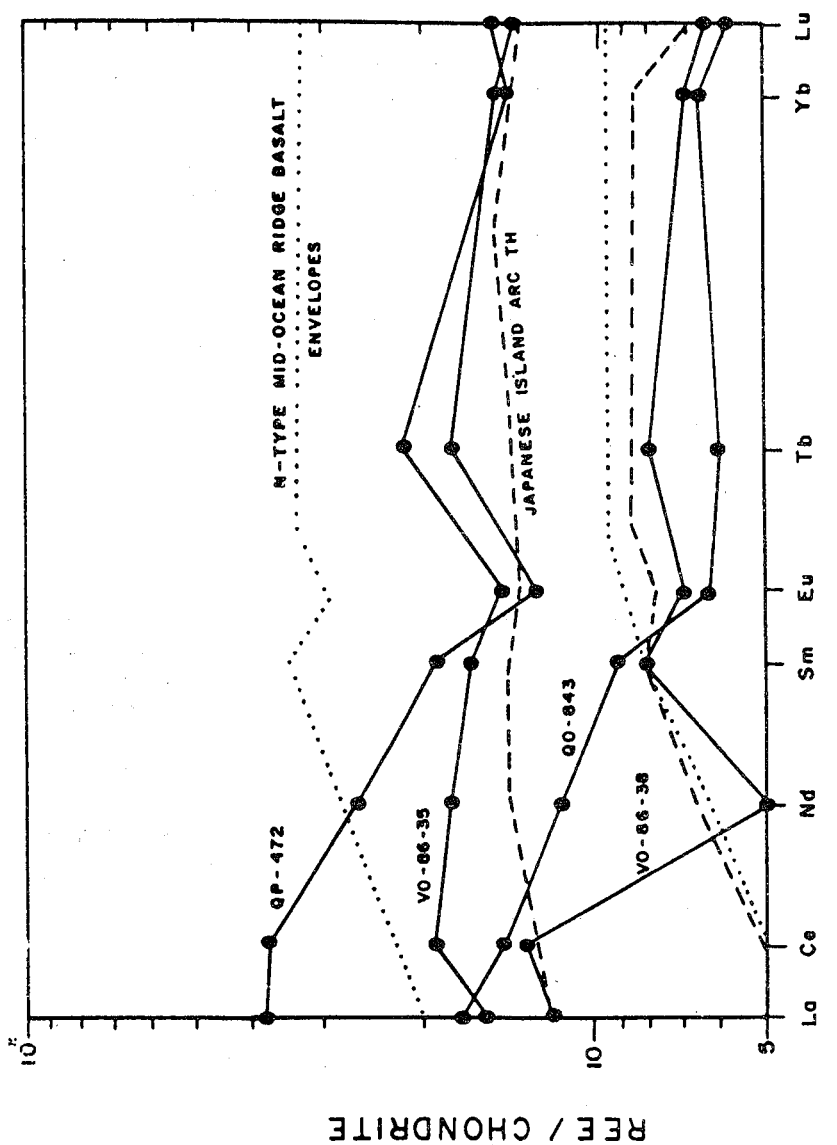

FIGURE 5.16 : REE PATTERNS OF METALAVAS FROM THE VILLA DE CURA GROUP NORTH OF THE TOWN OF SAN SEBASTIAN DE LOS REYES. THE N-TYPE MID-OCEAN RIDGE BASALT ENVELOPES IS FROM THE BASALTIC VOLCANISM STUDY PROJECT (1981) AND THE JAPANESE ISLAND ARC THOLEIITE ENVELOPES ARE FROM PHILPOTTS. et al. (1971)

clinopyroxene-rich source and/or of a more light-REE enriched source (Venturelli *et al.*, 1979). The samples have $(La/Ce)_n$ ratios within the range of the values described by Langmuir *et al.* (1977) for basalts from the famous area, which are enriched relative to the values proposed by Kay *et al.* (1970). Moreover, the Zr, Nb, Y, and transition metals content for the Villa de Cura lavas are quite similar to those of the mid-oceanic ridge basalts in the Famous area described by Langmuir *et al.* (1977). Similar patterns have been also described for andesites (Johnson, 1982) and island arc basalts from Java (Hutchinson, 1982). However, the Cr, Ni, and Zr contents of the two Villa de Cura samples do not correspond to those characteristic of island arc basalts (Baker, 1982; Ewart, 1982).

The fourth sample (VO-86-38) shows a similar pattern as sample QO-843. It has a SiO_2 content too high for a basalt; although, similar rocks have been described in marginal basins and seafloor sequences (Saunders and Tarney, 1979; Saunders *et al.*, 1979; Hawkins and Melchior, 1985). Thus, tentatively, it is assumed that these Villa de Cura samples have formed in a mid-oceanic ridge setting.

Conclusions

The metabasalts from the Villa de Cura Group near San Sebastian de los Reyes clearly have a tholeiitic affinity. They certainly have not formed within a plate. They may have formed at a divergent plate boundary. The REE abundances and patterns do not yield unequivocal evidence, but they are not inconsistent with magmatism in deep ocean basins.

Additionaly, the high P/T metamorphism that these rocks underwent (See Chapter 6 on Metamorphism) may support the notion that the protolith was oceanic.

The metabasalts in the Dos Hermanas Formation in Guatopo National Park are also tholeiites and do not resemble within-plate basalts. They may be related to an island arc, marginal basin, or mid-oceanic ridge. However, the large amount of metatuff interbedded with the lavas, would support an island arc tectonic setting.

Venezuelan Islands

The original tectonic setting of mafic rocks of Margarita was evaluated on the basis of composition of twenty amphibolite and eclogite samples from the Peninsula of Paraguachoa, northeast Margarita (Figure 5.17) and two eclogite samples from the Peninsula of Macanao, west Margarita. Eleven samples of metagabbro and metadiabase from

Los Roques Island were analyzed; the sample location is shown on the simplified geologic map of Figure 5.18.

Margarita Island

Average major- and trace-element abundances in rocks from Margarita Island are shown in Table A.5.6; the entire data set is shown in Table 5.9. The rocks are basic with a SiO_2 range between 43.26 and 53.02 % and a mean of 48.14 %; the TiO_2 contents are from 0.20 to 1.88 % with a mean of 0.88 %, while the mean K_2O content is and 0.32 ranging between 0.05 to 1.08 %. Disregarding the mobility of potassium, its abundance is characteristic of low-K tholeiites of the island arc suite, while the titanium contents vary between island arc and ocean floor abundances (Jakes and White, 1972; Condie, 1976; Baker, 1982). The mafic samples from Margarita Island reveal clearly a tholeiitic affinity on the Ti/Y-Nb/Y variation diagram (Figure 5.19 A).

The major-element ternary variation diagrams K_2O-P_2O_5-TiO_2 (Figure 5.19B) and $MnO*10$-P_2O_5*10-TiO_2 (Figure 5.20A) indicate an ocean floor affinity and a MORB and IAT affinity, respectively, assuming again that these elements were not mobile. It is difficult even to rule out a within-plate origin, because the common discrimination diagrams include the incompatible elements (during basalt fractionation) Zr and Ti, which have anomalously low and high abundances, respectively. The Zr values are even lower than the common abundance in low-K volcanic arc tholeiites, while the titanium abundances are higher than the common values used by Pearce and Cann (1973) for characterising the different magma types. Thus, the data do not plot in the various fields proposed by the diverse authors (Pearce and Cann, 1973; Meschede, 1986).

However, the samples with the lowest Zr abundances (3 to 5 ppm) correlate well with the lowest Y abundances (1 ppm), but as both were determined by inductively coupled plasma mass spectrometry (Table A.5.0), an analytical problem is suggested. The within-plate affinity was only ruled out on the basis of the Zr/Y-Ti/Y (Figure 5.20B). The Zr abundances reported by Langmuir *et al.* (1977) from the Mid-Atlantic ridge in the Famous area are ranging from 31 to 67 ppm, which is less than the average of ocean ridge basalts (122 ppm) found by Erlank and Kable (1976). Similar low Zr abundances were recognized in the axial sequences of the Troodos Massif in Cyprus (from 5 to 118 ppm; Smewing *et al.*, 1975) and values less than 10 ppm are reported for gabbros from the same complex by Kay and Senechal (1976). In addition, low Zr values (6 to 22 ppm) are reported in the mafic dikes from the Northern Pindos Ophiolite in Greece

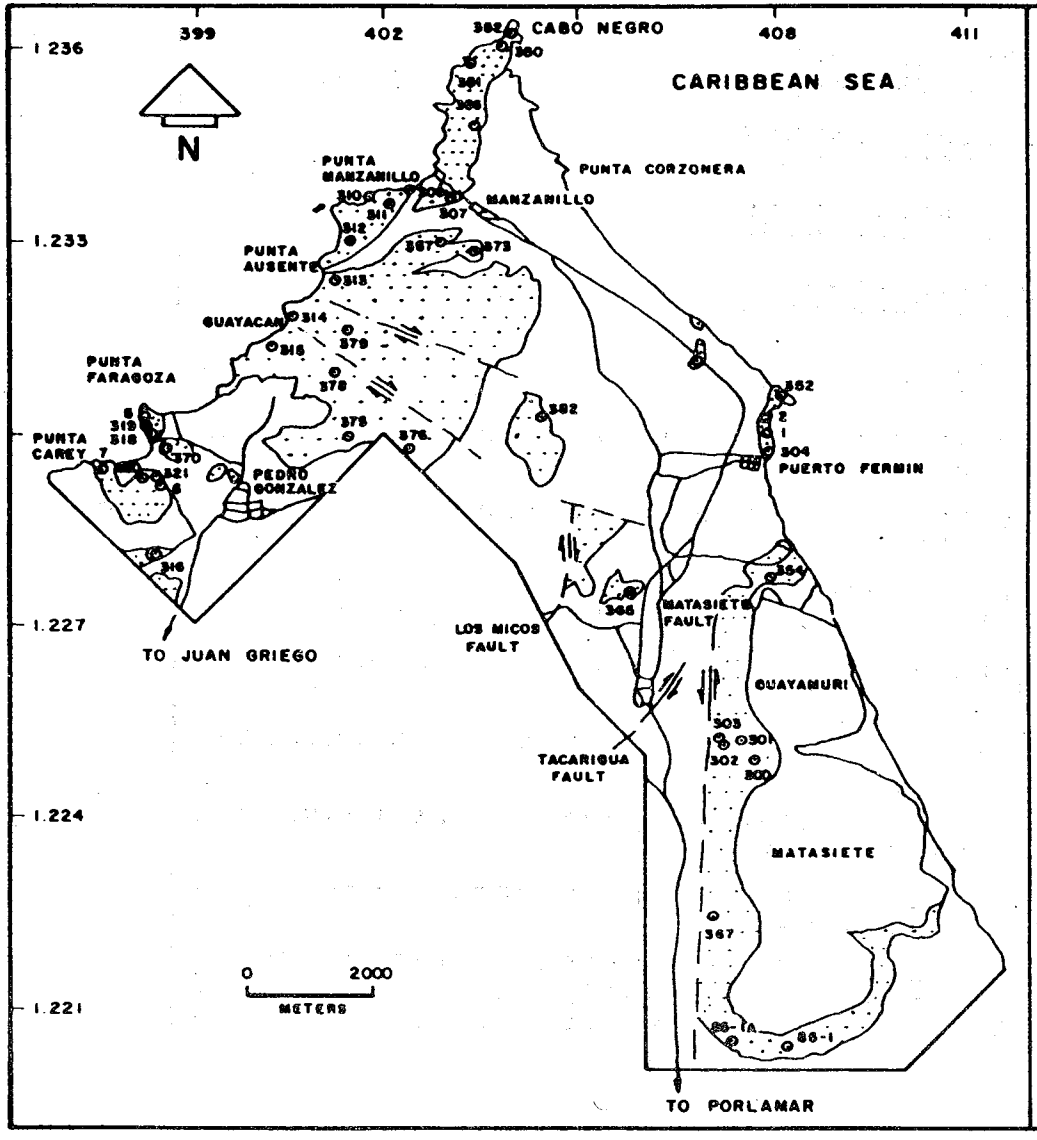

FIGURE 5.17: LA RINCONADA GROUP IN NORTHEASTERN PARAGUACHOA PENINSULA, MARGARITA ISLAND, VENEZUELA (FROM MARESCH, 1973; VIGNALI, 1979; CARRILLO AND VIVAS, 1986; CHEVALIER, 1987).

- LA RINCONADA GROUP.
- RIGHT LATERAL STRIKE-SLIP FAULT.
- LEFT LATERAL STRIKE-SLIP FAULT.
- SAMPLE LOCATION 301

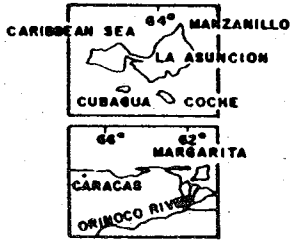

TABLE 5.9: Major- and trace-element data of mafic rocks from Margarita Island (major element values in percent; trace elements in ppm).

SAMPLES	SiO2	Al2O3	TiO2	Fe2O3	MnO	MgO	CaO	Na2O	K2O	P2O5	LOI	SUM
VO-83-302	49.76	10.71	0.30	9.41	0.13	14.53	7.66	0.56	0.05	0.07	5.12	98.30
VO-83-3028	53.02	13.61	0.30	7.91	0.12	10.17	8.49	3.41	1.04	0.07	0.75	98.89
VO-83-3058	50.00	17.00	1.21	12.52	0.12	3.74	9.50	4.24	0.22	0.22	0.14	98.91
VO-83-307	43.34	16.61	0.98	13.45	0.15	4.54	9.46	4.45	1.08	0.15	6.12	100.33
VO-83-308	43.26	17.03	0.81	12.97	0.16	6.93	12.64	3.23	0.25	0.09	1.38	98.75
VO-83-3088	46.58	14.54	0.64	8.70	0.11	12.14	8.00	3.12	0.32	0.09	4.02	98.26
VO-83-309	47.64	16.20	0.70	12.26	0.15	5.71	10.17	2.76	0.16	0.09	2.76	98.60
VO-83-310	49.10	15.37	0.64	11.07	0.14	7.52	10.00	3.88	0.19	0.12	1.65	99.68
VO-83-311	47.64	17.44	0.75	11.78	0.11	4.54	10.00	3.98	0.50	0.12	1.99	98.85
VO-83-3138	49.10	14.95	1.04	9.41	0.15	8.42	10.45	3.55	0.20	0.05	1.35	98.67
VO-83-315	51.33	15.37	0.65	10.12	0.12	6.79	11.58	2.87	0.16	0.10	1.07	100.16
VO-83-316	49.83	15.78	0.58	8.46	0.08	7.73	12.50	2.87	0.08	0.06	1.41	99.38
VO-83-317	47.06	16.20	0.31	9.65	0.11	9.78	11.79	2.22	0.66	0.01	2.70	100.49
VO-83-318	47.00	16.20	1.13	10.84	0.11	6.79	11.54	3.25	0.12	0.13	1.70	98.81
VO-83-319	48.13	16.62	1.06	9.41	0.13	6.79	12.10	3.23	0.18	0.12	1.56	99.33
VO-83-321	48.53	15.68	1.20	10.13	0.15	7.71	10.55	3.31	0.15	0.10	n.d.	97.51
VO-83-322	43.87	14.52	1.80	17.00	0.18	7.63	11.00	3.59	0.07	0.09	0.96	100.71
VO-83-323	50.08	15.78	0.20	5.62	0.08	9.94	10.95	2.58	1.02	0.01	3.46	99.72
VO-83-324	49.83	16.61	0.99	13.44	0.02	6.16	8.40	3.44	0.12	0.07	0.05	99.13
VO-83-326	47.00	14.95	1.07	14.39	0.15	7.94	10.24	2.51	0.12	0.12	1.38	100.47
VO-86-5	48.72	15.16	1.15	9.89	0.16	7.95	10.91	3.39	0.16	0.09	0.96	98.54
VO-86-6	48.34	16.20	1.26	10.36	0.15	7.47	11.37	3.23	0.12	0.12	0.64	99.26

	Cr	Ni	Zr	Y	Nb	Rb	Sr
VO-83-302	1000	380	3	9	1.00	12	519
VO-83-3028	85	126	60	26	13.97	7	166
VO-83-3058	6	17	1	18	2.00	11	225
VO-83-307	619	132	21	14	7.47	7	199
VO-83-308	240	37	30	13	7.45	11	297
VO-83-3088	12	36	8	21	1.00	14	468
VO-83-309	41	32	45	19	7.98	8	276
VO-83-310	180	59	3	19	1.00	11	190
VO-83-311	2	18	5	18	1.00	15	180
VO-83-3138	190	28	21	21	5.19	6	234
VO-83-315	11	12	24	21	6.44	9	201
VO-83-316	897	328	21	23	5.09	9	43
VO-83-317	57	67	30	28	6.22	5	199
VO-83-318	58	33	27	16	6.77	5	199
VO-83-319	54	37	21	15	7.09	7	78
VO-83-321	64	41	27	21	7.28	2	154
VO-83-322	144	48	33	23	8.09	8	191
VO-83-323	128	32	30	22	5.23	6	453
VO-83-324	171	86	21	21	10.20	12	224
VO-83-326	921	249	39	10	5.49	12	219
VO-86-5	234	69	30	21	5.20	2	235
VO-86-6	150	68	4	23	1.00	19	209

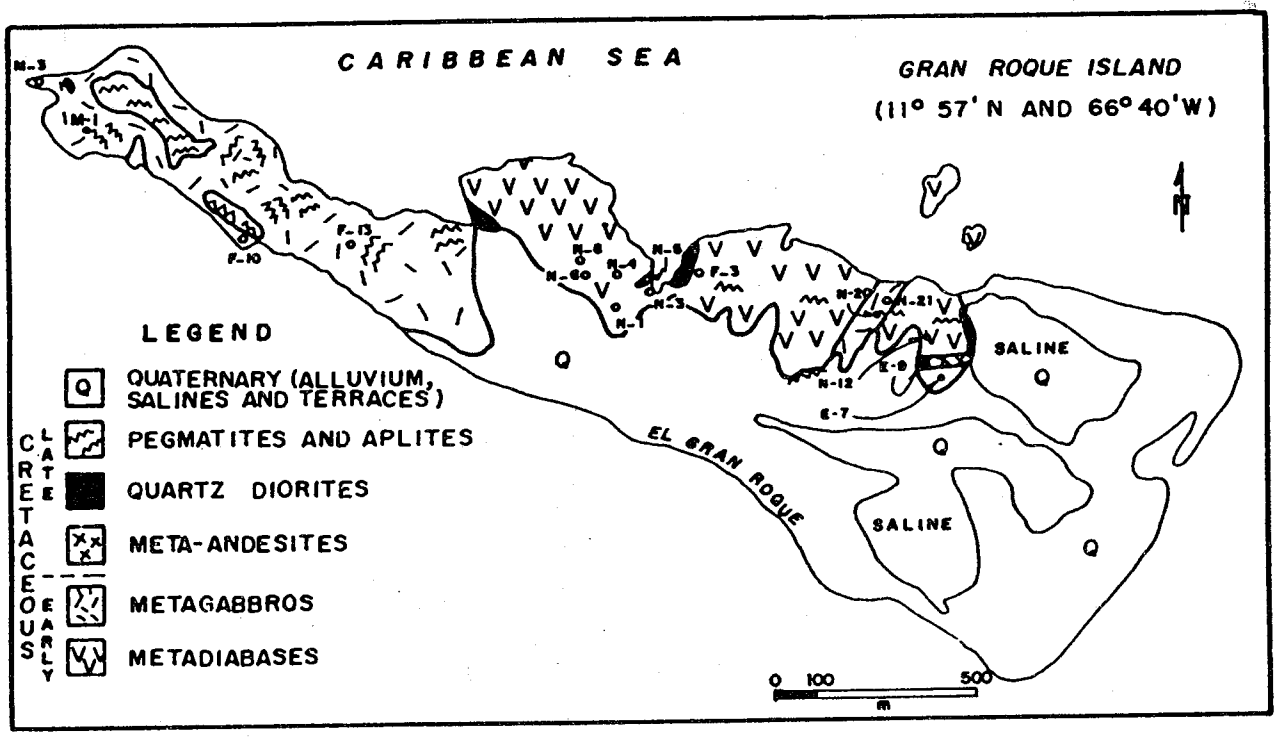

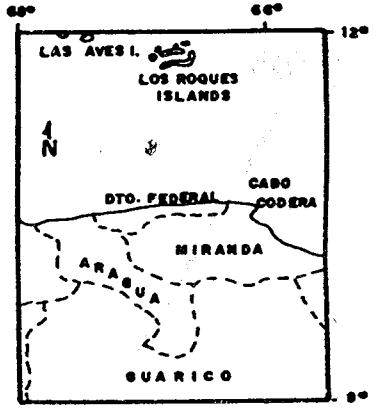

FIGURE 5.18 : SIMPLIFIED GEOLOGIC MAP OF THE GRAN ROQUE ISLAND (FROM GONZALEZ DE JUANA et al, 1980) AND THE LOCATION OF THE SAMPLES ANALYZED CHEMICALLY.

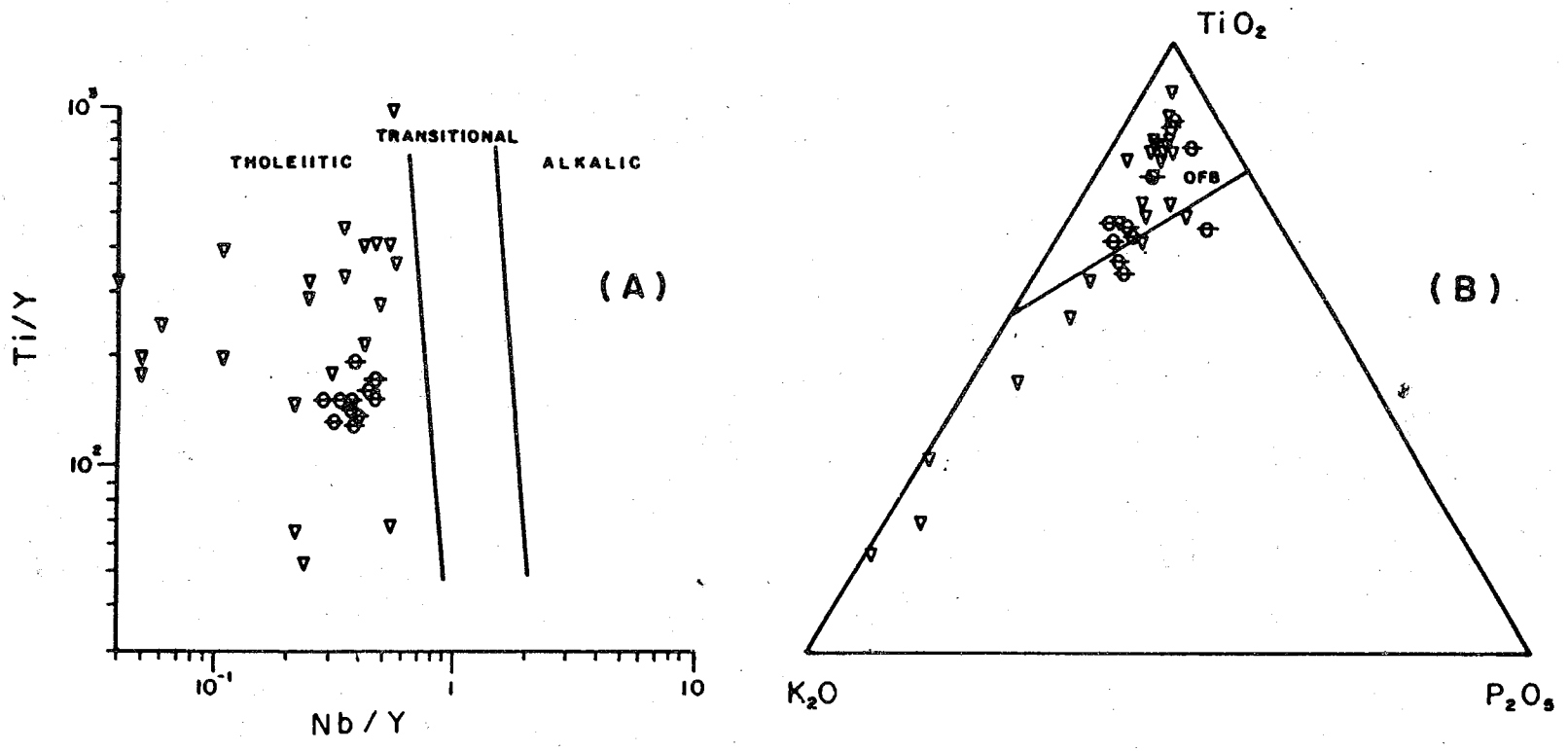

FIGURE 5.19 A-B : TECTONIC DISCRIMINANT DIAGRAMS FOR MAFIC ROCKS FROM THE MARGARITA AND LOS ROQUES ISLANDS. ▽ MARGARITA ISLAND, ⊖ LOS ROQUES ISLAND. A Ti/Y - Nb/Y DISCRIMINANT DIAGRAM OF PEARCE (1982). B TiO_2 - K_2O - P_2O_5 DISCRIMINANT DIAGRAM OF PEARCE *et al.* (1975)

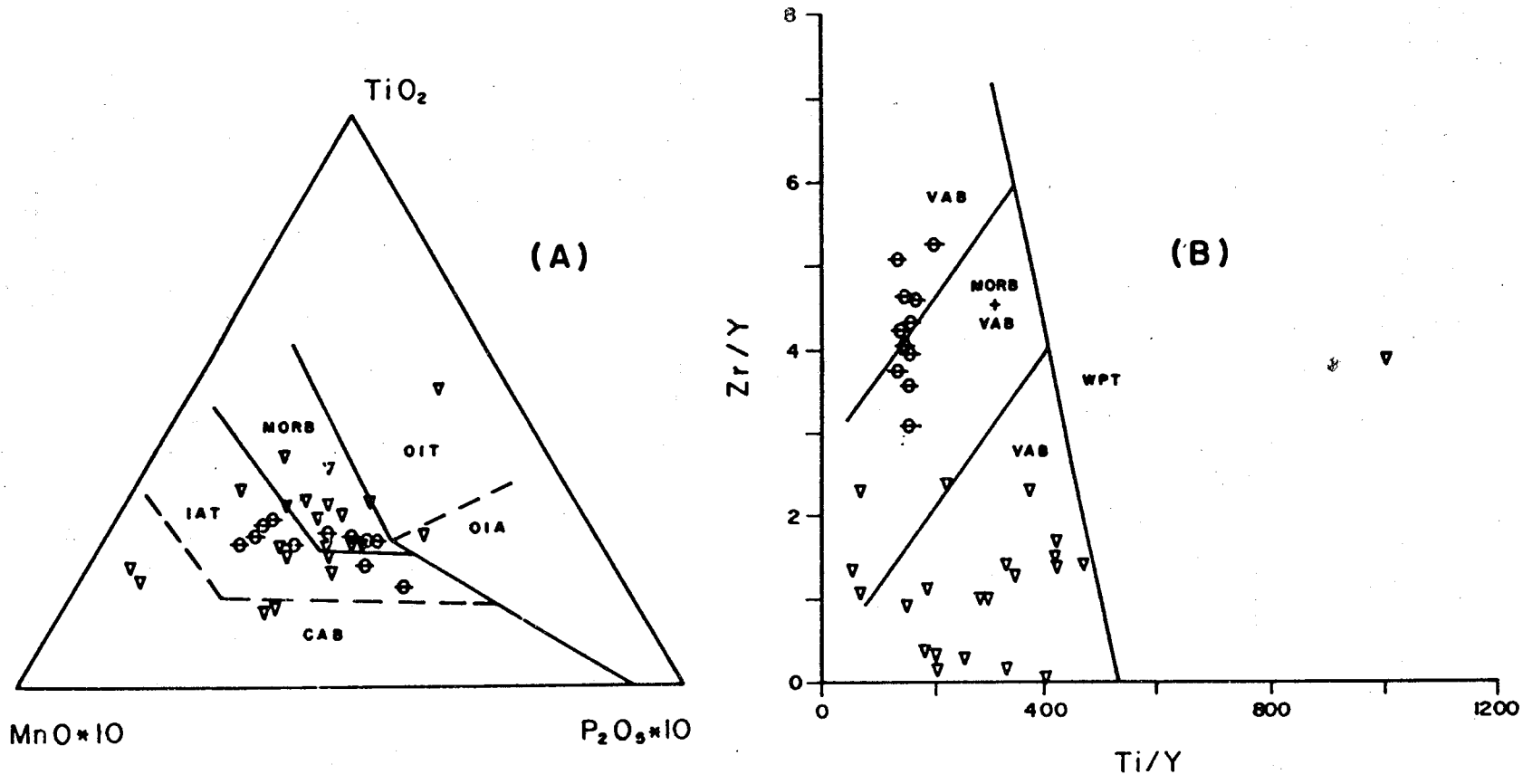

FIGURE 5.20 A-B : TECTONIC DISCRIMINATION DIAGRAMS FOR MAFIC ROCKS FROM THE MARGARITA AND LOS ROQUES ISLAND. ▽ MARGARITA ISLAND, ⊖ LOS ROQUES ISLAND. A TiO_2 - MnO*10 - P_2O_5*10 DISCRIMINATION DIAGRAM OF MULLEN (1983). B Zr/Y - Ti/Y DISCRIMINATION DIAGRAM OF PEARCE AND GALE (1979).

(Dupuy *et al.*, 1984). Thus, abnormally low Zr abundances are found in young ocean floor and in ancient ophiolites, with which the mafic samples from Margarita with Zr contents between 21 and 60 ppm can be correlated (Table 5.9).

A within-plate affinity can be discounted on the basis of the Zr/Y-Ti/Y diagram (Figure 5.20B), while no discrimination can be made between VAB and MORB on a Ti/Cr-Ni (Figure 5.21A), and the Ni-Y ratio (Figure 5.21B) favors an IAT affinity. This may suggest that the tectonic environment was composite or transitional: VAB and MORB or a back arc basin close to an island arc. The first seems more likely, because the samples can be separated into two populations: (a) One with lower TiO_2 values, high Cr and Ni, and variable Zr, Nb, and Y, which plot in the mid-oceanic ridge field (samples mainly from Cerro Matasiete, the schist-amphibolite sequence near Manzanillo, Juan Griego Formation near Altagracia, and two localities of eclogite boudins in Macanao), and (b) the other set with higher TiO_2 values, Cr less than 100 ppm, Ni less than 86 ppm, and variable abundances of the other trace elements, which plot mainly in the IAT field (these are eclogite samples from northeastern Paraguachoa between Manzanillo and Pedro Gonzalez, gabbro sample from the Morro de Porlamar, and three mafic boudins, one from Macanao and two from Paraguachoa).

The first group consisting of the mafic boudins in the Juan Griego Group or interlayered with the Matasiete Trondhjemite may have formed at a mid-oceanic ridge or marginal basin. It is possible however, that the eclogites and gabbros of the second group originally formed in an island arc or back arc basin close to a volcanic arc.

Los Roques Island

The major- and trace-element abundances in eleven mafic samples from Los Roques Island are shown in Table 5.10 and the element averages appear in Table A.5.7 in the Appendix. The SiO_2 contents are indicative of the mafic composition of the analyzed samples. The TiO_2 content varies from 0.72 to 1.12 % with a mean of 0.92 and the K_2O abundances are very low with a range between 0.05 and 0.41 % and a mean of 0.21 %. If the potassium content is original, the rocks are in the range of island arc tholeiites (Jakes and White, 1972; Baker, 1982; Ewart, 1982).

The data of the metagabbros and metadiabases plotted on a Ti/Y-Nb/Y diagram (Figure 5.19A) indicate a tholeiitic affinity. The K_2O-P_2O_5-TiO_2 major-element ternary diagram indicates that eight of the eleven samples can be identified

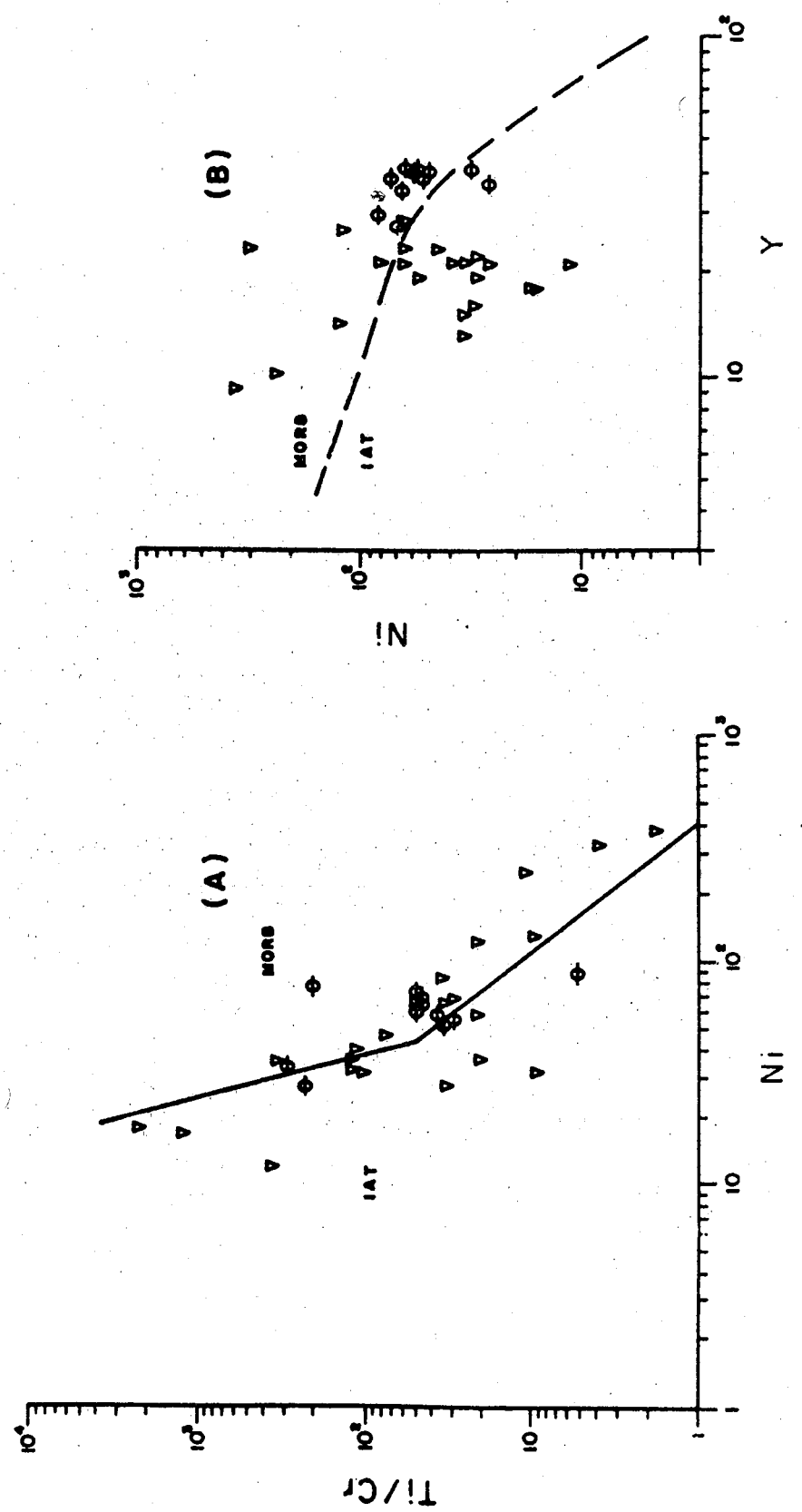

FIGURE 5.21 A-B: TECTONIC DISCRIMINANT DIAGRAMS FOR MAFIC ROCKS FROM THE MARGARITA AND LOS ROQUES ISLANDS. ▽ MARGARITA ISLAND, ⊕ LOS ROQUES ISLAND. A Ti/Cr-Ni DISCRIMINANT DIAGRAM OF BECCALUVA et al. (1979). B Ni-Y DISCRIMINANT DIAGRAM OF CRAWFORD AND KEAYS (1978) AND CAPEDRI et al. (1980)

TABLE 5.10: Major- and trace-element data of metagabbros and metadiabases from Los Roques Island (major element values in percent; trace elements in ppm).

SAMPLES	SiO2	Al2O3	TiO2	Fe2O3	MnO	MgO	CaO	Na2O	K2O	P2O5	LOI	SUM
N-1	47.79	13.68	0.72	12.73	0.16	8.94	13.00	1.36	0.05	0.06	1.12	99.13
N-3	49.32	14.52	0.80	12.80	0.16	8.56	13.00	1.79	0.12	0.23	0.29	104.29
N-4	50.48	15.65	0.81	9.26	0.16	8.21	11.24	1.99	0.27	0.07	n.d.	98.14
N-6	49.53	14.08	0.96	9.26	0.14	8.65	12.50	1.31	0.30	0.15	n.d.	96.88
N-8	50.25	14.92	1.02	10.13	0.19	9.02	12.95	2.21	0.18	0.12	n.d.	100.99
N-12	49.32	14.10	0.86	11.80	0.14	8.31	12.70	1.75	0.07	0.07	1.61	100.73
N-20	48.47	16.01	0.95	9.23	0.17	8.51	9.09	2.77	0.39	0.19	n.d.	95.78
N-21	48.34	15.32	1.04	9.47	0.14	8.77	10.14	2.85	0.41	0.17	n.d.	96.65
E-7	49.32	14.10	0.86	12.70	0.15	8.42	12.80	1.64	0.11	0.07	0.91	101.08
F-3	49.32	14.52	0.99	10.60	0.14	8.47	11.60	2.58	0.07	0.14	1.73	100.16
F-13	51.07	15.02	1.12	10.25	0.17	9.58	11.97	2.43	0.34	0.14	n.d.	102.0

	Cr	Ni	Zr	Y	Nb	Rb	Sr
N-1	90	74	116	27	12.54	22	176
N-3	914	89	133	29	12.33	20	169
N-4	22	28	182	36	11.18	27	282
N-6	170	53	180	39	14.57	30	146
N-8	131	67	158	40	14.74	20	157
N-12	182	56	156	37	14.46	34	149
N-20	29	79	132	37	12.24	19	175
N-21	22	34	123	40	11.39	39	218
E-7	105	61	146	39	14.97	37	153
F-3	162	59	162	40	14.71	33	149
F-13	147	70	178	34	13.24	19	175

as OFB's (Figure 5.19B). The data plotted on a MnO*10-P_2O_5*10-TiO_2 discrimination diagram indicate a mid-ocean ridge or an island arc tectonic settings (Figure 5.20A). The rocks were not within-plate basalts as indicated by the Zr/Y-Ti/Y variation diagram (Figure 5.20B); instead, this diagram suggests a volcanic arc or a mid-ocean ridge environment. However, the diagrams Ti/Cr-Ni (Figure 5.21A) and Ni-Y (Figure 5.21B) fit a mid-ocean ridge affinity somewhat better.

Rare earth elements (REE)

Rare-earth element abundances of four samples from Margarita Island were determined (Table 5.4) and the chondrite normalized patterns are shown in Figure 5.22. Sample VO-83-308B is from an undeformed post-metamorphic mafic dike, intrusive into the La Rinconada Group. The pattern shows a slight negative Eu anomaly and a light REE enrichment. The pattern can be included in the oceanic ridge envelopes of Kay *et al.* (1970) and the Basaltic Volcanism Study Project (1981); it is also similar to the enriched pattern for the Mid-Atlantic ridge basalts from close to Tristan da Cunha (Humphris *et al.*, 1985) or with the E-type MORB (transitional between depleted N-type MORB and OIB) described by Nye and Reid (1986) in Okmok volcano, Central Aleutians.

The other samples are eclogites (VO-83-305, VO-83-315, and VO-83-318). Their REE pattern fall within the ocean floor envelopes of the Basaltic Volcanism Study Project (1981). Sample VO-83-318 is not included in the ocean floor or island arc envelopes. However, the samples show a similar pattern as the Pleistocene-Miocene lavas of the Iceland hotspot (Schilling *et al.*, 1982). They resemble the enriched pattern of the Mid-Atlantic ridge described by Humphris *et al.* (1985). The similarity of these samples with sample VO-83-308B, discussed above, indicates also a correlation with N-type and E-type MORB. Furthermore, the fact that these rocks underwent eclogite metamorphism suggests also an oceanic origin.

Conclusions

The mafic rocks from Margarita have a complex origin; they are tholeiites with low Zr and high Ti contents. Their original tectonic setting is debatable. The eclogites may represent marginal basin tholeiites extruded close to an island arc. The mafic dikes intruding the eclogite-bearing formations have MORB or E-type MORB affinity. The mafic boudins and layers in the Matasiete Trondhjemite and the Juan Griego Group show a mid-ocean ridge affinity.

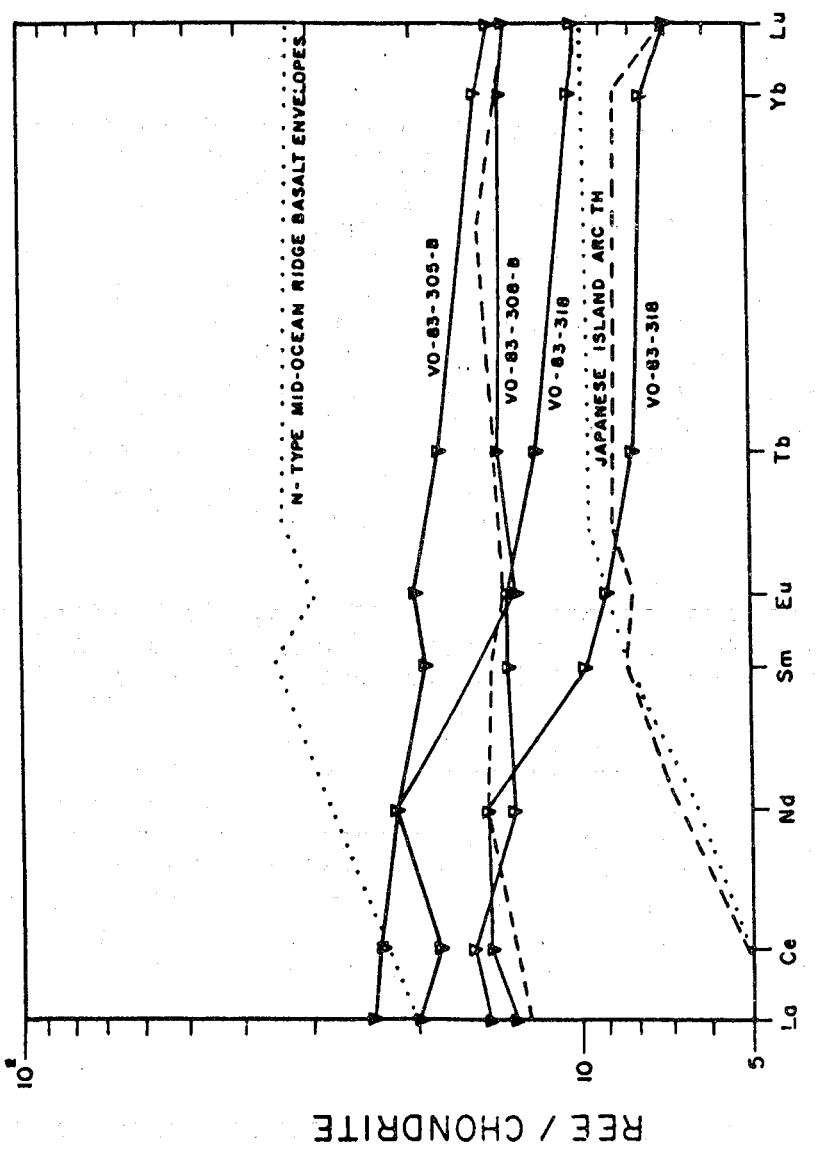

FIGURE 5.22: REE PATTERNS OF MAFIC ROCKS FROM MARGARITA ISLAND. THE N-TYPE MID-OCEAN RIDGE ENVELOPES ARE FROM THE BASALTIC VOLCANISM STUDY PROJECT (1981) AND THE JAPANESE ISLAND ARC THOLEIITE ENVELOPES ARE FROM PHILPOTTS et al. (1971).

The composition of the metagabbros and metadiabases from Los Roques Island indicates that they are tholeiitic and may have formed in a mid-ocean ridge tectonic setting.

Granitoid Rocks

The original scope of this research did not include the determination of the tectonic setting of the granitoid rocks of the Caribbean Mountains System. However, during the present study it became clear that the granitoid rocks were very extensive and that their tectonomagmatic affinity was as well important. Therefore, several granitoid rocks were analyzed to establish the tectonic affinity on the basis of the discrimination diagrams of Pearce *et al.* (1984).

Cordillera de la Costa Belt

The major- and trace-element compositions of nineteen granitoid rock samples from the Cordillera de la Costa belt are shown in Tables 5.11 and 5.12. The analyzed samples were collected from the Peña de Mora Formation at two different localities: (a) along the Chichiriviche-La Victoria transect (Plate 1), and (b) El Avila National Park (Figure 5.2). Sample DF-9155 (Table 5.12) has a low Rb content (7 ppm), which suggest an analytical problem during its analysis. Figure 5.23A shows the variation diagram Nb-Y with the tectonic affinity fields from Pearce *et al.* (1984). The diagram clearly reveals a within-plate affinity for the granitoid rocks from the Cordillera de la Costa belt. The Rb-Y+Nb diagram shows also a within-plate tectonomagmatic affinity, although two samples plot in the ocean-ridge granite field (Figure 5.23B).

Table A.5.9 in the Appendix shows the whole-rock Rb/Sr data for samples from the Caribbean Mountains System. The complete data set is included in Chapter 7. The Sr isotope ratio is an important petrologic indicator. The initial isotopic ratio of a derivative magma is the same as that of the original magma prior to differentiation, and the same as that of the original rock prior to partial melting.

Therefore, Sr isotope ratios of igneous rocks may give a direct clue about the original material from which it was derived.

The initial $^{87}Sr/^{86}Sr$ ratios are also important to discriminate between the tectonic settings. The initial isotopic ratio of the analyzed samples from the Cordillera de la Costa basement is 0.711 ± 0.007. The standard desviation is too large to definetely asign a tectonic

TABLE 5.11: Major- and trace-element data of granitoid rocks from the Cordillera de la Costa belt, along the Chichiriviche-La Victoria transect (major element values in percent; trace elements in ppm).

SAMPLE	SiO2	Al2O3	TiO2	Fe2O3	MnO	MgO	CaO	Na2O	K2O	P2O5	LOI	SUM
VO-83-1	75.83	11.29	0.44	2.16	0.32	1.52	0.91	2.53	5.82	0.09	n.d.	100.91
VO-83-4	68.99	16.15	0.32	2.67	0.27	1.90	1.66	3.39	2.69	0.02	n.d.	98.06
VO-83-7	68.08	16.45	0.30	2.29	0.25	1.45	0.98	3.99	2.98	0.18	1.32	98.27
VO-83-8	68.71	16.57	0.26	2.05	0.23	1.37	0.76	4.60	2.82	0.16	n.d.	97.53
VO-83-12	70.91	16.09	0.42	2.95	0.20	2.08	0.14	1.21	3.64	0.09	n.d.	97.73
VO-83-12B	68.65	16.09	0.32	2.32	0.25	1.21	0.66	4.86	2.98	0.18	n.d.	97.52
VO-83-13	68.38	16.57	0.27	2.51	0.30	1.76	0.38	2.90	4.13	0.13	n.d.	97.33
VO-83-21	75.03	12.01	0.32	1.99	0.23	1.23	1.08	2.73	6.02	0.08	n.d.	100.72
VO-83-27	68.98	17.35	0.62	3.32	0.20	1.18	0.55	2.95	2.35	0.18	n.d.	97.68
VO-83-34	69.99	16.85	0.45	2.89	0.24	1.24	0.24	3.09	2.45	0.21	n.d.	97.65
VO-86-9	73.73	14.12	0.15	1.10	0.02	0.35	1.85	5.03	1.66	0.03	1.35	99.39
PM-1	70.30	13.00	0.37	3.74	0.05	0.34	1.45	3.10	5.33	0.08	1.23	98.99
PM-2	72.50	13.00	0.35	3.86	0.02	0.43	0.62	3.60	5.17	0.06	0.70	100.31
PM-3	70.10	13.00	0.48	4.63	0.05	0.59	1.62	2.56	5.11	0.12	0.85	99.11

	Cr	Ni	Zr	Y	Nb	Rb	Sr
VO-83-1	12	32	382	110	44.32	201	65
VO-83-4	10	30	393	82	32.18	171	87
VO-83-7	14	22	304	104	42.64	187	93
VO-83-8	35	40	334	88	48.17	128	275
VO-83-12	20	30	338	104	50.18	191	66
VO-83-12B	37	45	336	80	56.82	121	231
VO-83-13	29	48	346	104	42.28	153	63
VO-83-21	19	28	324	87	41.63	124	177
VO-83-27	30	50	328	80	33.25	146	36
VO-83-34	32	45	304	75	30.47	120	209
VO-86-9	24	30	362	86	48.68	167	79
PM-1	12	46	442	137	45.00	269	111
PM-2	14	31	471	154	41.00	228	42
PM-3	10	28	621	92	33.00	162	186

TABLE 5.12: Major- and trace-element data of intermediate and felsic rocks from the Cordillera de la Costa belt, El Avila National Park (major element values in percent; trace elements in ppm).

SAMPLE	SiO2	Al2O3	TiO2	Fe2O3	MnO	MgO	CaO	Na2O	K2O	P2O5	LOI	SUM
DF-9024	67.11	15.93	0.34	6.02	0.06	0.47	1.58	3.62	3.91	0.15	n.d.	99.19
DF-9062	69.18	15.07	0.30	4.09	0.04	0.61	0.63	3.96	5.07	0.08	n.d.	99.03
DF-9155	61.54	12.31	0.64	9.68	0.08	9.31	3.04	3.01	0.23	0.11	n.d.	99.95
DF-10042	69.53	15.07	0.42	3.98	0.03	0.33	0.83	4.96	5.03	0.15	n.d.	100.33
DF-10064	72.15	14.82	0.18	1.99	0.07	0.10	0.51	4.81	4.37	0.40	n.d.	99.4

	Cr	Ni	Zr	Y	Nb	Rb	Sr
DF-9024	23	24	174	82	54.22	189	87
DF-9062	35	39	168	95	60.7	132	234
DF-9155	57	42	135	52	53.92	7	154
DF-10042	30	32	198	75	53.16	198	83
DF-10064	28	39	176	68	47.16	207	91

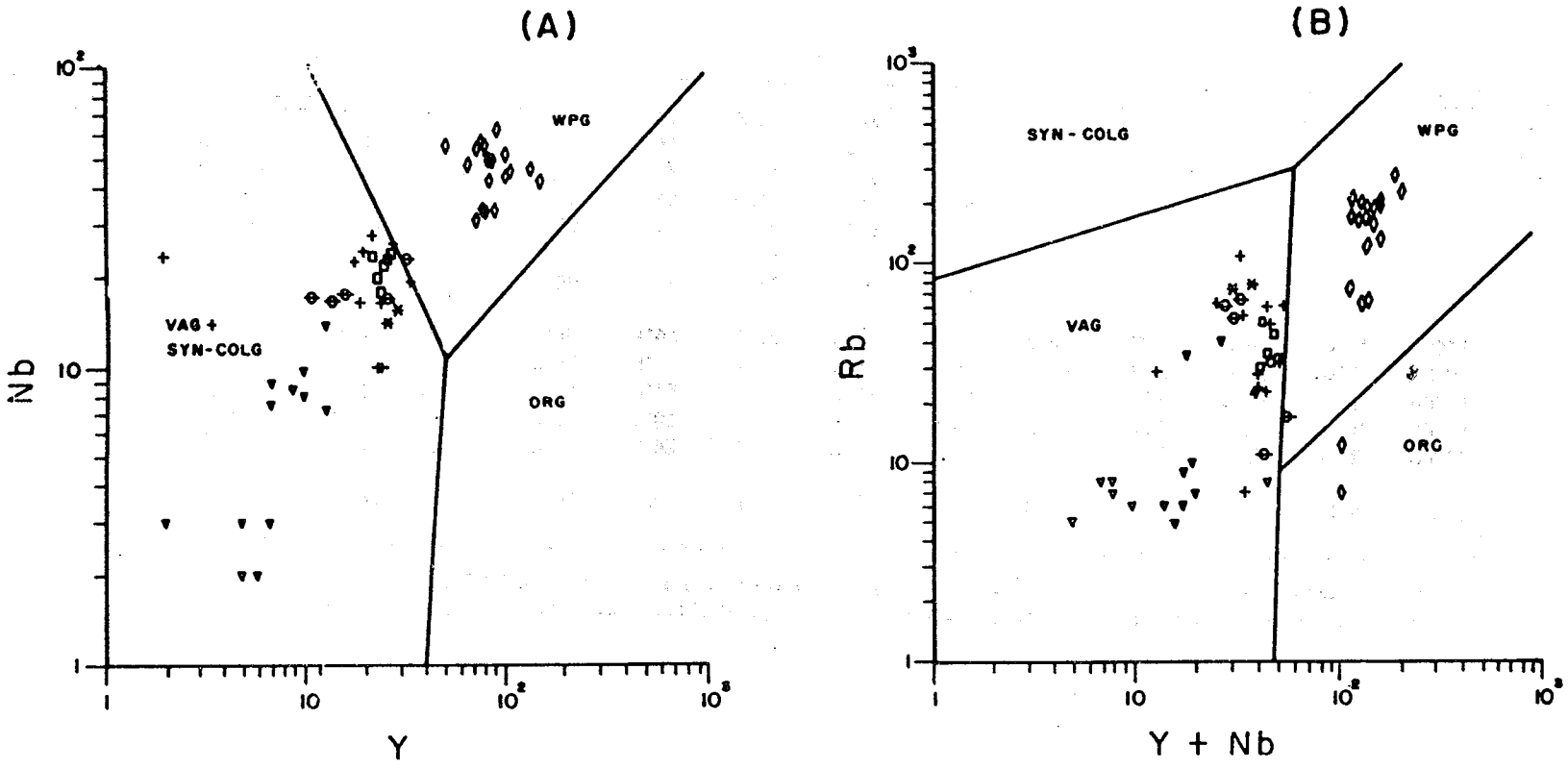

FIGURE 5.23 A-B : TECTONIC DISCRIMINANT DIAGRAMS FOR FELSIC ROCKS FROM THE CARIBBEAN MOUNTAINS SYSTEM. ◊ CORDILLERA DE LA COSTA (PEÑA DE MORA FORMATION), □ TINACO COMPLEX (LA GUACAMAYA METADIORITE), + TINACO COMPLEX (LA AGUADITA GNEISS), ⊖ LOS ROQUES ISLAND, ▽ MATASIETE AND GUAYACAN TRONDHJEMITES AND * EL SALADO GRANITE, MARGARITA ISLAND. A AND B DISCRIMINANT DIAGRAMS OF PEARCE et al. (1984)

setting. However, it is more likely that the ultimate source for the granitoid magmas was a heterogeneous, older continental crust comparable to the Mid-Proterozoic (1.7 to 1.4 or 1.2 Ga) anorogenic granites in the Rio Negro Province in northern Brazil (Dall'Agnol *et al.*, 1987).

Caucagua-El Tinaco Belt

The major- and trace-element contents of twenty six intermediate and felsic rocks of the Caucagua-El Tinaco belt are shown in Tables 5.13 and 5.14. The sample locations are shown on the maps of the La Victoria-San Sebastian and the Tinaco River-Casupo transects (Plates 2 and 3). Although the Si, Sr, and K contents are lower and the Ti, Zr, Nb, Fe, and Rb abundances are higher in the La Guacamaya Metadiorite (La Victoria-San Sebastian transect) than in the La Aguadita Gneiss of the Tinaco Complex (Tinaco River-Casupo transect), the differences are small and the two complexes can be grouped into one class.

Sample VO-83-202 (Table 5.14) has a very low Nb content (1ppm), which suggests an analytical problem with the inductively coupled plasma mass spectrometer during the analyses of Nb. The K_2O is highly variable (Table 5.14) with some values lower than 1%, which may have been the consequence of an extensive alteration after the metamorphism.

Figure 5.23A shows the Nb-Y discrimination diagram with the geotectonic fields from Pearce *et al.* (1984). The abundances of these trace-element in the La Guacamaya Metadiorite are very similar to those in the La Aguadita Gneiss. The diagram indicates VAG or SYN-COLG affinities. Both localities have also similar Rb-Y+Nb ratios (Figure 5.23B). If one believes that Rb was relatively immobile, this ratio suggests a VAG affinity.

The samples from La Guacamaya show a $^{87}Sr/^{86}Sr$ ratio between 0.70266 and 0.70674, while the isotopic ratios of the samples from the La Aguadita Gneiss (Tinaco River) are between 0.72005 and 0.71760 (Samples RT-87-4 and RT-87-5) and the initial ratio is 0.70475 $\pm$ 0.00197 (Table A.5.9 in the Appendix). The initial strontium ratio of the samples from the Aguadita Gneiss is within the range of island arc volcanic rocks observed by Faure and Powell (1972) and the isotopic ratios are somewhat higher than those of ordinary abyssal tholeiites and consequently at least one other isotopically distinct source of Sr for the samples is suggested. This material is either a different component of the subducted oceanic lithosphere such as the pelagic sediments or the peridotite layer (McNutt *et al.*, 1975), or

TABLE 5.13: Major- and trace-element data of metadiorites and metagranodiorites from the La Guacamaya Metadiorite, in La Victoria-San Sebastian transect (major element values in percent; trace elements in ppm).

SAMPLE	SiO2	Al2O3	TiO2	Fe2O3	MnO	MgO	CaO	Na2O	K2O	P2O5	LOI	SUM
VO-83-59	60.01	16.03	0.67	8.12	0.12	3.96	4.32	3.61	2.02	0.05	n.d.	98.91
VO-83-60	57.86	15.31	0.70	8.22	0.10	4.41	7.00	2.32	1.72	0.08	1.81	99.53
VO-83-62B	69.54	8.10	0.15	2.13	0.03	2.92	4.40	1.79	3.68	0.06	6.42	99.22
VO-83-64	57.19	14.91	0.64	8.46	0.10	3.78	7.10	2.40	1.24	0.09	4.23	100.14
VO-83-66	59.82	15.71	0.59	7.04	0.08	4.20	4.04	3.88	1.77	0.07	2.07	99.27
VO-83-67	66.72	14.51	0.64	5.15	0.03	2.38	0.99	2.07	3.74	0.18	2.34	98.75
VO-83-68	67.02	14.83	0.72	5.02	0.07	2.09	0.78	2.31	4.01	0.20	n.d.	97.05
VO-83-71	61.28	12.31	1.21	9.89	0.12	4.20	4.53	2.72	0.99	0.14	1.83	99.22
LV-87-1	55.90	16.10	0.69	8.57	0.16	4.19	8.15	2.21	1.51	0.09	2.08	99.65
LV-87-2	53.80	16.90	0.67	8.90	0.17	5.02	9.61	2.51	0.84	0.07	2.23	100.72
LV-87-3	54.60	16.20	0.73	9.01	0.16	4.27	8.07	2.12	1.39	0.09	2.47	99.11
LV-87-4	57.60	15.70	0.65	7.91	0.14	3.57	7.68	2.45	1.19	0.09	2.27	99.25

	Cr	Ni	Zr	Y	Nb	Rb	Sr
VO-83-59	39	41	100	26	22.83	45	260
VO-83-60	41	34	96	23	19.67	52	260
VO-83-62B	36	27	101	24	17.72	31	239
VO-83-64	44	38	89	25	21.62	33	208
VO-83-66	51	39	98	27	23.66	34	203
VO-83-67	31	24	106	27	30.09	197	91
VO-83-68	37	32	130	21	29.89	202	88
VO-83-71	44	46	128	22	23.32	36	210
LV-87-1	28	19	74	19	17.00	51	223
LV-87-2	46	38	26	12	11.00	36	266
LV-87-3	30	24	101	11	19.00	54	240
LV-87-4	29	39	69	25	10.00	48	245

TABLE 5.14: Major- and trace-element data of intermediate and felsic rocks from the Tinaco Complex, along the Tinaco River-Casupo transect (major element values in percent; trace elements in ppm).

SAMPLE	SiO2	Al2O3	TiO2	Fe2O3	MnO	MgO	CaO	Na2O	K2O	P2O5	LOI	SUM
VO-83-202	56.40	12.51	0.25	10.12	0.33	4.85	7.60	3.86	1.95	1.56	0.39	99.82
VO-83-205B	69.55	14.91	0.18	2.50	0.03	0.61	1.30	5.64	2.07	0.07	4.22	101.08
VO-83-207	70.32	14.45	0.18	2.10	0.25	1.64	0.85	2.60	5.59	0.19	n.d.	98.17
VO-83-208	59.32	14.91	0.64	8.94	0.12	3.03	6.20	4.67	1.60	0.21	0.11	99.75
VO-83-210B	66.92	15.85	0.34	3.24	0.17	3.31	2.80	2.45	1.45	0.25	n.d.	29.86
VO-83-211	56.00	9.70	0.19	8.55	0.13	11.10	10.00	2.72	1.30	0.03	1.18	100.9
VO-83-212	57.86	14.91	0.64	8.23	0.10	3.51	6.00	5.02	1.03	0.30	1.12	98.72
VT-82-133	71.07	14.55	0.17	1.95	0.45	1.87	0.98	2.86	5.89	0.23	n.d.	100.02
VT-82-134	67.25	13.42	0.20	5.17	0.07	2.01	5.01	4.38	0.87	0.10	n.d.	98.48
VT-82-136	68.34	15.15	0.23	3.06	0.13	1.84	3.21	4.45	0.98	0.14	n.d.	97.53
VO-82-136B	72.09	13.67	0.20	1.97	0.30	1.53	0.89	2.98	6.01	0.22	n.d.	27.77
VTOG-45	75.50	12.94	0.20	0.85	0.01	0.17	1.74	5.92	0.55	0.03	0.62	98.53
RT-87-4	62.10	17.20	0.45	3.64	0.07	1.58	2.70	3.07	8.37	0.19	0.85	100.22
RT-87-5	55.70	16.30	0.74	7.39	0.17	4.12	6.12	3.74	4.27	0.37	1.62	100.54

	Cr	Ni	Zr	Y	Nb	Rb	Sr
VO-83-202	75	45	77	12	1	29	285
VO-83-205B	41	26	78	2	23.44	53	372
VO-83-207	38	31	87	20	24.01	59	278
VO-83-208	92	67	83	18	22.33	24	389
VO-83-210B	26	49	91	20	24.31	33	1063
VO-83-211	71	66	90	19	16.18	7	133
VO-83-212	99	77	65	21	23.41	23	401
VT-82-133	27	41	60	28	25.39	60	264
VT-82-134	30	23	93	22	27.26	45	921
VT-82-136	33	21	80	24	22.34	49	198
VO-82-136B	13	29	67	24	16.27	66	418
VTOG-45	19	19	90	34	19.12	68	329
RT-87-4	12	29	10	23	10.00	109	381
RT-87-5	40	21	49	24	10.00	54	192

it is derived from a mantle or crust source above a Benioff zone.

Venezuelan Islands

Margarita Island

Major- and trace-element abundances of sixteen granitoid samples from Margarita are shown in Table 5.15. The sample locations are shown in Figure 2.5. Most samples are trondhjemites from the Cerro Matasiete and from the area near the Village of Guayacan and granitic augengneiss from the neighborhood of El Salado. The major- and trace-element abundances in the Matasiete and Guayacan metatrondhjemites are very similar, so that a common origin is suggested. However the granitic augengneiss from El Salado contains more Si, K, Zr, Y, Nb, and Rb, which may indicate a different source.

The Nb-Y values of the felsic samples from Margarita Island plot in the VAG and SYN-COLG fields (Figure 5.23A). The Rb-Y+Nb variation diagram shows that they have a VAG affinity (Figure 5.23B). Therefore, based on the discrimination diagrams for felsic rocks of Pearce *et al.* (1984) a volcanic arc tectonomagmatic affinity for the rocks studied seems to be obvious.

The strontium isotopic ratios of the trondhjemites included in Table A.5.9 in the Appendix are about 0.703, which is in the range of oceanic island arc volcanic rocks. These ratios are lower than the average of oceanic plagiogranites (0.7045-0.7059; Coleman, 1977), but they are close to the average of ordinary abyssal tholeiites (0.703-0.704; Miyashiro *et al.*, 1982). Thus, the trondhjemites may be a partial melting product of oceanic crust in a subduction zone.

Los Roques Island

Figure 5.18 shows the location of the five analyzed samples from Los Roques Island. The major and trace-element abundances are given in Table 5.16. Sample F-10 has very high Cr and Ni contents, which are higher than similar samples analyzed by similar methods. The high values can be the consequence of contamination during sample preparation.

The analyzed samples are intermediate aplites and they plot within the VAG + SYN-COLG field of the Nb-Y discrimination diagram (Figure 5.23A). The Rb-Y+Nb discrimination diagram (Figure 5.23B) indicates a VAG tectonomagmatic affinity. Therefore, the data are in agreement with the interpretation

TABLE 5.15: Major- and trace-element data of felsic rocks from the Matasiete-Guayacan metatrondhjemites and El Salado metagranite, Margarita Island (major elemeny values in percent; trace elements in ppm).

SAMPLE	SiO2	Al2O3	TiO2	Fe2O3	MnO	MgO	CaO	Na2O	K2O	P2O5	LOI	SUM
MTS-85-1	73.81	14.78	0.10	1.77	0.02	0.92	2.13	5.80	0.80	0.05	0.78	100.18
MTS-85-2	68.04	15.78	0.20	2.60	0.03	1.60	3.40	5.49	0.80	0.13	0.76	98.83
MTS-85-3	68.26	16.20	0.11	2.40	0.02	1.02	3.20	5.86	0.84	0.09	0.79	98.79
GUAY-85-1	68.20	16.20	0.13	1.90	0.02	1.55	3.47	5.42	0.73	0.11	1.11	98.84
VO-83-300	77.18	12.91	0.09	0.90	0.02	0.44	1.30	5.64	0.84	0.01	1.01	100.34
VO-83-301	70.88	14.91	0.15	1.95	0.02	1.17	3.20	5.61	0.64	0.07	1.27	99.87
VO-83-303	71.01	15.31	0.12	1.15	0.01	0.55	1.00	6.47	1.10	0.04	2.27	99.03
VO-83-303B	68.58	16.11	0.17	1.83	0.02	1.27	2.64	6.22	0.98	0.12	1.15	99.09
VO-83-304	67.62	16.51	0.19	2.09	0.02	1.56	3.54	5.75	0.84	0.10	1.27	99.49
VO-83-304B	67.16	16.11	0.20	2.70	0.03	1.87	3.47	5.75	0.63	0.11	0.85	98.88
VO-83-306B	61.88	18.31	0.14	2.84	0.03	1.88	4.33	8.27	0.15	0.08	0.96	98.87
VO-83-313	69.64	15.90	0.13	1.45	0.02	0.95	2.85	6.15	0.80	0.08	0.77	98.74
VO-83-314	69.84	15.32	0.15	1.82	0.03	1.39	3.40	5.24	0.48	0.12	1.20	98.99
VO-83-320	59.16	16.62	0.58	5.62	0.06	3.91	7.20	6.04	0.10	0.15	1.15	100.59
VO-85-352	68.35	16.41	0.13	1.96	0.02	1.42	2.94	5.99	0.91	0.11	n.d.	98.24
VO-85-385	76.32	12.95	0.30	1.36	0.02	0.76	0.18	5.60	1.80	0.02	n.d.	99.31

	Cr	Ni	Zr	Y	Nb	Rb	Sr
MTS-85-1	39	50	215	7	3.00	28	592
MTS-85-2	31	48	197	6	2.00	23	524
MTS-85-3	30	52	174	5	2.00	15	544
GUAY-85-1	29	58	254	5	3.00	15	650
VO-83-300	34	47	201	2	3.00	22	287
VO-83-301	40	50	217	4	1.00	23	616
VO-83-303	30	48	189	9	8.57	18	389
VO-83-303B	23	29	200	7	7.55	23	403
VO-83-304	29	54	224	7	8.91	20	354
VO-83-304B	34	40	199	10	8.06	27	724
VO-83-306B	46	32	139	13	13.81	41	239
VO-83-313	27	34	231	13	7.24	28	499
VO-83-314	30	40	226	10	9.74	30	547
VO-83-320	50	30	126	10	8.14	35	195
VO-85-352	34	45	215	29	15.90	78	350
VO-85-385	10	31	154	26	14.06	73	41

TABLE 5.16: Major- and trace-element data of granodiorites from Los Roques Island (major element values in percent; trace elements in ppm).

SAMPLE	SiO2	Al2O3	TiO2	Fe2O3	MnO	MgO	CaO	Na2O	K2O	P2O5	LOI	SUM
N-5	61.56	15.46	0.52	8.30	0.09	3.17	6.50	2.87	0.79	0.11	0.33	99.70
E-9	61.77	16.65	0.55	8.35	0.10	2.83	5.31	1.59	0.67	0.09	n.d.	97.91
F-10	61.01	15.86	0.40	7.98	0.17	4.05	6.60	0.90	0.39	0.13	n.d.	97.49
M-1	65.62	16.78	0.50	5.68	0.09	1.93	5.86	2.62	1.66	0.06	n.d.	100.80
M-3	64.07	16.01	0.62	5.91	0.12	2.02	6.32	2.97	0.98	0.10	n.d.	99.12

	Cr	Ni	Zr	Y	Nb	Rb	Sr
N-5	19	47	177	33	22.79	17	156
E-9	15	43	162	11	17.02	61	135
F-10	387	177	142	26	17.03	11	53
M-1	19	37	159	14	16.67	53	162
M-3	17	41	144	16	17.42	65	148

of Santamaria and Schubert (1974) that the Los Roques Islands are underlain by oceanic crust upon which a volcanic island arc was built.

Rare earth elements (REE)

The REE abundances of one sample from the Peña de Mora Formation in El Avila National Park (Figure 5.2) were determined and the data are shown in Table 5.4. The REE pattern (Figure 5.24) displays an important negative Eu anomaly, a small HREE depletion, and a strong LREE enrichment. The pattern compares well with the alkali-rich post-tectonic granite from Serra Do Iran in southwestern Goias, Brazil (Martins-Pimentel and Fuck, 1987). It is quite different from the REE patterns of the quartz diorites of Troodos (Kay and Senechal, 1976), Atlantic plagiogranite (Shih, 1972), and the island arc trondhjemite from the Sparta ophiolite (Phelps and Avé Lallemant, 1980).

Moreover, the high silica and REE abundances of the sample, suggest an incompatible behavior of the REE during crystallization, which together with the presence of the negative Eu anomaly, indicates that feldspar played an important role in the origin of this rock and suggests a relatively important crustal source component. Therefore, the REE pattern for this rock from the basement of the Cordillera de la Costa belt (Peña de Mora Formation) is also in agreement with the within-plate affinity deduced before on the basis of the trace elements.

The REE abundances of a metatrondhjemite (Sample VO-83-207) from the El Tinaco River were determined (Table 5.4) and the chondrite normalized REE pattern is shown in Figure 5.24.

The (La/Yb)n value for this sample is 15.02 which is markedly different from the mafic La Aguadita Gneiss (5.87). Therefore, it is likely that the magma source of the metatrondhjemites is different from the source of the mafic rocks, into which the trondhjemites were intruded.

The metatrondhjemite pattern is light-REE enriched and shows a slight negative Eu anomaly. This pattern is not similar to the plagiogranites of Canyon Mountain Complex (Gerlach *et al.*, 1981) and the Samail ophiolite (Pallister and Knight, 1981) and it is also different from island arc plagiogranites (Phelps and Avé Lallemant, 1980) and island arc metarhyolites of Santa Cruz Island (Sorensen, 1985). However, the pattern can be well correlated with the seriate tin granites of the Seward Peninsula, Alaska (Hudson and Arth, 1983) and with the granophyres of the Sarmientos ophiolite, that are interpreted to be fusion products of

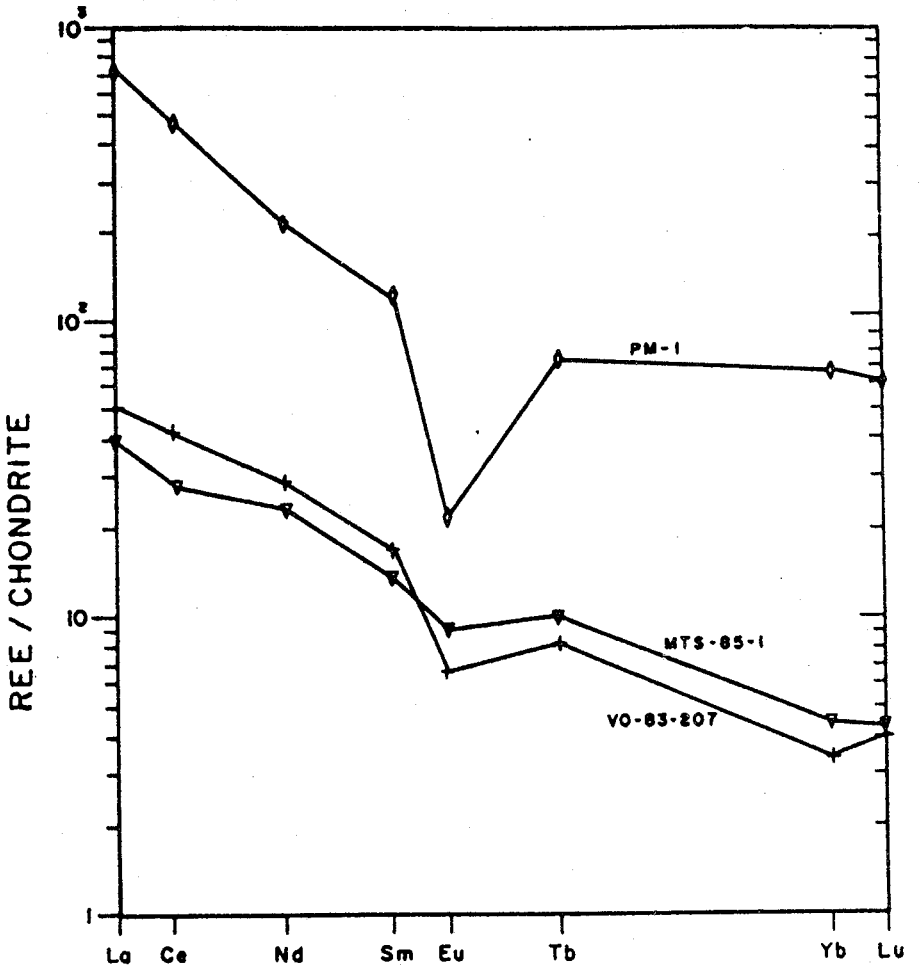

FIGURE 5.24 : REE PATTERNS OF FELSIC ROCKS FROM THE CARIBBEAN MOUNTAINS SYSTEM. PM-1 CORDILLERA DE LA COSTA BELT (PEÑA DE MORA FORMATION, MTS-85-1 MARGARITA ISLAND (MATASIETE TRONDHJEMITE), VO-83-207 CAUCAGUA - EL TINACO BELT (LA AGUADITA GNEISS).

continental crust (Saunders *et al.*, 1979). Therefore, the VAG affinity found on the basis of the discrimination diagrams is also supported by the rare earth element pattern.

The REE abundances of a sample of the Matasiete metatrondhjemite (Sample MTS-85-1) are shown in Table 5.4 and the normalized REE pattern is shown in Figure 5.24. The sample has a light REE enrichment with a $(La/Yb)_n$ value of 8.26, which is between 5 and 6 times the ratio in the mafic rocks from the island (Figure 5.22). The REE pattern is similar to the pattern of the felsic sample from the Tinaco River. The difference of this ratio with the felsic and mafic rocks may indicate that the magmas of the felsic rocks are the partial-melt products of a different source. Furthermore, the pattern does not compare well that of the oceanic plagiogranites of Canyon Mountain Complex (Gerlach *et al.*, 1981) and Samail ophiolite (Pallister and Knight, 1981), nor with that of the island arc plagiogranites of Sparta (Phelps and Avé Lallemant, 1980) and the Santa Cruz island-arc (Sorensen, 1985). The pattern of this rock resembles much more that of the seriate tin-granite from the Seward Peninsula, Alaska (Hudson and Arth, 1983) and the granophyres of continental origin in the Sarmiento Ophiolite (Saunders *et al.*, 1979).

Conclusions

Based on the trace-element discrimination diagrams, the strontium isotopic ratios, and the REE abundances of felsic rocks from the Caribbean Mountains System and Venezuelan islands, the following conclusions can be made: (a) the Peña de Mora Formation shows a within-plate granite affinity and it is likely that its source was an older heterogeneous continental crust, (b) the felsic basement of the Caucagua-El Tinaco belt shows a VAG affinity and various rock sources above a Benioff zone could have been the protolith, (c) the Matasiete trondhjemite of Margarita Island shows a VAG affinity on the discrimination diagrams and it must represent a suprasubduction zone magmatism, (d) The aplites on the Los Roques Island have also a VAG tectonomagmatic affinity, and (e) the various tectonic settings of the basement in the Caribbean terranes suggest a complex tectonic history. The basement of the Cordillera de la Costa and Caucagua-El Tinaco belts are pieces of Precambrian and Paleozoic continental lithosphere, while the granites of the northernmost terranes were part of Mesozoic volcanic arc.

CHAPTER VI

METAMORPHISM

Introduction

As discussed before, northern Venezuela can be divided into several east-west trending tectonostratigraphic belts. The belts of interest in this study are from north to south: Cordillera de la Costa-Margarita terrane, Cordillera de la Costa belt, Caucagua-El Tinaco belt, Paracotos belt, and Villa de Cura belt. The Cordillera de La Costa-Margarita terrane is a tectonic melange that consists of metasedimentary and metaigneous rocks metamorphosed to greenschist and epidote amphibolite facies (Stephan *et al.*, 1980; Navarro, 1981; Talukdar and Loureiro, 1982) which overprints an earlier metamorphism of the eclogite and blueschist facies. The interpretation of these rocks has been controversial: some geologists argued for a polymetamorphic history with first an eclogite/blueschist event, and later a low P/T metamorphism (Blackburn and Navarro, 1977; Navarro, 1977; Talukdar *et al.*, 1979; Ostos, 1981; Stephan *et al.*, 1980; Navarro, 1981; Talukdar and Loureiro, 1982;; Stephan, 1982; Navarro, 1987). Several other authors proposed a single metamorphic cycle to explain the metamorphic assemblages of the terrane with the greenschist to epidote amphibolite facies due to a late-stage decompression resulting from uplift and exhumation of the once deeply buried eclogites and blueschists (Maresch, 1971; Maresch and Abraham, 1981; Beets *et al.*, 1984; Chevalier, 1987).

The highest pressures determined by Navarro (1974) from the pair garnet-clinopyroxene in eclogites are 8-9 Kbar at temperatures of 200° to 300° C, while Maresch and Abraham (1981) calculated pressures higher than 11.5 Kbar at temperatures of 450° to 525° C, and Chevalier (1987) proposed a minimum pressure of 11.8 Kbar and a temperature of 500° C.

The basement of the Cordillera de la Costa Belt (Peña de Mora Formation and the Sebastopol Complex) consists of granites metamorphosed to the greenschist facies with biotite and garnet as characteristic minerals (Wehrmann, 1972; Urbani and Ostos, 1987). The Caracas Group and the Tacagua Formation were metamorphosed in the greenschist facies at intermediate P/T conditions with muscovite and chlorite as common index minerals, although biotite has been described in the Las Brisas Formation (Talukdar *et al.*, 1979; Talukdar and Loureiro, 1982). The metamorphism in the

Cordillera de la Costa belt corresponds with the later metamorphic assemblages developed in the Cordillera de la Costa-Margarita terrane.

The Caucagua-El Tinaco belt consists of a basement which is formally defined as the Tinaco Complex (consisting of the La Aguadita Gneiss and the Tinapu Schist). The La Aguadita Gneiss was metamorphosed in the amphibolite facies (Menéndez, 1965; Ostos, 1984), while the Tinapu Schist underwent a greenschist metamorphism with chlorite as the most frequent index mineral (Menendez, 1965; MacKenzie, 1960; González de Juana *et al.*, 1980). The metasedimentary and metavolcanic sequences of Permian and Cretaceous age overlying the Tinaco Complex has undergone greenschist facies metamorphism with muscovite and/or chlorite as typical index minerals. The metamorphism of the basement and the cover in the Cordillera de la Costa and Caucagua-El Tinaco belts are similar with the only difference that the metamorphic grade in the basement of the Tinaco Complex is somewhat higher (Menendez, 1965). The Tinaquillo Peridotite Complex is also part of the Caucagua-El Tinaco belt. The metagabbros of the complex shows a relict granulite assemblage, which was overprinted by an amphibolite facies metamorphism (Ostos, 1984).

The Paracotos belt is metamorphosed at a very low grade (prehnite-pumpellyite facies) and the serpentinites lying along the northern and southern contacts of this belt show greenschist metamorphic assemblages (Konigsmark, 1958; Shagam, 1960; Beck, 1985b). The Villa de Cura Group in the Villa de Cura belt is metamorphosed at high P/T; a metamorphic zonation exists with the following zones from north to south: pumpellyite-actinolite, lawsonite-albite, lawsonite-glaucophane, glaucophane-epidote, barroisite, and glaucophane-barroisite (Navarro, 1983). Some other units in the belt (Dos Hermanas and Tiara formations) reveal very low metamorphic assemblages of zeolite and prehnite-pumpellyite facies (Navarro, 1983; Beck, 1985b).

Metamorphism in the Study Area

The metamorphic grade and history of the different belts is based on mineral assemblages and textural relatioships between the mineral phases. Minerals were identified in thin section with the petrographic microscope and by X-ray diffraction. The percentages shown in the tables (Table 6.1 to 6.11) are only estimates; no modal analysis was done.

Cordillera de la Costa-Margarita Terrane

The Cordillera de la Costa-Margarita terrane was studied on the mainland in the northernmost part of the Chichiriviche-La Victoria transect (Plate 1 and Figure 5.1) and in El Avila National Park (Figure 5.2) and offshore on Margarita Island (Fig. 2.5 and 5.17).

Chichiriviche-La Victoria Transect

The Cordillera de la Costa-Margarita terrane crops out in the northernmost part of this transect. It consists of the Nirgua and Antimano formations. The lithologies encountered are tremolite marble, muscovite-garnet schist, sheared serpentinite, and garnet amphibolite but due to the initial objective of this work the marble and serpentinite were not sampled. The petrography of the studied samples from these units is shown in Table 6.1.

The following metamorphic assemblages have been distinguished in the studied samples:

(1) Pelitic Rocks

Albite ± muscovite ± chlorite ± biotite ± garnet ± epidote. Texturally, the pelitic rocks are lepidoblastic; the schistosity is defined by muscovite, chlorite, and biotite preferred orientation; epidote is also orientated parallel to the schistosity. Garnet shows snow-ball texture. The metamorphic assemblage in the pelitic rocks is characteristic of greenschist facies metamorphism, and particulary of the almandine + chlorite + muscovite zone of Winkler (1979). The breakdown of muscovite in presence of quartz (Helgeson *et al.*, 1978) to sillimanite is often used to determine the temperature range of metamorphism. Thus, the lack of sillimanite suggest that these rocks never reached the conditions to form sillimanite by destruction of muscovite. The only conclusion, that can be made, is that the metamorphic assemblage is characteristic of the greenschist facies and is similar to these assemblages in the greenschist facies of the Otago Schist terrane in New Zeland (Turner, 1981) and comparable to these assemblages in the Bessi-Ino and Barrovian regions (Miyashiro, 1979), which are typical of intermediate P/T conditions.

(2) Mafic Rocks

Albite ± muscovite ± chlorite ± biotite + garnet ± epidote ± zoisite + actinolite ± barroisite (?) ± omphacite (?).
The mafic rocks are garnet amphibolites with relicts of clinopyroxene (omphacite ?), amphibole (barroisite ?), and

TABLE 6.1: PETROGRAPHY OF SAMPLES FROM THE CORDILLERA DE LA COSTA-MARGARITA TERRANE AND CORDILLERA DE LA COSTA BELT (CHICHIRIVICHE-LA VICTORIA TRANSECT).

	NUMBER	QUARTZ	K-FELD.	PLAG.	MUSC.	CHL.	BIOT.	GARNET	ACT.	BARR.	CPX	EPID.	ZOIS.	SPH.	OPAQ.	CARB.	GRAPH.	NAME
CCMT	VO-83-1	32	19	39	6	0	1	0	0	0	0	3	0	0	0	0	0	Feld. biot. augengneiss
	VO-83-4	21	8	57	3	0	6	0	0	0	0	0	4	0	1	0	0	" " "
	VO-83-5	0	0	35	3	1	0	14	45	3	0	0	1	0	1	0	0	Garnet amphibolite
	VO-83-5A	0	0	8	4	0	0	16	55	0	2	0	14	1	0	0	0	" "
	VO-83-5B	0	0	3	3	0	1	12	67	0	1	0	0	0	1	0	0	" "
	VO-83-5C	39	0	20	30	2	0	5	0	0	0	3	0	1	0	0	0	Musc. garnet schist
	VO-83-7	20	24	49	0	0	5	0	0	0	0	2	0	0	0	0	0	Plag. biotite schist
	VO-83-9	11	0	21	4	14	0	9	34	1	0	4	0	1	1	0	0	Garnet amphibolite
	VO-83-9b	15	0	25	3	12	0	10	28	1	0	5	0	1	1	0	0	" "
	VO-83-10	0	0	22	0	6	0	5	54	0	0	10	2	1	0	0	0	" "
	VO-83-15	50	35	0	11	0	3	0	0	0	0	1	0	0	0	0	0	Plag. biotite gneiss
	VO-83-17	48	13	26	10	1	1	0	0	0	0	1	0	0	0	0	0	Feld. biot. augengneiss
	VO-83-21	10	0	1	15	0	0	0	0	0	0	0	0	0	1	72	0	Quartz musc. marble
	VO-83-27	58	0	8	30	1	1	0	0	0	0	1	0	1	0	0	0	Muscovite quartzite
	VO-83-28	51	8	36	3	1	1	0	0	0	0	0	0	0	0	0	0	Feldspar gneiss
	VO-83-31	78	0	3	12	0	3	0	0	0	0	4	0	0	0	0	0	Muscovite quartzite
	VO-83-34	39	21	32	7	0	1	0	0	0	0	0	0	0	0	0	0	Feldspar gneiss
	VO-83-44	83	0	0	11	5	0	0	0	0	0	0	0	0	1	0	0	Muscovite quartzite
	VO-83-45	42	3	48	6	0	0	0	0	0	0	0	0	0	1	0	0	Feldspar gneiss
	VO-83-45B	80	0	0	18	0	0	0	0	0	0	0	0	0	2	0	0	Muscovite quartzite
	VO-83-46	26	0	0	2	0	0	0	0	0	0	0	0	0	1	70	1	Quartz marble
	VO-83-47	5	0	0	1	0	0	0	0	0	0	0	0	1	0	91	2	" "
	VO-83-52	38	25	20	15	0	1	0	0	0	0	0	0	1	0	0	0	Quartz feld. gneiss
	VO-83-55	71	0	0	13	6	0	0	0	0	0	0	0	1	0	0	1	Calcareous quartzite
	VO-86-8	32	13	41	2	0	9	1	0	0	0	1	0	0	1	0	0	Feld. biotite augengneiss
	VO-86-9	32	25	30	6	0	1	1	0	0	0	4	0	0	1	0	0	" " "
CCMT	VO-86-9B	7	0	3	1	0	0	18	60	6	0	4	0	0	1	0	0	Garnet amphibolite
	VO-86-10	0	0	21	0	0	0	21	50	7	0	0	1	0	0	0	0	" "
	VO-86-11	37	4	36	20	0	2	0	0	0	0	0	0	1	0	0	0	Feld. biotite gneiss
	VO-86-12	24	0	39	18	4	1	0	0	0	0	11	2	1	0	0	0	Albite muscovite schist
	VO-86-15	5	0	0	1	0	0	0	0	0	0	0	0	1	0	92	1	Quartz marble
	VO-86-16	25	0	0	8	0	0	0	0	0	0	0	0	2	0	65	0	Calcareous qz. marble

CCMT Samples from the Cordillera de la Costa-Margarita Terrane; Qz: quartz; K-feld: K-feldspar, Plag: Plagioclase; Musc: Muscovite; Chl: Chlorite; Biot: Biotite; Act: Actinolite; Barr: Barroisite; Cpx: Clinopyroxene; Epid: Epidote; Zois: Zoisite; Sph: Sphene (Titanite); Carb: Carbonate; Opaq: Opaque; Graph: Graphite.

titanite (sphene). The garnet in some samples shows a zonation, defined by inclusions; whether this zonation is also compositional is not known. The garnet porphyroclasts have textures that indicate that they were formed during a pre-D_1 deformation. The relict mineral paragenesis may represent an eclogite facies metamorphism similar to that described in the Bessi area of the high P/T Sanbagawa belt in Japan (Banno, 1966; Miyashiro, 1979), in the high P/T Mesozoic-Cenozoic belts of the Mediterranean region, and in the Paleozoic Urals-Mongolia orogenic belt (Dobretsov and Sobolev, 1984; Dobretsov *et al.*, 1987).

The eclogites are interpreted by Fry and Fyfe (1969) as formed under exceptional anhydrous conditions, while the greenschists, epidote amphibolites, and blueschists may have formed instead of eclogites, under hydrated conditions. The stability of eclogites has been determined by Ringwood and Green (1966), Green and Ringwood (1967,1972), and Ito and Kennedy (1971) using various basaltic compositions. The stability field of eclogites based on experimental work of the last authors is indicative of stability over a very large temperature range (450°-1200° C), if pressure is high (>8 Kb, maximum pressure for the stability of plagioclase at the minimum temperature).

Texturally, the barroisite is as a rim around pyroxene porphyroclast; while the actinolite defines the nematoblastic foliation and it is being formed from the barroisite. The amphibole composition of the studied amphibolites is indicative of different metamorphic conditions; thus, barroisite forms at the higher pressure in the epidote amphibolite facies (Ernst, 1979), glaucophane above 10 Kb (Carman and Gilbert, 1983) in the eclogite and blueschist facies (Miyashiro, 1979; Turner, 1981), and actinolite in the greenschist facies (Apted and Liou, 1983). Therefore, a high P/T assemblage (eclogite facies) and a subsequent intermediate P/T assemblage (greenschist facies) is proposed for the rocks of La Cordillera de la Costa-Margarita terrane along the Chichiriviche-La Victoria transect.

El Avila National Park

The petrography of the samples from El Avila National Park is shown in Table 6.2. and the sample locations are included on Figure 5.2. The predominant lithologies are garnet amphibolite, glaucophane amphibolite, garnet-clinozoisite amphibolite, epidote amphibolite, and quartz-garnet-actinolite schist. Pelitic rocks are subordinate and occur as layers interfoliated with the amphibolites. The following

TABLE 6.2: PETROGRAPHY OF SAMPLES FROM EL AVILA NATIONAL PARK, NORTH OF CARACAS (CORDILLERA DE LA COSTA-MARGARITA TERRANE).

SAMPLE NUMBER	QUARTZ	PLAG.	MUSC.	CHL.	BIOT.	GARNET	ACT.	BARR.	GLAU.	CLINOZ.	ZOIS.	EPIDOTE	CPX.	SPHENE	RUTILE	OPAQ.	K-FELDS.	CARB.	NAME
DF-9024	40	15	0	25	0	2	0	0	0	0	0	13	0	0	0	5	0	0	Feld. quartz. augengneiss
DF-9062	24	59	12	0	3	0	0	0	0	0	0	1	0	0	0	1	0	0	" " " "
DF-9092	4	27	0	4	0	0	47	0	0	0	4	13	0	1	0	0	0	0	Epidote amphibolite
DF-9131	5	19	1	0	0	25	48	0	0	0	1	0	0	1	0	0	0	0	Garnet amphibolite
DF-9134	0	3	0	0	0	28	47	0	0	0	20	0	1	0	1	0	0	0	" " "
DF-9147	0	19	0	4	0	13	63	0	0	0	0	0	0	0	0	1	0	0	" " "
DF-9153	0	8	0	0	0	18	43	0	0	0	2	28	0	0	0	1	0	0	" " "
DF-9155	0	20	0	0	0	35	43	0	0	0	0	0	0	0	1	1	0	0	" " "
DF-9159	0	17	0	0	0	11	53	8	0	0	3	7	0	0	0	1	0	0	" " "
DF-9162	7	0	6	0	0	14	58	0	0	0	4	9	0	0	0	2	0	0	" " "
DF-9358	1	5	3	0	0	23	61	0	0	0	1	1	0	1	0	2	0	0	" " "
DF-9359	2	1	3	0	0	23	63	0	0	2	0	0	5	0	0	1	0	0	" " "
DF-9360	43	17	15	0	0	14	10	0	0	0	0	0	0	0	0	1	0	0	Qz. act. garnet schist
DF-9361	5	7	4	1	0	32	47	0	0	1	2	0	0	0	0	1	0	0	Garnet amphibolite
DF-9362	3	1	5	0	0	25	45	0	0	20	0	0	0	1	0	0	0	0	Garnet clinoz. amphibolite
DF-9363	0	0	7	0	0	27	27	8	8	16	0	0	3	0	1	1	0	0	Glaucophane amphibolite
DF-10042	13	60	10	2	4	1	0	0	0	0	0	5	0	2	0	1	0	2	Feld. quartz augengneiss
DF-10064	20	57	13	1	2	1	0	0	0	0	0	4	0	1	0	1	0	0	" " " "
DF-91288	5	0	0	0	0	16	74	0	0	0	0	3	0	1	0	1	0	0	Garnet amphibolite
DF-91508	3	0	6	0	0	8	66	0	0	0	4	12	0	1	0	0	0	0	" " "
DF-91528	0	1	7	0	0	35	54	0	0	0	0	0	1	0	1	1	0	0	" " "
PM-2	55	25	5	0	3	0	0	0	0	0	0	2	0	0	0	0	10	0	Feld. quartz augengneiss
PM-1A	40	29	1	3	7	0	0	0	0	0	0	3	0	0	0	1	16	0	" " " "

Qz: Quartz; PLAG: Plagioclase; MUSC: Muscovite; CHL: Chlorite; BIOT: Biotite; ACT: Actinolite; BARR: Barroisite; GLAU: Glaucophane; CLINOZ: Clinozoisite; CPX: Clinopyroxene; OPAQ: Opaques; K-FELDS: K-feldspar; CARB: Carbonate.

metamorphic minerals have been found in the mafic rocks: ± Albite ± muscovite ± chlorite ± garnet + actinolite ± barroisite (?) ± glaucophane ± epidote ± clinozoisite ± ± zoisite ± omphacite (?) ± rutile.

The mafic rocks have a nematoblastic texture defined by amphibole preferred orientations. Actinolite is the most common amphibole; it occurs as rims around a blue-green amphibole (barroisite ?). Glaucophane is only present in one of the studied samples as a rim around clinopyroxene grains. The contacts between any pair of amphiboles or between amphibole and pyroxene are simplectitic. Albite crystals have inclusions defining a helicitic texture. Garnet porphyroblasts have two different types of textures: first, they occur as large zoned porphyroblasts with inclusion-rich cores (sieve texture), inclusion-free rims, and well-developed pressure shadows; the second type displays the snow-ball texture. The textural relationships suggest that there was an earlier eclogite/blueschist metamorphism overprinted by a greenschist metamorphism. The textures of barroisite (?) suggest that it formed during the final stages of the blueschist metamorphism or the early stages of the greenschist metamorphism. The association of eclogite with glaucophane and epidote define the type-C eclogite of Coleman *et al.* (1965).

Margarita Island

Margarita Island has been proposed to be the northeast extension of the high P/T belt on the mainland (Stephan *et al.*, 1980). The petrographic description of the samples from this terrane are given in Table 6.3. The metamorphic assemblages on the island are:

(1) Granitic rocks

Albite + K-feldspar + muscovite + biotite.

(2) Trondhjemitic rocks

Albite ± muscovite ± chlorite + epidote ± zoisite ± clinozoisite ± actinolite.

(3) Calcareous rocks

Calcite and/or dolomite ± chlorite ± muscovite + tremolite.

(4) Pelitic rocks

Albite + muscovite ± chlorite ± biotite + zoisite ± clinozoisite.

TABLE 6.3: PETROGRAPHY OF SAMPLES FROM MARGARITA ISLAND.

SAMPLE NUMBER	QUARTZ	K-FELD.	PLAG.	MUSC.	CHL.	BIOT.	GARNET	ACT.	BARR.	TREM.	SERP.	CPX	EPID.	ZOIS.	CLINOZ.	CARB.	SPH.	RUTILE	GRAPH.	OPAQ.	NAME
GUAY-1	52	0	55	5	2	0	0	0	0	0	0	0	3	2	0	0	0	0	0	0	Plagioclase quartz gneiss
MA-037B	50	0	10	37	0	3	0	0	0	0	0	0	0	18	1	0	0	0	0	1	Muscovite biotite schist
MA-108	6	0	0	3	0	0	0	0	0	2	0	0	0	0	0	89	0	0	0	0	Tremolite marble
MA-133	36	0	38	20	1	0	0	0	0	0	0	0	0	4	0	0	0	0	0	1	Quartz feldspar musc. schist
MA-151	30	49	13	6	0	1	0	0	0	0	0	0	0	0	0	0	0	0	0	1	Feldspar augengneiss
MA-155A	38	0	2	55	0	3	0	0	0	0	0	0	0	0	0	0	0	0	0	2	Musc. biotite graph. schist
MA-157	3	0	2	2	0	0	0	0	0	1	0	0	0	0	0	91	0	0	0	1	Tremolite marble
MA-158	3	0	1	0	3	0	0	0	0	1	0	0	0	0	0	92	0	0	0	0	Quartz tremolite marble
MA-86-5	20	0	67	1	4	0	0	0	1	0	0	0	3	4	0	0	0	0	0	0	Plag. quartz chlorite gneiss
MTS-85-1	34	0	57	1	3	0	0	0	0	0	0	0	3	0	0	0	0	0	0	1	Metatrondhjemite
MTS-85-2	39	0	50	1	4	0	0	0	0	0	0	0	3	0	0	0	0	0	0	0	" "
MTS-85-3	36	0	58	0	3	0	0	0	0	0	0	0	2	0	0	0	0	0	0	0	" "
VO-83-300	57	0	40	2	0	0	0	0	0	0	0	0	1	0	0	0	0	0	0	0	" "
VO-83-302	2	0	15	0	8	0	0	59	0	0	0	0	15	0	0	0	0	0	0	1	Amphibole schist
VO-83-305	59	0	25	3	2	0	0	0	0	0	0	0	10	0	0	0	0	0	0	1	Metatrondhjemite
VO-83-305B	34	0	10	3	0	0	0	0	50	0	0	0	2	0	0	0	0	0	0	1	Quartz amphibolite
VO-83-304	35	0	54	0	2	0	0	0	0	0	0	0	8	0	0	0	0	0	0	1	Metatrondhjemite
VO-83-305	0	0	0	0	0	0	0	0	0	0	98	0	0	0	0	0	0	0	0	2	Serpentinite
VO-83-305B	0	0	45	0	25	0	0	0	20	0	0	2	0	0	7	0	0	0	0	1	Clinoz. cpx amphibolite
VO-83-306B	20	0	65	0	3	0	0	0	0	0	0	0	8	4	0	0	0	0	0	0	Metatrondhjemite
VO-83-308	0	0	29	1	0	0	0	0	48	0	0	6	0	0	15	0	0	1	0	0	Clinoz. cpx amphibolite
VO-83-309	0	0	0	5	3	0	2	0	44	0	0	20	0	0	25	0	0	0	0	1	Amphibole eclogite
VO-83-309B	0	0	3	1	0	0	0	47	0	0	0	0	1	20	28	0	0	0	0	0	Epidote amphibolite
VO-83-310	0	0	27	2	2	0	2	0	55	0	0	7	0	0	3	0	0	1	0	1	Amphibole eclogite
VO-83-311	0	0	45	0	2	0	2	0	17	0	0	23	0	0	10	0	0	1	0	1	Clinoz. cpx amphibolite
VO-83-315	1	0	33	1	0	0	0	0	30	0	0	20	0	0	13	0	1	1	0	0	" " "
VO-83-318	0	0	44	2	0	0	0	0	13	0	0	31	0	1	8	0	0	1	0	0	Amphibole eclogite
VO-83-320	20	0	59	1	0	0	0	10	0	0	0	0	2	4	4	0	0	0	0	0	Metatrondhjemite
VO-83-321	1	0	18	2	0	0	23	0	18	0	0	28	0	0	9	0	0	1	0	0	Amphibole eclogite
VO-86-2	50	0	39	3	2	0	0	0	0	0	0	0	4	0	0	0	0	0	0	2	Metatrondhjemite
VO-86-38	3	0	9	0	1	0	0	0	69	0	0	0	0	17	0	0	1	0	0	0	Zoisite amphibolite
VO-86-46	3	0	30	0	3	0	24	0	28	0	0	7	0	0	8	0	0	0	0	0	Cpx garnet amphibolite
VO-86-5	0	0	8	1	1	0	0	0	57	0	0	12	0	0	20	0	0	1	0	0	Eclogitic amphibolite
VO-86-58B	0	0	22	2	0	0	5	0	51	0	0	4	0	0	15	0	0	1	0	0	" " "
VO-86-50	0	0	23	5	0	0	0	0	26	0	0	38	0	0	7	0	0	1	0	0	" " "
VO-86-7	2	0	23	1	0	0	13	0	40	0	0	12	0	0	7	0	0	1	0	1	" " "

K-FELD: K-FELDSPAR; PLAG: PLAGIOCLASE; MUSC: MUSCOVITE; CHL: CHLORITE; BIOT: BIOTITE; ACT: ACTINOLITE; TREM: TREMOLITE; SERP: MINERALS OF THE SERPENTINE GROUP; CPX: CLINOPYROXENE; ZOIS: ZOISITE; CLINOZ: CLINOZOISITE; CARB: CARBONATE; SPH: SPHENE; GRAPH: GRAPHITE; OPAQ: OPAQUES.

(5) Mafic rocks

Albite ± white mica ± chlorite ± garnet ± epidote ± zoisite ± clinozoisite ± actinolite ± barroisite ? ± clinopyroxene (omphacite ?).

Texturally, the granitoid rocks are gneisses showing well developed feldspar "augen" with pressure shadows. The quartz crystals are neoblasts and have a shape preferred orientation parallel to the mica foliation. The trondhjemites are granoblastic to foliated. The gneissic texture is defined by the orientation of elongate quartz and albite neoblasts, muscovite, chlorite, and epidote. The granoblastic trondhjemites show little schistosity. Zoned plagioclases are common relict igneous textures. The pelitic rocks have a well developed lepidoblastic texture, defined by the orientation of muscovite, although quartz neoblasts and zoisite are also well orientated. The mafic rocks (eclogite and amphibolite) have granoblastic to nematoblastic texture. The eclogites are commonly granoblastic. They contain post-tectonic white mica, albite, and garnet porphyroblasts. The white mica is frequently rimmed by albite crystals, although the albite also shows helicitic texture; garnet shows a zonation with inclusion-rich cores and inclusion-free rims. The foliated mafic rocks are eclogitic amphibolites and amphibolites, which show pressure shadows around garnet porphyroclasts and sometimes rotated albite crystals.

The chemical compositions of some mineral phases of the mafic rocks have been determined by Navarro (1977): garnet is essentially almandine with moderate grossularite and little spessartite and pyrope; the clinopyroxene is an omphacite with very high acmite content; the amphibole is subcalcic having a composition between barroisite and Ca-glaucophane; and, the white mica is essentially paragonite with minor potassium in solid solution. As on the mainland, the mafic rocks of Margarita show a relict eclogite facies which is overprinted by an epidote-amphibolite facies metamorphism. Some amphibolites interlayered with the Matasiete Trondhjemite and some of the amphibolite boudins in the Juan Griego Group underwent greenschist facies metamorphism, which may have been caused by locally lower values of fO_2, which decrease the P-T stability field of the epidote amphibolite facies and move it to higher pressures (Apted and Liou, 1983).

The granite, trondhjemite, and the calcareous and pelitic rocks have a metamorphic paragenesis characteristic of the greeschist facies.

Conclusions

Based on the metamorphic assemblages and textures recognized in the Cordillera de la Costa-Margarita terrane, the following conclusions can be made:

(a) The high P/T assemblage recognized along the Cordillera de la Costa-Margarita terrane on the mainland and on Margarita is generated at a convergent plate boundary (Ernst, 1971; Miyashiro, 1979; Platt, 1986; Ernst, 1988). The retrograde intermediate P/T assemblage may have formed when the rocks were uplifted due to underplating, where upon they were denudated by extension and erosion (Cloos, 1982; 1984; Platt, 1986). Alternatively, the uplift may have been the result of buoyancy and isostatic readjustment when subduction ceased possibly due to collision (Ernst, 1988).
(b) The high P/T metamorphic rocks in the Cordillera de la Costa-Margarita terrane can be separated into two groups:

(1) the rocks that have relicts of blueschist and eclogite facies metamorphism, which were overprinted by a greenschist facies metamorphism (Cordillera de la Costa-Margarita terrane on the mainland) and (2) the rocks showing eclogite facies metamorphism and a later overprint of epidote amphibolite facies (Margarita Island). The different metamorphic overprints may be related to differential uplift in the accreationary wedge or to different thermal configurations depending on the maturity of the island arc. If the latter is the case, the high P/T rocks of the mainland are older and they were overprinted when the island arc was immature and the thermal conditions of the epidote amphibolite facies were not yet developed.

Cordillera de la Costa Belt

The Cordillera de la Costa belt was studied along the Chichiriviche-La Victoria transect (Plate 1 and Figure 5.1), in El Avila National Park (Figure 5.2), and along the northern part of the Tinaco River-Casupo transect (Plate 3). It underlies tectonically the Cordillera de la Costa-Margarita terrane and consists of a Precambrian-Paleozoic basement overlain by metasediments. The basement consists mainly of granitoid gneisses (e.g. Sebastopol Complex, Peña de Mora Formation, and the Colonia Tovar Granite). The overlying metasediments are included formally in the Caracas Group.

Granitoid rocks

Granitoid rocks of the Peña de Mora Formation and the Colonia Tovar Granite were studied along the Chichiriviche-

La Victoria transect and in El Avila National Park. The petrography of the samples is included in Tables 6.1 and 6.2. Albite and less frequently microcline porphyroclasts have asymmetric pressure shadows indicating rotations. The "S" and "C" surfaces (Berthé et al., 1979) are well defined with quartz neoblast and "mica fish" orientated along these surfaces. Also common are broken and rotated feldspar crystals. Rare garnet crystals are tiny, idioblastic, and commonly post-tectonic. Biotite crystals are frequently rimmed by chlorite.

The metamorphic assemblage of the Peña de Mora Formation in both areas is the same and consists of:

Albite $\pm$ K-feldspar $\pm$ muscovite $\pm$ chlorite $\pm$ biotite $\pm$ epidote $\pm$ garnet.

The mineralogic assemblage is characteristic of the quartz-albite-epidote-biotite subfacies of the greenschist facies of Turner (1960). The presence of garnet (almandine ?) and albite is indicative of low to medium grade metamorphism (Winkler, 1979). Almandine garnet is widely distributed in intermediate P/T regional metamorphic terranes (Miyashiro, 1979). The petrography of the Colonia Tovar Granite is shown in Table 6.1. The metamorphic assemblage consists of albite, muscovite, chlorite, biotite, and epidote. The assemblage is equally characteristic of the quartz-albite-epidote-biotite subfacies of the greenschist facies (Turner, 1960).

Caracas Group

The Caracas Group was studied along the Chichiriviche-La Victoria transect (Plate 1) and near the northern contact of the Tinaquillo Peridotite Complex (Plate 3). The units in the study areas are the Las Brisas and the Las Mercedes formations. The Las Brisas Formation is exposed near La Victoria, State of Aragua (Plate 1) and consists of quartzo-feldspathic and quartzose calcareous metasediments. The petrography of one sample from this formation is shown in Table 6.1 (Sample VO-83-55). It consists of quartz, muscovite, chlorite, calcite, dolomite, and graphite. The assemblage is indicative of a greenschist facies metamorphism in a low P/T regime (Miyashiro, 1979).

The Las Mercedes Formation is well exposed in the north and south flanks of the Cordillera de la Costa Range and toward the northern contact of the Tinaquillo Peridotite Complex (Plates 1 and 3). The petrography is shown in Tables 6.1 and 6.4. The rocks in this formation are mainly calcareous; calcareous schists, phyllites, and marbles are the common

TABLE 6.4: PETROGRAPHY OF SAMPLES FROM LAS MERCEDES FORMATION, ALONG THE TINACO RIVER-CASUPO TRANSECT.

SAMPLE NUMBER	CARBONATE	QZ	MUSC.	PYRITE	HAEM.	GRAPH.	NAME
VTO-82-5	88	9	1	1	1	0	Calcareous quartz phyllite
VTO-82-16	77	17	3	1	0	2	Quartz muscovite marble
VTO-82-17	95	3	1	0	0	1	Quartz marble
VTO-82-29	79	14	4	2	1	0	Calcareous qz. musc. phyllite
VTO-83-141	93	2	0	1	1	3	Quartz marble
VTO-83-142	94	4	0	0	1	1	Quartz marble

QZ: Quartz; MUSC: Muscovite; HAEM: Haematite; GRAPH: Graphite.

lithologies. Texturally, the rocks are granoblastic to foliated, depending on the calcite-dolomite content. The schistosity is defined by calcareous and quartz-muscovite rich laminations (foliated marbles) or by the preferred shape orientation of tiny quartz neoblasts, muscovite, calcite, and dolomite. Pyrite crystals frequently show quartz "pressure fringers" and extensional calcite veins are also common. The most common mineral assemblage is:

Calcite + quartz ± dolomite ± muscovite ± graphite ± pyrite.

Winkler (1979) described the association calcite-dolomite-quartz-white mica as characteristic of marls subjected to very low grade metamorphism but he pointed out that these rocks usually contain graphite which probably reduced the activity of water in favor of methane in the fluid phase. If this is the case, the temperatures in these rocks could have been higher (French, 1966) than the 584 ± 4° at X_{CO2}= 0.50 ± 0.06 and 6 Kb of fluid pressure as determined by Hewitt (1973) in the reaction: Muscovite + Calcite + 2Quartz = K-feldspar + Anorthite + CO_2 + H_2O.

Turner (1981) extended the stability field of calcite-dolomite-quartz in siliceous magnesian marbles up to the amphibolite facies where tremolite is present. According to Winkler (1979) this assemblage is stable at the transition of the low to the medium grade of regional metamorphism. However, there is no textural or mineralogical evidence of the reversed reaction. The influence of graphite on the metamorphic temperature is not known, but tremolite is not present. Thus, the association is characteristic of the greenschist facies and is comparable to that in the Ryoke belt in Japan, which according to Miyashiro (1979) formed at the lowest temperature of the greenschist facies in a low P/T regime.

Caucagua-El Tinaco Belt

The Caucagua-El Tinaco belt was studied along the La Victoria-San Sebastian and Tinaco River-Casupo transects (Plates 2 and 3). The studied units were the La Guacamaya Metadiorite, the Tucutunemo Formation, and the Tinaco (La Aguadita Gneiss) and Tinaquillo Peridotite complexes.

La Victoria-San Sebastian Transect

The units of the Caucagua-El Tinaco belt studied along the La Victoria-San Sebastian transect are the Guacamaya Metadiorite and the Tucutunemo Formation. The Guacamaya Metadiorite is interpreted as Paleozoic basement in this area (MacLachlan *et al.*, 1960). The Tucutunemo Formation is

a metasedimentary, metavolcaniclastic, and metavolcanic cover in which fossils were recently identified as Permian (Benjamini *et al.*, 1987). The petrography of samples from the Guacamaya Metadiorite and the Tucutunemo Formation are shown in Tables 6.5 and 6.6, respectively.

The Guacamaya Metadiorite has mostly granoblastic textures although locally a well developed foliation is observed. The rocks are coarse and only locally quartz has recrystallized to smaller shape orientated neoblasts, defining with chlorite and epidote the banded gneissic foliation. The feldspar and hornblende are porphyroclastic, showing incipient recrystallization; some have been broken and rotated. Relict igneous textures such as zoning in plagioclase are also frequent. The mineral assemblage of the La Guacamaya Metadiorite consists of:

Quartz ± Oligoclase ± K-feldspar + green hornblende ± augite ± muscovite ± chlorite ± biotite ± epidote.

The metamorphic assemblage is indicative of amphibolite facies metamorphism (Turner, 1981), or medium metamorphic grade of Winkler (1979). It has been suggested (Miyashiro, 1979) that the green colour of the amphiboles is characteristic of the lower part of the amphibolite facies, but this is apparently not always the case (Sisson; personal communication, 1990). There is not textural evidence of the epidote-breakdown but the association hornblende + oligoclase is typical of the amphibolite facies (Apted and Liou, 1983). The association is also characteristic of low P/T, which according to Ernst (1984) is consistent with conditions in a volcanic-plutonic complex. Tectonically, the metamorphism is representative of a Paleozoic Andean-type convergent boundary.

The petrography of the studied metasedimentary rocks of the Tucutunemo Formation is shown in Table 6.6 and the mineral assemblage of the pelitic rocks consists of: Quartz + muscovite ± chlorite ± epidote.

In addition, volcanic rock fragments were identified in a metaconglomerate of this unit. The mineralogic assemblage of the pelitic rocks is characteristic of the quartz-albite-muscovite-chlorite subfacies (Turner, 1968) of the greenschist facies. The mineral assemblage of the calcareous samples consists of calcite, dolomite, quartz, and muscovite which also is indicative of greenschist facies metamorphism. Therefore, there is a metamorphic discontinuity between the La Guacamaya Metadiorite metamorphosed in the amphibolite facies and Tucutunemo Formation metamorphosed in the greenschist facies, which supports the mapped tectonic

TABLE 6.5: PETROGRAPHY OF SAMPLE FROM LA GUACAMAYA METADIORITE, ALONG THE LA VICTORIA-SAN SEBASTIAN TRANSECT.

SAMPLE NUMBER	QUARTZ	PLAG.	K-FELD.	HBL	BIOTITE	AUG.	CHL.	MUSC.	EPID.	OPAQ.	MAGN.	SPH.	NAME
VO-83-59	12	53	6	26	0	1	0	1	0	1	0	0	Plag. hornblende cpx gneiss
VO-83-60	15	53	0	27	0	3	0	1	0	1	0	0	" " " "
VO-83-61	12	53	0	25	0	8	1	0	0	1	0	0	" " " "
VO-83-62	12	58	0	22	0	5	2	0	0	1	0	0	" " " "
VO-83-63	10	55	0	25	0	5	1	1	1	1	1	0	" " " "
VO-83-64	15	44	0	20	0	15	3	2	0	1	0	0	" " " "
VO-83-65	17	54	0	23	0	3	1	0	0	0	1	1	" " " "
VO-83-66	9	55	3	19	0	10	2	2	0	0	0	0	" " " "
VO-86-17	30	41	1	25	0	3	0	0	0	0	0	0	" " " "
VO-86-21	22	42	0	30	1	0	0	1	3	1	0	0	Plagioclase hornblende gneiss

PLAG: Plagioclase; K-FELD: K-feldspar; HBL: Hornblende; AUG: Augite; CHL: Chlorite; MUSC: Muscovite; EPID: Epidote; OPAQ: Opaques; MAGN: Magnetite; SPH: Sphene.

TABLE 6.6: PETROGRAPHY OF SAMPLES FROM THE TUCUTUNEMO FORMATION, ALONG THE LA VICTORIA-SAN SEBASTIAN TRANSECT.

SAMPLE NUMBER	QUARTZ	PLAG.	MUSC.	CHL.	OPAQ.	CARBONATE	EPID.	ROCK FRAGMENT	APHANITIC MATRIX	NAME
VO-83-67	69	3	10	17	1	0	0	0	0	Muscovite chlorite schist
VO-83-72	85	2	13	0	0	0	0	0	0	Muscovite schist
VO-86-20	10	0	1	0	0	87	0	0	0	Quartz marble
VO-86-22	64	1	20	10	0	0	1	0	0	Muscovite chlorite schist
VO-86-23	64	1	25	7	0	0	0	0	0	Muscovite chlorite schist
VO-86-25	0	0	7	1	0	0	0	85	7	Metaconglomerate

PLAG: Plagioclase; MUSC: Muscovite; CHL: Chlorite; OPAQ: Opaques; EPID: Epidote.

contact (Plate 2). A similar discontinuity is reported in the Tinaco area between La Aguadita Gneiss and the Tinapu Schist (Menendez, 1965).

Tinaco River-Casupo Transect

The units of the Caucagua-El Tinaco belt studied along the Tinaco River-Casupo transect are the Tinaco Complex (La Aguadita Gneiss) and the Tinaquillo Peridotite Complex (Plate 3). The La Aguadita Gneiss has several different lithologies: plagioclase-quartz gneiss, quartz-feldspar schist, amphibolite, and amphibole gneiss. The plagioclase-quartz gneiss is a metatrondhjemite. It locally preserves the intrusive relations with the country rock. The amphibolite and amphibole plagioclase gneiss include a wide range of lithologies, resulting from variations in the plagioclase and amphibole contents. The mineralogic composition of the gneiss may be related to the original igneous composition, although a strong metamorphic differentiation resulting in the well-defined gneissic texture may have modified the original composition. The Tinaquillo Peridotite Complex consists of harzburgite, dunite, clinopyroxenite, serpentinite, and metagabbro (granulite). The metagabbros are located at the contacts with the La Aguadita Gneiss and the Las Mercedes Formation. They occur interlayered with the ultramafics.

The petrography of the La Aguadita Gneiss is shown in Table 6.7. The mineral assemblage of the amphibolite and amphibole gneiss consists of:

Oligoclase + quartz + green hornblende $\pm$ K-feldspar $\pm$ epidote $\pm$ clinopyroxene $\pm$ actinolite $\pm$ garnet $\pm$ chlorite.

Garnet is a very rare mineral component of these rocks, as well as actinolite which is rimming the green hornblende crystals. Clinopyroxene is a relict mineral occurring in the core of hornblende porphyroblasts. The clinopyroxene in the metamorphic assemblage and its zoned texture suggest that the rocks first may have been metamorphosed at granulite facies conditions and later at amphibolite facies conditions. The amphibole colour is indicative of a lower temperature than the temperatures reached in the Tinaquillo Peridotite Complex. The plagioclase composition is also indicative of a higher pressure metamorphism in the Tinaco River area.

TABLE 6.7: PETROGRAPHY OF SAMPLES FROM THE CAUCAGUA-EL TINACO BELT (TINACO RIVER-CASUPO TRANSECT).

SAMPLE NUMBER	QUARTZ	K-FELD.	PLAG.	MUSC.	CHL.	BIOT.	GARNET	ACT.	HBL	CPX	EPID.	SPH.	ZIRCON	APAT.	MAGN.	HEM.	OPAQ.	NAME
VO-83-200	1	0	54	0	0	0	0	0	40	1	3	1	0	0	0	0	0	Plag. hbl. epidote gneiss
VO-83-201	2	0	50	0	4	0	0	0	40	0	4	0	0	0	0	0	0	Plag. hbl. chlorite gneiss
VO-83-202	5	0	36	0	1	0	1	0	55	0	2	0	0	0	0	0	0	Plag. hbl. garnet gneiss
VO-83-202A	30	5	62	0	2	0	0	0	0	0	1	0	0	0	0	0	0	Metatrondhjemite
VO-83-203	16	0	45	0	2	0	0	0	30	0	3	0	0	0	1	1	0	Plag. quartz hbl. gneiss
VO-83-204	32	0	40	0	0	0	0	0	25	0	1	1	0	0	1	0	0	Plag. hbl. gneiss
VO-83-205	7	3	46	0	0	0	0	0	35	2	5	0	1	0	1	0	0	" "
VO-83-205B	49	0	47	0	1	0	0	0	0	0	2	0	0	0	1	0	0	Plag. quartz gneiss
VO-83-206	5	0	65	0	1	0	0	1	48	0	0	0	0	0	0	0	0	Hbl. plag. quartz gneiss
VO-83-206B	43	1	53	0	1	0	0	0	1	0	1	0	0	0	0	0	0	Metatrondhjemite
VO-83-207	60	4	30	0	2	0	0	0	0	0	4	0	0	0	0	0	0	" "
VO-83-208	30	0	46	0	0	1	0	0	20	0	1	1	0	0	1	0	0	Plag. hbl. biotite gneiss
VO-83-209	25	0	43	0	0	0	0	0	25	0	5	1	0	0	1	0	0	Plag. quartz hbl. gneiss
VO-83-210	40	0	47	0	3	0	1	0	6	0	1	1	1	0	0	0	0	Plag. quartz gneiss
VO-83-211	28	0	20	0	0	0	0	0	50	0	2	0	0	0	0	0	0	Plag. hbl. gneiss
VO-83-212	27	0	55	0	0	0	0	0	15	0	3	0	0	0	0	0	0	Plag. hbl. epidote gneiss
VTO-82-63	0	0	42	0	0	0	0	0	19	27	0	0	0	0	0	0	1	Pyroxene granulite
VTO-82-65B	0	0	37	0	0	0	0	0	22	28	0	0	0	0	0	0	1	Pyroxene granulite
VTO-82-83	17	0	43	1	0	0	0	0	31	0	6	1	0	0	0	0	1	Plag. hbl. gneiss
VTO-82-92	0	0	56	0	0	0	0	0	30	13	0	0	0	0	0	0	1	Plag. cpx. hbl. gneiss
VTO-82-101	0	1	49	0	0	0	0	0	33	15	0	0	1	0	1	0	0	" " "
VTO-82-102	0	0	49	0	0	2	0	0	21	19	0	0	0	0	0	0	1	Pyroxene granulite
VTO-82-104	0	16	48	0	0	1	0	0	0	25	0	0	0	0	0	0	1	" " "
VTO-82-105	0	0	49	0	0	1	0	0	32	17	0	0	0	0	0	0	1	Plag. cpx. hbl. gneiss
VTO-82-107	0	0	57	0	0	1	0	0	0	31	0	0	0	1	1	0	0	Pyroxene granulite
VTO-82-132	19	6	62	0	0	1	0	0	11	0	0	0	0	1	0	0	0	Plag. hbl. gneiss
VTO-82-133	18	10	66	3	0	0	0	0	0	0	1	1	0	1	0	0	0	Plag. quartz gneiss
VTO-82-134	5	0	56	0	0	0	2	0	36	0	1	0	0	0	0	0	0	Plag. hbl. garnet gneiss
VTO-82-136	0	7	70	0	0	0	0	0	18	0	3	1	0	1	0	0	0	Plag. hbl. gneiss
VTO-82-136B	4	1	66	0	1	0	0	0	25	0	3	0	0	0	0	0	0	Plag. hbl. gneiss

K-FELD: K-FELDSPAR; PLAG: PLAGIOCLASE; MUSC: MUSCOVITE; CHL: CHLORITE; BIOT: BIOTITE; ACT: ACTINOLITE; EPID: EPIDOTE; SPH: SPHENE; OPAQ: OPAQUES; CPX: CLINOPYROXENE; HBL: HORNBLENDE; APAT: APATITE; MAGN: MAGNETITE; HEM: HEMATITE.

The plagioclase-quartz gneiss (metatrondhjemite) of the La Aguadita Gneiss consists of:

Quartz + oligoclase ± microcline ± muscovite ± chlorite ± epidote ± biotite ± green hornblende ± garnet.

The mineral assemblage and the field relations of the trondhjemites are indicative of a metamorphic grade similar to the second metamorphism of the amphibole gneiss and amphibolite. No granulite relicts were found. Therefore, the La Aguadita Gneiss and the trondhjemites were affected by an amphibolite facies metamorphism at low P/T conditions subsequent to the granulite facies metamorphism and intrusion of the trondhjemites.

The mineral association of the metagabbros of the Tinaquillo Peridotite Complex is shown in Table 6.8. The rocks consists of:

Plagioclase ± diopside ± brown hornblende ± hypersthene ± garnet ± biotite.

Garnet and biotite are very rare. Hornblende has a preferred orientation and it rims the pyroxene. Thus, two assemblages were distinguished. The older assemblage consists of plagioclase, diopside, hypersthene, and garnet. Turner (1981) has shown that the zonal sequence in the granulite facies can be based on the relative amount of hornblende and biotite with respect to pyroxenes. An increase in pyroxene and garnet is to be correlated with increasing metamorphic grade, decrease in water fugacity, increase in temperature, and perhaps an increase in pressure. Turner (1981) proposed also a few temperature and pressure estimates for the granulite facies. In summary, it is suggestive that the metagabbros were formed in the granulite facies of the low pressure-type of Miyashiro (1979), at temperatures of 700° to 900° C and pressures less than 15 Kb.

The granulite metamorphism occurred probably after the separation of the gabbroic melt from the peridotite (Tinaquillo Peridotite), close to the Mohorovicic discontinuity as Dawson (1980) has suggested. Therefore, the Tinaquillo Complex could represent an Alpine-type tectonic massif. Alternatively, the Tinaquillo Peridotite Complex could have been an ophiolite which first was burried deeply and subsequently uplifted, emplaced, and dismembered.

The younger metamorphic assemblage in the metagabbros consists of andesine, brown horblende, and biotite. Miyashiro (1979) established that brown amphiboles in metabasites indicate the highest temperatures of the

TABLE 6.8: PETROGRAPHY OF SAMPLES FROM THE TINAQUILLO PERIDOTITE COMPLEX, STATE OF COJEDES.

SAMPLE NUMBER	HYP.	ENS.	AUG.	DIOP.	OLIV.	PLAG.	SPINEL	HBL.	OPAQ.	SERP.	K-FELDS.	PEROSK.	BIOT.	GARNET	NAME
VTO-82-1	7	0	16	0	0	56	0	19	2	0	0	0	0	0	Pyroxene granulite
VTO-82-18	0	9	0	6	82	0	3	0	0	0	0	0	0	0	Harzburgite
VTO-82-22	0	16	0	7	70	0	7	0	0	0	0	0	0	0	"
VTO-82-32	0	90	0	0	0	0	3	0	1	6	0	0	0	0	Orthopyroxenite
VTO-82-38	0	12	0	7	67	0	5	0	0	10	0	0	0	0	Harzburgite
VTO-82-40	0	10	0	4	83	0	3	0	0	0	0	0	0	0	"
VTO-82-51	5	0	13	0	0	65	3	16	1	0	0	0	0	0	Pyroxene granulite
VTO-82-52	4	0	13	0	0	51	0	27	3	0	0	0	2	0	" " "
VTO-82-55	0	10	0	5	76	0	0	0	0	4	0	0	0	0	Harzburgite
VTO-82-80	0	5	0	3	90	0	5	0	0	0	0	0	0	0	Dunite
VTO-82-87	0	11	0	8	78	0	2	0	0	0	0	0	0	0	Harzburgite
VTO-82-88	1	0	0	0	0	88	3	9	0	0	2	0	0	0	Plagioclase gneiss
VTO-82-99	0	16	0	5	77	0	0	0	0	0	0	0	0	0	Harzburgite
VTO-82-100	0	0	5	0	0	78	2	13	2	0	0	0	2	0	Plagioclase gneiss
VTO-82-108	0	0	8	0	0	55	0	24	1	0	4	0	3	5	Plag. cpx. gar. gneiss
VTO-82-112	0	13	0	4	79	0	0	0	0	4	0	0	0	0	Harzburgite
VTO-82-114	9	0	23	0	0	43	0	23	2	0	0	0	0	0	Pyroxene granulite
VTO-82-116	29	0	11	0	0	56	0	0	1	0	0	0	3	0	" " "
VTO-82-118	8	0	12	0	0	71	0	0	2	0	6	1	0	0	" " "
VTO-82-121	0	12	0	6	76	0	6	0	0	0	0	0	0	0	Harzburgite
VTO-82-123	0	15	0	82	0	0	0	0	0	3	0	0	0	0	Clinopyroxenite
VTO-82-140	0	15	0	9	67	0	7	0	0	2	0	0	0	0	Harzburgite

HYP: Hypersthene; ENS: Enstatite; AUG: Augite; DIOP: Diopside; OLIV: Olivine; PLAG: Plagioclase; HBL: Hornblende; OPAQ: Opaques; SERP: Serpentinite; K-FELDS: K-Feldspar; PEROSK: Peroskite; BIOT: Biotite; Gar: Garnet

amphibolite facies. The plagioclase composition changes with pressure; although the relations are not clear, the data of the Aracena, Ryoke, and Central Abukuma terranes suggest that plagioclase becomes more calcic with decreasing pressure (Miyashiro, 1979). Turner (1981) characterized the almandine zone of the amphibolite facies by the assemblage: hornblende-andesine-(epidote-almandine-biotite). Miyashiro (1979) suggested that the formation of garnet is strongly dependent on the original composition (ferrous iron/magnesium). As garnet was not formed during the younger event, the mineralogic association may have formed at transitional conditions between the biotite and garnet zone of the amphibolite facies where the pressure was not high enough to form garnet, or the original rock did not have the requiered composition.

Paracotos Belt

The Paracotos belt consists primarely of the Paracotos Formation. Dismembered ophiolites occur along the northern and southern contacts of this belt. The Paracotos Formation consists of flysch which includes limestone olistoliths. The petrography of the samples of the Paracotos Formation is shown in Table 6.9. The following lithologies have been recognized: phyllite, lithic metagraywacke, metaconglomerate and aphanitic marble.

The characteristic metamorphic assemblage of Paracotos is defined by the association prehnite-pumpellyite, although detrital quartz, plagioclase, epidote, chlorite, muscovite, and rock fragments are presents. The metamorphic assemblage is characteristic of a very low metamorphic grade, but it occurs in low P/T as well as in high P/low T series (Miyashiro, 1979). However, Ernst (1976, 1984) recognized this facies in basaltic and quartzo-feldespathic rocks as part of a high P/T series, characteristic of an accreationary complex.

The Paracotos Formation consists of flysch probably deposited in a foreland basin. The metamorphism could be the consequence of a very low thermal gradient produced by the obduction of a cold ophiolite slab or by regional burial metamorphism or by metamorphism in an accreationary wedge (Miyashiro, 1979; Winkler, 1979; Turner, 1981; Platt, 1986).

Villa de Cura Belt

The Villa de Cura belt was studied along the La Victoria-San Sebastian transect (Plate 2 and Figure 5.11) and in Guatopo National Park (Figure 5.12). The Villa de Cura belt consists of the Villa de Cura Group and undeformed

TABLE 6.9: PETROGRAPHY OF SAMPLES FROM THE PARACOTOS FORMATION, ALONG THE LA VICTORIA-SAN SEBASTIAN TRANSECT.

SAMPLE NUMBER	QUARTZ	PLAG.	EPID.	CHL.	MUSC.	OPAQ.	ROCK FRAGMENTS	P-P	CARB.	NAME
PAR-87-0	3	0	0	0	10	1	0	0	86	Aphanic marble
PAR-87-1	18	3	1	0	18	1	57	2	0	Lithic metaconglomerate
PAR-87-2	23	8	0	0	12	2	54	1	0	" " "
PAR-87-3	1	0	0	0	0	6	0	0	93	Aphanic marble
PAR-87-4	12	8	0	0	15	32	61	1	0	Lithic metaconglomerate
PAR-87-4A	16	10	0	1	9	1	63	0	0	" " "
PAR-87-5	26	8	0	0	13	1	52	0	0	" " "
VO-86-26	77	0	0	0	20	2	0	1	0	Quartz sericite phyllite
VO-86-28	51	35	9	1	3	1	0	0	0	Quartz metagrauwacke
VO-87-29A1	33	30	0	0	12	1	23	0	0	Lithic metagrauwacke
VO-87-28A2	37	26	0	0	8	1	27	0	0	" " "

PLAG: Plagioclase; EPID: Epidote; CHL: Chlorite; MUSC: Muscovite; OPAQ: Opaques; P-P: Prehnite-pumpellyite; CARB: Carbonate.

metavolcaniclastic and metaandesitic rocks of the Dos Hermanas or Tiara Sur formations. Murray (1973) described the occurrence in this belt of an Alaska-type ultramafic complex (Chacao Complex). Urbani (1987b) recognized an ultramafic complex, consisting of dunite, wherlite, clinopyroxenite, and gabbro in Guatopo National Park (Figure 5.12). The metamorphic petrology of the Villa de Cura Group was extensively studied by Navarro (1983). The petrographic description of samples studied during the present research are given in Tables 6.10 and 6.11. The most abundant lithologies in the Villa de Cura Group are granofels, clinopyroxene metalava, metatuff, and quartz sericite schist, while the Dos Hermanas Formation consists of tuff, lava, and volcanic agglomerate. The Villa de Cura Group, north of San Sebastian de los Reyes shows the following mineral associations:

(a) Mafic rocks

.- Albite + chlorite $\pm$ lawsonite $\pm$ muscovite $\pm$ actinolite $\pm$ glaucophane.

.- Quartz + chlorite + actinolite $\pm$ epidote + glaucophane.

.- Lawsonite + albite + chlorite + actinolite + epidote + pumpellyite.

.- Quartz + albite + muscovite + actinolite + glaucophane + clinopyroxene $\pm$ pumpellyite.

(b) Metatuff

.- Albite + chlorite + actinolite + clinopyroxene + stilpnomelane.

(c) Granofels

.- Quartz + albite + stilpnomelane + prehnite-pumpellyite.

The pair glaucophane-lawsonite in some of the assemblages indicate high P/low T blueschist facies metamorphism (Turner, 1981; Dobretsov and Sobolev, 1984). The assemblages bearing glaucophane or lawsonite are transitional to the blueschist facies (Ernst *et al.*, 1970). The conditions leading to the formation of glaucophane were reversed by Carman and Gilbert (1983). The reaction albite + sodium phlogopite-talc solid solution= glaucophane took place at 600^{o} C and 14.8 Kb; the slope of the lower boundary of the glaucophane stability field is 13.3 b/^{o}C. The upper pressure limit is 21 Kb at 262^{o} C and 30.7 Kb at 600^{o} C (Carman and

TABLE 6.10: PETROGRAPHY OF SAMPLES FROM THE VILLA DE CURA BELT, NORTH OF SAN SEBASTIAN DE LOS REYES.

SAMPLE NUMBER	QUARTZ	LAWS.	PLAG.	K-FELD.	MUSC.	CHL.	ACT.	GLAUC.	CPX	CARB.	STIL.	EPID.	ROCK FRAGMENT	OPAQ.	LEUCOXENE	P-P	SPH.	NAME
OH;682	1	0	14	0	14	8	10	9	21	1	0	18	0	0	1	0	3	Pyroxene glaucophane metabasalt
OH-6898	4	0	18	0	23	1	3	13	20	0	0	13	0	0	0	1	4	" " " "
QO-839	0	0	4	0	26	20	25	12	43	0	0	0	0	0	0	0	0	" " " "
QO-843	0	0	10	0	6	25	16	12	14	0	0	0	0	5	0	0	12	" " " "
VO-86-31	99	0	0	0	0	0	0	0	0	0	0	0	0	1	0	0	0	Chert
VO-86-32	0	0	18	0	0	3	13	0	3	0	5	0	57	1	0	0	0	Metatuff
VO-86-33	17	0	8	0	0	0	0	0	0	0	7	0	63	1	0	4	0	Granofels
VO-86-34	6	4	17	0	4	1	0	1	0	2	0	0	64	1	0	0	0	Metatuff
VO-86-35	0	6	76	0	0	3	7	0	0	0	0	5	0	2	0	1	0	Lawsonite actinolite metalava
VO-86-35A	0	5	70	0	0	5	10	0	0	0	0	5	0	2	0	3	0	" " " "
VO-86-36	5	0	63	0	7	0	12	4	6	0	0	0	0	1	0	2	0	Glaucophane metalava
VO-86-36B	12	0	62	0	13	0	0	0	10	0	0	0	0	0	0	3	0	Pumpellyite metalava
VO-86-37	0	0	65	0	0	3	6	12	13	0	0	0	0	*	0	0	0	Glaucophane metalava
VO-86-38	2	1	59	3	0	5	0	11	13	3	0	0	0	0	0	3	0	" " "

LAWS: Lawsonite; PLAG: Plagioclase; K-FELD: K-feldspar; MUSC: Muscovite; CHL: Chlorite; ACT: Actinolite; GLAUC: Glaucophane; CPX: Clinopyroxene; CARB: Carbonate; STIL: Stilpnomelane; EPID: Epidote; OPAQ: Opaques; P-P: Prehnite-pumpellyite; SPH: Sphene.

TABLE 6.11: PETROGRAPHY OF SAMPLES FROM THE VILLA DE CURA BELT IN THE GUATOPO NATIONAL PARK.

AMYGDULES	SAMPLE NUMBER	CARBONATE	CHL.	QUARTZ	P-P	NAME
	VC-51	0	0	0	0	Plag. amphibole metalava
	VC-60	0	0	0	0	" " "
	VC-75	0	7	8	0	" " "
	VC-208	5	5	5	0	Plag. pyroxene metalava
	VC-22C	8	9	0	9	" " "
	VC-23A	0	0	0	0	Plagioclase metalava
	VC-24A	0	0	0	0	" " "
	VC-30A	0	0	0	0	Plag. amphibole metalava
	VC-71A	0	0	0	0	Plagioclase metalava

PHENOCRYSTS		PLAG.	CPX	OPAQUES	AMPH.	QUARTZ	CHL.	EPIDOTE	SPH.
	VC-51	66	5	0	10	2	2	8	7
	VC-60	5	0	0	15	0	0	0	0
	VC-75	20	0	0	1	0	0	0	0
	VC-208	2	39	0	0	0	0	0	0
	VC-22C	10	15	0	0	0	0	0	0
	VC-23A	25	3	2	0	0	0	0	0
	VC-24A	5	0	0	0	0	0	0	0
	VC-30A	10	0	0	15	0	0	0	0
	VC-71A	65	0	0	0	15	5	10	2

MATRIX		PLAG.	CARBONATE	CHL.	EPID.	CLINOZ.	SPH.	PUMP.	HAEM.	PYRITE	MAGN.	LEUCOX.	CPX	AMPH.	QUARTZ
	VC-51	0	0	0	0	0	0	0	0	0	0	0	0	0	0
	VC-60	16	0	0	28	0	0	0	0	0	0	0	0	20	15
	VC-75	26	0	1	1	0	3	0	0	0	1	0	1	13	18
	VC-208	15	0	11	1	0	1	0	0	0	0	0	6	0	10
	VC-22C	37	1	1	1	0	0	1	0	0	1	0	8	0	0
	VC-23A	36	1	20	5	1	5	1	1	0	0	0	0	0	0
	VC-24A	53	5	12	5	0	0	15	0	1	2	1	1	0	0
	VC-30A	46	8	0	0	3	0	0	0	1	1	1	0	15	0
	VC-71A	3	0	0	0	0	0	0	0	0	0	0	0	0	0

CHL: Chlorite; P-P: Prehnite-pumpellyite; PLAG: Plagioclase; CPX: Clinopyroxene; AMPH: Amphiboles; SPH: Sphene; EPID: Epidote; CLINOZ: Clinozoisite; PUMP: Pumpellyite; HAEM: Haematite; LEUCOX: Leucoxene.

Gilbert, 1983). Thus, glaucophane forms at high P/low T conditions in the blueschist and eclogite facies as has been proposed by Miyashiro (1979), Dobretsov and Sobolev (1984) and Banno (1986).

The association lawsonite-albite-chlorite-pumpellyite-epidote -actinolite is a frequent assemblage in the pumpellyite-actinolite facies (Winkler, 1974; Brown, 1977; Liou *et al.*, 1985). The stability fields of lawsonite coexisting with glaucophane have been determined by Newton and Kennedy (1963), Crawford and Fyfe (1965), and Carman and Gilbert (1983). The data are indicative of a pressure higher than 12 Kb at temperatures lower than 500° C, which are characteristic of a high P/T regime (Miyashiro, 1979). Furthermore, the assemblages with lawsonite and without glaucophane indicate pressures lower than 12 kb at temperatures lower than 440° C, which is also characteristic of a high P/T regime.

The assemblage prehnite + chlorite is stable in the presence of a fluid phase below 10 Kbar if the temperature is lower than 200° C, but at temperatures higher than 200° C, the stable assemblage is pumpellyite + actinolite (Hinrichsen and Schurmann, 1969). However, Nitsch (1971) also established that the association prehnite + chlorite is stable up to 400° C, at a pressure of 3 Kbar. Miyashiro (1979) indicated that stilpnomelane is widely distributed in high-pressure metamorphic rocks, that it is sometimes present in medium-pressure rocks, and that it is extremely rare in low-pressure metamorphic rocks. However, in the present area stipnomelane is associated with prehnite-pumpellyite and albite-chlorite-actinolite which are characteristic of low grade pumpellyite-actinolite facies metamorphism (Turner, 1981). The mineral assemblages described above are indicative of the following metamorphic facies: (1) pumpellyite-actinolite facies, (2) lawsonite-albite-chlorite facies, and (3) blueschist facies. Elsewhere, Navarro (1983) recognized a fourth assemblage which is characteristic of the greenschist facies at high pressure and is transitional to the blueschist facies.

However, the foliation of some glaucophane-bearing rocks is defined by actinolite-chlorite. The igneous clinopyroxene (Girard, 1981) is rimmed by glaucophane and/or actinolite. The textural relationships between pyroxene and amphiboles suggest that the igneous protolith first underwent the blueschist facies metamorphism. The actinolite-albite-chlorite assemblage is characteristic of the greenschist facies metamorphism in mafic rocks (Apted and Liou, 1983). Therefore, the metamorphic assemblage and the textures of the high P/T rocks indicate that some of the earlier formed

blueschist assemblages were overprinted by greenschist facies assemblages.

The Villa de Cura belt in the studied transect and in Guatopo National Park (Figure 5.12), also include a metatuff, metalava, and metabreccia unit (Dos Hermanas Formation). This unit is undeformed and shows a prehnite-pumpellyite assemblage (Table 6.11) indicative of a very low metamorphic grade (Winkler, 1979). Perchuk and Aranovich (1980) determined an equilibrium temperature of 250^{o} C at 2 Kbar for the assemblage pumpellyite-prehnite-calcite-epidote-chlorite-quartz. Thus, this assemblage was formed at the lowest pressures and temperatures of the entire belt.

The metamorphic series in the Villa de Cura belt records the prograde high P/low T trajectory, typical for a convergent boundary and a retrograde intermediate P/T assemblage formed during uplift due to underplating and denudation by extension and erosion (Cloos, 1982, 1984; Platt, 1986) or uplift resulting from bouyancy and isostatic readjustment when subduction ceased due to collision (Ernst, 1988).

The metamorphic path of the Villa de Cura Group is similar to that in the Cordillera de la Costa-Margarita terrane. However, the Villa de Cura Group underwent somewhat higher P/T conditions during the first metamorphic event (blueschist facies; there is no evidence of eclogite metamorphism) and may be higher P/T conditions during the retrograde metamorphism (greenschist facies). The higher P/T conditions in the Villa de Cura belt in comparison to the Cordillera de la Costa-Margarita terrane may be the result of the age of the volcanic arc: the Villa de Cura metamorphism is probably older than the Margarita high P/T metamorphism (Chapter VIII) and thus related to a more immature arc, where the P/T ratio is higher than in a mature arc. Another possibility is that the Villa de Cura rocks were never subducted as deep as the Margarita rocks.

CHAPTER VII

Rb/Sr AGE DETERMINATIONS

The interpretation of the geology of the south-central Caribbean is problematic, largely because of the scarcity of good crystallization and metamorphism ages for the Caribbean Mountains system orogenic belt. The "Consejo Nacional de Investigaciones Cientificas de Venezuela, CONICIT", made it possible to have several whole rock Rb/Sr analyses performed for the present study. The analyses were made by TELEDYNE ISOTOPES in New Jersey.

The samples were chosen from the following units in the Caribbean Mountains system: (a) Matasiete and Guayacan metatrondhjemites, Margarita Island, (b) basement of the Cordillera de la Costa belt (Peña de Mora Formation) in El Avila National Park and south of the Village Chichiriviche (the Chichiriviche-La Victoria transect), (c) the La Aguadita Gneiss (Tinaco Complex), basement of the Caucagua-El Tinaco belt along the Tinaco River, State of Cojedes (Tinaco River-Casupo transect), (d) the La Guacamaya metadiorite, basement of the Caucagua-El Tinaco belt south of the town La Victoria, State of Aragua (along La Victoria-San Sebastian transect), and (e) the Todasana Complex, south of the Village Todasana, Cordillera de la Costa belt.

The data obtained for the Matasiete and Guayacan (Table 7.1) indicate isotopic similarities between both trondhjemites and a unique source and tectonic setting may be suggested. The metatrondjemites have very low Rb abundances, high Sr contents, and the $^{87}Sr/^{86}Sr$ ratios are very similar; thus, unfortunately, an isochron could not be calculated.

The whole-rock isochron for the three samples from the Peña de Mora Formation (Table 7.2) was calculated using the least square regression computer program after York (1968) and a decay constant of $1.42 * 10^{-11}$ yr^{-1}. The best slope determined is 0.02240 ± 0.00121. The initial $^{87}Sr/^{86}Sr$ ratio obtained is 0.71103 ± 0.00734. The age of crystallization of the Peña de Mora Formation may be 1560 ± 83 Ma, which is close to the Early-Middle Proterozoic boundary. Thus, the Peña de Mora Formation represents the basement upon which the Jurassic-Cretaceous Caracas Group was deposited.

Four samples from the Tinaco Complex (La Aguadita Gneiss) were analyzed (Table 7.3); the samples were chosen taking into account the great lithologic variations of the complex and its apparent cogenetic igneous character. The selection

of the samples was difficult, because the wide-spread alteration of plagioclase in the gneissic rocks. An isochron was calculated using the least square regression computer program of York (1968). The best slope found is 0.01351 $\pm$ 0.00257 and the best intercept is 0.70475 $\pm$ 0.00197 (initial 87Sr/86Sr) resulting in an apparent age of 945 $\pm$ 178 Ma.

TABLE 7.1: Rb/Sr age determinations of the Matasiete and Guayacan metatrondhjemites, Peninsula of Paraguachoa, Margarita Island.

SAMPLE	Rb (ppm)	Sr (ppm)	$^{87}Rb/^{86}Sr$	$^{87}Sr/^{86}Sr$
MTS-85-1	7.190	506.7	0.0411	0.70302 ± 0.00010
MTS-85-2	5.83	626.1	0.0269	0.70324 ± 0.00011
MTS-85-3	5.97	629.0	0.0275	0.70344 ± 0.00009
MTS-85-4	13.6	1040.0	0.0378	0.70331 ± 0.00016
GUAY-85-4	6.12	738.4	0.0240	0.70298 ± 0.00011

TABLE 7.2: Rb/Sr age determination of the Peña de Mora Formation, in El Avila National Park and south of the Village Chichiriviche, Cordillera de la Costa belt.

SAMPLE	Rb (ppm)	Sr (ppm)	$^{87}Rb/^{86}Sr$	$^{87}Sr/^{86}Sr$
CH-86-1	155.4	162.1	2.793	0.77486 ± 0.00012
PM-86-1	227.4	106.9	6.269	0.84784 ± 0.00012
PM-86-2	227.0	83.9	7.940	0.89125 ± 0.00014

TABLE 7.3: Rb/Sr age determination of the Tinaco Complex (La Aguadita Gneiss), basement of the Caucagua-El Tinaco belt.

SAMPLE	Rb (ppm)	Sr (ppm)	$^{87}Rb/^{86}Sr$	$^{87}Sr/^{86}Sr$
RT-87-1	34.0	377	0.261	0.71010 ± 0.00023
RT-87-2	28.7	505	0.165	0.70519 ± 0.00015
RT-87-4	96.2	226	1.234	0.72005 ± 0.00014
RT-87-5	64.2	218	0.853	0.71760 ± 0.00014

This age corresponds to Middle to Late Proterozoic. The large error bar may be a consequence of a complex thermal history, although the variability of lithologies may also indicate that not all the rocks are cogenetic. Although the results are not ideal, the age may indicate that the rocks are part of the Precambrian Guayana Shield. Thus, the Tinaco Complex may represent the northern extension of the shield, but other interpretations are possible as will be discussed in the Chapter VIII.

Four samples from the La Guacamaya Metadiorite were analyzed (Table 7.4). They have very similar Rb and Sr contents. Thus, it is probably not justified to calculate an age from this data set. However, it was determined anyway and the best slope found is 0.01275 $\pm$ 0.00748, the initial $^{87}Sr/^{86}Sr$ ratio is 0.70070 $\pm$ 0.00297, and the age calculated is 892 $\pm$ 520 Ma. This age and the large error are the consequence of the similar isotopic abundances. Consequently, this Rb/Sr age is meaningless and it can not be used in the regional geologic interpretations.

Three samples from the Todasana Complex in the Cordillera de la Costa belt were analyzed (Table 7.5). They have very low Rb abundances and very high Sr content. The calculated age of 4924 $\pm$ 484 Ma is clearly meaningless.

TABLE 7.4: Rb/Sr age determination of the La Guacamaya Metadiorite, basement of the Caucagua-El Tinaco belt, south of La Victoria.

SAMPLE	Rb (ppm)	Sr (ppm)	$^{87}Rb/^{86}Sr$	$^{87}Sr/^{86}Sr$
LV-87-1	50.4	249	0.586	0.70674 ± 0.00013
LV-87-2	24.8	250	0.287	0.70600 ± 0.00012
LV-87-3	24.1	275	0.254	0.70266 ± 0.00017
LV-87-4	30.8	239	0.37 3	0.70651 ± 0.00017

TABLE 7.5: Rb/Sr age determination of the Todasana Complex, Cordillera de la Costa belt.

SAMPLE	Rb (ppm)	Sr (ppm)	$^{87}Rb/^{86}Sr$	$^{87}Sr/^{86}Sr$
TOD-22	27.4	428	0.1850	0.71270 ± 0.00020
TOD-25	11.3	655	0.0499	0.70323 ± 0.00011
TOD-26	27.7	929	0.0863	0.70486 ± 0.00011

CHAPTER VIII

TECTONIC MODELS

Introduction

A large number of plate tectonic models have been proposed to explain the origin and evolution of the Caribbean and its borderlands (Ladd, 1976; Beck, 1977; Burke *et al.*, 1978; Stephan *et al.*, 1980; Pindell and Dewey, 1982; Anderson and Schmidt, 1983; Burke *et al.*, 1984; Duncan and Hargraves 1984; Mattson, 1984; Beck. 1985; Bertrand and Bertrand, 1985; Leclere and Stephan, 1985; Burke, 1988; Pindell *et al.*, 1988; Ross and Scotese, 1988). These models are based mainly on paleomagnetic data, and to some extent on regional geology, structural geology, geochronology, petrology, and geochemistry and they try to explain the tectonic evolution of the Caribbean plate, using the reconstructions of western Pangea from the Permo-Triassic period until the present time.

All models are to large extent speculative because they are based on rotations of small blocks which are necessary to explain the gaps or overlaps that occur in the reconstructions of Africa and America for the Permian and Triassic according to the Bullard fit (Bullard *et al.*, 1965). Uncertainties results from the scarcity of geophysical data for the continental margins. Several plate tectonic models have been proposed specifically for northern Venezuela (Bell, 1972; Santamaria and Schubert, 1974; Maresch, 1974; Mascle *et al.*, 1979; Talukdar *et al.*, 1981; Talukdar and Loureiro, 1982; Navarro, 1983; Ostos and Navarro, 1985; Speed, 1985; Robertson and Burke, 1989; Avé Lallemant, 1989). These models are based mainly on petrologic and structural data of the Caribbean Mountains system, the Dutch Leeward Islands, and the Venezuelan Islands, but all models are rather unsubstantiated because of the lack of detailed geologic knowledge of these areas and the complex geologic history.

Almost all recent models proposed to explain the evolution of northern Venezuela are rather similar and differ only in details. The models of Talukdar *et al.* (1981), Navarro (1983), and Ostos and Navarro (1985) show the largest differences with the others. These models will be discussed later in this chapter and modifications will be suggested based on the new information presented in the previous chapters. First, however, the pertinent data will be reviewed under the following subheadings: Radiometric ages,

Fossil ages, Unconformities, Igneous rocks, Regional metamorphism, Sedimentary basins, and Mesozoic rift facies.

Isotopic Ages

The Paleozoic and Mesozoic history of the south-central Caribbean and northern Venezuela is not well known due to the lack of a systematic study of the Caribbean Mountains system, poor exposure, and the younger sedimentary cover. However, several radiometric ages have been published for the area and will be reviewed.

Dutch Leeward and Venezuelan Islands

Table 8.1 shows all published K/Ar and Rb/Sr ages of igneous rocks from the islands Aruba, Curacao, Los Roques, La Blanquilla, Los Hermanos, Los Frailes, Los Testigos, and Los Monjes (Figure 2.1). Bar graphs of the thirty four (34) radiometric ages included in Table 8.1 are shown in Figure 8.1. Analyzed samples were metamorphosed in the zeolite and prehnite-pumpellyite facies (Aruba, Curacao, Bonaire, Los Testigos, and Los Frailes) and in the greenschist facies (Los Monjes, Los Roques, and Los Hermanos). The graph shows a cluster of ages in the 60 to 80 Ma interval (Campanian to Paleocene). On Curacao and Bonaire occur Campanian to Paleocene turbidites (Midden Curacao Formation and Knip Group) and continental-platform deposits (Rincon and Soebi Blanco formations), which overlie Albian (Curacao Formation) and Albian-Turonian (Washikemba Formation) volcanic rocks (Beets, 1972; Beets, 1977; Beets *et al.*, 1984; Bellizia, 1985).

Los Monjes Island and the Los Roques islands (Figure 2.2) have an igneous-metamorphic basement, which has MORB affinities, although Los Roques also has the calc-alkaline suite (Bellizia *et al.*, 1969; Santamaria and Schubert, 1974). The ocean-floor basement yielded K/Ar ages from 114 to 130 Ma (Table 8.1). The basement has only a Quaternary sedimentary cover. Thus, the ages may represent a metamorphic age and the sea floor sequences may be older (Early Cretaceous).

The calc-alkaline basement in the Venezuelan islands underlies Quaternary sediments. The K/Ar ages range from 44 Ma on Los Testigos to 71 Ma on Los Hermanos, with a maximum between 60 and 70 Ma (Table 8.1). They may be uplift ages related to collision and the building of the arc onto the oceanic crust (e.g. Los Roques) may have occurred earlier.

Therefore, based on the data available the 60-80 Ma interval for the Dutch Leeward and Venezuelan Islands may coincide

TABLE 8.1: ISOTOPIC AGES FROM THE DUTCH AND VENEZUELAN ISLANDS, THE PENINSULA OF PARAGUANA, GULF OF VENEZUELA, AND THE VENEZUELAN PLATFORM.

	ROCK TYPE	METHOD	MIN./ROCK	AGE	REFERENCE
ARUBA	TONALITE	K/Ar	Biotite	74.5 ± 4 Ma	A
	Qz. DIORITE	K/Ar	Biotite	67.0 ± 4 Ma	B
	TONALITE	K/Ar	Hornblende	85 to 90 Ma	C
	TONALITE	Rb/Sr	Whole rock	72.5 ± 4 Ma	A
	TONALITE	Rb/Sr	Biotite (3) Whole rock (9)	72.0 ± 2 Ma	D
	TONALITE	Rb/Sr	Whole rock (9)	72.0 ± 29 Ma	D
CURACAO	DOLERITE	K/Ar	Whole rock	118 ± 10 Ma	B
	DOLERITE	K/Ar	Whole rock	126 ± 12 Ma	B
	DIABASE	K/Ar	Whole rock	93.0 ± 3 Ma	C
	DIABASE	K/Ar	Whole rock	73.0 Ma	C
	DIABASE	K/Ar	Whole rock	69.0 Ma	C
	Qz. TRACHIANDESITE	K/Ar	Whole rock	74.0 ± 5 Ma	B
	TRACHIANDESITE	K/Ar	Hornblende	76.0 ± 6 Ma	B
	TRACHIANDESITE	K/Ar	Whole rock	84.0 ± 6 Ma	B
LOS ROQUES	METADIABASE	K/Ar	Amphibol	127 ± 15 Ma	B
	METALAMPROPHYRE	K/Ar	Amphibol	130 ± 14 Ma	B
	PEGMATITE	K/Ar	?	66.0 ± 5 Ma	B
	Qz. DIORITE	K/Ar	Biotite	65.0 ± 3.6 Ma	B
	Qz. DIORITE	K/Ar	Hornblende	66.0 ± 6 Ma	B
LA BLANQUILLA	TRONDHJEMITE	K/Ar	Biotite	64.0 ± 3.5 Ma	B
	TRONDHJEMITE	K/Ar	Biotite	62.0 ± 3.2 Ma	B
	PEGMATITE	K/Ar	Feldspar	64.0 ± 3.4 Ma	B
	PEGMATITE	K/Ar	Biotite	62.0 ± 3.2 Ma	B
	TRONDHJEMITE	K/Ar	Biotite	64.0 ± 3.4 Ma	B
LOS HERMANOS	Hbl. GNEISS	K/Ar	Hornblende	71.0 ± 6 Ma	B
	Hbl. GNEISS	K/Ar	Hornblende	70.0 ± 5.4 Ma	B
	Hbl. GNEISS	K/Ar	Hornblende	67.0 ± 5.1 Ma	B
LOS FRAILES	DIABASE	K/Ar	Whole rock	66.0 ± 5.1 Ma	B
LOS TESTIGOS	METAGRANITE	K/Ar	Feldspar	44.0 ± 4.5 Ma	B
	METAGRANITE	K/Ar	Hornblende	47.0 ± 6.1 Ma	B
	METAGRANITE	K/Ar	Hornblende	44.0 ± 5.4 Ma	B
	METAGRANITE	K/Ar	Hornblende	44.0 ± 5.5 Ma	B
LOS MONJES	ORTHOAMPHIBOLITE	K/Ar	Amphibol	116 ± 13 Ma	B
	ORTHOAMPHIBOLITE	K/Ar	Whole rock	114 ± 12 Ma	B
PENINSULA OF PARAGUANA	METAGRANITE	U/Pb	Allanite	262 Ma	E
	METAGRANITE	U/Pb	Allanite	265 Ma	E
	METAANDESITE	K/Ar	Whole rock	63.0 ± 4.4 Ma	B
	METAGABBRO	K/Ar	Whole rock	120 ± 11 Ma	B
	METADOLERITE	K/Ar	Whole rock	118 ± 10 Ma	B
	METAANDESITE	K/Ar	Hornblende	73.5 ± 11 Ma	F
GULF OF LA VELA	Qz-Ser. PHYLLITE	K/Ar	Whole rock	83.5 Ma	G
	Qz. METAGABBRO	K/Ar	Feldspar	114 Ma	G
TUY-CARIACO BASIN	METAVOLCANIC	K/Ar	Whole rock	65.4 Ma	H
	METAVOLCANIC	K/Ar	Whole rock	69.5 Ma	H
	METAANDESITES	K/Ar	Whole rock	78.3 ± 3.9 Ma	H
CARUPANO BASIN	METAANDESITES	K/Ar	Whole rock	38.6 ± 2 Ma	I
	METAANDESITES	K/Ar	Whole rock	33.5 ± 1.8 Ma	I
	METABASALT	K/Ar	Whole rock	87.0 ± 9 Ma	I
	METABASALT	K/Ar	Whole rock	102.2 ± 10 Ma	I
GULF OF VENEZUELA	GRANITE	K/Ar	Whole rock ?	304 Ma	J
	GRANITE	K/Ar	Whole rock	138 ± 6.9 Ma	J

A: Priem et al. (1966). B: Santamaria and Schubert (1974). C: Priem et al. (1966). D: Priem et al. (1977). E: MacDonald (1968). F: Loubet et al. (1985). H: Talukdar and Bolivar (1983). I: Talukdar (1983). J: Feo Codecido et al. (1984).

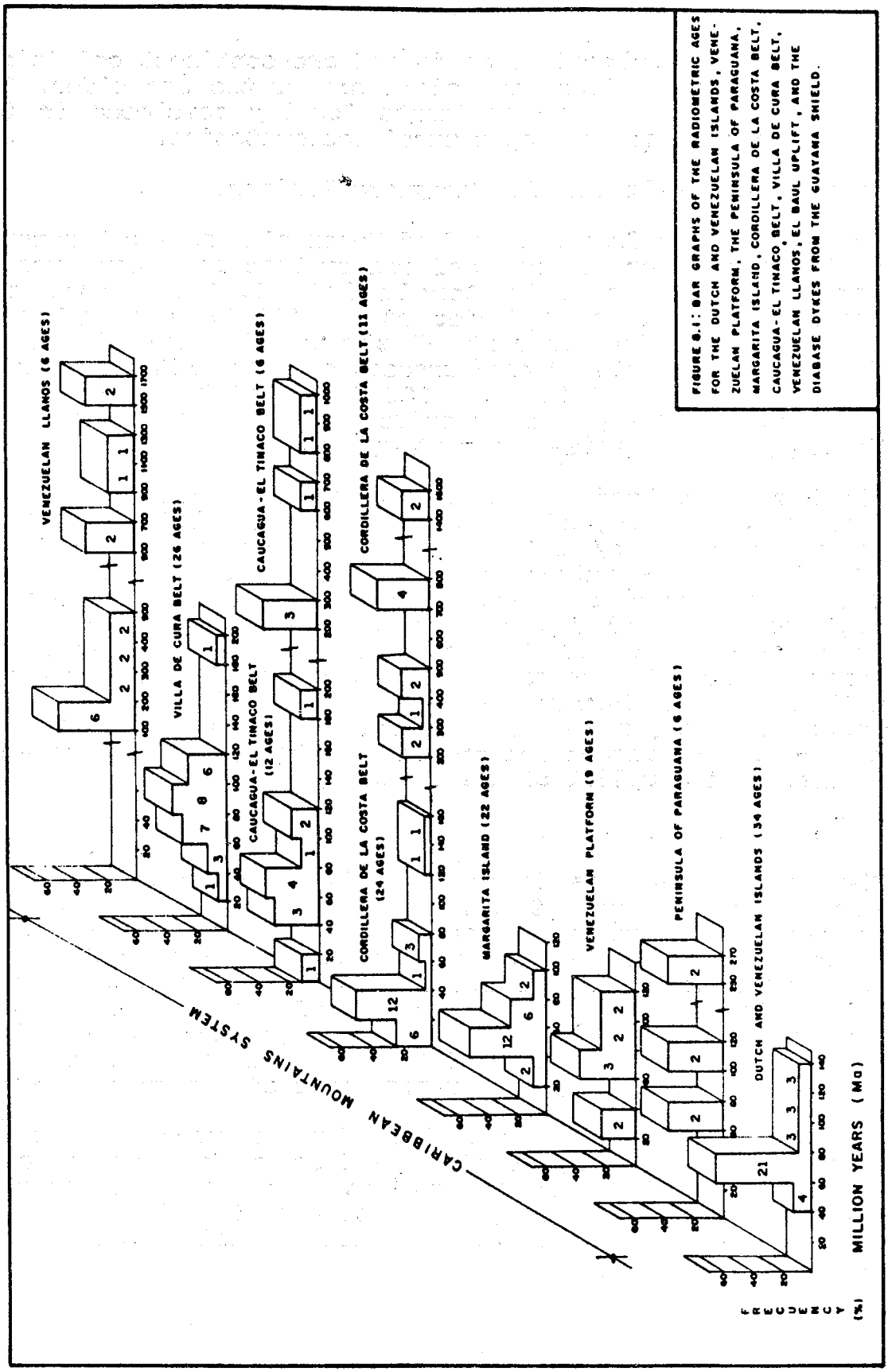

FIGURE 8.1: BAR GRAPHS OF THE RADIOMETRIC AGES FOR THE DUTCH AND VENEZUELAN ISLANDS, VENEZUELAN PLATFORM, THE PENINSULA OF PARAGUANA, MARGARITA ISLAND, CORDILLERA DE LA COSTA BELT, CAUCAGUA-EL TINACO BELT, VILLA DE CURA BELT, VENEZUELAN LLANOS, EL BAUL UPLIFT, AND THE DIABASE DYKES FROM THE GUAYANA SHIELD.

with uplift related to an island arc-continent collision, while the ocean-floor and island arc suites are older. The Campanian to Paleocene sediments locally developed in the islands may represent episutural sedimentation.

Gulf of Venezuela and the Paraguana Peninsula

Geological data from the Gulf of Venezuela and the Peninsula of Paraguana are scarce and radiometric data come mostly from the studies of MacDonald (1968), Santamaria and Schubert (1974), Feo Codecido *et al.* (1984), and Loubet *et al.* (1985). The basement of the southernmost Gulf of Venezuela consists of pre-Jurassic granites with K/Ar whole rock ages of 304 Ma and 138 Ma, which underlies a Cretaceous-Tertiary transgressive-regressive sequence and a Tertiary transgressive sedimentary cycle.

The Paraguana Peninsula consists of a granitic basement (Paraguana Granite) of early-Late Permian age (262-265 Ma). It is overlain by a Mesozoic metasedimentary sequence (Pueblo Nuevo Formation) and dismembered ophiolites (Table 8.1). K/Ar whole-rock ages of 63, 118, and 120 Ma and an amphibole age of 73.5 Ma have been determined in the dismembered ophiolites (Table 8.1). Therefore, the Paraguana Peninsula may also represent part of a collisional boundary, with the oldest Barremian-Aptian ages (similar to those of nearby Los Monjes Island) related to metamorphism of the ocean-floor sequences and the Late Cretaceous-Paleocene ages related to the uplift of the area.

La Vela and Triste Gulfs

The La Vela Gulf is located southeast of the Paraguana Peninsula (Figure 2.8). Its basement consists of metasediments and metaigneous rocks. A quartz phyllite yielded a K/Ar whole rock age of 83.5 Ma (Table 8.1) and feldspar from metagabbro has a 114 Ma age (Kiser *et al.*, 1984). The basement underlies unconformably a Tertiary-Quaternary sedimentary sequence. The younger age may date the uplift of the collisional boundary and the older age may indicate approximately the upper limit of the metamorphism.

The Triste Gulf is underlain by a very low-grade metamorphosed flysch, which underlies a Tertiary pelagic sequence. There are no radiometric dates, but the basement may correlate with the Upper Cretaceous flysch exposed on Curacao, suggesting a Late Cretaceous metamorphism and uplift.

Margarita Island

Twenty two (22) radiometric ages have been published for Margarita Island (Table 8.2 and Fig. 8.1). The data in figure 8.1 are clustered between 40 and 80 Ma, but fifty five (55) percent of the ages are in the 40 to 60 Ma interval. The metamorphic basement is overlain by an Early to Middle Eocene flysch deposit. The contact may be an unconformity (Gonzàlez de Juana *et al.*, 1980), suggesting that the metaigneous basement was metamorphosed during the

Late Cretaceous-Paleocene interval, probably in a subduction complex. Uplift must have taken place after or during the flysch sedimentation as a result of the deformation in the collisional boundary.

Tuy-Cariaco and Carupano Basins

The Tuy-Cariaco and the Carupano (North Paria) basins (Figure 2.1) were studied by the Venezuelan oil industry (Talukdar and Bolivar, 1982; Talukdar, 1983; Pereira, 1985). The Tuy-Cariaco basin is underlain by a metaigneous and metasedimentary basement, which has been correlated with the accreationary complex of Margarita Island. The metaigneous rocks have an IAT affinity (Talukdar and Bolivar, 1982); three samples yielded 65.4, 69.5, and 78.3 Ma K/Ar ages (Table 8.1). The igneous rocks underlie a Tertiary calcareous flysch uncomformably, which is similar to that exposed on Margarita Island (Talukdar and Bolivar, 1982).

The Carupano (North Paria) basin is underlain by basalts of MORB-affinity, metamorphosed to glaucophane-bearing assemblages, which are overlain by primitive (in the south) and mature (in the north) island arc complexes (Talukdar, 1983). Whole-rock K/Ar ages in the primitive island arc complex are 87.0 and 102 Ma, while the rocks from the mature island arc are 38.6 and 33.5 Ma old (Table 8.1). A Tertiary sequence of sandstones derived from a magmatic arc and recycled orogen overlies the basement unconformably (Talukdar, 1983).

Talukdar (1983) proposed that the mid-Cretaceous island arc was built on the older accreationary complex (glaucophane-containing MORB's), that the Late Cretaceous uncomformity was the consequence of the collision of the island arc with the continent, and that the younger island arc was the result of inversion in polarity of the subduction after the collision. However, the younger island arc may be part of the same island arc system, which collided diachronously against South America.

TABLE 8.2: RADIOMETRIC AGES FROM MARGARITA ISLAND

ROCK TYPE	METHOD	MIN./ROCK	AGE	REFERENCE
TRONDHJEMITE	K/Ar	Amphibole	71.0 ± 5 Ma	A
GRANITE	K/Ar	Amphibole	72.0 ± 6 Ma	B
TRONDHJEMITE	K/Ar	Hornblende	70.0 ± 6 Ma	B
PEGMATITE	K/Ar	Feldspar	32.0 ± 2 Ma	B
Amp. GNEISS	K/Ar	Amphibole	47.0 ± 4 Ma	C
Amp. GNEISS	K/Ar	Clinozoisite	43.0 ± 31 Ma	C
Amp. GNEISS	K/Ar	Muscovite	40.1 ± 2.5 Ma	C
Amp. GNEISS	K/Ar	Clinozoisite	57.5 ± 15 Ma	C
Amp. GNEISS	K/Ar	Chloritized Amp.	37.0 ± 19 Ma	C
Amp. GNEISS	K/Ar	Muscovite	50.5 ± 15 Ma	C
Amp. GNEISS	K/Ar	Clinozoisite	44.5 ± 3.5 Ma	C
Amp. GNEISS	K/Ar	Chloritized Amp.	45.5 ± 7.5 Ma	C
Amp. GNEISS	K/Ar	Muscovite	51.0 ± 1.5 Ma	C
Amp. GNEISS	K/Ar	Chlorite	56.5 ± 26 Ma	C
Amp. GNEISS	K/Ar	Clinozoisite	98.0 ± 30 Ma	C
Amp. GNEISS	K/Ar	Muscovite	59.5 ± 2 Ma	C
GRANODIORITES	K/Ar	Muscovite	67.5 ± 2 Ma	C
GRANODIORITES	K/Ar	Muscovite	54.0 ± 2 Ma	C
ORTHOGNEISS	K/Ar	Mica	62.51 ± 3.13 Ma	D
ORTHOGNEISS	K/Ar	Mica	57.07 ± 2.85 Ma	D
AMPHIBOLITE	K/Ar	Mica	84.65 ± 4.23 Ma	D
AMPHIBOLITE	K/Ar	Amphibole	79.33 ± 3.79 Ma	D

A: Olmeta (1968). B:Santamaria and Schubert (1974). C: Loubet et al. (1985).
D: Chevalier (1987).

Cordillera de la Costa Belt

Table 8.3 includes thirty six (36) K/Ar, Rb/Sr, and fission track ages from the Cordillera de la Costa belt, and Figure 8.1 shows the bar graph of the compiled data. Ten Rb/Sr whole rock ages range from 1560 to 220 Ma. Three K/Ar amphibole ages range from 753 to 155 Ma. Nine K/Ar and one Rb/Sr age determinations of muscovite and biotite separates yielded ages from 79 to 30 Ma. The fission track age of one sphene sample is 126 Ma; eleven apatite fission track determinations yielded ages of 24 to 16 Ma. Thus, it seems that the Cordillera de la Costa belt underwent several thermal events in the Precambrian and Paleozoic. The Tertiary ages may all be related to the uplift of the belt.

Caucagua-El Tinaco Belt

In Table 8.4 eighteen (18) K/Ar, Rb/Sr, and fission track age determinations from the Caucagua-El Tinaco belt are given and a bar graph for the age data (excluding the ninth sample) is shown in Figure 8.1. The ages of the basement (La Aguadita Gneiss) shown in Table 8.4 may indicate a Paleozoic and perhaps a Precambrian event. There is a possibility that a Triassic/Early Jurassic thermal event occurred. The 100-120 Ma range (K/Ar, biotite, hornblende) may be related to a metamorphic event. Most K/Ar whole rock analyses yielded ages between 64 and 88 Ma. The late Cretaceous and Tertiary ages are probably related to uplift; they are somewhat older than in the Cordillera de la Costa belt, but similar to the platform and offshore uplift ages.

Villa de Cura Belt

Table 8.5 includes twenty six (26) K/Ar ages determined for different tectonostratigraphic units of the Villa de Cura belt and Figure 8.1 shows the bar graph of the data. The ages range from 35 to 192 Ma; the range of amphibole ages is between 104 and 77 Ma. This range is typical for the Villa de Cura Group and the Chacao Complex. Older ages for the Tiara Sur Formation were determined on plagioclase separates and thus, are less reliable. Younger whole-rock ages (35 to 80 Ma) correspond to the Tiara Formation, Dos Hermanas Formation, and the Cantagallo Metagabbro.

The older ages may date the metamorphism of the accreationary complex, while the younger ages of the Dos Hermanas island arc complex may be uplift ages.

TABLE 8.3: RADIOMETRIC AGES FROM THE CORDILLERA DE LA COSTA BELT.

ROCK TYPE	METHOD	MIN./ROCK	AGE	REFERENCE
Sebastopol Metagranite				
METAGRANITE	K/Ar	Muscovite	41 ± 2 Ma	A
GRANITIC GNEISS	Rb/Sr	Whole rock	420 Ma	B
GRANITIC GNEISS	Rb/Sr	Whole rock	359 Ma	B
PARAGNEISS	Rb/Sr	Whole rock (5)	350-260 Ma	C
Guaremal Metagranite				
ORTHOGNEISS	K/Ar	Biotite	33 ± 3 Ma	D
ORTHOGNEISS	Rb/Sr	Biotite	79 ± 5 Ma	D
ORTHOGNEISS	K/Ar	Biotite	32 ± 2 Ma	E
ORTHOGNEISS	K/Ar	Biotite	31 ± 1.8 Ma	E
ORTHOGNEISS	K/Ar	Biotite	33 ± 2 Ma	E
ORTHOGNEISS	Rb/Sr	Whole rock (3)	402 ± 6 Ma	F
ORTHOGNEISS	Rb/Sr	Whole rock (3)	264 ± 4 Ma	G
Avila National Park Metagranites				
ORTHOGNEISS	Rb/Sr	Whole rock (3)	220 ± 20 Ma	H
AUGENGNEISS	Rb/Sr	Whole rock (3)	1560 ± 83 Ma	I
GNEISS	F.T.	Apatite	18.9 ± 1.9 Ma	J
GNEISS	F.T.	Apatite	23.9 ± 1.9 Ma	J
GNEISS	F.T.	Apatite	17.4 ± 2.1 Ma	J
GNEISS	F.T.	Apatite	18.8 ± 2.1 Ma	J
GNEISS	F.T.	Apatite	18.4 ± 1.9 Ma	J
GNEISS	F.T.	Apatite	17.5 ± 1.7 Ma	J
Avila National Park Metasediments				
Biotite GNEISS	Rb/Sr	Whole rock	787 Ma	H
Biotite GNEISS	Rb/Sr	Whole rock	714 Ma	H
Biotite GNEISS	Rb/Sr	Whole rock	1475 Ma	H
Choroni Granite				
METAGRANITE	K/Ar	Biotite	30.0 ± 1.9 Ma	E
METAGRANITE	K/Ar	Biotite	30.0 ± 1.8 Ma	E
METAGRANITE	F.T.	Apatite	24.1 ± 3.0 Ma	J
METAGRANITE	F.T.	Apatite	22.3 ± 2.3 Ma	J
METAGRANITE	F.T.	Apatite	17.5 ± 1.9 Ma	J
METAGRANITE	F.T.	Apatite	21.9 ± 2.9 Ma	J
METAGRANITE	F.T.	Sphene	126 ± 15 Ma	J
Colonia Tovar Granite				
GNEISS	F.T.	Apatite	16.4 ± 2.1 Ma	J
Oritapo Metadiorite				
METADIORITE	K/Ar	Biotite	76.0 ± 3.9 Ma	E
METADIORITE	K/Ar	Biotite	77.0 ± 4.0 Ma	E
Puerto Cabello Amphibolite				
Gn. AMPHIBOLITE	K/Ar	Amphibole	32.4 ± 1.2 Ma	K
Oricao Amphibolite				
Gn. AMPHIBOLITE	K/Ar	Amphibole	735 ± 30 Ma	K
Cabo Codera Complex				
Gn. AMPHIBOLITE	K/Ar	Amphibole	155 ± 7.0 Ma	K
Gn. AMPHIBOLITE	K/Ar	Amphibole	753 ± 31.0 Ma	K

F.T.: Fission tracks. A: Olmeta (1968). B: Hurley and Hess (1968). C: Pimentel et al. (1985). D: Morgan (1967). E: Santamaria and Schubert (1974). F: Urbani (1983). G: Urbani (1988). H: Kovach et al. (1977). I: Ostos (this work). J: Kohn et al. (1984). K: Loubet et al. (1985).

TABLE 8.4: RADIOMETRIC AGES FROM THE CAUCAGUA-EL TINACO BELT.

ROCK TYPE	METHOD	MIN./ROCK	AGE	REFERENCE
La Aguadita Gneiss				
Bio. GNEISS	K/Ar	Biotite	112.4 ± 3.0 Ma	A
Bio. GNEISS	K/Ar	Hornblende	117.5 ± 3.0 Ma	A
Hbl. GNEISS	K/Ar	Hornblende	235.8 ± 13 Ma	B
Hbl. GNEISS	K/Ar	Pyroxene	684.0 ± 55 Ma	C
Hbl. GNEISS	K/Ar	Plagioclase	191.1 ± 15 Ma	B
Hbl. GNEISS	K/Ar	Hornblende	204.0 ± 12 Ma	A
Hbl. GNEISS	K/Ar	Actinolite?	210.0 ± 10 Ma	A
Hbl. GNEISS	Rb/Sr	Whole rock (4)	945 ± 178 Ma	D
METADIORITE	Rb/Sr	Whole rock (4)	892 ± 520 Ma	D
GNEISS	F.T.	Apatite	49.0 ± 5.8 Ma	E
DIORITE	F.T.	Apatite	41.9 ± 4.9 Ma	E
DIORITE	F.T.	Apatite	43.4 ± 5.6 Ma	E
TRONDHJEMITE	F.T.	Apatite	6.1 ± 1.3 Ma	E
Tiramuto Formation				
METABASALT	K/Ar	Whole rock	64.2 ± 2.4 Ma	A
METABASALT	K/Ar	Pyroxene	77.0 ± 8.0 Ma	A
Pilancones Formation				
METALAVA	K/Ar	Whole rock	67.5 ± 4 Ma	F
METALAVA	K/Ar	Whole rock	88.0 ± 2.5 Ma	F
Tucutunemo Formation				
METALAVA	K/Ar	Whole rock	73.5 ± 1.9 Ma	F

F. T.: Fission track. A: Martin (1968). B: Hess (1966) in Urbani (1982). C: Kugler (1972). D: Ostos (this work). E: Kohn et al. (1984). F: Beck (1985).

TABLE 8.5: RADIOMETRIC AGES FROM THE VILLA DE CURA BELT.

ROCK TYPE	METHOD	MIN./ROCK	AGE	REFERENCE
Villa de Cura Group				
ACT. METATUFF	K/Ar	Whole rock	100.0 ± 10 Ma	A
METALAVA	K/Ar	Amphibole	77.0 ± 5 Ma	B
METALAVA	K/Ar	Phengite	87.0 ± 3 Ma	B
METALAVA	K/Ar	Plagioclase	99.0 ± 5 Ma	B
METALAVA	K/Ar	Amphibole	88.4 ± 3.1 Ma	B
METALAVA	K/Ar	White Mica	82.5 ± 2.5 Ma	B
METALAVA	K/Ar	Amphibole	90.8 ± 2.9 Ma	B
METALAVA	K/Ar	W.Mica + Epidote	192 ± 6 Ma	B
METALAVA	K/Ar	Plagioclase	107 ± 11 Ma	B
METALAVA	K/Ar	Amphibole	101 ± 58 Ma	B
Tiara Formation				
METALAVA	K/Ar	Whole rock	63.2 ± 2.0 Ma	C
METALAVA	K/Ar	Whole rock	80.0 ± 4.0 Ma	C
Tiara Sur Formation				
METALAVA	K/Ar	Plagioclase	119.0 ± 4 Ma	B
METALAVA	K/Ar	Plagioclase	112.0 ± 4 Ma	B
Dos Hermanas Formation				
METALAVA	K/Ar	Whole rock	34.7 ± 1.7 Ma	C
METALAVA	K/Ar	Whole rock	52.2 ± 1.3 Ma	C
Chacao Complex				
METAGABBRO	K/Ar	Hornblende	98.0 ± 4 Ma	B
METAGABBRO	K/Ar	Hornblende	104.0 ± 4 Ma	B
METAGABBRO	K/Ar	Plagioclase	58.5 ± 2 Ma	B
METAGABBRO	K/Ar	Hornblende	91.0 ± 3.5 Ma	B
METAGABBRO	K/Ar	Hornblende	101.0 ± 4 Ma	B
METAGABBRO	K/Ar	Plagioclase	49.8 ± 2 Ma	B
Cantagallo Metagabbro				
METAGABBRO	K/Ar	Whole rock	67.0 ± 6 Ma	D
METAGABBRO	K/Ar	Whole rock	65.0 ± 5 Ma	D
METAGABBRO	K/Ar	Whole rock	66.0 ± 6 Ma	D
METAGABBRO	K/Ar	Whole rock	67.0 ± 6 Ma	D

A: Piburn (1968). B: Loubet et al. (1985). C: Beck (1985). D: Santamaria and Schubert (1974).

Venezuelan Llanos Basin, El Baul Uplift, and younger magmatism in the Guayana Shield

Table 8.6 includes eighteen (18) K/Ar and Rb/Sr ages determined on rocks from the basement of the Venezuelan Llanos Basin, the El Baul Uplift, and from late intrusions in the Guayana shield. Figure 8.1 shows a bar graph of the data. The oldest dates are Precambrian, typical of the Guayana shield. The Paleozoic ages may be related to Silurian, Carboniferous, and Permian events. A major event is a Jurassic magmatic event that occurred in the Espino Graben (Llanos basin, well 17), represented by the Guacamaya volcanics in the El Baul uplift, and in the Guayana shield.

Discussion of the Radiometric Ages

The radiometric age distribution in the Venezuelan Llanos basin, the Caribbean Mountains system, the Venezuelan platform, and the Dutch Leeward and Venezuela islands may be related to the main tectonic events that affected the Caribbean-South American borderland (Table 8.7). The tectonic interpretation is speculative, because not enough radiometric data are available and many of the age dates are of poor quality. With this in mind, the Jurassic and younger isotopic ages may be related to the following tectonic events:

1.- A Jurassic rifting event.

2.- An Early to Late Cretaceous metamorphic event.

3.- A Late Cretaceous uplift, and

4.- A Tertiary uplift.

Fossil ages

Fossils are scarce along the South-Central Caribbean Plate boundary, because of the penetrative recrystallization and tectonic disruption of most rocks. In Table 8.8 all fossil data are tabulated from the Dutch Leeward Islands, Paraguana Peninsula, and Siquisique in the State of Lara, Venezuela (Fig. 2.1 and 2.8). The Aruba Lava Formation (on Aruba) and the Curacao Lava Formation (on Curacao) have both MORB characteristics; fossils in the first are Turonian and in the second Albian in age (Beets *et al.*, 1984). The Washikemba Formation (on Bonaire) consists of primitive island arc rocks; it has fossils of Albian to Coniacian age (Beets *et al.*, 1984). This indicates that an volcanic arc was being formed while rifting was still in progress.

TABLE 8.6: RADIOMETRIC AGES FROM THE VENEZUELA LLANOS BASIN, EL BAUL UPLIFT, AND THE DIABASE DYKES FROM THE GUAYANA SHIELD.

	ROCK TYPE	METHOD	MIN./ROCK	AGE	REFERENCE
Venezuelan Llanos Basin					
Well 4	PEGMATITE	Rb/Sr ?	?	433 Ma	A
Well 9	SCHIST	K/Ar	?	412 Ma	A
Well 13	GRANITE	K/Ar	Muscovite	321 Ma	A
Well 14	HORNFELS	K/Ar	Biotite	347.0 ± 10 Ma	A
Well 17	BASALT	K/Ar	Whole Rock	162.0 ± 8 Ma	A
Well 17	BASALT	K/Ar	Whole rock	160.0 ± 5 Ma	A
Well 17	BASALT	K/Ar	Whole rock	157.0 ± 5 Ma	A
Well 19	GRANITE	K/Ar	K-feldspar	1110 ± 33 Ma	A
Well 19	GRANITE	K/Ar	?	869 Ma	A
Well 19	GRANITE	K/Ar	?	708 Ma	A
Well 19	?	K/Ar	?	1366 ± 41 Ma	A
Well 22	Qz. DIORITE	Rb/Sr	Whole rock	1785 ± 15 Ma	A
Well 24	Qz. MONZONITE	Rb/Sr	Whole rock	1900 ± 10 Ma	A
El Baul Granite					
	GRANITE	K/Ar	Orthoclase	270.0 ± 10 Ma	B
	GRANITE	Rb/Sr	Biotite	287.0 ± 10 Ma	B
Guacamaya Volcanics					
	RHYOLITES	K/Ar	Whole rock	192.0 ± 3.8 Ma	C
	RHYOLITES	K/Ar	Whole rock	195.0 ± 3.9 Ma	C
Guayana Shield					
	DIABASE	K/Ar	Whole rock	198.0 ± 4 Ma	C

A: Feo Codecido et al. (1984). B: Martin (1968). C: MacDonald and Opdyke (1974).

TABLE 8.7: Main Mesozoic-Cenozoic tectonic events in the South Caribbean plate boundary, based on isotopic data.

AGE		GEOLOGIC INTERPRETATION
Dutch and Venezuelan Is.	60-80 Ma	Uplift age related to collision
Los Monjes Island	114-116 Ma	Metamorphic age related to a convergent boundary
Paraguana Peninsula	118-120 Ma	Metamorphic age related to a convergent boundary
	63-73.5 Ma	Uplift age related to collision
Gulf of La Vela	83.5 Ma	Uplift age related to collision
	11 Ma	Metamorphic (?) age related to convergent boundary
Margarita Island	40-60 Ma	Uplift age related to collision
Carupano Basin	87-102 Ma	Magmatism/uplift of a primitive island arc
	8.6-33.5 Ma	Uplift of a mature island arc
Tuy-Cariaco basin	65.4-78.3 Ma	Metamorphism (?)/uplift of an accreationary complex
Cordillera de la Costa belt	20-40 Ma	Uplift age (fission tracks)
	20-40 Ma	Uplift age (K/Ar ages)
Caucagua-El Tinaco belt	64-88 Ma	Uplift age
	110-120 Ma	Metamorphism (?)
Villa de Cura belt	35-80 Ma	Uplift, in an island arc complex
	77-104 Ma	Metamorphism (?)
Espino graben	157-162 Ma	Crystallization of an anorogenic alkaline basalt

TABLE 8.8: SEDIMENTARY AGES FOR THE NETHERLAND LEEWARD ISLANDS, THE PENINSULA OF PARAGUANA, AND THE SIQUISIQUE OPHIOLITE BASED ON THE FOSSILIFEROUS CONTENT.

UNIT	ENVIRONMENT	AGE	REFERENCE	REMARKS
NETHERLANDS LEEWARD IS.				
ARUBA				
Aruba Lava Fm.	Pelagic	Turonian	A	Intercalated with MORB sequences
CURACAO				
Curacao Lava Fm.	Pelagic	Middle Albian	B	Intercalated with IAT sequences
BONAIRE				
Washikemba Fm.	Pelagic	Albian	C	Intercalated with primitive IAT sequences
PARAGUANA PENINSULA				
Pueblo Nuevo Fm.		Late Jurassic	A	Quartzite, Phyllite, Schist, Metasandstone, Metaconglomerate, marble, metaradiolarites.
SIQUISIQUE				
Dismembered Ophiolite	Pelagic	Middle Jurassic	D	Prehnitized olivine gabbro, basaltic and andesitic extrusive, spilite, tuff, conglomeramerate, shale chert, and carbonate.

A: MacDonald (1968). B: Wiedmann (1978). C: Beets et al. (1984). D: Bartok et al. (1985).

Marble beds in the Pueblo Nuevo Formation on the Paraguana Peninsula contain Late Jurassic fossils. This age is one of the oldest recorded in northern Venezuela and it constrains the opening of the Caribbean.

In the Siquisique ophiolite in the State of Lara, Middle Jurassic ammonites were found (Bartok *et al.*, 1985). They may been deposited during the early stages of the opening of the ProtoCaribbean.

In Table 8.9 fossil ages are shown for the Cordillera de la Costa and the Caucagua-El Tinaco belts. The Cordillera de la Costa belt includes Jurassic, Late Jurassic (Kimmeridgian), Early Cretaceous (Neocomian), and undifferentiated Mesozoic faunas occurring in marble beds. The age of the sedimentation in the Caucagua-El Tinaco belt is not well constrained. A Permian fauna has been described in the Tucutunemo Formation, while Albian and undifferentiated Late Cretaceous fossils were recognized in the Chuspita and Urape formations.

The Paracotos belt contains limestone olistoliths and lenses, rich in Late Cretaceous pelagic and Late Cretaceous-Paleogene shallow water fossils (Table 8.10). Fossils in the Villa de Cura Group (Table 8.10) are rare and only Aptian-Albian shallow water faunas have been recognized.

Uncomformities

Hiatuses and unconformities are important indicators of tectonic events. Several have been identified in the south-central Caribbean (Table 8.11). The age range of these uncomformities is mainly based on the age of the basement dated by radiometric methods and the sedimentary age of the cover rocks determined by fossils.

In the Dutch Leeward and Venezuelan islands, the uplift and consequently the uncomformities may be related to a lithospheric plate collision. It seems that the collision in the western islands began earlier (±88 Ma, Aruba) than in the eastern part (±43 Ma, Los Testigos) of the boundary. The data do not show a systematic regional pattern in a north-south direction.

The Carúpano basin shows a well developed pattern in a southeast-northwest direction. The southernmost wells show a Paleocene to Oligocene hiatus. The uncomformity in the wells to the north is Oligocene in age.

TABLE 8.9: SEDIMENTARY AGES FOR THE CORDILLERA DE LA COSTA AND CAUCAGUA-EL TINACO BELTS BASED ON THE FOSSILIFEROUS CONTENT.

UNIT	ENVIRONMENT	AGE	REFERENCE	REMARKS
CORDILLERA DE LA COSTA BELT				
Las Brisas Fm.	Shallow water	Jurassic to Cretaceous	A	Marble layer
Las Brisas Fm.	Shallow water	L. Jurassic Kimmeridgian	B	Biohermic marble
Las Mercedes Fm.	Shallow water	Mesozoic	C	Marble layer
Las Mercedes Fm.	Shallow water	Mesozoic	D	Biohermic marble
Nirgua Fm.	Shallow water	E. Cretaceous Neocomian	E	Marble layer
CAUCAGUA - EL TINACO BELT				
Urape Fm.	Pelagic	L. Cretaceous	F	Metaconglomerate with volc. and met. source, metasand.,phyllite, marble, and metaradiolarite.
Chuspita Fm.	Outer continental shelf	Albian	G	Metaconglomerate, metasandstones, graphite phyllite and marble.
Tucutunemo Fm.	Platform	Permian	H	Calcareous metaconglomerate with marble lense carbonaceous phyllite and lithic metaconglomerate

A: Wolcott (1943). B: Urbani (1969). C: MacKenzie (1966). D: Spena, Furrer, and Urbani (1977). E: Bellizia (1972). F: Sellier De Civrieux (1953). G: Macsotay (1972). H: Benjamini et al. (1987).

TABLE 8.10: SEDIMENTARY AGES FOR THE PARACOTOS AND VILLA DE CURA BELTS BASED ON THE FOSSILIFEROUS CONTENT.

UNIT	ENVIRONMENT	AGE	REFERENCE	REMARKS
PARACOTOS BELT				
Paracotos Fm.	?	Turonian to Maastrichtian	A	Limestone olithostrom
Paracotos Fm.	Pelagic	L. Cretaceous Cenomanian	B	,, ,,
Paracotos Fm.	Pelagic	L. Cretaceous Camp.-Masstrich.	C	,, ,,
Paracotos Fm.	Shallow water	L. Cretaceous-Paleogene	D	Limestone lenses
Paracotos Fm.	Pelagic	L. Cretaceous Camp.-Maastrich.	D	,, ,,
Paracotos Fm.		L. Cretaceous Maastrichtian	E	,, ,,
VILLA DE CURA BELT				
Villa de Cura Group	Shallow water ?	E. Cretaceous Aptian - Albian	F	

A: Sellier De Civrieux (1953). B: Smith (1952). C: Konigsmark (1965). D: Oxburgh (1965). E: Shagam (1960). F: Johnson (1965).

TABLE 8.11: Major uncomformities in the Venezuelan platform and the Dutch Leeward and Venezuelan islands.

Locality	Age Ranges of the Major Uncomformities	
Aruba	Coniacian-Eocene	88.5-87.5 to 52 Ma
	Eocene-Neogene	52(?) to 23.7 Ma
Curacao	Cenomanian-Santonian	97.5 to 84 Ma
	Maastrichtian-Eocene	66.4 to 52 Ma
	Eocene-Neogene	52(?) to 23.7 Ma
Bonaire	Santonian-Campanian	87.5 to 74.5 Ma
	Paleocene-Eocene	60.6(?) to 52 Ma
	Eocene-Neogene	52(?) to 23.7 Ma
Los Roques	Maastrichtian-Quaternary	66 to 1.6 Ma
La Blanquilla	Maastrichtian-Quaternary	66 to 1.6 Ma
Los Hermanos	Maastrichtian-Quaternary	66 to 1.6 Ma
Los Frailes	Maastrichtian-Quaternary	66 to 1.6 Ma
Los Testigos	Late Eocene-Quaternary	43 to 1.6 Ma
Los Monjes	Aptian-Quaternary	119 to 1.6 Ma
La Vela Gulf	Santonian-Late Oligocene	83.5 to 23.7 Ma
	Early-Middle Miocene Boundary	16.6 Ma
	Miocene-Pliocene Boundary	5.3 Ma
Triste Gulf	Middle-Late Eocene Boundary	43.6 Ma
	Oligocene	38.6 to 23.7 Ma
	Late Miocene	11.2 to 5.3 Ma
	Pliocene-Pleistocene Boundary	1.6 Ma
Margarita	Late Cretaceous-Early Eocene	74.5 to 52.0 Ma
	Late Eocene-Middle Miocene	40.0 to 11.2 Ma
Tuy-Cariaco	Late Cretaceous-Paleocene	78.3 to 57.8 Ma
basin	Oligocene-Early Miocene	38.6 to 16.6 Ma
Carupano	Santonian-Campanian (?)	87.5 to 74.5 Ma
Basin	Paleocene-Oligocene	57.8 to 22.7 Ma

Priem et al. (1966), Schubert and Moticska (1972), Maresch (1974), Santamaria and Schubert (1974), Bellizia et al. (1976), Priem et al. (1977), González de Juana et al. (1980), Talukdar and Bolivar (1982), Biju-Duval et al. (1983), Talukdar (1983), Beets et al. (1984), Kiser et al. (1984), Priem et al. (1986), Chevalier (1987)

Igneous Rocks

The tectonic setting of several igneous complexes in the South Caribbean plate boundary zone was discussed in a previous chapter. That data and information previously published (See Chapter II), are used here to get a more regional framework of the area (Table 8.12). Precambrian intra-plate granites and Paleozoic calc-alkaline granites occur both in the Caucagua-El Tinaco and the Cordillera de la Costa belts. The Tinaquillo Peridotite Complex has MORB characteristics and may be of Paleozoic age.

Upper Jurassic anorogenic tholeiites occur in the Venezuelan Llanos basin (Espino graben) and they may be related to the Caribbean opening or to back-arc extension of the Andes subduction zone.

Undated, but probably Mesozoic ophiolitic complexes occur in the Paracotos belt (Loma de Hierro). The peridotite bodies in the Cordillera de la Costa belt may also be Mesozoic. The Siquisique ophiolites are of Middle Jurassic age. Upper Jurassic to Lower Cretaceous basaltic lavas of MORB affinity are found on Los Monjes, Aruba, Curacao, Los Roques, and Margarita. MORB-type volcanics were also encountered in wells in the Carůpano basin. The protolith of the high P/T Villa de Cura Group rocks has MORB characteristics as well. All these rocks may have formed at a mid-oceanic ridge (or marginal basin). Often it is assumed that these rocks represent the ProtoCaribbean crust, which was formed by rifting between North and South America.

Upper Cretaceous island arc activity occurred on Aruba, Bonaire, Los Roques, La Blanquilla, Los Hermanos, Los Frailes, Margarita, and in the Carůpano and Tuy-Cariaco basins. The metalavas of the Tiara Sůr and Dos Hermanas formations were also formed in a volcanic island arc, probably in late Cretaceous time (this is not supported by the isotopic ages but these ages are not reliable). Late Eocene mature island arc activity is also recognized in the northernmost part of the Carůpano basin and on Los Testigos Island.

The Andean terranes (Chapter II) have also ophiolites and dismembered ophiolites defining two north-south trending belts (a) The Jurassic Romeral terrane and (b) the Late Cretaceous Choco terrane in Colombia (Case *et al.*, 1984; MacCourty *et al.*, 1984). The igneous rocks with island arc affinity in the Andean terranes occur also in two north-south trending belts (MacCourty *et al.*, 1984): (a) Late Cretaceous-Paleogene Choco terrane and (b) the Neogene island arc complex of the Western Cordillera of Colombia.

TABLE 8.12: Tectonic affinity of Igneous Rocks from the Dutch Leeward and Venezuelan Islands, Venezuelan Platform, Caribbean Mountains System, and the Espino Graben.

LOCALITY	TECTONIC AFFINITY	AGE
Aruba	MORB	pre-Turonian
	Calc-alkaline	Turonian
Curacao	T-Type MORB	Albian or older
Bonaire	Primitive island arc	Albian to Turonian
Los Roques	MORB	Neocomian
	Calc-alkaline	Older than Campanian
La Blanquilla	Calc-alkaline	pre-Campanian
Los Hermanos	Calc-alkaline	pre-Campanian
Los Frailes	Calc-alkaline	pre-Campanian
Los Testigos	Calc-alkaline	pre-Middle Eocene
Los Monjes	MORB	Aptian or older
Margarita	MORB and/or marginal basin	pre-Campanian
	Calc-alkaline	Maastrichtian ?
Carupano Basin	MORB	pre-Coniacian
	Primitive island arc	Coniacian or older
	Mature island arc	pre-Late Eocene
Tuy-Cariaco basin	IAT	Campanian or older
Cordillera de la Costa belt	Within-plate granites	Precambrian
	MORB	Mesozoic (?)
Caucagua-El Tinaco belt	MORB	Paleozoic(?) and Mesozoic
	Calc-alkaline	Paleozoic
Villa de Cura belt	MORB and/ or marginal basin	pre-Albian
	IAT	Albian-Cenomanian
Espino graben	Anorogenic alkaline magmatism	Late Jurassic

Regional Metamorphism

The regional metamorphism in the tectonic belts of the south-central Caribbean was discussed in detail in Chapter VI. A summary of the tectonic interpretations of the entire range is given in Table 8.13. Ancient seafloor in an accreationary wedge was metamorphosed during late Early or early Late Cretaceous in the prehnite-pumpellyite, zeolite, eclogite, and blueschist facies. It is now exposed on Curacao, Margarita, in the Carůpano basin, Cordillera de la Costa-Margarita terrane, Paracotos belt, and Villa de Cura belt.

During the Late Cretaceous and Tertiary, an intermediate P/T metamorphic event occurred, characterized by prehnite-pumpellyite, greenschist, and epidote amphibolite facies assemblages in the volcanic island arc of Aruba, Bonaire, Los Roques, Los Hermanos, Los Testigos, Los Monjes, Margarita, Tuy-Cariaco basin, Carůpano basin, and Villa de Cura belt. During the Late Cretaceous, intermediate and low P/T metamorphism occurred in the Cordillera de la Costa and Caucagua-El Tinaco belt, probably related to the continentward movement of nappes during an island arc/Atlantic-type margin collision or related to the migration of a transpressional terrane.

Sedimentary Basins

Until Late Cretaceous time sediments were deposited in basins on the passive Atlantic-type South America continental margin. In Late Cretaceous-Paleogene time sedimentation in the south continued, although the basins became foreland basins (perisutural) and in the north, episutural basins developed as a consequence of the Caribbean/South America plate interaction.

Atlantic-type Basins

In northern South America, the largest Atlantic-type basins are the Maracaibo Lake basin, the Gulf of Venezuela basin, the Guarico basin, and the Maturin basin. They are all located south of the Caribbean Mountains system (Figure 1.5). The stratigraphy of these basins is similar to that in the Andean terranes (Sierra de Perijá and Mérida Andes) previously discussed in the Chapter II.

Continental conditions (conglomerates, red beds, and rare alkaline volcanics) during the Jurassic were replaced by pelagic conditions in the Cretaceous associated with a transgressive cycle, which continued in the Maracaibo Lake basin and the southern part of the Gulf of Venezuela basin

until the Santonian and until the Maastrichtian in the Guarico and Maturin basins. The similarity in pre-Santonian sedimentary facies of all basins suggests that they were part of one Atlantic-type basin, but in the Santonian time this large basin may have been divided into two separate basins.

The regression in the basins was diachronous from west to east (Figure 8.2) and it may indicate the beginning of subduction or collision in northwestern South America. The erosion associated with the regression in the Maracaibo and the southern Gulf of Venezuela basins may have started in the southern part of the Maracaibo basin during the Paleocene (Gonzàlez de Juana *et al.*, 1980), although southeasterly migrating deltas have also been recognized (Audemard; personal communication, 1989), but it is only in the Oligocene when the uncomformity became regional. A major Miocene uncomformity developed in the Guarico and Maturin basins which may correlate with the Oligocene hiatus of the Maracaibo and Gulf of Venezuela basins. Thus, a west to east diachronism exists also in the major Tertiary erosional period.

Episutural Basins

Relatively little is known of the Cretaceous-Tertiary sediments in the northern part of the South Caribbean plate boundary zone as discussed in a previous chapter (Chapter II). However, several tentative conclusions can be made based on the available data. According to Talukdar and Bolivar (1982), Talukdar (1983), Case *et al.* (1984), Kiser *et al.* (1984), and Pereira (1985) the Venezuelan platform is partly continental and partly oceanic. In the west, the boundary between oceanic and continental crust lies between the Dutch Leward islands and the Peninsula of Paraguana; in the central part, this boundary lies south of the small Venezuelan islands (Los Roques Archipelago) , and in the east south of Margarita. The oldest (Upper Cretaceous) sediments in the area are deposited on oceanic or island arc sequences; they are recognized in the west on Curacao and Bonaire; in the east, they occur in the southern part of the Carupano basin. These sediments may be associated with deep sea trench or a forearc basin, and related to a Late Cretaceous convergent margin in northern South America.

Eocene volcanigenic sediments are exposed on Margarita and were recovered from wells in the Carùpano basin and in the Triste Gulf. In many areas a hiatus occurs between Eocene and Miocene and locally the Miocene overlies the Upper Cretaceous basement uncomformably (Chapter II). Thus, the timing of the regional uplift of the platform is consistent

TABLE 8.13: Tectonic Interpretation of the Regional Metamorphism in the South-Central Caribbean Plate Boundary Zone.

LOCALITY	TECTONIC INTERPRETATION	AGE
Aruba	Prehnite-pumpellyite and zeolite facies. Metamorphism in a volcanic-plutonic complex.	Campanian or older
Curacao	Prehnite-pumpellyite and zeolite facies. Metamorphism in an accreationary complex or in a divergent plate boundary.	Campanian or older
Bonaire	Prehnite-pumpellyite and zeolite facies. Metamorphism in a volcanic-plutonic complex.	Campanian or older
Los Roques	Greenschist facies. Metamorphism in a volcanic-plutonic complex.	Campanian or older
Los Hermanos	Greenschist facies. Metamorphism in a volcanic-plutonic complex.	Campanian or older
Los Frailes	Prehnite-pumpellyite facies. Metamorphism in a volcanic-plutonic Complex.	Campanian or older
Los Testigos	Prehnite-pumpellyite facies. Metamorphism in a volcanic-plutonic Complex.	pre-Middle Eocene
Los Monjes	Greenschist facies. Metamorphism in an accreationary complex.	Aptian
Margarita	Eclogite, greenschist, and epidote amphibolite facies. Metamorphism in an accreationary complex and in a volcanic-plutonic conplex.	Campanian or older
Tuy-Cariaco basin	Very-low metamorphic grade (?). Metamorphism in a volcanic-plutonic complex.	Campanian or older

TABLE 8.13: CONTINUATION

LOCALITY	TECTONIC INTERPRETATION	AGE
Carupano Basin	High P/T metamorphism Metamorphism in an accreationary complex. Unmetamorphosed to prehnite-pumpellyite facies (island arc). Metamorphism in a volcanic-plutonic complex.	pre-Coniacian Coniacian to Tertiary
Cordillera de la Costa-Margarita terrane	Eclogite, greenschist, and blueschist facies. Metamorphism in an accreationary complex.	late - early Cretaceous ?
Cordillera de la Costa belt	Greenschist facies. Metamorphism in an accreationary complex predating collision of an island arc and Atlantic-type margin.	late Cretaceous
Caucagua-El Tinaco belt	Greenschist, epidote amphibolite, and amphibolite facies. Metamorphism in a volcanic-plutonic complex.	Campanian or older
Paracotos belt	Prehnite-pumpellyite facies. Metamorphism in an accreationary complex or related with the continentalward-movement of nappes during an island arc/Atlantic-type margin collision or developed during the migration of a transpressional terrane.	late Cretaceous ?
Villa de Cura belt	Prehnite-pumpellyite to blueschist facies. Metamorphism in a accreationary complex and in a volcanic complex.	Albian-Cenomanian?

with that in the tectonic belts of the mainland. During the Miocene the platform subsided, while the mainland remained above sea level. Thus, the Neogene basins were best developed north of the Cordillera de la Costa belt, on the Venezuelan platform. They formed as pull-apart basins related to the Tertiary strike-slip faulting.

FIGURE 8.2: Simplified regional events in the Atlantic-type basins of northern South America (After Salvador, 1964; Salvador and Stainforth, 1968; González de Juana, 1972; González de Juana *et al.*, 1980; Yoris, 1985).

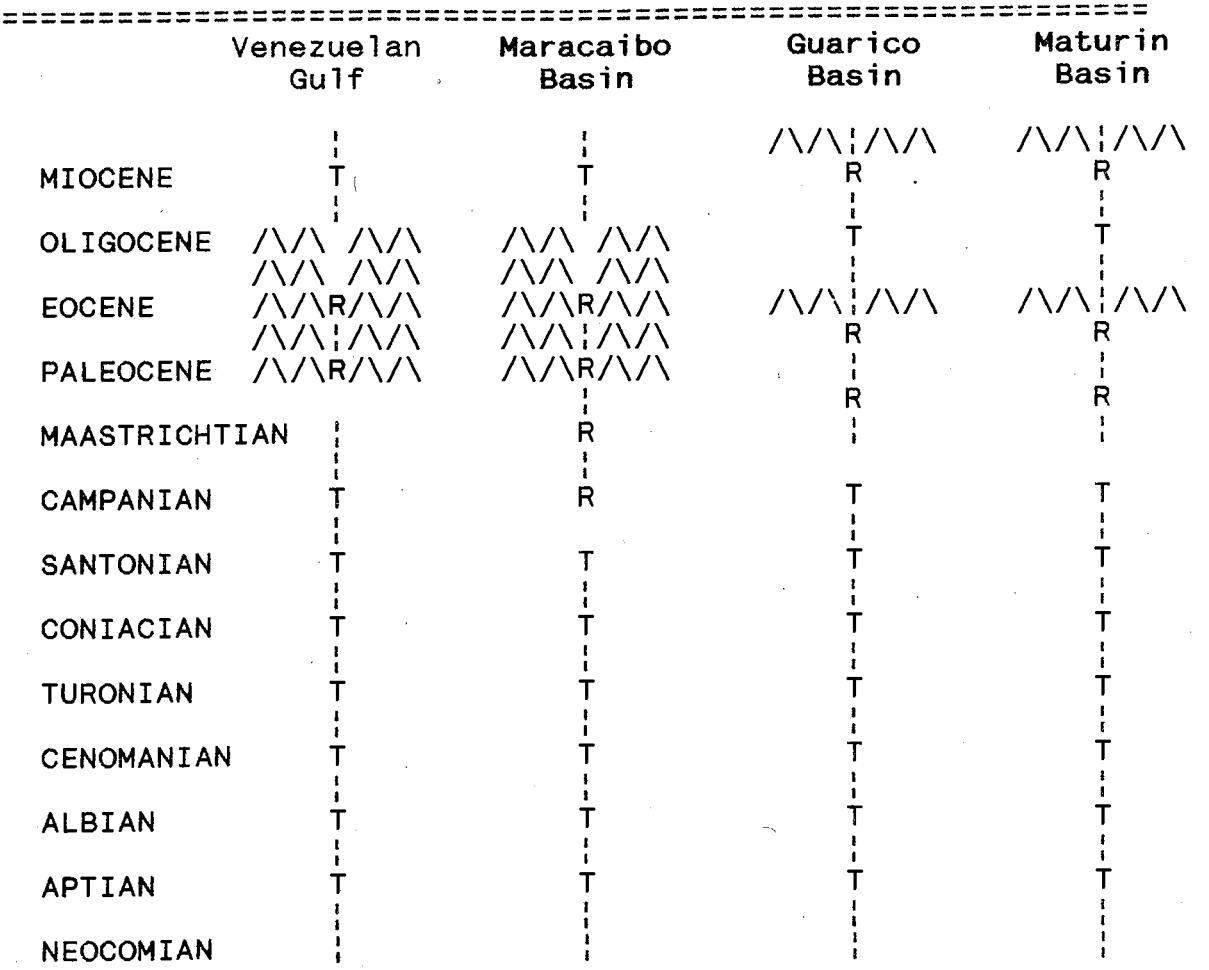

Mesozoic rift facies in northern South America

Mesozoic rift facies in the central Caribbean Mountains System are restricted to the overturned belt of the Guarico foreland basin and the Espino Graben in the basement of the Venezuela Llanos basin (González de Juana *et al.*, 1980; Feo Codecido *et al.*, 1984; Moticska, 1985). Mesozoic rift facies in northwestern South America have been described in the Sierra de Perijá (Kellogg and Bonini, 1982), Mérida Andes (Schubert *et al.*, 1979), Peninsula of la Goajira (Bellizia, 1985), and the Eastern Colombian Cordillera (Shagam, 1975). Mesozoic rift facies in northeastern South America is suggested by the Valanginian (González de Juana *et al.*, 1980) evaporite-rich Patao Member of the Cariaquito Formation, in the Peninsula of Paria (González de Juana *et al.*, 1972).

However, the Mesozoic rift facies in northwestern South America are located in the allochthonous Andean terranes (Chapter II). They may be related to the convergent plate boundary of western South America or to the extension related to the Jurassic North and South America rifting event (Maze, 1984).

The Mesozoic rift facies in north-central and northeastern South America can be separated into two groups: (a) the autochthonous rift facies located in the basement of the Venezuela Llanos basin (Espino Graben), which clearly is a relict intracratonic basin related to the Caribbean opening and (b) the allochthonous rift facies of the Cordillera de la Costa belt in the Peninsula of Paria and in the Guarico foreland basin. Therefore, the only rift facies proven to be related to the ProtoCaribbean plate is the Espino graben rift sequence (Ipire Formation).

Late Triassic-Early Jurassic Plate Configuration

The plate configuration of North and South America during the Triassic and Jurassic has been the object of debate. However, lately the location of the Yucatan or Maya block between North and South America has been widely accepted (Dengo, 1983; Burke *et al.*, 1984; Ghosh *et al.*, 1984; Pindell, 1985; Burke, 1988; Pindell *et al.*, 1988). Anderson and Schmidt (1983) and Ross and Scotese (1988), used a similar reconstruction, but proposed that Cuba was also located between North and South America; others assume that Cuba is allochthonous and was formed in the Pacific as part of the Greater Antilles arc. The reconstruction of the northwestern corner of South America is still an unsolved problem.

Figure 8.3 depicts the Late Triassic-Early Jurassic reconstruction, which is mainly based on the one proposed by Dengo (1983). It defines a Paleozoic belt, which trends north-south in the west and east-west in northern South America. This belt had magmatic activity during the Late Paleozoic. The north-south belt consists of the Central and Eastern Cordillera of Colombia, the Santa Marta Massif (Irving, 1975; Shagam, 1975; González de Juana *et al.*, 1980; Ramirez *et al.*,1983; Restrepo and Toussaint, 1988), and the Oaxaca and Chortis blocks (Dengo, 1983). In northern South America the belt includes the Peninsula of la Goajira (González de Juana *et al.*, 1980; Bellizia, 1985), the Paleozoic megasuture of northern Venezuela (Feo Codecido *et al.*, 1984), and the Yucatan block, and Catoche terrane (Case *et al.*, 1984). The southern limit of the Paleozoic megasuture is shown on Figure 8.3 but the northern limit is not clearly defined, because of the younger superimposed Mesozoic megasuture. The basement of the Caribbean Mountains system could be the northern part of the Paleozoic megasuture in the central and eastern parts of Venezuela; alternatively, it may have been transported from the west.

Plate Tectonic Model

Introduction

Several plate tectonic models have been proposed to explain the origin and evolution of the Caribbean, thus having implications on the evolution of the northern Venezuela. Some models have been proposed specifically to explain the Venezuelan geology (Maresch, 1974; Talukdar *et al.*, 1981; Talukdar and Loureiro, 1982; Navarro, 1983; Beck, 1985; Ostos and Navarro, 1985; Stephan, 1985). Most models are very similar and differ only in details. The models of Talukdar *et al.* (1981), Navarro (1983), and Ostos and Navarro (1985) which are based solely on the geology of Venezuela are very different. However, in all models, the evolution of northern Venezuela began with rifting of North and South America and the formation of an Atlantic-type margin.

The different belts of the Caribbean Mountains system are thought to have been formed after the drifting episode, that is after mid- Cretaceous time. However, in most older models, subduction and volcanic island arc formation started before drifting was terminated. For example, Maresch (1974) proposed that a south-facing volcanic island arc was formed north of Venezuela already in Jurassic time. This arc became extinct, while a new south-dipping subduction zone developed south of the extinct arc. During the Coniacian this arc

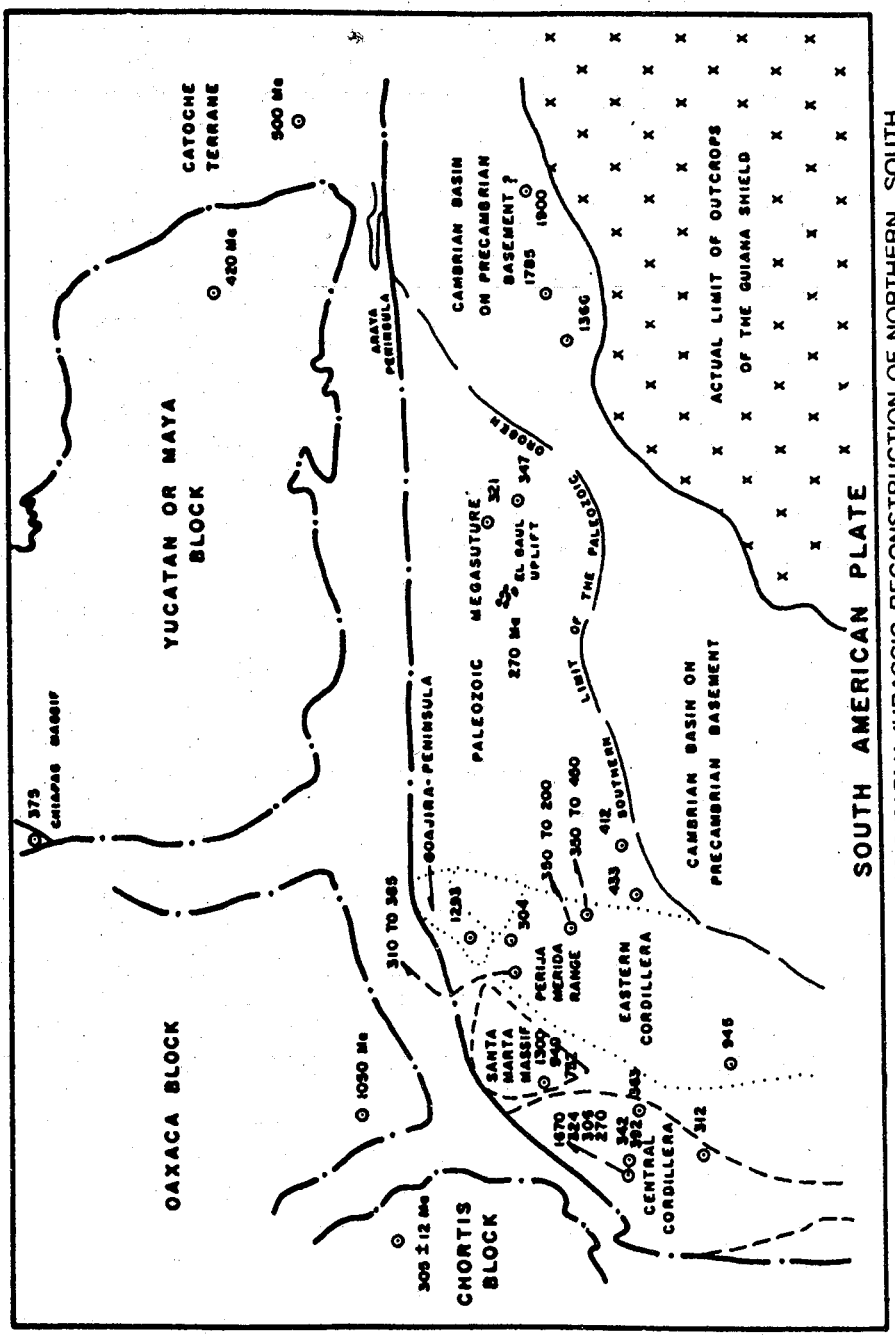

FIGURE 8.3: LATE TRIASSIC-EARLY JURASSIC RECONSTRUCTION OF NORTHERN SOUTH AMERICA WITH ISOTOPIC AGES OF SOME BASEMENT COMPLEXES (MACDONALD AND IRVING, 1971; IRVING, 1975; RESTREPO AND TOUSSAINT, 1978; RESTREPO AND TOUSSAINT, 1982; GONZALEZ DE JUANA et al., 1980; FEO CODECIDO et al., 1984).

collided with South America and a new south-dipping subduction zone was formed which became deactivated in the Paleocene. A similar model was proposed by Talukdar and Loureiro (1982), but they suggested that the Cretaceous subduction zone was north dipping. An Early Cretaceous history for northern Venezuela is also proposed by Beck (1985b) and Stephan (1985). They proposed in their tectonic model three main periods of compressional tectonics: (a) a lowermost Cretaceous island arc-continent collision, which emplaced high P/low T rocks (Villa de Cura belt and Cordillera de la Costa-Margarita terrane) onto the continent, (b) a Senonian phase during which the Villa de Cura belt was transported further southward and approximately to the present position (Beck, 1985b, 1986; Stephan, 1985), and (c) a Senonian to Neogene phase of more superficial folding and thrusting, above a shallow north dipping decollement exposed in the piedmont. In more recent models (Duncan and Hargraves, 1984; Ross and Scotese, 1988; Pindell *et al.*, 1988) the arc and the Caribbean Mountains system of northern South America were formed by the interaction of the Farallon plate with South America near northwestern Colombia. They were transported eastward during the Late Cretaceous and Paleocene, and were emplaced onto the South America plate in Venezuela from Eocene to Miocene time as transpressional terranes.

Constraints for the Tectonic Model

The tectonic model that is proposed here tries to accomodate the following geologic data:

(a) There is no evidence for convergence between North and South America during the Cretaceous (Pindell *et al.*, 1988). Thus, during the Cretaceous no compressional deformation should have happened in northern South America as is indeed shown by the sedimentary history of the Atlantic-type basins. The Cretaceous deformation in the allochthonous belts of northern Venezuela must have occurred elsewhere.

(b) The structural data indicate that the entire Caribbean Mountains system , which includes the Precambrian-Paleozoic continental basement, the Mesozoic metasedimentary cover, ophiolites, and island arc complexes, was influenced by dextral strike-slip tectonics.

(c) The development of magmatism, unconformities, Tertiary east-west trending pull-apart basins, and of foredeeps has occurred earlier in the west (Late Cretaceous to Eocene) than in the east (Eocene to Miocene).

(d) The geochemistry of basaltic rocks and the metamorphic

assemblages indicate that the Cordillera de la Costa-Margarita terrane and the Villa de Cura Group are pieces of ancient ocean floor or marginal basin, which were metamorphosed under high P/low T conditions and later overprinted by lower P/T assemblages. The metamorphic path may be related to collision (Ernst, 1988) or to the development of a transpressional terrane (Avé Lallemant and Guth, 1990). However, this terrane contains also calc-alkaline magmatic rocks.

(e) Radiometric ages suggest that the metamorphism in the Caribbean Mountains system is early-Late Cretaceous. The Villa de Cura, Los Monjes, and Los Frailes ocean floor rocks have, however, an older metamorphic history than the rest of the Caribbean Mountains system.

(f) The P/T ratio during the metamorphism of the Villa de Cura Group is higher than of the Cordillera de la Costa-Margarita terrane. The Villa de Cura subduction may be related to an older, immature, and short lived volcanic island arc.

(g) There are no Late Cretaceous granitic intrusions typical of an Andean-type plate boundary in northern South America. The granitic rocks previously interpreted as Late Cretaceous are pieces of Precambrian-Paleozoic basement which were involved in the deformation and metamorphism during the Late Cretaceous-Tertiary. The Precambrian-Paleozoic granitic basement and the Paleozoic sedimentary cover are exposed in the Caribbean Mountains system and deformed with the entire orogenic chain, which indicates that during the Late Cretaceous-Tertiary orogenic event, the decollement extended down into the basement.

(h) Kinematic indicators suggest south directed thrusting in the Cordillera de la Costa belt and north directed thrusting in the Villa de Cura belt. Both belts show a component of dextral slip along east-west trending shear zones.

(i) The Albian age of shallow water fossils in the oceanic Villa de Cura belt is doubtful. These fossils are poorly preserved. Even if they are Albian, they may have been included in the belt during Late Cretaceous-Tertiary tectonism or they may belong to the younger Paracotos belt. Thus, it is quite possible that the Villa de Cura protolith is older and may be correlated with the 125 Ma old blueschist of the Romeral ophiolite in Colombia.

(j) The Caribbean seafloor is thought to be of Coniacian-Santonian age (the age of the B" reflector; see Donnelly *et al.*, 1973). It has been proposed that the Caribbean seafloor

collided with the Mid-America Caribbean island arc at about 80 Ma, after which the polarity of subduction was reversed. However, it is suggested here that this collision is much older (100 Ma) because subduction underneath the Dutch and Venezuelan islands started around 90 to 100 Ma.

Tectonic model

Using the constraints described above, a plate tectonic model will be discussed, based on the plate motion vectors proposed by Pindell *et al.* (1988). In the model the Caribbean Mountains system, the Dutch and Venezuelan islands, and the Venezuelan platform are allochthonous and deformed as the result of two collisions: an earlier collision of a microcontinent with an island arc and a later collision of the Caribbean island arc system and northwestern South America. The easterly tectonic transport of the terranes is a consequence of oblique plate convergence (Avé Lallemant and Oldow, 1988). The Caribbean Mountains system, the Dutch and Venezuelan islands, and the Venezuelan platform initially might have been coupled to the overriding South American plate, but because of the large obliquity were displaced eastward as part of the Farallon (Caribbean) plate.

Neocomian (144 to 120 Ma)

The Late Triassic-Early Jurassic configuration of northern South America (Figure 8.3) was radically changed during the mid-Late Jurassic, when ridge branches of the North Atlantic spreading system developed between South America and the Chortis, Oaxaca, and Yucatan blocks. A southernmost rift branch (Espino graben) was also formed, but it was aborted in the Late Jurassic (Feo Codecido *et al.*, 1984). The proto-Caribbean spreading center is displaced along several transform faults. The faults are plotted as extensions of the much younger El Baul and Urica faults on the mainland of Venezuela (Figure 8.4A), which may represent old weakness surfaces developed during a Paleozoic orogeny.

The Baul fault is a major structure that divides the extensive lower Upper Cretaceous continental platform deposits in the Maracaibo Lake basin from the restricted sediments of the Guarico basin. The Urica fault separates relatively thin sediments in the Guarico basin from thick deposits in the Maturin basin.

The Maracaibo-Santa Marta block was located south of its present location; rotations between the Sierra de Perijá and Mérida Andes (Maze and Hargraves, 1984) had already occurred. The origin of the Atlantic-type Maracaibo Lake

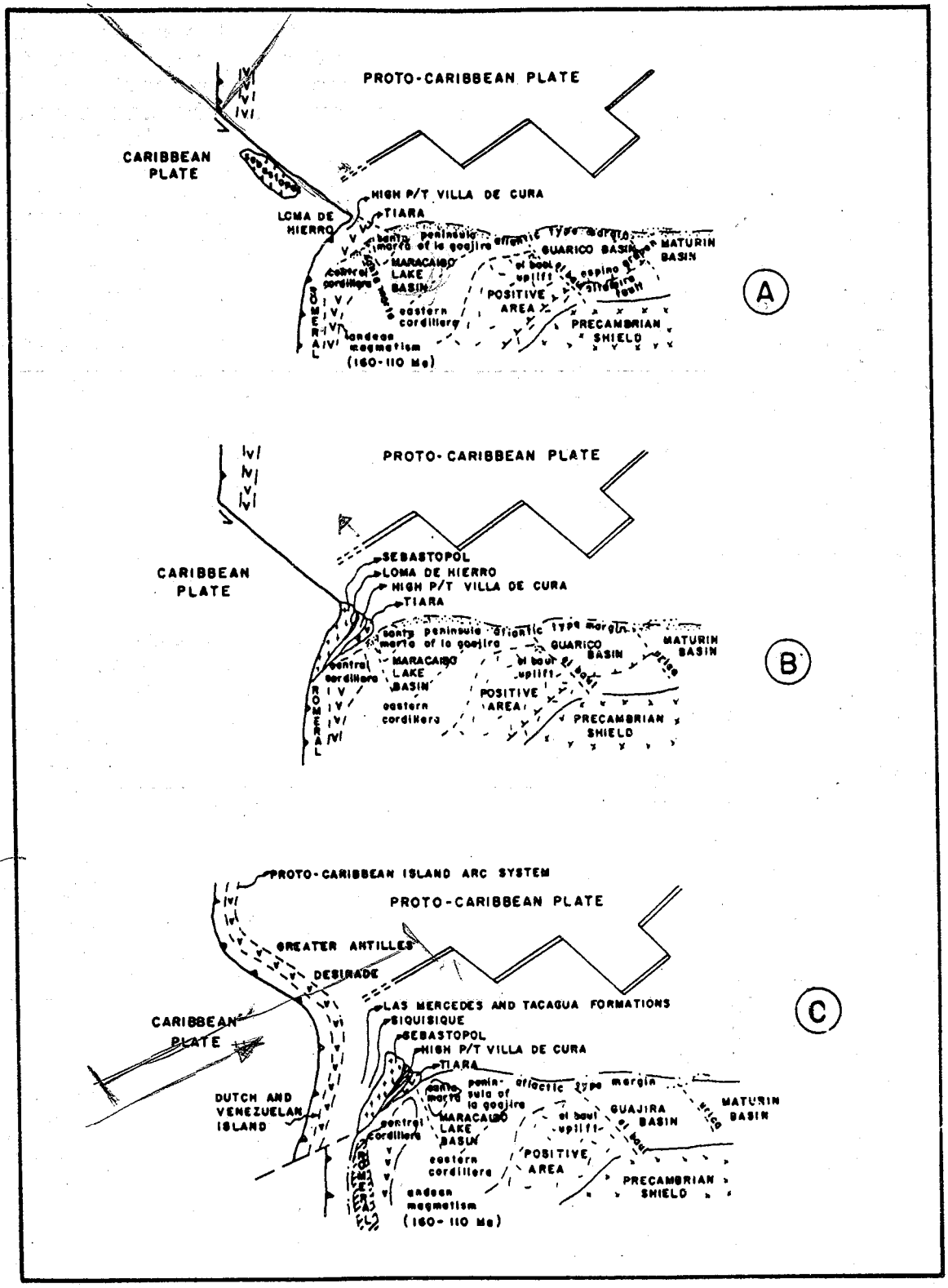

FIGURE 8.4 : TECTONIC EVOLUTION OF NORTHERN SOUTH AMERICA DURING THE NEOCOMIAN (A : 144 Ma ; B : 125 Ma ; C : 120 Ma).

basin may be related to the opening of the Proto-Caribbean ocean. Atlantic-type basins developed in northern South America (Maracaibo Lake, Santa Marta massif, Peninsula of la Goajira, Guarico, and Maturin basins) and on the Sebastopol block (Figure 8.4). The Sebastopol block which is exposed in the Cordillera de la Costa and Caucagua-El Tinaco belts may represent a microcontinent rifted from the Chortis and/or Oaxaca blocks. The Jurassic to Early Cretaceous sediments of the Caracas Group were deposited on the Atlantic-type margins of the Sebastopol block. Figure 8.4A shows the Berriasian (144 Ma) reconstruction; at that time the Farallon plate migrated southeasterly and the following plate boundaries were developed: (a) a southeast trending conservative boundary between the Farallon (Caribbean) and Proto-Caribbean plates, (b) a Mariana-type subduction boundary in northwestern South America, and (c) an Andean-type subduction boundary in western South America (Toussaint and Restrepo, 1982; Apsden and McCourt, 1986). The Sebastopol block moved southeasterly parallel to the transform boundary. The Loma de Hierro ophiolite was part of the Caribbean plate and it was located between the Sebastopol block and the convergent boundary of the Tiara arc (Figure 8.4A). The oceanic rocks of the Villa de Cura belt were metamorphosed at blueschist facies conditions in the accreationary wedge (144 Ma). The Tiara arc was build on the Proto-Caribbean plate. In this model, the high P/low T rocks of Romeral are correlated with the Villa de Cura. The Tiara magmatism is contemporaneous with the Andean felsic magmatism (160-110 Ma) in the Central Cordillera of Colombia (Toussaint and Restrepo, 1982; Bourgois *et al.*, 1985).

Figure 8.4B shows the Hauterivian (125 Ma) tectonic reconstruction of northern South America. At that time, the Sebastopol block collided with the Tiara arc which subsequently became extinct. The Villa de Cura blueschists were uplifted and underwent greenschist and pumpellyite-facies retrograde metamorphism. The uplift of the high P/low T Villa de Cura was facilitated by north-directed thrusting. The sediments south of the Sebastopol block (Caucagua-El Tinaco belt) were metamorphosed during the northward thrusting. The Loma de Hierro ophiolite was thrust northward on the Sebastopol block. The Andean magmatism in the Central Cordillera of Colombia continued, as well as the sedimentation on the Atlantic-type margins of northern South America (Figure 8.4B).

Figure 8.4C shows the Barremian-Aptian (120 Ma) reconstruction. At this time the Farallon (Caribbean) plate changed its migration direction from southeasterly to northeasterly and a convergent boundary was developed west of the earlier conservative boundary. The Romeral ophiolite

was obducted in western South America and a new east dipping subduction zone was formed. However, the magmatism in the eastern flank of the Central Cordillera of Colombia continued until the Albian (Bourgois *et al.*, 1985). The southernmost extension of the Proto-Caribbean island arc and the correlation with the Western Cordillera of Colombia is not clear, because there are conflicting interpretations of the tectonic meaning of this belt. Pichler *et al.* (1974) suggest an oceanic origin; Restrepo and Toussaint (1975) interpreted it as a magmatic arc developed on oceanic crust and related to a subduction zone located to the west in the Pacific; Barrero (1977) postulated that the Western Cordillera represents a magmatic arc west of the Andean magmatic arc, but both related to the east-dipping subduction of the Farallon plate; Bourgois *et al.* (1985) thought that the Cordillera was formed in a marginal basin related to an east dipping subduction zone. Rocks of the Lower Cretaceous Proto-Caribbean island arc system (Figure 8.4C) are recognized in the following localities: (a) in Cuba: pegmatites (Meyerhoff *et al.*, 1969), (b) in Hispanola: felsic intrusions (Kesler *et al.*, 1977), (c) in Puerto Rico: ophiolitic and primitive island arc complexes (Lee and Mattson, 1976), (d) the Desirade island, and (e) the Dutch and Venezuelan islands (Los Monjes, Los Roques). During this time span sedimentation on the northern margin of the Sebastopol block and on the Siquisique ocean floor continued with the deposition of the euxinic Las Mercedes Formation and the volcaniclastic Tacagua Formation (Figure 8.4C).

Late Albian (~100 Ma)

During the mid Cretaceous major changes occurred in the tectonic evolution of the Caribbean. About 100 Ma, according to Ross and Scotese (1988) or 80 Ma (Duncan and Hargraves, 1984; Pindell *et al.*, 1988) the polarity of subduction in Central America (Proto-Caribbean island arc system) reversed. Generally, it is assumed that the polarity change resulted from the collision of an oceanic plateau with the Proto-Caribbean island arc (Duncan and Hargraves, 1984; Burke, 1988). This plateau ultimately became the thickened Caribbean seafloor. After the change of polarity (Figure 8.5), the Caribbean island arc system developed upon the Proto-Caribbean island arc system. Because of the subduction reversal, the Caribbean island arc system had to migrate northeasterly (Figure 8.5). The Caribbean island arc system consists of the Greater Antilles, Desirade Island, the Aves Ridge, and the Dutch and Venezuelan islands.

It is difficult to correlate the Caribbean island arc system with convergent margin magmatism in South America because the tectonic meaning of the Western Cordillera of Colombia

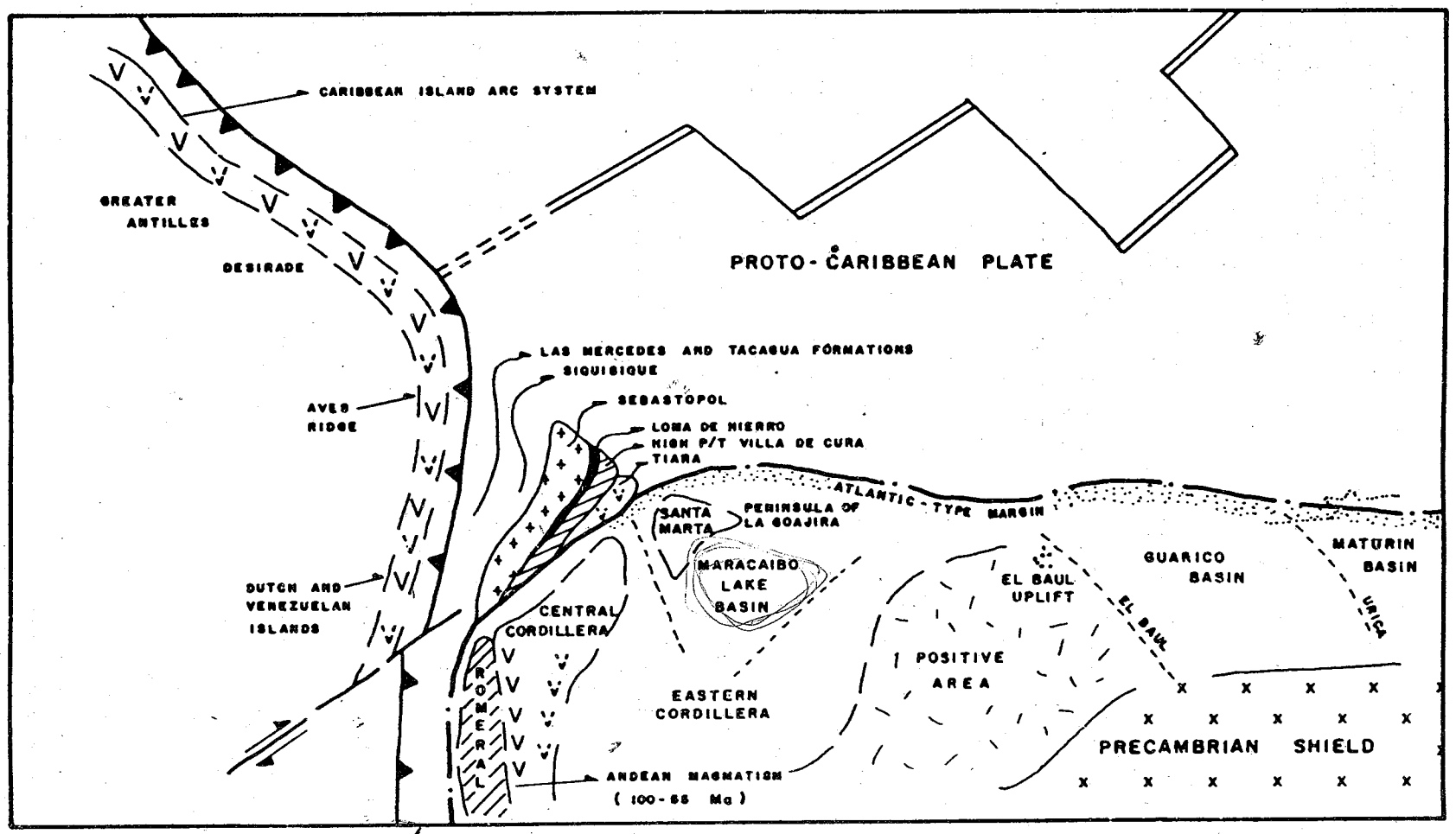

FIGURE 8.5: LATE ALBIAN (≈ 100 Ma) RECONSTRUCTION OF NORTHERN SOUTH AMERICA

is uncertain. The Andean-type boundary is still present in the Late Albian. This migration also occurred in the Andean plutonism, which moved from the eastern to the western flank of the Central Cordillera of Colombia (Toussaint and Restrepo, 1982; Apsden and McCourt, 1986).

During this time span, deposition of euxinic (Las Mercedes) and volcaniclastic (Tacagua Formation) continued. The northwestern corner of South America (Sebastopol block, Loma de Hierro, Villa de Cura, Tiara, and the northern part of the Central Cordillera of Colombia) was uplifted and became the source of sediments for the Santa Marta, Peninsula de la Goajira, and the Maracaibo Lake basin. The primitive Caribbean island arc system developed upon the older Proto-Caribbean arc and on older oceanic crust (Dutch islands). The high P/low T metamorphism of the oceanic rocks of the Cordillera de la Costa-Margarita terrane and Carúpano basin occurred in the accreationary wedge of the Caribbean island arc system.

Santonian to Early Eocene

During the Santonian-Campanian (~85 Ma) the mid-oceanic ridge between North and South America became extinct, the Proto-Caribbean plate reached its maximum size (Pindell *et al.*, 1988; Ross and Scotese, 1988), and the primitive Caribbean island arc was well developed upon the Proto-Caribbean island arc (Dutch Leeward and Venezuelan islands, Aves ridge, and the Greater Antilles). At this time, the southernmost part of the Caribbean island arc system collided against the Sebastopol block (Figure 8.6). As a result of the collision and subsequent northeast migration of the Caribbean until the Early Eocene, the following geologic events occurred: (a) Las Mercedes and Tacagua formations were metamorphosed under intermediate P/T greenschist facies conditions, (b) the calc-alkaline magmatism in the Caribbean island arc system becomes progresively extinct from west to east; the last calc-alkaline magmas intruded in the easternmost high P/low T metamorphic rocks of the plate boundary (Margarita Island and Carúpano basin), (c) the northernmost terranes (Dutch and Venezuelan islands, Venezuelan platform, Cordillera de la Costa-Margarita terrane, and Cordillera de la Costa belt) were thrust southward, (d) a regressive cycle began in the Maracaibo basin in the Santonian-Campanian, while in the eastern Guarico and Maturin basins, the major Cretaceous transgressive cycle continued until the Maastrichtian, and (e) the northwestern corner of South America was affected by transpression.

During its northeastward migration the Caribbean plate was

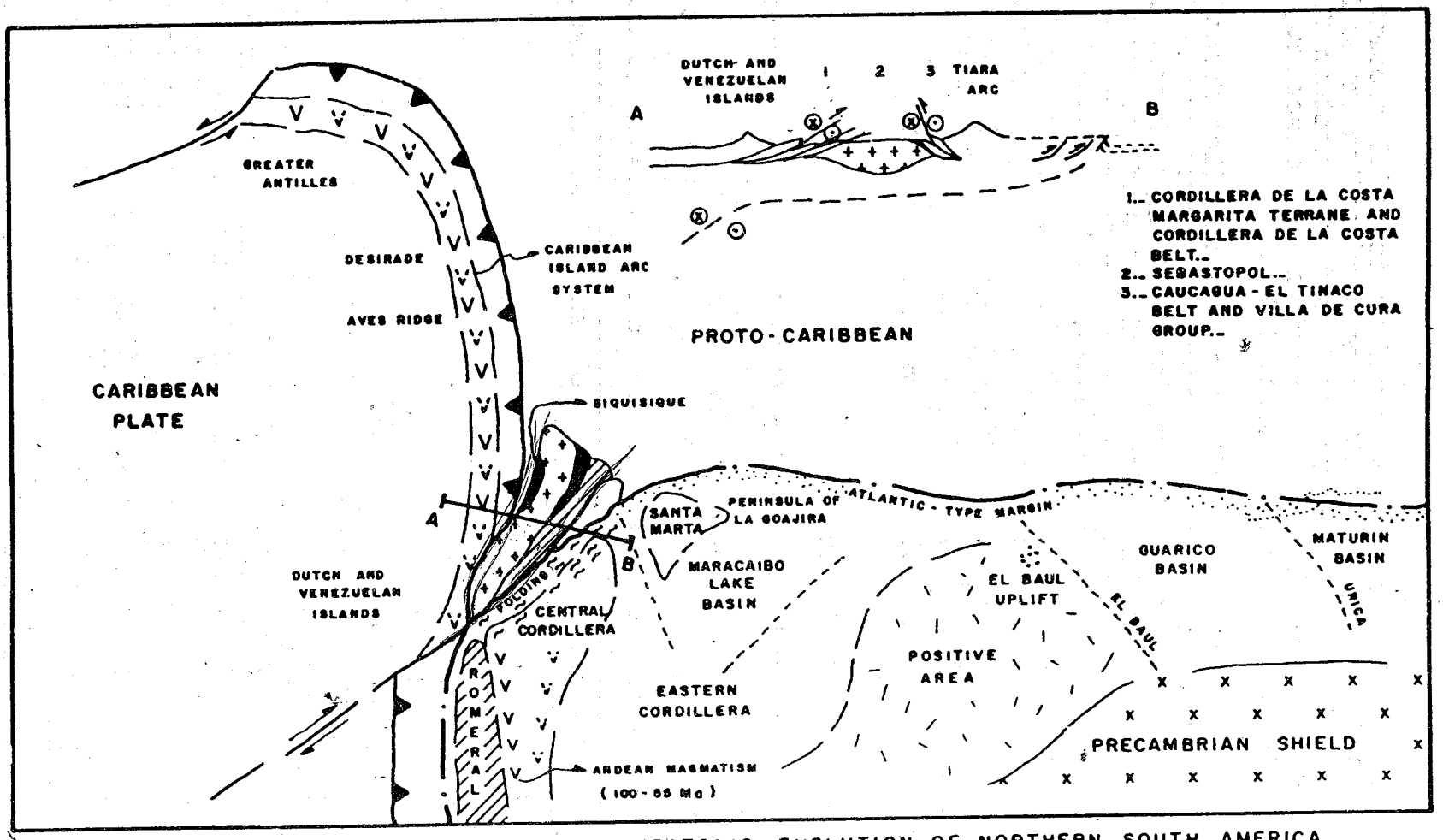

FIGURE 8.6 : SANTONIAN TO EARLY EOCENE TECTONIC EVOLUTION OF NORTHERN SOUTH AMERICA

affected by the back arc arc spreading resulting in the formation of the Grenada Basin in the Paleocene. The Aves Ridge is the inactive remnant part of the arc system (Pinet *et al.*, 1985).

Middle-Late Eocene (~40 Ma)

During the Tertiary the Greater Antilles collided with the Bahamas. The age of collision is controversial; Burke *et al.* (1984) and Pindell and Dewey (1982) proposed an Early Eocene age (53 Ma), Duncan and Hargraves (1984) and Ghosh *et al.* (1984) suggested a Late Eocene age (38 and 36 Ma respectively), and Mattson (1984) proposed a Late Cretaceous-Paleocene age (66 Ma). After the collision the Caribbean plate moved in an easterly direction. This caused a clockwise rotation of the transpressional terrane of Venezuela (Figure 8.7). The postmetamorphic east-northeast trending folds and south vergent thrust faults in northeastern Venezuela (Avé Lallemant, 1989) and the southwest-northeast fold axes and extensional structures on Margarita (Guth and Avé Lallemant, 1989) are consistent with eastward migration of the Lesser Antilles volcanic arc along northern South America.

At the same time the relative motion of South America with respect to North America changed to convergence (Pindell *et al.*, 1988), which may have increased the northwest-southeast compression in the northern South American margin. The major Eocene compressional event in northern Venezuela has been widely recognized in the Piemontine zone (Bell, 1968; Beck, 1978, 1985; Stephan *et al.*, 1980).

The eastward migration of the transpressional terranes along northern South America caused the diachronous development of perisutural flysch deposits (Figure 8.7), from the Paleocene-Eocene deposits in the west (Matatere Formation) to Eocene in the east (Guarico Formation). Episutural basins were locally developed on the transpressional terrane, such as in the Triste Gulf, Margarita, and Tuy-Cariaco basin.

The available data from the South American platform and islands (Dutch and Venezuelan islands, La Vela Gulf, Triste Gulf) and from the mainland (Caucagua-El Tinaco Belt, Villa de Cura Belt) indicate that the transpressional terrane was uplifted, as well as the sub-Andean basin (Barinas basin), the Maracaibo Lake basin, and the southermost part of the Guarico and Maturin basins (Figure 8.7).

Late Oligocene (28 Ma)

During the Oligocene the Falcón, Bonaire, and the Baja

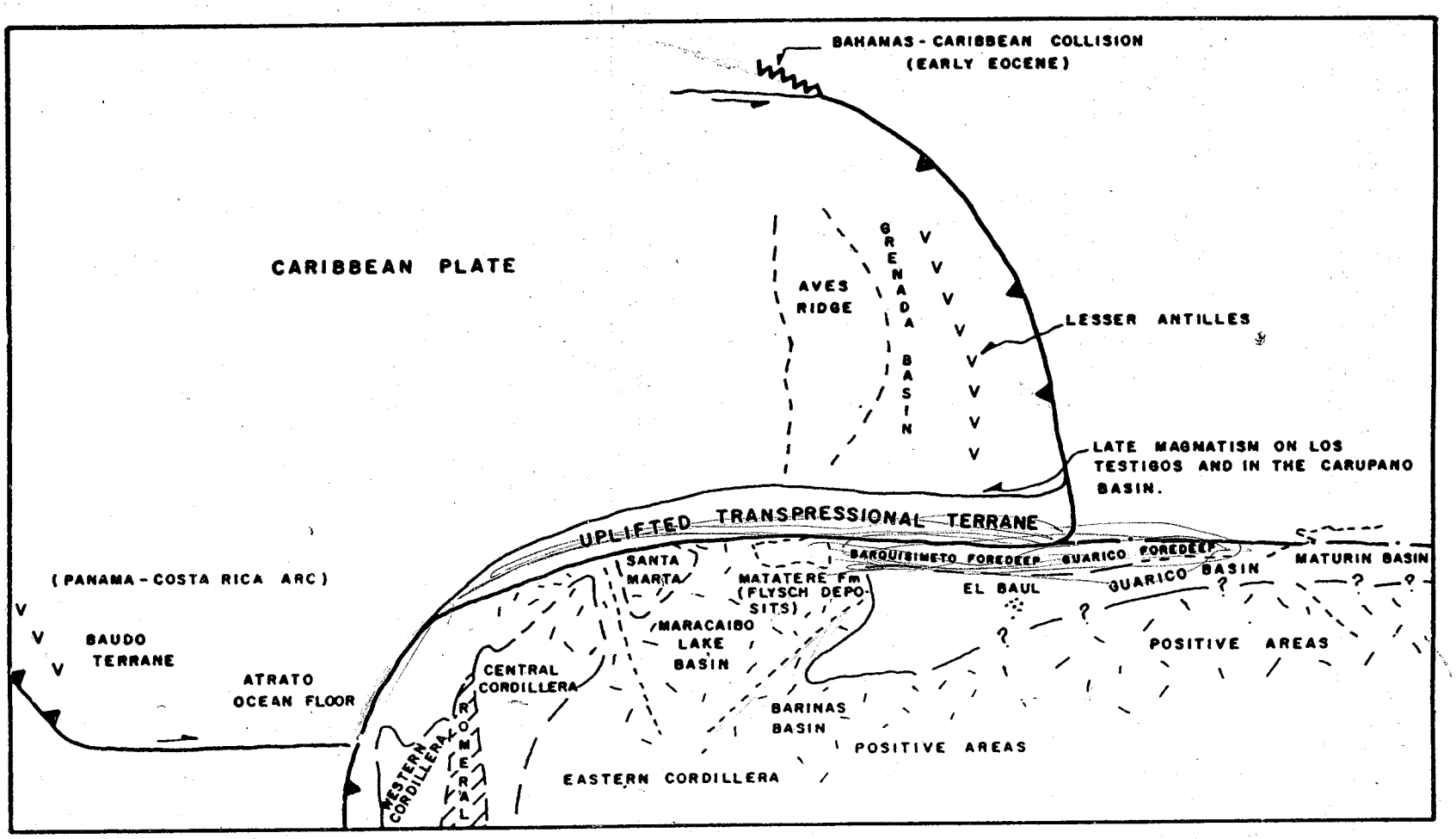

FIGURE 8.7 : MIDDLE - LATE EOCENE (40 Ma) RECONSTRUCTION OF NORTHERN SOUTH AMERICA.

Goajira pull-apart basins developed as a result of right-lateral strike-slip faulting along northern South America. The Siquisique ophiolite, south of the Falcon basin was thrust southward before the development of the pull-apart basins (Figure 8.8). The Oca right-lateral strike-slip fault may have caused the offset of the Peninsula of La Goajira, although it was inactive during the Oligocene. The Maracaibo-Santa Marta block started to move northward along the Bocono megashear (Late Oligocene-Early Miocene), related to the Andean-type subduction boundary in western South America, resulting in the development of the South Caribbean deformed belt (Case *et al.*, 1984).

The transpressional terrane continued to move eastward in a wide strike-slip fault zone (Figure 8.8). The central axis of magmatism in western South America migrated from the western flank of the Western Cordillera of Colombia to the Central Cordillera of Colombia. Locally, the Mérida Andes and Sierra de Perijá were uplifted, which may be related to the northwest-southeast convergence of North and South America. Sedimentation in northern South America became restricted. In the Guarico Basin only continental or shallow marine sediments were deposited. Sedimentation on the Maracaibo-Santa Marta block occurred only locally during the Oligocene, while toward the north in the Peninsula of la Goajira and the Gulf of Venezuelan, an Oligocene-Pliocene transgressive cycle was initiated.

Late Miocene-Present

The northward migration of the Maracaibo-Santa Marta block, which started in the Late Oligocene-Early Miocene, was enhanced in the Miocene and subsequently, as a consequence of collision of the Baudo (Panama-Costa Rica) arc with the west coast of South America along the Atrato suture (Figure 8.9). The South Caribbean deformed belt continued to be active as shown by the deformation of the Neogene sediments and the seismic activity along the Bocono, Santa Marta, and San Sebastian faults, while the eastward tectonic transport of the tranpressional terrane along the plate boundary continued (Figure 8.9).

The eastern termination of the South Caribbean deformed belt is along the Orchila basin (Figure 8.9), which is bordered by north-northwest trending fault systems having both normal and strike-slip components of motion (Case *et al.*, 1984). Some east-west trending faults in the Maracaibo-Santa Marta block, previously developed as strike-slip faults, were reactivated as reverse faults (Figure 11 in Biju-Duval *et al.*, 1983) as a result of the northward migration of the Maracaibo-Santa Marta block.

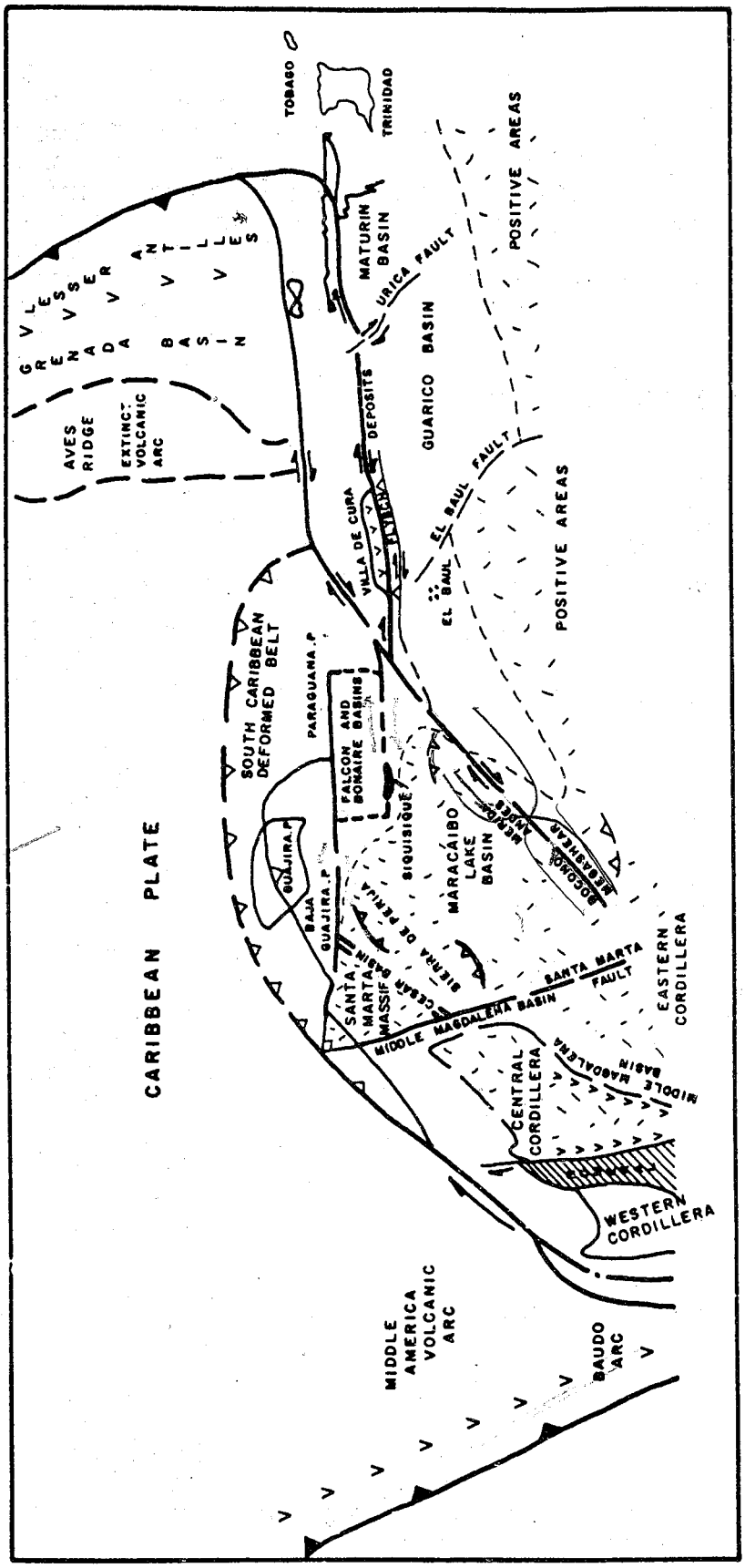

FIGURE 8.8 : LATE OLIGOCENE RECONSTRUCTION OF NORTHERN SOUTH AMERICA.

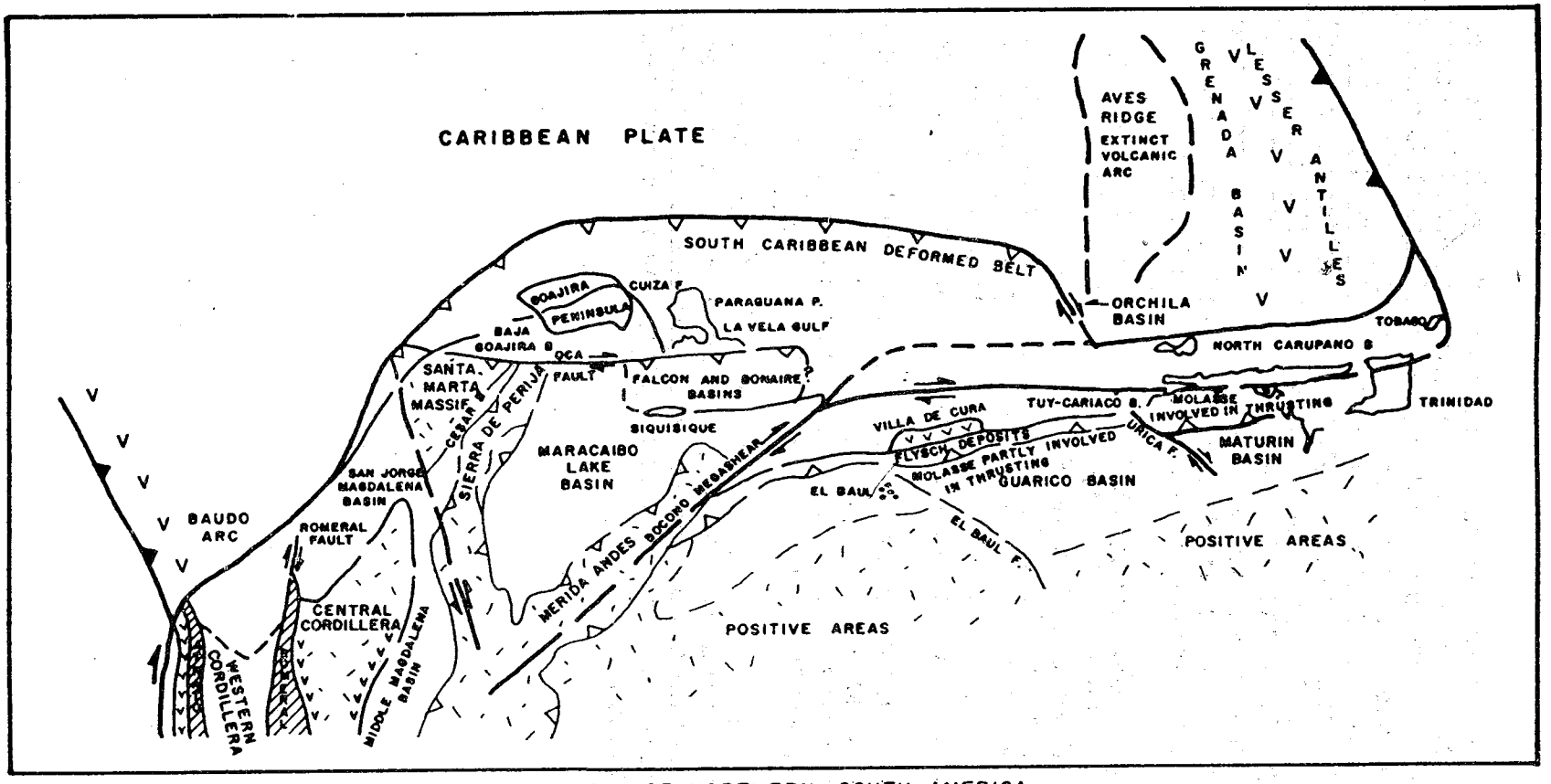

FIGURE 8.9 : LATE MIOCENE RECONSTRUCTION OF NORTHERN SOUTH AMERICA.

: Evidencias de los corrimientos en ambos lados de la cordillera de la Costa. Tomado de (Tesis de Marino ostos).

The Caribbean Mountains system on the mainland continued to be uplifted and the deformation was mostly restricted to faulting. There are Quaternary pull-apart basins (Schubert, 1984) related to east-west trending right-lateral faults, such as the La Victoria and El Avila faults, but there are also pull-apart basins related to northwest trending faults such as the Tacagua fault, which is still seismically active today (Rial, 1978). In the Guarico and Maturin basins, south of the uplifted Araya-Paria terrane, molasse becomes progresively deposited and deformed from west to east, in the Eastern Venezuelan fold and thrust belt.

The Falcòn and Maracaibo basins were invaded by the seas. There is a record of a transgressive cycle in the La Goajira basin. However, the Gulf of La Vela and the Triste Gulf basins were uplifted (Table 8.11) in the Late Miocene, which may be related to reactivation of east-west strike-slip faults or to north-south to northeast-southwest trending strike-slip faults, conjugate to the Bocono megashear.

The well data of northeastern Venezuela (Tuy-Cariaco and Carùpano basins) and the stratigraphy of Margarita suggest that a Miocene transgression occurred north of the Caribbean Mountains system, which was already uplifted.

The tectonic evolution of the southern Caribbean plate boundary during the Pliocene-Quaternary is characterized by the continuous northward and eastward migration of the Maracaibo-Santa Marta block and the transpressional terrane, respectively.

SUMMARY AND CONCLUSIONS

Geologically, north-central South America consists from north to south of the following east-west trending tectonostratigraphic belts: Dutch and Venezuelan islands, the Venezuelan platform, and the Caribbean Mountains system. The Caribbean Mountains system can be divided into the following belts from north to south: Cordillera de la Costa-Margarita terrane, Cordillera de la Costa belt, Caucagua-El Tinaco belt, Paracotos belt, and Villa de Cura belt. These tectonostratigraphic belts have characteristic structural, petrologic, sedimentologic, and geochronologic features, which were analyzed to test the tectonic evolution of the south-central Caribbean.

Tectonic belts

The Dutch and Venezuelan islands terrane consists of Lower to mid Cretaceous oceanic rocks and Upper Cretaceous island arc volcanics. This terrane has been correlated with the lithologic units of the Villa de Cura belt in the mainland and with the Venezuelan platform in northeastern Venezuela. The Caribbean Mountains system on the mainland consists of five tectonostratigraphic belts with three major east-west trending faults, separating the four southernmost belts. The Cordillera de la Costa-Margarita terrane consists of rocks which underwent high P/low T metamorphism overprinted by an intermediate P/T metamorphism. The Cordillera de la Costa belt consists of a Precambrian granitic basement and a Mesozoic metasedimentary cover, which underwent only the second intermediate P/T metamorphism. The Caucagua-El Tinaco belt consists of a Paleozoic metamorphic basement overlain by Permian metasediments mixed with alkalic non-orogenic metavolcanics and Cretaceous metasediments and metavolcanics. The basement underwent low P/T metamorphism in the amphibolite facies, while the Permian and Cretaceous sequences have undergone greenschist facies metamorphism.

The Paracotos belt consists of Campanian-Maastrichtian flysch and wildflysch deposits, serpentinite slices, and dismembered ophiolites. Locally, this belt underwent very-low grade metamorphism. The Villa de Cura belt consists of metasedimentary (mostly volcaniclastic) and metavolcanic rocks of the Villa de Cura Group, island arc volcanics, and mafic-ultramafic plutonic complexes. The Villa de Cura belt underwent locally high P/low T metamorphism overprinted by intermediate P/T metamorphism.

Isotopic ages

Most isotopic ages in northern South America are related to the orogeny that affected the Caribbean-South America plate boundary. They may be correlated with the following tectonic events: (a) Jurassic rifting event, (b) Early to Late Cretaceous metamorphic event, (c) Late Cretaceous uplift, and (d) Tertiary uplift.

Fossil ages

Fossils are scarse along the south-central Caribbean, because of tectonic disruption and recrystallization. However, based on the fossil data available, the following constraints exist: (a) Jurassic and Neocomian fossils are found in marbles on the Peninsula of Paraguana, in the Siquisique ophiolite, and in the Cordillera de la Costa belt. These ages are the oldest Mesozoic ages in northern Venezuela and they constrain the opening of the Proto-Caribbean, (b) Turonian and Albian fossils are found in the MORB sequences of Aruba and Curacao, while Albian to Coniacian fossils are found in the primitive island arc sequences of Bonaire. They indicate that a volcanic island arc was being formed while rifting was still in progress, (c) Permian, Albian, and undifferentiated Upper Cretaceous fossils were reported in the sediments of the Caucagua-El Tinaco belt, (d) the metamorphosed flysch deposits of the Paracotos Formation contain Upper Cretaceous and Upper Cretaceous-Paleogene fossils. They indicate sedimentation associated with a deep sea trench, a forearc basin, or an episutural basin related to transpressional terranes, and (e) Aptian-Albian shallow water fossils have been described in the Villa de Cura belt. The belt may thus be correlated with the ocean-floor sequences of the Dutch islands. However, the origin of the fossils in the Villa de Cura rocks is suspect. The fossils may have been collected from another unit or they may have been inserted tectonically into the Villa de Cura. Furthermore, the Villa de Cura ocean floor appears to be older (radiometrically) than that in the Dutch islands and thus, it may be correlated with the Romeral ophiolite in Colombia and with the ocean floor rocks of Los Monjes and Los Roques.

Uncomformities

Based on the age of the basement dated by radiometric methods and the sedimentary age of the cover rocks, several hiatuses and unconformities have been identified in the south-central Caribbean, which are important indicators of

tectonic events. In the Dutch and Venezuelan islands, such an uncomformity may be related to the collision of the Caribbean and South American plates. It seems that the collision in the western islands began earlier than in the eastern part of the Dutch and Venezuelan islands. In the Venezuelan platform (Gulf of La Vela and Triste Gulf) the uncomformities may be related to the Upper Cretaceous-Eocene collisional boundary and the development of the Oligocene pull-apart basins, and the Miocene northward migration of the Maracaibo-Santa Marta block.

The Carúpano basin in the eastern Venezuelan shows a Paleocene to Oligocene hiatus in the southeast while the uncomformity in wells to the northwest are Oligocene in age.

In the Tuy-Cariaco basin Late Cretaceous-Paleocene and Oligocene-Early Miocene uncomformities occur. These two uncomformities may be related to collision and the subsequent development of episutural flysch basins. A Miocene uncomformity may indicate the generation of pull-apart basins in the collisional boundary zone. The Eastern Venezuela basin (Guarico and Maturin basins) shows a west to east diachronism in the sedimentation of the Miocene and Pliocene molasses. The uncomformities in the Cordillera de la Costa-Margarita terrane are well exposed on Margarita island. Late Cretaceous-Early Eocene and Late Eocene-Middle Miocene uncomformities can be correlated with the collision and the Late Miocene generation of pull-apart basins in the collisional boundary.

The Caribbean Mountains system on the mainland shows a Late Cretaceous-Pliocene to Pleistocene uncomformity, which can be related to uplift and the Neogene development of pull-apart basins in the collisional terrane.

Tectonic affinity of igneous rocks

The tectonic setting of several igneous complexes in the south-central Caribbean was determined by discrimination diagrams of the most immobile major elements, the transition elements of the iron group (Cr and Ni), the high-charge imcompatible elements (Zr, Y, Nb, and some of the rare earth elements), and the elements of low ionic potential (e.g. Rb). On the basis of geochemical data previously published and those obtained in the present study a regional framework can be constructed for the south-central Caribbean: (a) Precambrian intra-plate granites and Paleozoic calc-alkaline granites occur in the Cordillera de la Costa and Caugagua-El Tinaco belts, (b) Paleozoic volcanic arc tholeiites and MORB's occur in the Caucagua-El Tinaco belt, (c) Late

Jurassic anorogenic tholeiites extruded in the Venezuelan LLanos basin (Espino Graben), which may be related to the opening of the Caribbean or to back-arc extension behind the Andes subduction zone, (d) ophiolitic complexes in the Paracotos and Cordillera de la Costa belts and Cordillera de la Costa-Margarita terrane are undated, but probably Mesozoic, (e) The Siquisique ophiolite is of Middle Jurassic age, (f) the Late Jurassic to Early Cretaceous basalts of Los Monjes, Aruba, Curacao, Los Roques, Carůpano basin, and Margarita are MORB's, (g) the Villa de Cura belt consists of Lower Cretaceous (?) mid-oceanic ridge or marginal basin basalts, (h) Late Cretaceous island arc activity occurred on the islands Aruba, Bonaire, Los Roques, La Blanquilla, Los Hermanos, Los Frailes, and Margarita, in the Carůpano and Tuy-Cariaco basins, and in the Villa de Cura belt, and (i) Late Eocene volcanic island activity occurred in the northernmost part of the Carůpano basin and on Los Testigos island.

Regional metamorphism

The conditions of regional metamorphism in the tectonic belts of the south-central Caribbean are based on mineral assemblages and textural relationships between mineral phases. In summary, the following constraints have been derived: (a) granulite facies metamorphism may have occurred in the basement of the Caucagua-El Tinaco belt in the Permian, (b) Upper Jurassic to Lower Cretaceous seafloor was metamorphosed in a subduction complex during the late Early or early Late Cretaceous at conditions of the prehnite-pumpellyite, zeolite, eclogite, and blueschist facies. These metamorphic rocks are found on the Dutch and Venezuelan islands (Curacao), in the Venezuelan platform (Carůpano basin), in the Cordillera de la Costa-Margarita terrane, and in the Paracotos and Villa de Cura belts, (c) a Late Cretaceous intermediate P/T metamorphic event occurred in the volcanic island arc of the Dutch and Venezuelan islands (Aruba, Bonaire, Los Roques, Los Hermanos, Los Testigos, and Los Monjes), in the Venezuelan platform (Tuy-Cariaco and Carůpano basins), in the Cordillera de la Costa-Margarita terrane, and in the Villa de Cura belt. The metamorphic event is characterized by prehnite-pumpellyite, greenschist, and epidote amphibolite assemblages, and (d) an intermediate to low P/T metamorphism (greenschist, epidote amphibolite, and amphibolite facies) occurred in the Cordillera de la Costa and Caucagua-El Tinaco belts during the Late Cretaceous.

Structural Geology

The belts of the Caribbean Mountains system have been deformed severely. Four phases of folding were recognized. The first two were only found in the Caucagua-El Tinaco belt, may be related to Permian orogenesis. The Cordillera de la Costa basement must also have been deformed in pre-Cretaceous time, but the structures are obscured by later deformation. The third and fourth phases of folding were recognized in all the belts. Both the third and the fourth folding events may have taken place during the Late Cretaceous-Tertiary orogenic event.

Three generations of faults were recognized. East-west trending dextral strike-slip and thrust faults and northwest-southeast trending dextral strike-slip faults are thought to be related to the fourth phase of folding. East-west trending normal faults are interpreted to have formed later and are still active.

Kinematic indicators suggest south directed shear on the foliation planes related to the third folding event in the Cordillera de la Costa-Margarita terrane and in the Cordillera de la Costa belt and north directed shear in the Caucagua-El Tinaco, Paracotos, and Villa de Cura belts. Both show a component of dextral slip. Therefore, if the kinematic indicators were developed during the Late Cretaceous-Tertiary orogeny, the entire Caribbean Mountains sytem underwent dextral shear parallel to the belts.

Sedimentary basins in northern South America

The history of the sedimentary basins of northern South America can also contrain the tectonic evolution of the plate boundary. The basins can be divided into passive Atlantic-type and episutural basins. The following inferences can be made: (a). Until Late Cretaceous time, the sediments were deposited in basins on the passive Atlantic-type South American continental margin. The pre-Santonian sedimentary facies is everywhere the same suggesting that there existed only one large Atlantic-type basin, but in the Santonian this large basin may have been divided into two separate basins. (b). In Late Cretaceous-Paleogene time sedimentation in the southern parts of the Atlantic-type basins continued, but in the north the Maracaibo basin became a foreland basin (perisutural). (c). During the Late Cretaceous, flysch basins developed north of the Atlantic-type and perisutural basins. They occur on the Dutch and Venezuelan islands (Curacao and Bonaire) and in the Venezuelan platform (Carúpano basin). These basins may

be associated with a deep sea trench or a forearc basin, and related to a Late Cretaceous convergent boundary along northern South America. (d). Eocene volcanigenic sediments are recognized east of the Maracaibo-Santa Marta block, in the Venezuelan platform (Carúpano basin and Triste Gulf) and in the Cordillera de la Costa-Margarita terrane on Margarita. They may be related to a Tertiary convergent boundary along northern South America. (e). Oligocene east-west trending pull-apart basins developed in the western part of the Caribbean-South America plate boundary, and (f). Miocene and Pliocene to Quaternary east-west trending episutural pull-apart basins formed in the central and western parts of the plate boundary (Venezuelan platform and Caribbean Mountains system).

Plate Tectonic model

On the basis of the available geological data, a plate tectonic model is proposed. The model tries to accomodate all the features discussed above. In the model the east-west trending belts of northern South America are allochthonous and deformed as a result of collision of a microcontinent and an island arc against west-northwest South America during the Neocomian. The belts were initially coupled to the overriding South American plate, but because of the large obliquity were transported northeasterly in a transpressional terrane. The tectonic transport occurred since the Santonian-Campanian, after the collision of the Caribbean plateau and the generation of a west-dipping subduction zone in the eastern boundary of the Caribbean plate.

The northeasterly motion of the terranes and of the Caribbean plate changed to an easterly direction after the collision of the Greater Antilles island arc with the Bahamas in the Late Eocene. The change of transport direction was manifested by northwest-southeast compression in northern South America and the development of Oligocene east-west trending pull-apart basins.

In the Late Oligocene northward migration of the Maracaibo-Santa Marta block was initiated and it continues to do so today. The migration was enhanced in the Miocene by the collision of the Panama-Costa Rica arc. The northward migration of the Maracaibo-Santa Marta block is causing the development of the South Caribbean deformed belt. The plate boundary east of the South Caribbean deformed belt has been characterized by dextral strike-slip tectonics.

REFERENCES

Abbey, S. (1977) Studies in "Standard Samples" for use in the general analysis of silicate rocks and minerals. Part 5: 1977 Edition of "Usable" values. *Geological Survey of Canada Paper* 77-34; 31p.

Aguerrevere, S.E. and Zuloaga, G. (1938) Nomenclatura de las formaciones de la parte central de la Cordillera de la Costa. *Bol. Geol. y Minas, Caracas*, 2(2-4): 281-284.

Alvarez, W. (1967) Geology of the Siruma and Carpintero areas, Guajira Peninsula, Colombia. *Ph.D. Thesis, Princenton University, USA*,168 p.

Anderson, T. H. and Schmidt, V. A. (1983) The evolution of Middle America and the Gulf of Mexico-Caribbean Sea region during Mesozoic time. *Geol. Soc. Amer. Bull.* 94: 941-966.

Apted, M. J. and Liou, J. G. (1983) Phase relations among greenschist, epidote-amphibolite, and amphibolite in a basaltic system. *American Journal of Science, Vol.* 283-A: 328-354.

Aspden, J.A. and McCourt, W.J. (1986) Mesozoic oceanic terrane in the central Andes of Colombia. *Geology, Vol.* 14: 415-418.

Audemard, F. (1985) Neotectónica de la Cuenca del Tuy. *Memoria VI Cong. Geol. Venezolano,* Caracas, *Noviembre* 1985, *Tomo* III: 2339-2377.

Avé Lallemant, H.G. and Oldow, J.S. (1988) Early Mesozoic southward migration of Cordilleran transpressional terranes. *Tectonics*, 7(5): 1057-1075.

,, (1989) The Caribbean South America plate boundary in the Caribbean Mountains Province, Eastern Venezuela. *Abstracs of the Twelfth Caribbean Geological Conference, St. Croix.*

,, and Guth, L.R. (1990) Blueschists, eclogites, oblique subduction, and extensional tectonics in northeastern Venezuela. *Geology*. In press.

Baker, P.E. (1982) Evolution and classification of orogenic volcanic rocks. In: *Andesite: Orogenic Andesites and Related Rocks. Thorpe, R.S.* editor, *John*

Wiley & Sons, New York:11-24.

Bally, A.W. and Snelson, S. (1980) Realms of subsidence in facts and principles of world petroleum ocurrence. *Canadian. Soc. Petrol. Geol., Memoir* 6: 9-94.

Banno, S. (1986) The high-pressure metamorphic belts of Japan: A Review. *In Blueschist and Eclogites. Geol. Soc. of Am. Memoir* 164: 365-374.

Barrero, D. (1977) Geology of the Central Western Cordillera west of Buga and Roldanillo, Colombia. *Colorado School of Mines, Publ. Geol. Espec.* 4 (75).

Bartok, P.E., Renz, O., and Westermann, G.E.G. (1985) The Siquisique Ophiolite, Northern Lara State, Venezuela: A discussion on their Middle Jurassic ammonites and tectonic implications. *Geol. Soc. Amer. Bull.*, 96: 1050-1055.

Basaltic Volcanism Study Project (1981) *Basaltic Volcanism on the Terrestrial Planets. Pergammon Press, New York.* 1286 p.

Beccaluva, L., Ohnenstetter, D., and Ohnenstetter, M. (1979) Geochemical discrimination between ocean-floor and island arc tholeiites: application to some ophiolites. *Canadian Journal of Earth Sciences,* 16: 1874-1882.

Beck, C. (1977) El subestrato Cretàceo de la Faja Piemontina en la parte central de la Serrania del Interior en Venezuela Septentrional. Relaciones con la tectogénesis del Cretàceo Superior. *VIII Conf.Geol. Caribe , Curacao, Julio 1977, Resumenes*; 8-9.

,, (1978) Polyphasic Tertiary tectonics of the Interior Range in the Central part of Western Caribbean Chain, Guarico State, Northern Venezuela. *Geologie en Mijnbouw, vol.* 57 (2): 99-104

,, (1985) Caribbean colliding, Andean drifting and the Mesozoic-Cenozoic evolution of the Caribbean. *VI Cong. Geol. Venezolano. Tomo* X: 6575-6614.

,, (1985b) La Chaine Caraibe au meridien de Caracas: Geologie, tectogenese, place dans l'evolution geodynamique Mesozoique-Cenozoique des Caraibes meridionales. *Theses de Doctorat D'etat és*

Sciences Naturelles. L'Universite des Sciences et Techniques de Lille, France. 462 p.

,, (1986) Géologie de la Chaine Caraibe au meridien de Caracas (Venezuela). *Société Géologique du Nord.* Publication 14: 462 p.

Beckinsale, R.D. (1979) Granite magmatism in the tin belt of South-East Asia. *In: Origin of Granite Batholiths: Geochemical Evidences.* M.P. Atherton & J. Tarney *Editors. Orpington, Kent: Shiva Publishing Ltd*: 34-44.

Beets, D. J. (1972) Lithology and Stratigraphy of the Cretaceous and Danian sucessions of Curacao. *Publ. of Natuurwet. Studierkring Sur and Netherland Antilles*, 70: 135 p.

,, (1977) Cretaceous and Early Tertiary of Curacao. *Guide to Field Excursions in the 8th Caribbean Geological Conference, GUA Papers of Geology, Amsterdam,* 10: 7-17.

,, Klaver, G. Th., and Mac Gillavry, H.J. (1977) Geology of the Cretaceous and Early Tertiary of Bonaire. *Guide to the Field Excursions in the 8th Caribbean Geological Conference, GUA Papers of Geology, Amsterdam,* 10: 18-28. ,, Maresch, W., Klaver, G. Th., Mottana, A., Bocchio, R., Beunk, F., and Monen, H. (1984) Magmatic rock series and high-pressure metamorphism and constraints on the tectonic history of the Southern Caribbean. The Caribbean South America plate boundary and regional tectonics. *Geol. Soc. Amer. Memmoir* 162, *Bonini, W.E., Hargraves, R.B., and Shagam, R.* editors: 95-130.

Bell, J. S (1968) Geologia del Area de Camatagua, Estado Aragua, Venezuela. *Bol. Geol., Caracas.*9 (18): 291-440.

,, (1972) Tectonic evolution of the central part of the Venezuelan Coast Ranges. *Geol. Soc. Amer. Memoir* 130: 107-118.

Bellizia, A. (1967) Rocas Ultrabásicas en el Sistema Montañoso del Caribe y yacimientos minerales asociados. *Bol. Geol., Caracas,* 8 (16): 160-193. ,, and Rodriguez G., D. (1968) Consideraciones sobre la estratigrafia de los Estados Lara, Yaracuy, Cojedes, y Carabobo. *Bol. Geol., Caracas,*

9 (18): 515-563.

,, Carmona, C., and Graterol, M. (1969) Reconocimiento geolòǵico de las islas Los Monjes del sur, Archipiélago de los Monjes, Venezuela. *Bol. Geol., Caracas.* 10(20): 225-234.

,, (1972) Sistema Montañoso del Caribe, borde sur de la placa Caribe, es una cordillera alòctona?. *Memorias VI Conf. Geol. Caribe, Porlamar* 1971: 247-258.

,, Rodriguez G, D., and Graterol, M. (1972) Ofiolitas de Siquisique y Rio Tocuyo y sus relaciones con la Falla de Oca. *Memorias VI Conf. Geol. Caribe, Porlamar* 1971: 182-183.

,, and Rodriguez G.,D. (1976) Geologia del Estado Yaracuy. *Memorias IV Cong. Geol. Venez., Caracas 1969, Bol. Geol., Caracas, Public. Esp. 5 (VI)*: 3317-3417.

,, Perez, H., and Graterol, M. (1976) Reconocimiento geolòǵico del Archipielago de Los Monjes. *Memorias II Cong. Geol. Latinoamericano, Caracas* 1973, *Bol. Geol. Publ. Esp.* 7 (II): 509-516.

,, and Pimentel, N. (1976) Mapa Geolòǵico estructural de Venezuela a escala 1:500.000, y tablas de Correlaciones Estratigràficas. *Min. Energia y Minas, Direcciòn de Geologia, Caracas.*

,, (1985) Sistema Montañoso del Caribe- Una Cordillera Aloctona en la parte norte de America del Sur. *Memorias VI Cong. Geol. Ven., Caracas* 1985, *Tomo* X: 6657-6836.

Benjamini, C., Shagam, R., and Menendez V., A. (1987) (Late?) Paleozoic age for the "Cretaceous" Tucutunemo Formation, northern Venezuela: Stratigraphy and tectonic implications. *Geology, Vol.* 15: 922-926.

Berthé, D., Choukroune, P., and Jegouzo, P. (1979) Orthogneiss, mylonite and non-coaxial deformation of granites. *Journal of Structural Geology,* 1: 31-42.

Bertrand, A. E. S. and Bertrand, W. G. (1985) Plate Tectonic Evolution of the Southeast Caribbean.

Transactions of the First Geological Conference of the Geological Society of Trinidad and Tobago, Port Spain, Trinidad: 242-260.

Biju-Duval, B., Mascle, A., Montadert, L., and Wannesson, J. (1978) Seismic investigations in the Colombia, Venezuela, and Grenada Basin, and on the Barbados Ridge for future I.P.O.D. drilling. *Geologie en Mijnbouw*, 57: 99-104.

,, Mascle, A., Rosales, H., and Young, G. (1983) Episutural Oligo-Miocene Basins along the North Venezuelan Margin. *Amer. Ass. Petr. Geol. Memoir* 34. J. Watkins and C.L. Drake *Editors*: 347-358.

Blackburn, W.H. and Navarro, E. (1977) Garnet zoning and polimetamorphism in the eclogitic rocks of isla de Margarita, Venezuela. *Canadian Mineralogy*, 15: 257-266.

Bonini, W.E., Hargraves, R.B., and Shagam, R. (1984) The Caribbean-South America Plate Boundary and Regional Tectonics. *Geol. Soc. Am. Memoir* 162, 421 p.

Bourgois, J., Toussaint, J.F., González, H., Orrego, A., Azema, J., Calle, B., Desmet, A., Murcia, A., Pablo, A., Parra, E., and Tournon, J. (1985) Les ophiolites des Andes de Colombie: évolution structurale et signification géodynamique. *Symposium Géodynamique des Caraïbes, Paris, Février* 1985, *Mascle, A.* editor: 475-494.

Bowen, J.M. (1972) estratigrafía del precretáceo en la parte norte de la Sierra de Perijá. *Memoria IV Cong. Geol. Ven., Bol. Geol. Publ. Esp.* 5 (II): 729-761.

Bouysse, .P, Andreieff, P., Richard, M., Baubron, J.C., Mascle, A., Maury, R.C., and Westercamp, D. (1985) Aves Swell and northern Antilles Ridge: rock-dredging from ARCANTE III cruise. *Symposium Geodynamique des Caraibes, Paris, Février* 1985, *Mascle, A.* editor: 35-52.

Brown, E.H. (1977) Phase equilibria among pumpellyite, lawsonite, epidote, and associated minerals in low grade metamorphic rocks. *Contrib. Mineral. Petrol., Vol.* 64: 123-136.

Brown, G.C. (1982) Calc-alkaline intrusive rocks: their

diversity, evolution, and relation to volcanic arcs. In:*Andesites: Orogenic Andesites and Related Rocks, Thorpe, R.S.* editor, *John Wiley & Sons, New York:* 437-464.

Bullard, E. C., Everett, J. E., and Smith, A. H. (1965) The fit of the continents around the Atlantic. *Phil. Trans. Royal. Soc. London*, A1088: 41-51.

Burke, K., Fox, P.J., and Sengor, A.M.C. (1978) Buoyant ocean floor and the evolution of the Caribbean. *Jour. Geophys. Res.*, 83: 3949-3954.

,, Cooper, C., Dewey, J. F, Mann, J.P., and Pindell, J. (1984) Caribbean Tectonics and relative plate motions. *Geol. Soc. Amer. Memoir* 162. W.E.

Bonini, R. B. Hargraves, and R. Shagam *Editors*: 31-64.

,, (1988) Tectonic Evolution of the Caribbean. *Ann. Rev. Earth Planet. Sci.*, 16: 201-230.

Burkley, L.A. (1976) Geochronology of the Central Venezuelan Andes. *Ph.D Thesis. Department Geology, Case Western Reserve University.* USA. 150p.

Cann, J. R. (1970) Rb, Sr, Y, Zr, and Nb in some ocean floor basaltic rocks. *Earth Planet. Sci. Lett.* 10: 7-11.

Capedri, S., Venturelli, G., Bocchio, G., Dostal, J., Garuti, G., and Rossi, A. (1980) The geochemistry and petrogenesis of a ophiolite sequence from Pindos, Greece. *Contrib. Mineral. Petrol.*, 74: 189-200.

Carman, J.H. and Gilbert, M.C. (1983) Experimental studies on glaucophane stability. *American Journal of Science, Vol.* 283-A: 414-437.

Carrillo, M.E. and Vivas, B.C. (1986) Petrologia y Petrogénesis de las rocas felsicas metamorfizadas, de la region norte de la Isla de Margarita. *Trabajo Especial de Grado, UCV (Caracas)*, 92 p.

Case, J.E., Barnes, J., Paris, G., Gonzàlez, H., and Viña, A. (1973) Trans-Andean geophysical profile, southern Colombia. *Geol. Soc. Am. Bull.*, 84(9): 2895-2903.

,, (1975) Geophysical Studies in the Caribbean. *In: The Ocean Basins and Margins*, Vol. 3: *The Gulf of Mexico and the Caribbean*, 107-180, A.E.M. Nairm and F.G. Stehli *Editors, Plenun Press, New York*: 706 p.

,, and Holcombe, T.L. (1980) Geologic-tectonic map of the Caribbean region: Miscellaneous Investigations Series Map I-1100, Scale 2.500.000, *U.S. Geological Surrvey, Reston, Va.*

,, Holcombe, T.L., and Martin, R.G., (1984) Map of Geologic provinces in the Caribbean region. *Geol. Soc. Amer. Memoir* 162, E.E. Bonini, R.B. Hargraves, and R. Shagam *Editors*: 1-30.

Castro, M. and Mederos, A. (1985) Litoestratigrafía de la Cuenca de Carupano. *Memorias VI Cong. Geol. Ven., Caracas, Noviembre* 1985, *Tomo* I: 201-225.

Chachati, B. and Macsotay, O. (1985) Estudio geodinámico y geoquímico de rocas meta-acidas de Paraguachoa, Venezuela nororiental. *Memorias VI Cong. Geol. Ven., Caracas, Noviembre* 1985, *Tomo* II: 1586-1622.

Chappell, B.W. and White, A.J.R. (1974) Two contrasting granite types. *Pacific Geology* 8: 174-174.

Chevalier, Y. (1987) Les Zones internes de la chaine sud-Caraibe sur le transect ile de Margarita-peninsula d'Araya (Venezuela). *Théses de Doctorat de L'Université de Bretagne Occidentale. France.* 464 p.

Choudhuri, A. (1978) Geochemical trends in tholeiite dykes of different ages from Guiana. *Chemical Geology.* 22: 79-85.

Christofferson, E. (1973) Linear magnetic anomalies in the Colombia Basin, Central Caribbean Sea. *Geol. Soc. Am. Bull., Vol.* 84: 3217-3220.

,, (1976) Colombian Basin magnetism and Caribbean plate tectonics.*Geol. Soc. Am. Bull., Vol.*87: 1255-1258.

Closs, M. (1982) Flow melanges: Numerical modeling and geologic constraints on their origin in the Franciscan subduction complex. *Geol. Soc. Am. Bull., Vol* 93: 330-345.

,, (1984) Flow melanges and the structural evolution

of accreationary wedges. *Geol. Soc. Am., Special Paper* 198, *Raymond, L.A. editor:* 71-80.

Coleman, R.G. and Peterman, Z.E. (1975) Ocean Plagiogranite. *Jour. Geophys. Res.*, 80: 1099-1108.

,, (1977) *Ophiolites, Ancient Oceanic Lithosphere?.* Springer-Verlag, New York. 229 p.

,, Lee, D.E., Beatty, L.B., and Brannock, W.W. (1982) Eclogites and eclogites: Their differences and similarities. *Geol. Soc. Am. Bull., Vol.* 76: 483-508.

Collins, W.J., Bearns, S.D., White, A.J.R., and Chappell, B.W. (1982) Nature and origin of A-type granites with particular reference to Southeastern Australia. *Contrib. Miner. Petrol.*, 10: 189-200.

Condie, K.C. (1976) Trace-element geochemistry of Archean greenstone belts. *Earth Planetary Reviews*, 12: 393-417.

,, (1982) *Plate Tectonics and Crustal Evolution.* 2th Edition, Pergamon Press, New York, 310 p.

Crawford, W.A. and Fyfe, W.S. (1965) Lawsonite equilibria. *American Journal of Science.*, 263:262-270.

,, and Keays, R.R. (1978) Cambrian greenstone belts in Victoria: marginal sea-crust slices in the Lachlan fold belt of Southeastern Australia. *Earth Planet. Sci. Letter*, 41: 197-208.

Dall'Agnol, R., Silva B., J., Xafi Da Silva, J.-J., De Medeiros, H., Costi, H.T., and Buenano M., M.J. (1987) granitogenesis in northern Brazilian region: A review. *Revista Brasileira de Geociencias*, 17(4): 382-403.

Dawson, J.B. (1980) *Kimberlites, Minerals and Rocks.* Vol. 15, Springer-Verlag, New York, 252 p.

De Roever, W.P. (1972) Glaucophane problems. *Tschemarks Mineralogische und Petrographische Mitteilungen*, Vol. 18: 64-85.

Dengo, G. (1951) Geologia de la region de Caracas. *Bol. Geol., Caracas*, 1 (1): 39-115.

,, (1953) Geology of the Caracas region, Venezuela.

Geol. Soc. Am. Bull., 64 (1): 7-40.

,, (1962) Tectonic-igneous sequence in Costa Rica: Petrologic Studies. *Geol. Soc. Am., Volume to honor A.F. Buddington:* 133-161.

,, (1983) Mid-America: Tectonic Setting for the Pacific margin from the southern Mexico to northwestern Colombia. *Centro de Estudios Geolôgicos de America Central, Guatemala,* 96 p.

Dewey, J.F. and Bird, J.M. (1970) Mountains belts and the new global tectonics. *Jour. Geophys. Res.*, 75: 2625-2647.

,, (1972) Seismicity and tectonics of western Venezuela. *Bull. Seismol. Soc. Am.*, 62: 1711-1751.

Diaz de Gamero, M.L. (1969) Identificaciòn y significaciòn cronoestratigràfica de los pelecipodos de la Formaciòn Las Brisas. *A.V.G.M.P., Bol. Inform, Caracas.*, 13 (2): 455-464.

Dickinson, W.R. (1970) Interpreting Detrital Modes of and Arkose. *Jour. Sed. Petrol.* 40: 695-707.

Dobretsov, N.L. and Sobolev, N.V. (1984) Glaucophane schists and eclogites in the folded systems of northern Asia. *Ofioliti, Vol.* 9: 401-424.

,, Coleman, R.G., Liou, J.G., and Maruyama, S. (1987) Blueschist belts in Asia and possible periodicity of blueschist facies metamorphism. *Ofioliti, Vol.* 12: 445-424.

Donnelly, T. W. (1973) Circum-Caribbean explosive volcanic activity: evidence from Leg 15 sediments. *In: Initial Reports of the Deep Sea Drilling Project,* 15: 969-988, Edgar, N. T. *et al. Editors, U.S. Goverment Printing Office, Washington,* 1137 p.

,, Melson, W., Kay, R., and Rogers, J.J.W. (1973) Basalts and dolerites of Late Cretaceous age from the Central Caribbean. *In: Initial Reports of the Deep Sea Drilling Project,* 15: 989-1004, Edgar, N.T. *et al. Editors, U.S. Goverment Printing Office, Washington,* 1137 p.

,, and Rogers, J.J.W. (1978) The distribution of igneous rocks throughout the Caribbean. *Geologie en Mijnbouw,* 57(2): 151-162.

,, (1989) Geologic history of the Caribbean and Central America. *Geol. Soc. Am., The Geology of North America, Vol. A (Chapter 11):* 299-321.

Dostal, J., Dupuy, C., and Coulon, C. (1976) Rare-earth elements in high-alumina basaltic rocks from Sardinia. *Chemical Geology,* 18: 251-262.

,, Coulon, C., and Dupuy, C. (1982) Cainozoic andesitic rocks of Sardinia (Italy). In: *Andesites*: Orogenic Andesites and Related Rocks, Thorpe, R.S. *editor. John Wiley & Sons, New York:* 353-370.

Dougan, T.W. (1972) Origen y metamorfismo de los gneises de Imataca y Los Indios, rocas precámbricas de la región de Los Indios-El Pilar, Estado Bolivar, Venezuela. *IV Cong. Geol. Ven., Caracas, Publ. Esp.* 5 (III): 1337-1548.

Drury, M.R. and Humphreys, F.J. (1988) Microstructural shear criteria associated with grain-boundary sliding during ductile deformation. *Journal of Structural Geology,* 10(1): 83-90.

Duncan, R.A. and Hargraves, R.B. (1984) Plate Tectonic evolution of the Caribbean region in the mantle reference frame. *Geol. Soc. Am., Memoir* 162, *Bonini, W.E., Hargraves, R.B., and Shagam, R.* editors. 81-94.

Dupuy,C., Dostal, J., Capedri, S., and Venturelli, G. (1984) Geochemistry and Petrogenesis of Ophiolites from Northern Pindos (Greece). *Bull. Volcanol.,* 47-1: 39-46.

Edgar, N. T., Ewing, J. I., and Hennion, J. (1971) Seismic refraction and reflection in Caribbea Sea. *Am. Assoc. Petrol. Geol. Bull.,* 55 (6): 833-870.

,, Saunders, J. B., Bolli, M. M., Donnelly, T. W., Hay, W. W., Maurasse, F., Perez Nieto, H., Premoli Silva, I., Riedel, W. R., and Schneiderman, N. (1973) Site 147. *In: Initial Reports of the Deep Sea Drilling Project,* 15: 169-215, Edgar, N. T. *et al. Editors, U.S. Goverment Printing Office, Washington,* 1137 p.

Epp, D., Grim, P., and Langreth, M.G.Jr. (1970) Heat flow in the Caribbean and Gulf of Mexico. *Jour. Geophys. Res.,* 75 (29): 5155-5169.

Erickson, A.J, Helsley, C.E., and Simmons, G. (1972) Heat flow and continuous seismic profiles in the Cayman Trough and Yucatan Basin. *Geol. Soc. Am. Bull.*, 83: 1241-1260.

Erlank, A.J. and Kable, E.J.D. (1976) The significance of incompatible elements in Mid-Atlantic Ridge basalts 45° N with particular reference to Zr/Nb. *Contrib. Mineral. Petrol.*, 54: 281-291.

Ernst, W.G., Seki, Y., Onuki, H., and Gilbert, M.C. (1970) Comparative study of low-grade metamorphism in the California Coast Ranges and the Outer Metamorphic Belt of Japan. *Geol. Soc. Am., Memoir* 124: 276 p.

,, (1976) Mineral chemistry of eclogites and related rocks from the Voltri Group, western Liguria, Italy. *Schweizerische Mineralogische und Petrographische Mitteilungen, Vol.* 56: 293-343.

,, (1979) Coexisting sodic and calcic amphiboles from high-pressure metamorphic belts and the stability of barroisitic amphibole. *Mineralogical Magazine, Vol.* 43: 269-278.

,, (1984) California blueschist, subduction, and the significance of tectonostratigraphic terranes. *Geology, Vol.* 12: 436-441.

,, (1988) Tectonic history of subduction zones inferred from retrograde blueschist P-T paths. *Geology, Vol.* 16: 1081-1084.

Espejo C., A. (1980) Geocronologia de intrusivas àcidas en la Sierra de Perijà, Venezuela. *Bol. Geol., Caracas,* XIV(26): 245-254.

Etchecopar, A. and Malavielli, J (1987) Computer model of pressure-shadows: a method for strain measurements and shear-sense determination. *Journal of Structural Geology,* 9(5/6): 667-677.

Ewart, A. and Bryan, W.B. (1973) The petrology and geochemistry of the Tongan islands, in the western Pacific.*Island arcs, marginal seas, geochemistry, Coleman, P.J.* editor, *University of Western Australia Press.*

,, (1982) Tertiary-Recent orogenic volcanic rocks. In: *Andesites: Orogenic Andesites and Related Rocks. Thorpe, R.S.* Editor,*John Wiley & Sons, New*

York,25-98.

Faure, G. and Powell, J.L. (1972) *Strontium Isotope Geology*. Springer-Verlag, Berlin, 188 p.

Feo Codecido, G., Smith, F.D., Aboud, N., and de Di Giacomo, E. (1984) Basement and Paleozoic rocks of the Venezuela LLanos basins. *Geol. Soc. Am., Memoir* 162, *Bonini,W.E., Hargraves, R.B., and Shagam, R.* editors: 175-188.

Fry, N. and Fyfe, W.S. (1969) Eclogites and water pressures. *Contrib. Mineral. Petrol., Vol.* 24: 1-6.

Firstbrook, P.L., Funnel, B.M., Smith, A.M., and Smith, A.G. (1979) *Paleoceanic reconstructions. Publication of D.S.D.P., National Science Foundation,* 41 p.

Floyd, P. A. and Winchester, J. A. (1975) Magma type and Tectonic setting discrimination using immobile elements. *Earth Planet. Sci. Lett.* 27: 211-218.

Fox, P. J. and Hezzen, B. C. (1975) Geology of the Caribbean Crust. *In: The Ocean Basins and Margins. Vol. 3: The Gulf of Mexico and the Caribbean*, 421-466, A.E.M. Nairn and F.G. Stehli, *Editors, Plenun Press, New York*, 706 p.

French, B.M. (1966) Some geological implications of equilibrium between graphite and a C-H-O gas phase at high temperatures and pressures. *Rev Geophysics, Vol.* 4: 223-253.

Frey, F.A., Haskins, M.A., Poetz, J., and Haskins, L.A. (1968) Rare earth abundances in some basic rocks. *Jour. Geophys. Res.*, 73 (18): 6085-6098.

,, Bryan, W.B., and Thompson, G. (1974) Atlantic Ocean Floor: Geochemistry and Petrology of Basalts from Legs 2 and 3 of the Deep-Sea Drilling Project. *Jour. Geophys. Res.*, 79(35): 5507-5526.

Gamond, J.F. (1987) Bridge structures as sense of displacement criteria in brittle fault zones. *Journal of Structural Geology,* 9(5/6): 609-620.

Garcia, M.O. (1978) Criteria for the identification of ancient volcanic arcs.*Earth Science Reviews,* 14: 147-165.

Gale, G.H. and Pearce, J.R. (1982) Geochemical Patterns in Norwegian Greenstones. *Canadian Journal of Earth Sciences,* 19: 385-397.

Gerlach, D. C., Avé Lallemant, H.G., and Leeman, W.P (1981) An island arc origin for the Canyon Mountain ophiolite complex, Eastern Oregon, U.S.A. *Earth Planet. Sci. Letters.* 53: 255-265.

Ghosh, S. K. (1977) Geologia del Grupo Roraima en el Territorio Federal Amazonas-Venezuela. *Memorias V Cong. Geol. Ven., Caracas* 1977, *Tomo* I: 167-193.

Ghosh, N., Hall, S.A., and Casey, J.F. (1984) Seafloor spreading magnetic anomalies in the Venezuelan Basin. *Geol. Soc. Am. Memoir* 162, *Bonini, W.E., Hargraves, R.B., and Shagam, R.* editors, 65-80.

Girard, D. (1981) Pétrologie de quelques séries spilitiques Mésozoiques du domaine Caraïbe et des ensambles magmatiques de l'ile de Tobago. *Thése Doct. 3th. Cycle, Brest, Francia,* 229p.

,, Beck, C., Stephan, J.F., Blanchet, R., and Maury, R.C. (1982) Pétrologie, géochimie et signification géodynamique de quelques formations volcaniques crétacées péricaraïbes. *Geol. Soc. France, Bulletin,* (7), XXIV,3: 535-544.

Goldsmith, R., Marvin, R.F., and Mehnert, H.H. (1971) Radiometric ages in the Santander massif, eastern cordillera, Colombia Andes. *U.S. Geol. Surv. Prof. Paper,* 750-D: p.D44-D49.

González de Juana, C. (1968) Guia de la excursiòn geològica a la parte oriental de la Isla de Margarita (Estado Nueva Esparta). *Asoc. Ven. Geol. Min. y Petr., Guia de Excursiòn,* 30 p.

,, (1971) Guia de la excursiòn a la estructura de la Vela de Coro (Falcòn). *IV Congreso Geol. Venez., Caracas, Noviembre* 1969, *Memoria, Bol. Geol., Caracas, Publicacion Esp.* 5 (I): 317-328.

,, and Vignali, M. (1972) Rocas Metamòrficas en la Peninsula de Macanao, Margarita, Venezuela. *Memorias VI Conf. Geol. Caribe, Porlamar* 1971: 63-68.

,, (1972) Guia de la Excursiòn PC-4 Primera parte: Recorrido a lo largo de la costa venezolana entre

Cumana y Pertigalete. *Memorias VI Conf. Geol. Caribe, Porlamar* 1971, 54-57.

,, Muñoz, N.G., Vignali, M. (1972) Reconocimiento Geológico de la Peninsula de Paria, Venezuela. *IV Cong. Geol. Venez., Caracas, Noviembre* 1969, Memoria, Bol. Geol., Caracas, Publ. Especial 5 (III): 1569-1588.

,, Iturralde de Arozena, J., and Picard, X. (1980) Geologia de Venezuela y de sus Cuencas Petroliferas. FONINVES *Editions, Vol.* I *and* II, 1031 p.

González S., L.A. (1972) Geologia de la Cordillera de la Costa, Zona centro-occidental. *IV Cong. Geol. Ven., Caracas, Noviembre* 1969,*Memoria, Bol. Geol., Publ. Esp.*5 (III): 1589-1616.

Govindaraju, K. (1986) 1984 Compilation of working values and sample description for 170 International reference samples of mainly silicate and minerals. *Geostandards Newsletter. Supplement to Volume X.*Govindaraju, Gaudé, and Monnier editors: 16 p.

Grauch, R. I. (1975) Metamorphic petrology and thermal history of the central Andes. *II Cong. Latinoamericano Geol., Caracas Noviembre* 1973 *Memoria, Bol. Geol. Publ. Esp.* 7(I): 214-232.

Green, D.H. and Ringwood, A.E. (1967) An experimental investigation of the gabbro to eclogite transformation and its petrological applications. *Geoch. Cosmochim. Acta,* 31: 767-833.

,, and Ringwood, A.E. (1972) The Origin of Basalt Magmas. *In: Plate Tectonics, Bird, J.M.* editor, *Selected Papers from Publications of the American Geophysical Union, 2nd enlarged edition,* 126-130.

Guth, L. and Avé Lallemant, H.G. (1989) Kinematic history for eastern Margarita island, Venezuela. *Abstracts of the Twelfth Caribbean Geological Conference, St. Croix.*

Haskin, L.A., Haskin, M.A., Frey, F.A., and Waldeman, T.R. (1968) Relative and absolute terrestrial abundance of rare earths. In: *Origin and distribution of the elements.* L.H. Ahrens editor. Pergamon Press. New York: 889-912.

Hawkes, D.D. (1966) The petrology of the Guiana Dolerites. *Geological Magazine, Vol.* 103 (4).

Hawkesworth, C.J. (1982) Isotope characteristics of magmas erupted along destructive plate margins. In: *Andesites: Orogenic Andesites and Related Rocks, Thorpe, R.S.* editor, *John Wiley & Sons, New York,* 549-574.

Hawkins, J.W. and Melchior, J.T. (1985) Petrology of Mariana Trough and Lau Basin Basalts. *Jour. Geophys. Res.,* 90 (B13): 11431-11468.

Helgeson, H.C., Delany, J.M., Nesbitt, H.W., and Bird, D.K. (1978) Summary and critique of the thermodynamic properties of rock-forming minerals.*American Journal of Science, Vol.* 278-A, 229 pp.

Hellman, P.L. and Henderson, P. (1977) Are rare earth elements mobile during spilitization?.*Nature, Vol.* 267: 38-40.

Helmers, H. and Beets, D.J. (1977) Cretaceous of Aruba. *Guide to Field Excursions of the 8th Caribbean Geological Conference, GUA Papers of Geology, Amsterdam,* 10: 29-35.

Hess, H.H. and Maxwell, J. C. (1953) Caribbean Research Project. *Geol. Soc. Am. Bull.*, 64 (1): 1-6.

,, and Maxwell, J.C. (1949) Geological reconnaissance of the island of Margarita. *Geol. Soc. Am. Bull.,* 60 (12): 1857-1868.

,, and Maxwell, J.C. (1953) Caribbean Research project. *Geol. Soc. Am. Bull.*, 64(1): 1-6.

,, (1966) Caribbean Research Project, 1965 and bathymetric chart. *In: Caribbean Geological Investigations*, 1-10, *Geol. Soc. Am. Memoir* 98, 310 p.

Hewitt, D.A. (1973) Stability of the assemblage Muscovite-Calcite-Quartz. *American Mineralogy, Vol.* 58: 785-791.

Hezzen, B.C., Perfit, M.R., Dreyfus, M., and Catalano, R. (1973) The Cayman Ridge. *Geol. Soc. Am. Abstracs with Programs,* 5(7): p. 663.

Higgins, M.W. (1971) Cataclastic Rocks. *Geological Survey*

Professional Paper 687, U.S. Goverment Printing Office, Washington. 96 p.

Hinrichsen, T.V. and Schurmann, K. (1969) Untersuchungen zur stabilitat von pumpellyit. *Neues Jahrb. Mineral. Monatsh.*, 10: 441-445.

Hoffman, C. and Keller, J. (1979) Xenoliths of lawsonite-ferroglaucophane rocks from a Quaternary vulcano of Milos (Aegean Sea, Greece). *Lithos*, 12: 209-219.

Houtz, R.E and Ludwig, W.J. (1977) Structure of Colombia Basin, Caribbean Sea, from profiler-sonobuoy measurements. *Abstracts VIII Caribbean Geol. Conference, Curacao* 1977, *GUA Paper, Amsterdam*, 130; 74.

Hudson, T. and Arth, J.G. (1983) Tin Granites of Seward Peninsula, Alaska. *Geol Soc. Am. Bull.*, 94 (6): 768-790.

Hurley, P. and Hess, H.H. (1968) Basament gneiss, Cordillera de la Costa, Venezuela. *16th Ann. Prog. Rep. U.S. Atomic Energy Comm., Contract* AT (30-1)-1381, M.I.T., p.81.

,, Melchier, G.C., Pinson, W.H., and Fairbairn. H. W. (1976) Progress Report on Early Archean rocks in Liberia, Sierra Leone, and Guayana and their general stratigraphic setting. In: *The Early history of the Earth*, Windley, B.F. *editor., Proc. NATO Adv. Study Inst., John Wiley and Sons, New York:* 511-521.

Humphris, S.E. and Thompsom, G. (1978) Trace-element mobility during hydrothermal alteration of oceanic basalts. *Geochim. Cosmochim. Acta*, 42: 127-136.

,, Thompson, G., Schilling, J.-G., and Kingsley, R.H. (1985) Petrological and geochemical variations along the Mid-Atlantic Ridge between 46° N and 32° S: Influence of the Tristan da Cunha mantle plume. *Geochim. Cosmochim. Acta*, 49: 1445-1464.

Hutchinson, C.S. (1982) Regional distribution and character of active andesite Volcanism: Indonesia. In:*Andesites: Orogenic Andesites and Related Rocks, Thorpe, R.S.* editor, *John Wiley & Sons, New York:* 207-224.

Ibrahim, A.K., Latham,. G.V., and Ladd, J. (1979) Seismic refraction and reflection measurements in the Middle America Trench, offshore Guatemala. *Jour. Geophys. Res.*, 84(B10): 5643-5649.

Innocenti, F., Manetti, P., Mazzuoli, R., Pasquaré, G., and Villari, L. (1982) Regional distribution and character of active andesite volcanism: Anatolia and north-western Iran. In: *Andesites: Orogenic Andesites and Related Rocks, Thorpe, R.S.* editor, *John Wiley & Sons, New York:* 327-352.

Irving, E.M. (1971) La evolución estructural de los Andes mas septentrionales de Colombia. *Bol. Geol., Bogota, Vol. XIX (2):* 1-90.

,, (1975) Structural evolution of the northernmost Andes. *U.S. Geological Survey Professional Paper* 846: 47 p.

Ito, K. and Kennedy, G.C. (1971) An experimental study of the basalt-garnet granulite-eclogite transition. In: *The Structure and Physical Properties of the Earth's Crust. Geophys. Monogr. Ser., Vol.* 14, *Heacock, J.G.*editor, *AGU, Washington D.C.:* 303-314.

Jacobi, R.D. (1984) Modern submarine sediment slides and their implications for melange and the Dunnage Formation in north-central Newfoundland. In: *Melanges: Their nature, Origin, and Significance. Raymond, L.A.* editor, *Geol. Soc. Am., Special Paper* 198: 81-102.

Jahn, B.-M., Shih, C.-Y, and Murthy, V.R. (1974) Trace element geochemistry of Archean volcanic rocks.*Geochim. Cosmochim. Acta,* 38: 611-627.

Jakes, P. and White, A.J.R. (1972) Major and trace element abundances in volcanic rocks of orogenic areas. *Geol. Soc. Am. Bull.*, 83: 29-40.

Jam, P. and Mendez A., M. (1962) Geologia de las Islas de Margarita, Coche y Cubagua. *Soc. Ciencias. Naturales La Salle, Memoir* 22 (61): 51-93.

Jarrad, R.D. (1986) Terrane motion by strike-slip faulting of forearc slivers. *Geology, Vol.* 14: 780-783.

Jhonson, J.H. (1965) Three lower cretaceous algae new to the Americas. *Journal of Paleontology,* 39(4): 719-720.

Jhonson, R.W. (1982) Regional Distribution and Character of Active Andesite Volcanism: Papua New Guinea. In: *Andesites: Orogenic Andesites and Related Rocks, Thorpe, R.S* editor, *John Wiley & Sons:* 225-244.

Kafka, A.L. and Weidner, D.J. (1981) Earthquake focal mechanism and tectonic processes along the southern boundary of the Caribbean plate. *Jour. Geophys. Res.*, 86 (B4): 2877-2888.

Kay, R.W., Hubbard, N.J., Gast, P.W. (1970) Chemical Characteristics and Origin of Oceanic Ridge Volcanic Rocks. *Jour. Geophy. Res.*, 75(8): 1585-1613.

,, and Senechal, R.G. (1976) The rare earth geochemistry of the Troodos Ophiolite Complex. *Jour. Geophys. Res.*, 81(5): 964-970.

Kellogg, J.N. and Bonini, W.E. (1982) Subduction of the Caribbean plate and basement uplifts in the overriding South American plate.*Tectonics,* 1(3): 251-276.

,, (1984) Cenozoic tectonic history of the Sierra de Perijà, Venezuela-Colombia, and adjacent basins. *Geol. Soc. Am. Memoir 162, Bonini, W.E., Hargraves, R.B., and Shagam, R.* editors: 239-262.

Kesler, S.E., Lewis, J.F., Jones, L.M., and Walker, R.L. (1977) Early island-arc intrusive activity, Cordillera Central, Dominican Republic. *Contrib. Mineral. Petrol.*, 65: 91-99.

Kiser, D., Escalona, N., Portilla, A., Monsalve, O., Ramirez P., E., and Colina, G. (1984) Plataforma Continental Venezolana, La Vela-Golfo Triste. *Petroleos de Venezuela, Coordinaciòn de Exploraciòn, Grupo Interfilial,* Vol. II: 75 p.

Khon, B.P., Shagam, R., and Subieta, T. (1984) Results and preliminary implications of sixteen fission-track ages from rocks of the western Caribbean Mountains System. *Geol. Soc. Am. Memoir* 162, *Bonini, W.E., Hargraves, R.B., and Shagam, R.* editors: 415-421.

Konigsmark, T.A. (1958) Geology of the northern Guàrico-Lake Valencia area, Venezuela. *Ph.D. Thesis, Princenton University.*

,, (1965) Geologia del àrea de Guàrico septentrional-

Lago de Valencia, Venezuela. *Bol. Geol., Caracas*, 6(11): 209-285.

Kovach, A., Hurley, P., and Fairbairn, H. (1977) Rb-Sr whole rock dating of metamorphic events in the Iglesias Group, Venezuelan Andes. *Unpublished Report, Mass. Inst. Technol., Cambridge*, 15 p.

Kugler, H.G. (1972) The Dragon Gneiss of Paria Peninsula (Eastern Venezuela). *Memorias VI Conf. Geol. Caribe. Porlamar* 1971: 113-116.

Ladd, J.W. (1976) Relative motion between North and South America and Caribbean tectonics. *Memorias VII Conf. Geol. Caribe, Guadalupe* 1974: 63-68 p.

,, Worzel, J.L., and Watkins, J.S. (1977) Multifold seismic reflection records from the northern Venezuela Basin and the north slope of the Muertos trench. In: *Island arcs, deep sea trenches, and back arc basins.* Talwani, M. and Pitman, W.C. *editors. American Geophysical Union,* Maurice Ewing Series 1: 41-56.

,, and Watkins, J.S. (1978) Active margin structures within the north slope of the Muertos trench. *Geologie en Mijnbouw,* 57(2): 255-260.

,, (1980) Seismic stratigraphy of the western Venezuela basin. *Marine Geology, Vol.* 35: 21-41.

,, Ibrahim, A.K., McMillen, K.M., Latham, G.V., and von Huene, R.E. (1982) Interpretation of seismic reflection data of the Middle America Trench off Guatemala. In: *Initial reports of the Deep Sea Drilling Project, Leg 67,* 675-689.

,, Truchman, M., Talwani, M., Stoffa, P.L., Buhl, P., Houtz, R., Mauffret, A., and Westbrook, G. (1984) Seismic reflection profiles across the southern margin of the Caribbean. *Geol. Soc. Am. Memoir 162.* Bonini, W.E., Hargraves, R.B., and Shagam., R. *editors*: 153-160.

Laffaille, J. and Estévez, R. (1986) Modelo sismotectonico para la serrania de el Escorial. *Acta Científica Venezolana* 37: 675-679.

Laird, J., Lanphere, M.A., and Albee, A.L. (1984) Distribution of Ordovician and Devonian metamorphism in mafic and pelitic schists from

northern Vermont. *American Journal of Science,* 284(4-5): 376-413.

Langer, C.J. and Bollinger, G.A. (1979) Secondary faulting near the terminus of a seismogenic strike-slip fault: Aftershocks of the 1976 Guatemala earthquake. *Seismol. Soc. Am. Bull.*, 69: 427-444.

Langmuir, C.H., Bender, J.F., Bence, A.E., Hanson, G.N., and Taylor, S.R. (1977) Petrogenesis of basalts from the Famous area: Mid-atlantic Ridge. *Earth Planet. Sci. Letters,* 36: 133-156.

,, Voeke, R.D., and Hanson, G.N. (1978) A general mixing equation with application to Icelandic basalts. *Earth Planet. Sci. Letters,* 37: 380-392.

Leake, B., Lancaster, G., Kemp, A., Plant, A.G., Harrey, P., Wilson, J.R., Coats, J.S., Aucott, J.W., Lunel, T., and How Arth, R.J. (1969) The chemical Analysis of rock powders by Automatic X-ray Fluorescense. *Chemical Geology,* 5: 7-86.

Leclere Vanhoeve, A. and Stephan, J.F. (1985) Evolution géodynamique des Caraibes dans le system points chauds. In: *Symposium Géodynamique des Caraibes, Paris, Février 1985, Mascle, A.* editor: 21-34.

Lee, V. and Mattson, P.H. (1976) Metamorphosed oceanic crust or early volcanic products in Puerto Rico basement rock association. *Transactions 7th Caribbean Geological Conference, Guadeloupe:* 263-270.

Le Pichon, X. and Fox, P. J. (1971) Marginal offsets, fracture zones, and the early opening of the North Atlantic. *Jour. Geophys. Res.* 76 (26): 6294-6308.

Le Roex, A.P., Dick, H.J.B., Erlank, A.J., Reid, A.M., Frey, F.A., and Hart, S.R. (1983) Geochemistry, mineralogy and petrogeneses of lavas erupted along the Southwest Indian Ridge between the Bouvet Triple Junction and 11 degrees east. *Journal of Petrology,* 24: 267-318.

Liou, J.G., Maruyama, S., and Cho, M. (1985) Phase equilibria and mineral parageneses of metabasites in low-grade metamorphism. *Mineralogical Magazine,* 49: 321-333.

Lister, G.S. and Snokes, A.W. (1984) S-C Mylonites. *Journal of Structural Geology,* 6: 283-297.

Lopez-Escobar, L., Frey, F.A., Vergara, M. (1977) Andesites and high-alumina basalts from the central-south Chile: geochemical evidence bearing on their petrogenesis. *Contrib. Mineral. Petrol.*, 63: 199-228.

Loubet, M., Montigny, R., Chachati, B., Duarte, N., Lambret, B., Martin, C., and Thuizat, R. (1985) Geochemical and geochronological constraints on the geodynamic development of the Caribbean Chain of Venezuela. In: *Symposium Géodynamique des Caraibes, Paris, Février*1985, *Mascle, A.* editor: 553-566.

Loureiro, D. (1981) Geoquímica de los elementos mayoritarios de las anfibolitas de la Cordillera de la Costa: fragmentos de la corteza oceánica Caribe. *Trabajo de ascenso, Escuela de Geol., Minas y Geofísica, UCV, Caracas,* 186 p.

MacCourt, W.J., Apsden, J.A., and Brook, M. (1984) New geological and geochronological data from the Colombia Andes: Continental growth by multiple accretion. *Geol. Soc. London,* 141: 831-845.

MacDonald, W.D. (1965) Geology of the Serrania de Macuira area Guajira Peninsula, northeast Colombia. *Fourth Caribbean Conference, Trinidad:* 267-274.

,, (1968) Status of Geological research in the Caribbean. *Universidad de Puerto Rico* 14: 40.

MacDonald, W. D. (1968) Estratigrafía, estructura y metamorfismo, rocas del Jurásico Superior, Península de Paraguana, Venezuela. *Bol. Geol., Caracas,* 9(18): 441-458.

,, and Opdyke, N. D. (1974) Triassic paleomagnetism of northern South America. *Am. Assoc. Petr. Geol. Bull.*, 58 (2): 208-215.

MacDonald, K.C. and Holcombe, T.L. (1978) Inversion of magnetic anomalies and sea-floor spreading in the Cayman trough. *Earth Planet. Sci. Letters.* Vol. 40: 407-414.

MacKenzie, D. B. (1960) La Peridotita de Tinaquillo. *III Cong. Geol. Venez., Caracas, Noviembre* 1959, *Memoir, Bol. Geol., Caracas, Pub. Esp.* 3 (II): 761-826.

,, (1966) Geología de la región norte-central de

Cojedes. *Bol. Geol., Caracas,* 8 (15): 3-72.

MacLachlan, J.C., Shagam, R., and Hess, H. H. (1960) Geology of the La Victoria Area, Aragua, Venezuela. *Geol. Soc. Am. Bull.* 71. 241-248.

McNutt, R.H., Crockett, J.H., Clark, A.H., Caelles, J.C., Farrar, E., Haynes, S.J., and Zentilli, M. (1975) Initial $^{87}Sr/^{86}Sr$ ratios of plutonic and volcanic rocks of the central Andes between latitudes 26° and 29° south. *Earth Planet. Sci. Letters,* 27: 305-313.

Macsotay, O. (1972) Observaciones sobre la edad y paleoecologia de algunas formaciones de la regiòn de Barquisimeto, Estado Lara, Venezuela. IV *Cong. Geol. Ven. Memoria Caracas:* Tomo III: 1673-1689.

MainPrice, S.JI.D. and Boudier, F. (1988) Sense of shear in high-temperature movement zones from the fabric asymmetry of plagioclase feldspar. *Journal of Structural Geology,* 10(1): 73-82.

Mann, P. and Burke, K. (1984) Neotectonics of the Caribbean. *Reviews of Geophysics and Space Physics, Vol.* 22(4): 309-362.

Marechal, Ph. (1983) Les témoins de chaine hercynienne dans le noyau ancien des Andes de Mérida (Venezuela): structure et évolution tectono-métamorphique. *Thése Doct. 3éme cycle, Brest, France:* 178 p.

Maresch, W. V. (1971) The metamorphism and structure of northeastern Margarita island, Venezuela. *Ph.D. thesis, Princeton University* USA. 278 p.

,, (1973) Metamorfismo y estructura de Margarita nororiental, Venezuela. *Bol. Geol., Caracas,* 12 (22): 3-172.

,, (1974) Plate Tectonics origin of the Caribbean Mountains System of northern South America: discussion and proposal. *Geol. Soc. Am. Bull.,* 85 (5): 669-682.

,, and Abraham, K. (1981) Petrography, mineralogy, and metamorphic evolution of an eclogite from the island of Margarita, Venezuela. *Journal of Petrology.* Vol. 22: 337-362.

Martin B., C. (1968) Edades isotòpicas de rocas venezolanas.

Bol. Geol. Caracas. 9 (19): 356-380.

,, and Arozena I., J. (1972) Complejo ultramàfico zonado de Tausabana-El Rodeo, gabro zonado de Siraba-Capuana y Complejo subvolcànico estratificado de Santa Ana, Paraguanà, Estado Falcòn. *VI Conf. Geol. Caribe Memoria, Porlamar 1971.* Petzall, C. *editor:*337-356.

,, (1974) Paleotectònica del Escudo de Guayana. *IX Conf. Geol. Inter-Guayanas Memoria, Ciudad Guayana* 1972, *Venezuela, Bol. Geol. Pub. Esp.*6: 251-305.

,, (1975) Excursiòn Geològica N° 6, Puerto Ordaz-la Vergareña. *II Cong. Latinoamericano de Geologia Memoria, Noviembre* 1973, *Bol. Geol. Publ. Esp.*7: 371-388.

Martins-Pimentel, M. and Fuck, R. A. (1987) Late Proterozoic Granitic magmatism in southwestern Goiàs, Brazil. *Revista Brasileira de Geociencias,* 17(4): 415-425.

Mascle, A., Biju-Duval, B., Letouzey, J., Montadert, L., and Ravenne, C. (1977) Sediments and their deformations in active margins of different geological settings. In: *International symposium on geodynamics in south-west Pacific, Nouméa* 1976, Paris: 327-344.

,, Biju-Duval, B., Letouzey, J., Bellizia, A., Auboin, J., Blanchet, R., Stephan, J.F., and Beck, C. (1979) Estructura y evolución de los margenes este y sur del Caribe. *Bulletin du B.R.G.M. (deuxiéme série),* Section IV (3/4): 171-184.

,, Cazes, M., and Le Quellec, P. (1985) Structure des marges et bassins Caraïbes: une revue. In: *Symposium Géodynamique des Caraibes, Février* 1985. *Mascle, A.* editor: 1-20.

Mattson, P.H. (1984) Caribbean structural breaks and plate movements. *Geol. Soc. Ame. Memoir* 162. *Bonini, W. E., Hargraves, R.B., and Shagam, R.* editors: 131-152.

Maury, R.C. and Westercamp, D. (1985) Variations chronologiques et spatiales des basalts néogenes des Petites Antilles; implications sur l'évolution de l'arc. *Symposium Géodynamique des Caraïbes, Février* 1985, *Paris. Mascle, A.* editor: 77-90.

Mawer, C.K. (1987) Shear criteria in the Grenville Province, Ontario, Canada. *Journal of Structural Geology*, 9(5/6): 531-540.

Maze, W.B (1984) Jurassic La Quinta Formation in the Sierra de Perijà, northwestern Venezuela: Geology and tectonic environment of red beds and volcanic rocks. *Geol. Soc. Am. Memoir* 162. *Bonini, W.B., Hargraves, R.B., and Shagam, R.* editors: 263-282.

,, and Hargraves, R.B. (1984) Paleomagnetic results from the Jurassic la Quinta Formation in the Perijà Range, Venezuela, and their tectonic significance. *Geol. Soc. Am. Memoir* 162. *Bonini, W.B., Hargraves, R.B., and Shagam, R.* editors: 287-294.

Mendoza, V. (1977) Evolución tectónica del Escudo de Guayana. *Memoria II Cong. Geol. Latinoamericano, Noviembre* 1973, *Bol. Geol. Publ. Esp.* 7 (III): 2237-2270.

Menendez, A. (1965) Geologia del área de El Tinaco, centro del Estado Cojedes, Venezuela. *Bol. Geol., Caracas*, 6 (12): 417-543.

,, (1966) Tectónica de la parte central de las Montañas Occidentales del Caribe, Venezuela. *Bol. Geol., Caracas*. 8 (15): 116-139.

Meschede, M. (1986) A method of discriminating between different types of mid-ocean ridge basalts and continental tholeiites with the Nb-Zr-Y diagram. *Chemical Geology*, 56: 207-218.

Meyerhoff, A.A., Khudoley, K.M., and Hatten, C.W. (1969) Geologic significance of radiometric dates from Cuba. *Am. Ass. Petrol. Geol. Bull.* 53(12): 2494-2500.

Miyashiro, A. (1972) Metamorphism and related magmatism in plate tectonics. *American Journal of Science* 272: 629-656.

,, (1975) Volcanic rock series and tectonic setting. *Annu. Rev. Earth Planet. Sci.* 3: 251-269.

,, (1979) Metamorphism and Metamorphic Belts. *George Allen & Unwin. London. Fourth impression.* 492p.

,, Aki, K., and Celal Sengor, A.M. (1982) Orogeny. *John Wiley & Sons, New York.* 242p.

Molnar, P. and Sykes, L. (1969) Tectonics of the Caribbean and Middle America regions from focal mechanism and seismicity. *Geol. Soc. Am. Bull.,* 80: 1639-1684.

Morgan, B.A. (1967) Geology of the Valencia area, Carabobo, Venezuela. *Ph.D. Thesis. Princenton University.* 220p.

,, (1969) Geologia de la regiòn de Valencia, Carabobo, Venezuela. *Bol. Geol. 20, Caracas:* 3- 136.

Moticska, P. (1972) Geologia del Archipielago de Los Frailes. *Memoria VI Conf. Geol. Caribe, Porlamar. Julio* 1971. *Petzall, C.* editor: 69-73.

,, (1985) Volcanismo Mesozoico en el subsuelo de la faja petrolifera del Orinoco, Estado Guarico, Venezuela. *Memoria VI Cong. Geol. Venezolano. Tomo* III: 1929-1943.

Mottana, A., Bocchio, R., Liborio, G., Morten, L., and Maresch, W.V. (1985) The eclogite-bearing metabasaltic sequence of isla Margarita, Venezuela: a geochemcal study. *Chemical Geology,* 50: 351-368.

Muessig, K. W. (1984) Paleomagnetic data on the basic igneous intrusions of the Central Falcòn basin, Venezuela. *Geol. Soc. Am. Memoir* 162, Bonini, W.E., Hargraves, R.B., and Shagam, R, *editors*: 231-238.

Mullen, E.D. (1983) $MnO/TiO_2/P_2O_5$: a minor element discriminat for basaltic rocks of oceanic environments and its implications for petrogenesis. *Earth Planet. Sci. Letters,* 62: 53-62.

Murray, C. G. (1973) Estudios petrològicos de complejos ultramàficos zonados en Venezuela y Alaska. *Bol. Geol., Caracas,* 12 (22): 173-279.

Navarro F., E. (1974) Petrogenesis of the eclogitic rocks of Isla de Margarita, Venezuela. *Ph.D. Thesis, the Graduate School, University of Kentucky, U.S.A.,* 213 p.

,, (1977) Eclogitas de Margarita: evidencias de

polimetamorfismo. *V Cong. Geol. Venez., Caracas, Noviembre* 1977, *Memoir, Ministerio Energia y Minas-Soc. Ven. Geol.*, II: 651-661.

,, (1981) Relaciones mineralògicas en rocas eclogìticas de la isla de Margarita. *GEOS* 26, Caracas: 3-44.

,, (1983) Petrologìa y Petrogénesis de las rocas metavolcànicas del Grupo Villa de Cura. *GEOS* 28, Caracas: 170-317.

,, (1987) Anfiboles y micas blancas de la isla de Margarita, Venezuela: Su uso como indicadores petrogenéticos. *Acta Cientifica Venezolana*, 38: 490-502.

Newton, R.C. and Kennedy, G.S. (1963) Some equilibrium reactions in the join $CaAl_2Si_2O_8$-H_2O. *Jour. Geophys. Res.*, 68: 2967-2984.

Nitsch, K.-H. (1971) Stabilitatsbeziehungen von Prehnit- und Pumpellyt-haltigen Paragenesen. *Contrib. Mineral. Petrol.*, 30: 240-260.

Noiret, G., Montigny, R., and Allégre, C.J. (1981) Is the Vourinos Complex an island arc complex?. *Earth Planet. Sci. Letters*, 56: 375-386.

Nye, C.J. and Reid, M.R. (1986) Geochemistry primary and least fractionated lavas from Okmok Volcano, Central Aleutians: Implications for arc magmagenesis. *Jour. Geophys. Res.*, 91(B10): 10271-10278.

Officer, C. B., Ewing, J. I., Hennion, J. F., Harkrider, D.G., and Miller, D. E. (1959) Geophysical investigations in the eastern Caribbean: summary of 1955 and 1956 cruises. *In: Physics and Chemistry of the Earth*, 3 : 17-109, L.H. Ahrens *et al. Editors, Pergamon Press*, 464 p.

Olmeta, M.A. (1968) Determinaciòn de edades radiomètricas en rocas de Venezuela y su procedimiento por el método K/Ar. *Bol. Geol.*, Caracas. 10 (9): 339-344.

Ostos R., M. (1981) Geologia de una zona ubicada entre el estribo de Galindo y la autopista Caracas-La Guaira, Parque Nacional El Avila. *Trabajo de Ascenso, Universidad Central de Venezuela. Inédito*. 279p.

,, (1984) Structural interpretation of the Tinaquillo Peridotite and its country rock, Cojedes State, Venezuela. *Rice University, Houston, USA, Master thesis.* 135 p.

,, (1985) Peridotita de Tinaquillo: Ofiolita Paleozòica en el Sistema Montañoso del Caribe. VI *Cong. Geol. Venez., Caracas, Tomo IV*: 2557-2602.

,, and Navarro, E. (1985) Faja de Villa de Cura. Realmente un complejo de arco de isla alòctono?. *VI Cong. Geol. Venez., Caracas, Tomo* X: 6615-6638.

,, Urbani, F., and Navarro, E. (1989) Rocas Precambricas en el borde sur de la placa del Caribe, Venezuela. *Memorias VII Congreso Geol. Venezolano,* Barquisimeto, Noviembre 1989. In press.

Oxburgh, E.R. (1965) Geologia de la regiòn oriental del Estado Carabobo, Venezuela. *Bol. Geol.,* Caracas, 6 (11): 103-208.

,, (1966) Geology and Metamorphism of Cretaceous rocks in Eastern Carabobo State, Venezuelan Coast Range. *Geol. Soc. Amer., Memoir* 98: 241-310.

Pallister, J.S. and Knight, R.J. (1981) Rare-earth element geochemistry of the Samail Ophiolite near Ibra, Oman. *Jour. Geophys. Res.,* 86(B4): 2673-2697.

Passchier, C.W. and Simpson, C. (1986) Porphyroclast systems as kinematic indicators. *Journal of Structural Geology,* 8: 831-843.

Pearce, J.A. and Cann, J.R. (1973) Tectonic Setting of basic volcanic rocks investigated using trace element analyses. *Earth Planet. Sci. Lett.* 19: 290-300.

,, (1975) Basalt Geochemistry used to investigate past tectonic environment on Cyprus. *Tectonophysics,* 25: 41-67.

,, Gorman, B.E., and Birkett, T.C. (1975) The TiO_2-K_2O-P_2O_5 diagram: A method of discrimination between oceanic and non-oceanic basalts. *Earth Planet. Sci. Letters,* 24: 419-426.

,, and Gale, G.M. (1977) Identification of ore-deposition environment from trace element geochemistry of associated igneous host rocks. In: *Volcanic Processes in Ore Genesis. Geol. Soc. London. Spec Publ.* 7: 14-24.

,, and Norry, M. J. (1979) Petrogenetic implications of Ti, Zr, Y, and Nb variation in volcanic rocks. *Contrib. Mineral. Petrol.*, 69: 33-47.

,, (1982) Trace element characteristics of lavas from destructive plate boundaries. *In: Andesites.* R.S. Thorpe *Editor. New York, John Wiley & Sons*: 525-548.

,, Lippard, S. J., and Roberts, S. (1984) Characteristics and tectonic significance of supra-subduction zone ophiolites. In: *Marginal Basin Geology.Geol. Soc. London. Special Publication* 16. B.P. Kokelar and Howells, M.F. *Editors*: 77-94.

Peccirillo, A. and Taylor, S.R. (1976) Geochemistry of Eocene calc-alkaline volcanic rocks from the Kastamonu area, northern Turkey. *Contrib. Mineral. Petrol.*, 58: 63-81.

Pennington, W.D. (1981) Subduction of the Eastern Panamá Basin and Seismotectonic of Northwestern South America. *Jour. Geophys. Res.*, 86: 10753-10770.

Perchuck, L.L. and Aranovich, L.Y. (1980) The thermodynamic regime of metamorphism in the ancient subduction zone. *Contrib. Mineral. Petrol.*, 75: 407-414.

Pereira, J.G. (1985) Evolución tectónica de la cuenca de Carúpano durante el Terciario. *Memorias VI Cong. Geol. Venezolano*, Caracas, Noviembre 1985, *Tomo* III: 2618-2648.

Perfit, M.R. and Hezzen, B.C. (1978) The geology and evolution of the Cayman Trench. *Geol. Soc. Am. Bull.*, 89 (8): 1155-1174.

Phelps, D. and Avé Lallemant, H. G. (1980) The Sparta Ophiolite Complex: a plutonic equivalent to low K_2O island-arc volcanism. *American Journal of Science, Vol.*280-A: 345-358.

Philpotts, J.A., Martin, W., and Schnetzler, C.C. (1971) Geochemical aspects of some Japanese lavas. *Earth*

Planet. Sci. Letters, 12: 89-96.

Piburn, M.D. (1968) Metamorfismo y estructura del Grupo Villa de Cura, venezuela Septentrional. *Bol. Geol.*, Caracas, 9(18): 184-290.

Pichler, H., Stibane, F.R., and Weyl, R. (1974) Basischer Magmatismus und Krustenbahn im sudlichen Mittelamerica, Kolumbien und Ecuador. *Neues. Jahrb. Geol. Palaontol. Monatsh.*, 102-126.

Pimentel B., N., Gaudette, H., and Olsewsky, W. (1985) Nuevas dataciones en el "basamento" de la Cadena Caribe. *Memorias VI Cong. Geol. Venez.*, Caracas, *Noviembre* 1985, *Tomo* II: 1979-1994.

Pindell, J. and Dewey, J.F. (1982) Permo-triassic reconstruction of western Pangea and the evolution of the Gulf of Mexico/caribbean region. *Tectonics*. 1(2): 179-211.

,, (1985) Alleghenian recontruction and the subsequent evolution of the Gulf of Mexico, Bahamas, and Proto-Caribbean Sea. *Tectonics*. 4: 1-39.

,, Cande, S.C., Pitman III, W. C., Rowley, D.B., Dewey, J.F., Labrecque, J., and Haxby, W. (1988) A plate-kinematic framework for models of Caribbean evolution. *Tectonophysics*. 155: 121-138.

,, and Barret, S.F. (1989) Geological evolution of the Caribbean region: A plate tectonics perspective. In: *The Caribbean Region. Case, J.E. and Dengo, G.* eds. *Geological Society of America, The Geology of North America. Volume H.* In press.

Pinet, B., Lajat, D., Le Quellec, P., and Bouysse, Ph. (1985) Structure of Aves Ridge and Grenada Basin from multichannel seismic data. *Symposium Geodynamique des Caraibes, Paris, Février 1985. Mascle, A.* editor: 53-64.

Pitcher, W.S. (1983) Granite: typology, geological environment, and melting relationships. In: *Migmatites, Melting, and Metamorphism. Atherton, M.P and Gribble, C.D.* eds. *Shiva Publications*. 277-287.

Platt, J.P. (1976) The petrology, structure, and geologic history of the Catalina Schist terrain, southern California. *University of California, Publications*

in Geological Sciences. Vol. 112: 111p.

,, (1986) Dynamics of orogenic wedge and the uplift of high-pressure metamorphic rocks. *Geol. Soc. Am. Bull., Vol.* 97: 1037-1053.

Priem, H.N.A., Boelrijk, N.A.I.M., Verschure, R.H., Hebeda, E.H., and Lagaay, R.A. (1966) Isotopic ages of the quartz-diorite batholith on the island of Aruba, Netherland Antilles. *Geologies en Mijnbouw.* 45: 188-190.

,, Hebeda, E.H., Boelrijk, N.A.I.M., and Verschure, R.H. (1968) Isotopic age determination on Suriman rocks, 3 Proterozoic and Permo-Triassic basalt magmatism in the Guiana Shield. *Geologies en Mijnbouw,* 47(1): 17-20.

,, Boelrijk, N.A.I.M., Hebeda, E.H., and Verschure, R.H. (1973) Age of Precambrian Roraima Formation in north-eastern South America: evidence from isotopic dating of Roraima pyroclastic volcanic rocks in Suriname. *Geol. Soc. Am. Bull.* 84(5): 1677-1684.

,, Andriessen, P.A.M., Beets, D.J., Boelrijk, N.A.I.M., Hebeda, E.H., Verdurmen, E.A., and Verschure, R.H. (1977) Isotopic dating of the quartz-diorite batholith of Aruba and the crystalline cores of Curacao and Bonaire. *Abstract VIII Geological Caribbean Conference, Curacao* 1977, *GUA Paper of Geology, Series* I (9): 149-155.

,, Beets, D.J., and Verdurmen, E. A. (1986) Precambrian rocks in an early Tertiary conglomerate on Bonaire, Netherlands Antilles (South Caribbean borderland): evidence for a 300 Km eastward displacement relative to the South America mainland?. *Geologies en Mijnbouw.* 65: 35-40.

Ramirez, J.E., Duque-Caro, H., Goberna, J.R., and Toussaint, J.F. (1983) Geodynamic Research in Colombia. *American Geophysical Union. Geodynamics series Vol. 9. Cabré, R* editor: 41-52.

Ramsay, J.G. and Huber, M.I. (1983) *The Techniques of Modern Structural Geology. Volume 1: Strain Analysis.* Academic Press, New York: 308 p.

Restrepo, J.J. and Toussaint, J.F. (1975) Edades radiométricas de algunas rocas de Antioquia-

Colombia. *Publicación Esp. Geol. Universidad Nacional de Colombia, Medellin,* 6: 1-24.

,, and Toussaint, J.F.(1978) Ocurrencia de Precámbrico en las cercanias de Medellin, Cordillera Central de Colombia. *Publicación Esp. Geol. Universidad Nacional de Colombia, Medellin,* 12: 1-11.

,, and Toussaint, J.F. (1982) Metamorfismos superpuestos en la Cordillera Central de Colombia. *V Congreso Latinoamericano de Geología, Argentina. Tomo* III: 505-512.

,, and Toussaint, J.F. (1988) Terranes and Continental Accretion in the Colombian Andes. *Episodes* 11(3): 189-193.

Rial, J.A. (1978) The Caracas, Venezuela earthquake of July 1967: A multiple-source event. *Jour. Geophys. Res.*, 83: 5405-5414.

Ringwood, A.E. and Green, D.H. (1966) An experimental investigation of the gabbro-eclogite transformation and some geophysical implications. *Tectonophysics,* 3: 383-427.

Robertson, P. and Burke, K. (1989) Evolution of Southern Caribbean plate boundary, vicinity of Trinidad and Tobago. *Am. Ass. Petrol. Geol. Bull.* 73(4): 490-509.

Rosales, H. (1972) La falla de San Francisco en el Oriente de Venezuela. *IV Congreso Geol. Ven. Caracas Noviembre* 1969, *Bol. Geol. Publ. Esp.* 5(IV): 2322-2336.

Ross, M. I. and Scotese, C. R. (1988) A hierarchical tectonic model of the Gulf of Mexico and Caribbean region. *Tectonophysics* 155: 139-168.

Roy, R.K., Kacker, R.N., and Chattopadhayay, B. (1982) Geochemical characteristics and tectonic setting of the Naga Hills Ophiolite Volcanics, India. *Ofioliti,* (2/3): 479-498.

Salvador, A. (1964) Proposed simplification of the stratigraphy nomenclature in the Eastern Venezuela basin. *Asoc. Ven. Geol. Min. Petrol., Bol. Inf.*, Caracas, 7(6): 153-202.

,, and Stainforth, R.M. (1968) Clues in Venezuela to

the geology of Trinidad and viceversa. *IV Caribbean Geol. Conference, Trinidad* 1965: 31-40.

Santamaria, F. and Schubert, C. (1974) Geochemistry and geochronology of the southern Caribbean-Northern Venezuela plate boundary. *Geol. Soc. Am. Bull.* 85 (7): 1085-1098.

Saunders, J.B., Edgar, N.T., Donnelly, T.W., and Hay, W. (1973) Cruise Synthesis. In: *Initial Reports of the Deep Sea Drilling Project. Edgar, N.T. and Saunders, J.B.* editors. *U.S. Goverment Printing Office, Washington.* 15: 1077-1111.

,, Tarney, J., Stern, C.R., and Dalziel, I.W.D. (1979) Geochemistry of Mesozoic marginal basin floor igneous rocks from southern Chile. *Geol. Soc. Am. Bull.*, 90: 237-258.

,, and Tarney, J. (1979) The geochemistry of basalts from back-arc spreading centre in the East Scotia Sea. *Geochim. Cosmochim. Acta,* 43: 555-572.

Schilling, J.-G. (1973) Iceland mantle plume: Geochemical study of Reykjanes ridge. *Nature,* 242: 565-571.

,, (1975) Rare-earth variation across "Normal Segments" of the Reykjanes Ridge, 60° -53° N, Mid-Atlantic ridge, 29° S, and East Pacific Rise, 2°-19° S, and Evidences on the composition of the underlying low-velocity layer. *Jour. Geophys. Res.,* 80(11): 1459-1473.

,, Meyer, P.S., and Kingsley, R.H. (1982) Evolution of the Iceland hotspot. *Nature,* 296: 313-320.

Schubert, C. and Sifontes, R. (1970) Boconò Fault, Venezuelan Andes: evidence of post-glacial movement. *Science,* 170: 66-69.

,, and Moticska, P. (1972) Geological reconnaissance of the Venezuelan islands in the Caribbean Sea between Los Roques and Los Testigos. *Memorias VI Conf. Geol. Caribe, Porlamar* 1971: 81-82.

,, and Moticska, P. (1973) Reconocimiento geològico de las islas venezolanas en el Mar Caribe, entre Los Roques y Los Testigos (Dependencia Federales). *Acta Cientifica Venezolana,* 24: 19-31.

,, Sifontes, R., Padron, V.E., Velez, J.R., and Loaiza,

P.A. (1979) Formaciòn La Quinta (Jurasico) Andes Merideños: Geologia de la seccion tipo. *Acta Cientifica Venezolana*, 30: 42-55.

,, (1982) Origin of the Cariaco Basin, southern Caribbean Sea. *Marine Geology*, 47: 345-360.

,, (1984) Basin formation along the Boconò-Morón-El Pilar fault system, Venezuela. *Jour. Geophys. Res.*, 89: 5711-5718.

Seiders, V.M. (1965) Geologia de Miranda central, Venezuela. *Bol. Geol., Caracas*, 6(12): 289-416.

Sellier de Civrieux, J.M. (1953) Informe paleontològico sobre muestras del Grupo Paracotos en la regiòn de Caucagua. *Informe inedito Ministerio de Energia y Minas*, 12(I): 53p.

Shagam, R. (1960) Geology of the central Aragua State, Venezuela. *Geol. Soc. Am. Bull.*, 71 (3): 249-302.

,, (1975) The northern termination of the Andes. In: *The Ocean Basins and Margins, Vol. 3: Gulf of Mexico and the Caribbean*, 325-420. *Plenun Press, New York*, 706 p.

Shih, C.Y. (1972) the rare-earth geochemistry of oceanic igneous rocks. *Ph.D. thesis, Columbia University.*

Sigurdsson, H., Sparks, R.S.J., Carey, S.N., and Huang, T.C. (1980) Volcanogenic sedimentation in the Lesser Antilles arc. *Journal of Geology*. 88(5): 523-540.

Silver, E.A., Case, J.E., and MacGillavry, H.J. (1975) Geophysical study of the Venezuelan Borderland. *Geol. Soc. Am. Bull.*, 86(2): 213-226.

Sillitoe, R.H., Jaramillo, L., Damon, P.E., Shafiqullah, M., and Escobar, R. (1982) Setting, Characteristics, and Age of the Andean Porphyry Copper Belt in Colombia. *Economic Geology*, 77: 1837-1850.

Simpson, C. and Schmid, S.M. (1983) An evaluation of criteria to deduce the sense of movement in sheared rocks. *Geol. Soc. Am. Bull.*, 94: 1281-1288.

Skerlec, G.M. and Hargraves, R.B. (1980) Tectonic significance of paleomagnetic data from Venezuela.

Jour. Geophys. Res., 85(B10): 5303-5315.

Smewing, J.D., Simonian, K.O., and Gass, I.G. (1975) Metabasalts from the Troodos Massif, Cyprus: Genetic implications deduced from petrography and trace element geochemistry. *Contrib. Mineral. Petrol.*, 51: 49-64.

Smit, J. (1977) Planktonic foraminiferal faunas from the upper part of the Washikemba Formation. *Abstracts VIII Caribbean Geol. Conference, Curacao, GUA Papers of Geology, Series* 1 (9):192-193.

Smith, R.J. (1952) Geologia de la regiòn Los Teques-Cúa, Venezuela. *Bol. Geol., Caracas,* 2(6): 333-406.

,, (1953) Geology of the Los Teques-Cúa region, Venezuela. *Geol. Soc. Am. Bull.*, 64(1): 41-64.

Smith, R.E. and Smith, S.E. (1976) Comments on the use of Ti, Zr, Y, Sr, K, P, and Nb in classification of basaltic magmas. *Earth Planet. Sci. Letters,* 32: 114-120.

Smith, A.G. and Briden, J.C. (1977) *Mesozoic and Cenozoic Paleo-continental Maps.* Cambridge University Press, New York, 63 p.

Sorensen, S.(1985) Petrologic evidence for Jurassic, island-arc-like basement rocks in the southwestern Transverse Ranges and California Continental borderland. *Geol. Soc. Am. Bull., Vol.* 96: 997-1006.

Soulas, J.P. (1985) Neotectònica y Tectònica activa en Venezuela y regiones vecinas. *Memorias VI Congreso Geològico Venezolano, Noviembre* 1985. *Tomo* X:6639-6656.

Speed, R.C. (1985) Cenozoic collision of the Lesser Antilles arc and continental South America and the origin of the El Pilar fault. *Tectonics,*4: 41-69.

,, and Laure, D.K. (1985) Tectonic evolution of Eocene turbidites of Grenada. *Symposium Geodynamique des Caraibes, Paris Février* 1985, *Mascle, A.* editor: 101-108.

Spena, F., Furrer, M., and Urbani, F. (1977) Fòsiles en las rocas metamòrficas de la regiòn de Birongo-Capaya, Barlovento, Estado Miranda. *Bol. A.V.G.M.P.*

Caracas, 19 (4): 169-176.

Stephan, J. F. (1977) El contacto Cadena Caribe-Andes Merideños entre Carora y el Tocuyo (Estado Lara Venezuela). *Memorias V Congreso Geol. Venezolano. Tomo* II: 789-816.

,, Beck, C., Bellizia, A., and Blanchet, R. (1980) La chaine caraibe du Pacifique à l'Atlantique. *26 Congrés Géologique International, Paris.* 39-59.

,, (1982) Evolution géodynamique du domain caraibe; Andes et Chaine Caraibe sur la Transversale de Barquisimeto (Venezuela). *Thése d'Etat, Brest, Francia.* 512 p.

,, (1985) Andes et chaine Caraibe sur la transversale de Barquisimeto (Venezuela); evolution géodynamique. *Symposium Géodynamique des Caraibes, Février* 1985: 505-529.

Sun, S.-S. and Hanson (1977) Rare earth element evidence for differentiation of McMurdo Volcanics, Ross Island, Antartica. *Contrib. Mineral. Petrol.*, 54: 139-155.

,, Nesbitt, R.W., and Sharaskin, A.Ya. (1979) Geochemical characteristic of midocean ridge basalts. *Earth Planet. Sci. Letters*, 44: 119-138.

Sykes, L.R. and Ewing, M. (1965) The seismicity of the Caribbean region. *Jour. Geophys. Res.*, 70 (20): 5065-5074.

,, McCann, W.R., and Kafka, A.L. (1982) Motion of the Caribbean plate during last 7 million years and implications for earlier Cenozoic movements. *Jour. Geophys. Res.*, 87: 10656-10676.

Takagi, H. (1982) On the definition of mylonite and the classification of mylonitic rocks. *Gakujutsu Kenkyu, Scholl of Education, Waseda University, Series of Biology and Geology, Vol.* 31: 49-57.

,, (1986) Implications of mylonitic microtextures for geotectonic evolution of the Median Tectonic Line, Central Japan. *Journal of Structural Geology*, 8(1):3-14.

Talukdar, S. and Colvee, G.P. (1974) Geologia y estratigrafia del área Meseta de El Viejo-Cerro

Danto, Territorio Federal Amazonas, Venezuela. *Bol. Soc. Ven. Geol.*, 9(2): 22-41.

,, Loureiro, D., Mendoza, J., Lara, A., and Serrano de Rojas, I. (1979) Historia metamórfica de la parte norcentral de la Cordillera de la Costa entre Carayaca y Puerto Cruz y su significado. *GEOS, Caracas,* 25: 67-68.

,, Loureiro, D., Navarro, E., Urbani, F., and Ostos, M. (1981) Modelo de tectónica de placas para la evolución del Sistema Montañoso del Caribe: una nueva hipótesis de trabajo. *ASOVAC, Noviembre* 1981, Resumen, 212.

,, and Bolivar, E. (1982) Petroleum Geology of Tuy-Cariaco-Basin, eastern Venezuela continental shelf: a preliminary appraisal. *INTEVEP Informe Técnico INT-00661, 82.* 78 p.

,, and Loureiro, D. (1982) Geología de una zona ubicada en el segmento norcentral de la Cordillera de la Costa, Venezuela: Metamorfismo y deformación. Evolución del margen septentrional de Suramérica en el marco de la tectónica de placas. *GEOS Caracas,* 27: 15-76.

,, (1983) Petrological study of volcanic and sedimentary rocks from offshore wells of the north of Paria area. *INTEVEP Informe técnico INT-00877, 83.* 126 p.

Talwani, M., Windisch, C.C., Stoffa, P.L., Buhl, P., and Houtz, R.E. (1977) Multichannel seismic study in the Venezuela Basin and the Curacao Ridge. In: *Island arcs, deep sea trenches and back-arc basins (Maurice Ewing Series). Talwani, M. and Pitman, W.C.III* editors, *American Geophysical Union, Washington,* N°1: 83-98.

Tarney, J., Saunders, A.D., and Weaver, S.D. (1981) Geochemistry of Volcanic rocks from the Island arcs and marginal basins of the Scotia arc region. In: *Island arcs, deep sea trenches and back-arc basins (Maurice Ewing Series). Talwani, M. and Pitman, W.C.III* editors, *American Geophysical Union, Washington,* N° 1: 367-378.

,, Weaver, S.D., Saunders, A.D., Pankhurst, R.J., and Baker, P.F. (1982) Volcanic evolution of the northern Antartic peninsula and the Scotia arc.

In: *Andesites: Orogenic Andesites and Related Rocks, Thorpe, R.S.* editor, *John Wiley & Sons, New York:* 371-402.

Taylor, G.C. (1960) Geologia de la Isla de Margarita, Venezuela. *Memorias III Cong. Geol. Ven., Caracas* 1959, *Bol. Geol. Publ. Esp.* 3, II: 838-893.

Teggin, D.E., Martinez, M., and Palacio, G. (1985) Un estudio preliminar de las diabasas del estado Bolivar, Venezuela. *Memoria VI Cong. Geol. Ven., Caracas, Noviembre* 1985: *Tomo* II: 2159-2206.

Tomblin, J.F. (1975) The Lesser Antilles and Aves Ridge. In: *The Ocean basins and margins, Vol. 2, The Gulf of Mexico and the Caribbean. Plenun Press, New York:*467-500.

Torrini, R., Speed, R.C., and Mattioli, G.S. (1985) Tectonic relationship between forearc-basin strata and the accreationary complex at Bath, Barbados. *Geol. Soc. Am. Bull.*, 96: 861-874.

Toussaint. J.F. and Restrepo, J.J. (1982) Magmatic evolution of the northwestern Andes of Colombia. *Earth-Science Reviews,* 18: 205-213.

Tschanz, C.M., Marvin, R.F., Cruz, B., Mehnert, H.H., and Cebula, G.T. (1974) Geologic evolution of the Sierra Nevada de Santa Marta, northeastern Colombia. *Geol. Soc. Am. Bull.*, 85: 273-284.

Turner, F.J. (1968) *Metamorphic Petrology.* Mc Graw Hill, New York.

,, (1981) *Metamorphic Petrology: Mineralogical, Field, and Tectonic Aspects.* Mc Graw Hill, New York. Second edition. 524 p.

Urbani, F. (1969) Primera localidad fosilifera del Miembro Zenda de la Formación Las Brisas: Cueva El Indio, La Guairita, Estado Miranda. *AVGMP, Caracas,* 12(12): 447-453.

,, (1972) Geologia del Granito de Guaremal y rocas asociadas, estado Carabobo. *Memorias IV Cong. Geol. Ven., Caracas* 1969, *Bol. Geol. Publ. Esp.*, 7 (IV): 2340-2371.

,, and Quesada, E.A. (1972) Migmatitas y rocas asociadas del área de la Sabana, Cordillera de la

Costa. *Memorias IV Cong. Geol. Ven., Caracas* 1969, *Bol. Geol. Publ. Esp.*, 5 (IV): 2375-2400.

,, (1973) Notas sobre el hallazgo de fósiles en rocas metamórficas de la parte central de la Cordillera de la Costa. *Â.V.G.M.P. Caracas, Bol. Informativo* 16 (4-5-6): 41-53.

,, (1982) Comentarios sobre algunas edades de las rocas de la parte central de la Cordillera de la Costa. *GEOS* 27, Caracas: 77-84.

,, (1983) Las rocas graniticas del área de las Trincheras-Mariara, Estado Carabobo: Geologia y edad. *Cientifica Venezolana, Vol.* 34, supl. 1: p. 93.

,, and Ostos, M. (1987) El Grupo Avila, Cordillera de la Costa. *Memorias Jornadas 50 Aniversario Escuela Geologia (UCV, Caracas)*, In press.

,, Marquina, M., and Chirinos, A. (1987b) Geologia del área de la Sabana-Guatopo, Distrito Federal y Edos. Miranda y Guárico. *Bol. Geociencias (UCV, Caracas)*,11.

,, Contreras, O., and Ugueto, G. (1988) Geologia de la región de Mariara-Maracay, Carabobo y Aragua. *ASOVAC, Noviembre* 1988.

,, (1988b) Algunos complejos de rocas metaígneas en la Cordillera de la Costa. *Revista de la Facultad de Ingeniería (UCV, Caracas)*, 3(2): 22-39.

Van Den Driessche, J. and Brun, J.P. (1987) Rolling structures at large shear strain. *Journal of Structural Geology*, 9: 691-704.

Van der Voo, R. and French, R.B. (1974) Apparent polar wandering for the Atlantic bordering continents: Late Carboniferous to Eocene. *Earth Sciences Reviews, Vol.* 10: 99-119.

,, (1983) A plate-tectonics model for the Paleozoic assembly of Pangea based on paleomagnetic data. *Geol. Soc. Am., Memoir 158,* Contributions to the Tectonics and Geophysics of Mountain Chains, Hatcher, *R.B., Williams, H., and Zietz, I.* editors: 19-24.

Venturelli, G., Capedri, S., Thorpe, R.S., and Potts, P.J.

(1979) Rare-earth and other element distribution in some ophiolitic metabasalts of Corsica, Western Mediterranean. *Chemical Geology*, 24: 339-353.

Vierbuchen, R.C. (1978) The tectonics of northeastern Venezuela and the southeastern Caribbean Sea. *Ph.D. thesis, Princenton University*, 175p.

,, (1984) The Geology of the El Pilar fault zone and adjacent areas in northeastern Venezuela. *Geol. Soc. Am., Memoir 162, Bonini, W.E., Hargraves, R.B., and Shagam, R.* editors, 189-212.

Vignali, M. (1976) the stratigraphy and structure of the metamorphic Eastern Cordillera, Venezuela (Araya-Paria Peninsula and Margarita island). *Ph.D. thesis, ETH, Zurich*, 129p.

,, (1979) Estratigrafia y estructura de las cordilleras metamòrficas de Venezuela oriental (Peninsula de Araya-Paria e isla de Margarita). *GEOS, Caracas*, 25: 19-66.

Watkins, J. and Cavanaugh, Th. (1976) Implications of magnetic anomalies in the Venezuela basin. *Transactions of the 7th Caribbean Geol. Conference, Guadaloupe:* 127-138.

Wehrmann, M. (1972) Geologia de la regiòn de Guatire-Colonia Tovar. *Memorias IV Congreso Geol. Ven., Caracas* 1969, *Bol. Geol. Pub. Esp.*, 5 (IV): 2093-2119.

Westbrook, G.K. (1975) The structure of the crust and upper mantle in the region of Barbados and the Lesser Antilles. *Royal Astronomical Society Geophysics Journal, Vol.* 43: 201-242.

Westercamp, D., Andreieff, P., Bouysse, Ph., and Mascle, A. (1985) The Grenadines, southern Lesser Antilles. Part I: Stratigraphy and volcano-structural evolution. *Symposium Géodynamique des Caraibes, Paris Février* 1985, *Mascle, A.* editor: 109-118.

White, A.J.R. and Chappell, B.W. (1977) Ultrametamorphism and granitoid gneiss. *Tectonophysics*, 43: 7-22.

,, (1979) Source of granitic magmas. *Geol. Soc. Am., Ann. Gen. Meeting*, 539.

Wiedmann, J. (1978) Ammonites from the Curacao Lava

Formation, Curacao, Caribbean. *Geologie en Mijnbouw, Vol. 57:* 361-364.

Winchester, J.A. and Floyd, P.A. (1977) Geochemical discrimination of different magma series and their differentiation products using inmobile elements. *Chemical Geology,* 20: 325-343.

,, and Max, M.D. (1982) The geochemistry and origin of the Precambrian rocks of the Rosslare Complex, southeast Ireland. *Journal Geol. Soc. London,* 139: 309-319.

Winkler, H.G.F. (1979) *Petrogenesis of Metamorphic rocks.* Springer-Verlag, New York, fifth edition. 348 p.

Wood, D.A., Gibson, I.L., and Thompson, R.N. (1976) Elemental mobility during Zeolite facies metamorphism on the Tertiary basalts of eastern Iceland. *Contrib. Mineral. Petrol.,* 55: 241.

,, Joron, J-L., and Treuil, M. (1979) A re-appraisal of the use of trace elements to classify and discriminate between magma series erupted in different tectonic settings. *Earth Planet. Sci. Letters,* 45: 326-336.

,, (1980) The application of Th-Hf-Ta diagram to problems of tectonomagmatic classification and to establishing the nature of crustal contamination of basaltic lavas of the British tertiary Volcanic Province. *Earth Planet. Sci. Letters,* 50: 11-30.

Wolcott, P.P. (1943) Fossils from metamorphic rocks of the Coast Range of Venezuela. *Am. Ass. Petr. Geol. Bull.,* 27(10): 1632.

Yoris, F. (1985) Revisiòn de la Estratigrafia del Cretaceo inferior al sur y este de la Serrania del Interior, Venezuela Nororiental. *Memorias VI Congr. Geol. Ven., Caracas, Noviembre* 1985, *Tomo* II: 1343-1393.

York, D. (1968) Least-square fitting of a straight line with correlated errors. *Earth Planet. Sci. Letters,* 5: 320-324.

TABLE A.5.0: INSTRUMENTS USED IN THE ANALYSES.

SAMPLE NUMBER	MAJOR-ELEMENTS PHILIPS 1410/70	PHILIPS PW-1400	X-RAY LAB.	TRACE-ELEMENTS PHILIPS 1410/70	PHILIPS PW-1400	X-RAY LAB.
DF-9092	X			X		
DF-9128B	X			X		
DF-9131	X			X		
DF-9134	X					
DF-9135	X					
DF-9147	X					
DF-9150	X					
DF-9150B	X					
DF-9153	X					
DF-9156	X					
DF-9159	X					
DF-9162	X					
VO-83-5	X					
VO-83-5C	X					
VO-83-9	X					
VO-83-9B	X					
VO-83-10	X					
DF-234A1	X			X		
DF-234A2		X			X	
DF-323B		X			X	
DF-412B	X			X		
DF-512	X			X		
DF-512B	X			X		
DF-517		X			X	
DF-689B		X				
DF-1123		X				
DF-1226		X				
DF-2227B		X				
DF-2229		X				
DF-2252		X				
DF-3012		X				
DF-3220		X				
DF-3233		X				X
DF-3248	X			X		
DF-3303		X			X	
DF-3309B	X			X		
DF-3406		X			X	
VO-83-61	X			X		
VO-83-62	X			X		
VO-83-63	X			X		
VO-83-65	X			X		
VO-86-17	X			X		

TABLE A.5.0: CONTINUATION.

SAMPLE NUMBER	MAJOR-ELEMENTS PHILIPS 1410/70	PHILIPS PW-1400	X-RAY LAB.	TRACE-ELEMENTS PHILIPS 1410/70	PHILIPS PW-1400	X-RAY LAB.
VO-86-19	X			X		
VO-83-200	X					X
VO-83-203	X			X		
VO-83-205	X			X		
VT-82-135	X			X		
VT-82-104	X			X		
VT-82-105	X			X		
VT-82-129	X					X
VT-82-130	X					X
VT-82-132B	X			X		
VT-82-139	X			X		
VT-82-2	X			X		
VT-82-44	X					X
VT-82-51	X			X		
VTO-82-52	X			X		
VTO-82-61	X					X
VT-82-100	X				X	
VT-82-101	X				X	
VT-82-114	X				X	
VT-82-116	X				X	
VT-82-116B	X					X
VT-82-118	X				X	
VTOG-31	X				X	
VTOG-82	X				X	
VO-86-35	X				X	
VO-86-35B	X				X	
VO-86-36	X				X	
VO-86-37	X				X	
VO-86-37B	X				X	
VO-86-38			X			X
VO-86-40	X				X	
QP-403	X			X		
QP-416	X			X		
QP-462	X			X		
QP-472	X			X		
QR-475	X			X		
QO-530	X			X		
QRR-534	X			X		
QH-682	X			X		
QH-689A	X			X		
QO-839	X			X		
QO-843	X			X		
VC-20	X			X		

TABLE A.5.0: CONTINUATION.

SAMPLE NUMBER	MAJOR-ELEMENTS PHILIPS 1410/70	PHILIPS PW-1400	X-RAY LAB.	TRACE-ELEMENTS PHILIPS 1410/70	PHILIPS PW-1400	X-RAY LAB.
VC-20B	X			X		
VC-22C	X			X		
VC-23A	X			X		
VC-30A	X			X		
VC-51	X			X		
VC-60	X			X		
VO-83-302	X					X
VO-83-302B	X			X		
VO-83-305B	X					X
VO-83-307	X			X		
VO-83-308	X			X		
VO-83-308B	X					X
VO-83-309	X			X		
VO-83-310	X					X
VO-83-311	X					X
VO-83-313B	X			X		
VO-83-315	X			X		
VO-83-316	X			X		
VO-83-317	X			X		
VO-83-318	X				X	
VO-83-319	X				X	
VO-83-321	X				X	
VO-83-322	X				X	
VO-83-323	X				X	
VO-83-324	X				X	
VO-83-326	X				X	
VO-86-5	X				X	
VO-86-6	X					X
N-1	X			X		
N-3	X			X		
N-4	X			X		
N-6	X			X		
N-8	X			X		
N-12	X			X		
N-20	X			X		
N-21	X			X		
E-7	X			X		
F-3	X			X		
F-13	X			X		
VO-83-1	X			X		
VO-83-4	X			X		
VO-83-7	X			X		

TABLE A.5.0: CONTINUATION.

SAMPLE NUMBER	MAJOR-ELEMENTS PHILIPS 1410/70	PHILIPS PW-1400	X-RAY LAB.	TRACE-ELEMENTS PHILIPS 1410/70	PHILIPS PW-1400	X-RAY LAB.
VO-83-12	X			X		
VO-83-12B	X			X		
VO-83-13	X			X		
VO-83-21	X			X		
VO-83-27	X			X		
VO-83-34	X			X		
VO-86-9	X			X		
PM-1			X			X
PM-2			X			X
PM-3			X			X
DF-9024		X			X	
DF-9062		X			X	
DF-9155		X			X	
DF-10042		X			X	
DF-10064		X			X	
VO-83-59	X			X		
VO-83-60	X			X		
VO-83-62B	X			X		
VO-83-64	X			X		
VO-83-66	X			X		
VO-83-67	X			X		
VO-83-68	X			X		
VO-83-71	X			X		
LV-87-1			X			X
LV-87-2			X			X
LV-87-3			X			X
LV-87-4			X			X
VO-83-202	X					X
VO-83-205B			X	X		
VO-83-207	X			X		
VO-83-208	X			X		
VO-83-210B	X			X		
VO-83-211	X			X		
VO-83-212	X			X		
VT-82-133	X			X		
VT-82-134	X			X		
VT-82-136	X			X		
VT-82-136B	X			X		
VTOG-45			X			X
RT-87-2			X			X
RT-87-4			X			X
RT-87-5			X			

TABLE A.5.0: CONTINUATION.

SAMPLE NUMBER	MAJOR-ELEMENTS PHILIPS 1410/70	MAJOR-ELEMENTS PHILIPS PW-1400	MAJOR-ELEMENTS X-RAY LAB.	TRACE-ELEMENTS PHILIPS 1410/70	TRACE-ELEMENTS PHILIPS PW-1400	TRACE-ELEMENTS X-RAY LAB.
MTS-85-1			X			
MTS-85-2			X			
MTS-85-3			X			
GUAY-85-1			X			
VO-83-300	X					X
VO-83-301	X					X
VO-83-303B	X			X		
VO-83-304	X			X		
VO-83-304B	X			X		
VO-83-306B	X			X		
VO-83-313	X			X		
VO-83-314	X			X		
VO-83-320	X			X		
VO-83-352	X			X		
VO-83-385	X			X		
N-5		X			X	
E-9		X			X	
F-10	X			X		
M-1	X			X		
M-3	X			X		
TOD-22			X			X
TOD-25			X			X
TOD-26			X			X

X-RAY LAB: Major-elements by X-ray fluorescense and trace-elements by inductively coupled plasma mass spectrometry.

Table A.5.1: International Geostandards used for calibration

REFERENCE SAMPLE	SAMPLE COMPOSITION	SAMPLE SOURCE
AGV-1	Andesite	United States Geological Survey
BCR-1	Basalt	,, ,, ,, ,, ,,
DTS-1	Dunite	,, ,, ,, ,, ,,
PCC-1	Peridotite	,, ,, ,, ,, ,,
GSP-1	Granodiorite	,, ,, ,, ,, ,,
BR	Basalt	Centre de Researches Petrographiques et Geochimiques
GA	Granite	,, ,, ,, ,, ,,
GH	Granite	,, ,, ,, ,, ,,
NIM-G	Granite	National Institue for Metallurgy
NIM-L	Norite	,, ,, ,, ,, ,,
NIM-P	Pyroxenite	,, ,, ,, ,, ,,
NIM-S	Syenite	,, ,, ,, ,, ,,
SY-3	Syenite	Canadian Certified Reference Materials Project.
UB-N	Serpentinite	Association Nationale de la Recherche Technique
DRN	Diorite	Association Nationale de la Recherche Technique
DTN	Kyanite	,, ,, ,, ,, ,,

Table A.5.2: Precision of the major element analyses

OXIDE	X (%)	S	C
SiO_2	49.30	1.99	2.82
Al_2O_3	15.05	0.55	2.29
Fe_2O_3	13.01	0.25	1.25
MgO	7.91	0.19	2.11
CaO	6.32	0.21	2.21
Na_2O	3.09	0.20	5.71
K_2O	1.54	0.10	2.61
TiO_2	0.99	0.011	1.40
MnO	0.18	0.005	1.48
P_2O_5	0.27	0.04	8.49

Sample analyzed: VO-83-5B; S: Standard desviation;
C: Variation coefficient.

TABLE A.5.3: Major- and trace-element averages of mafic samples from the Cordillera de la Costa belt (major element values in percent; trace elements in ppm).

Chichiriviche-La Victoria (6 samples)										
	SiO2	Al2O3	TiO2	Fe2O3	MnO	MgO	CaO	Na2O	K2O	P2O5
Mean	50.41	14.67	1.20	11.25	0.22	9.15	8.40	2.88	0.49	0.17
	Cr	Ni	Zr	Y	Nb	Rb	Sr			
Mean	165	62	42	21	5.66	29	261			
El Avila National Park (12 samples)										
	SiO2	Al2O3	TiO2	Fe2O3	MnO	MgO	CaO	Na2O	K2O	P2O5
Mean	50.27	13.93	0.77	11.03	0.16	8.68	11.08	2.27	0.19	0.14
Mean	175	75	61	20	6.37	21	204			
El Limon-Tacagua Rivers (20 samples)										
	SiO2	Al2O3	TiO2	Fe2O3	MnO	MgO	CaO	Na2O	K2O	P2O5
Mean	47.01	14.71	1.55	14.05	0.24	9.44	8.20	2.70	0.51	0.33
	Cr	Ni	Zr	Y	Nb	Rb	Sr			
Mean	160	60	68	29	8.10	28	213			

TABLE A.5.4: Major- and trace-element averages of mafic rocks from Caucagua-El Tinaco belt (major element values in percent; trace elements in ppm).

La Guacamaya Metadiorite (6 samples)

	SiO2	Al2O3	TiO2	Fe2O3	MnO	MgO	CaO	Na2O	K2O	P2O5
Mean	54.13	15.58	0.71	9.68	0.12	6.63	7.84	2.12	1.45	0.12

	Cr	Ni	Zr	Y	Nb	Rb	Sr
Mean	31	29	72	24	9.72	51	232

Tinaco Complex in the Tinaco River-Casupo Village Transect (10 samples)

	SiO2	Al2O3	TiO2	Fe2O3	MnO	MgO	CaO	Na2O	K2O	P2O5
Mean	49.33	14.72	0.76	10.27	0.24	9.58	8.82	2.63	1.29	0.21

	Cr	Ni	Zr	Y	Nb	Rb	Sr
Mean	281	75	41	16	6.27	28	426

Tinaquillo Peridotite Complex (12 samples)

	SiO2	Al2O3	TiO2	Fe2O3	MnO	MgO	CaO	Na2O	K2O	P2O5
Mean	47.42	16.00	0.80	9.47	0.19	11.86	11.18	1.93	0.23	0.04

	Cr	Ni	Zr	Y	Nb	Rb	Sr
Mean	520	130	26	16	5.04	16	355

TABLE A.5.5: Major- and trace-element averages of mafic samples from the Villa de Cura belt (major element values in percent; trace elements in ppm).

Villa de Cura Group in La Victoria-San Sebastian Transect (18 samples)

	SiO2	Al2O3	TiO2	Fe2O3	MnO	MgO	CaO	Na2O	K2O	P2O5
Mean	47.90	14.56	0.85	10.11	0.15	9.28	8.96	2.10	1.08	0.15

	Cr	Ni	Zr	Y	Nb	Rb	Sr
Mean	358	103	83	26	8.91	25	247

Dos Hermanas Formation in the Guatopo National Park (7 samples)

	SiO2	Al2O3	TiO2	Fe2O3	MnO	MgO	CaO	Na2O	K2O	P2O5
Mean	50.06	15.25	0.87	9.12	0.31	11.43	7.69	3.06	0.94	0.14

	Cr	Ni	Zr	Y	Nb	Rb	Sr
Mean	144	59	111	34	7.88	17	271

TABLE A.5.6: Major- and trace-element averages of mafic samples from Margarita island (major element values in percent; trace elements in ppm).

	SiO2	Al2O3	TiO2	Fe2O3	MnO	MgO	CaO	Na2O	K2O	P2O5
Mean	48.14	15.57	0.88	10.85	0.13	7.77	10.42	3.17	0.32	0.10
	Cr	Ni	Zr	Y	Nb	Rb	Sr			
Mean	239	88	23	19	5.55	9	235			

TABLE A.5.7: Major- and trace-element averages of mafic samples from Los Roques island (major element values in percent; trace elements in ppm).

	SiO2	Al2O3	TiO2	Fe2O3	MnO	MgO	CaO	Na2O	K2O	P2O5
Mean	49.38	14.72	0.92	10.75	0.16	8.68	11.91	2.06	0.21	0.13
	Cr	Ni	Zr	Y	Nb	Rb	Sr			
Mean	179	61	151	36	13.31	27	177			

Table A.5.8: Discrimination Diagrams originally chosen

DISCRIMINATION DIAGRAM	AUTHOR
TiO_2 - Zr	Floyd and Winchester (1975)
TiO_2 - Y/Nb	,, ,, ,, ,,
TiO_2 - Zr/P_2O_5	,, ,, ,, ,,
P_2O_5 - Zr	,, ,, ,, ,,
Nb/Y - Zr/P_2O_5	,, ,, ,, ,,
Ni - MgO	Humphris *et al.* (1985)
Cr - MgO	,, ,, ,,
Nb - Zr	,, ,, ,,
Y - Zr	,, ,, ,,
TiO_2 - Zr	,, ,, ,,
Zr/4 - Y - 2*Nb	Meschede (1986)
$Na_2O + K_2O$ - SiO_2	Miyashiro (1975)
FeO*/MgO - SiO_2	,, ,, ,,
FeO* - FeO*/MgO	,, ,, ,,
TiO_2 - FeO*/MgO	,, ,, ,,
Cr-Y	,, ,, ,,
Ni - FeO*/MgO	,, ,, ,,
Ni-Y	Crawford and Keays (1978)
	Capedri *et al.* (1980)
MnO*10 - P_2O_5*10 - TiO_2	Mullen (1983)
Ni - MgO/(MgO + Fe_2O_3)	Noiret *et al.* (1981)
Ti/100 - Zr - 3*Y	Pearce and Cann (1973)
Ti/100 - Zr - Sr/2	,, ,, ,,
Ti - Zr	,, ,, ,,
Ti - Cr	Pearce (1975)
TiO_2 - K_2O - P_2O_5	Pearce *et al.* (1975)
Ti/Cr - Ni	Beccaluva *et al.* (1979)
Ti/Y - Nb/Y	Pearce (1982)
Zr/Y - Zr	Pearce and Norry (1979)
Ti/Y-Zr/Y	Pearce and Gale (1977)
Ti/100 - Cr	Roy *et al.* (1982)
Zr - Fe/Mg	Saunders and Tarney (1979)
TiO_2 - Fe/Mg	,, ,, ,,
CaO/TiO_2 - TiO_2	Sun *et al.* (1979)
Al_2O_3/TiO_2 - TiO_2	,, ,, ,,

TABLE A.5.9: Whole-rock Rubidium-Strontium data for from the Caribbean Mountains System.

SAMPLE	BELT	$^{87}Rb/^{86}Sr$	$^{87}Sr/^{86}Sr$	Initial $^{87}Sr/^{86}Sr$
PM-86-1	Cordillera de la Costa	6.269	0.84784	
PM-86-2	,, ,,	7.940	0.89125	
CH-86-1	,, ,,	2.793	0.77486	0.71103 ±.00734
RT-87-1	Caucagua-El Tinaco	0.261	0.71010	
RT-87-2	,, ,,	0.165	0.70519	
RT-87-4	,, ,,	1.234	0.72005	
RT-87-5	,, ,,	0.853	0.71760	0.70475 ± .00197
LV-87-1	Caucagua-El Tinaco	0.586	0.70674	
LV-87-2	,, ,,	0.287	0.70600	
LV-87-3	,, ,,	0.254	0.70286	
LV-87-4	,, ,,	0.373	0.70651	
MTS-85-1	Margarita I.	0.0411	0.70302	
MTS-85-2	,, ,,	0.0269	0.70324	
MTS-85-3	,, ,,	0.0275	0.70344	
MTS-85-4	,, ,,	0.0378	0.70331	
GUAY-85-1	,, ,,	0.0240	0.70298	